Modeling of a Variable Frequency Drive Controller for Residential Air Conditioning System

BY

OMAR AHMED OMAR AL-TAMIMI

A Thesis Presented to the

DEANSHIP OF GRADUATE STUDIES

KING FAHD UNIVERSITY OF PETROLEUM & MINERALS

DHAHRAN, SAUDI ARABIA

In Partial Fulfillment of the
Requirements for the Degree of

MASTER OF SCIENCE

In

ELECTRICAL ENGINEERING

MAY, 2017

DHAHRAN- 31261, SAUDI ARABIA

DEANSHIP OF GRADUATE STUDIES

This thesis, written by **OMAR AHMED OMAR AL-TAMIMI** under the direction his thesis advisor and approved by his thesis committee, has been presented and accepted by the Dean of Graduate Studies, in partial fulfillment of the requirements for the degree of **MASTER OF SCIENCES IN ELECTRICAL ENGINEERING.**

Dr. Mahmoud Kassas

(Advisor)
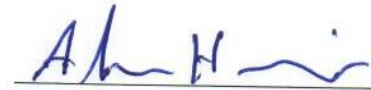
Dr. Ali Al-Shaikhi

Department Chairman

Dr. Chokri Belhadj Ahmed

(Member)

Dr. Salam A. Zummo

Dean of Graduate Studies

Dr. Alaa El-Din Hussein

(Member)

20/8/12

Date

بسم الله الرحمن الرحيم

ACKNOWLEDGMENT

"In the name of Allah, the Most Beneficent and the Most Merciful"

All praise, glory and thanks are due to Almighty Allah, Most Gracious, and Most Merciful for bestowing me with health, knowledge, opportunity, courage and patience to accomplish this work. May peace and blessings be upon the prophet Muhammad (PBUH), his family and his companions.

Firstly, acknowledgement is due to King Fahd University of Petroleum & Minerals for the support given to purse my graduate studies with financial support and conduct this research through its facilities.

I acknowledge with deep gratitude, the inspiration, encouragement, valuable time, guidance and appreciation given to me by my thesis advisor, Dr. Mahmoud Kassas .I am deeply grateful to Dr. Chokri Belhadj Ahmed and Dr. Alaa El-Din Hussein, my thesis committee members, for their valuable time, interest, cooperation and constructive advice.

Special thanks to my seniors at the university Waleed Mohammed, and Saleh Alawsh, who always helped me by providing proper guidance. I am thankful to my colleagues Fahed, Ali, Shihab,Majeed, Saeed, Ahmed, and all who provided wonderful company and good memories that will remain with me forever.

Lastly and the most important of all I am thankful to my parents for their love, support, prayers and encouragement throughout my life. I appreciate the efforts of my father and mother for

everything and I am and will remain in debt to them for my entire life time. I thank my wife, brothers and sister for their unconditional love, motivation and encouragement. I am also grateful to my uncle Mr. Khalid and cousins, Mr. Salem Saleh, Mr. Radi and their families.

TABLE OF CONTENTS

LIST OF TABLES

LIST OF FIGURES

LIST OF ABBREVIATIONS

HVAC	:	Heating, Ventilation and Air Conditioning
VFD	:	Variable Frequency Drive
VSD	:	Variable Speed Drive
MATLAB	:	Matrix Laboratory
rpm	:	Revolutions per minute
hp	:	Horsepower
BTU	:	British Thermal unit
LabVIEW	:	Laboratory Virtual Instrument Engineering Workbench
DAQ	:	Data Acquisition
PC	:	Personal Computer
cDAQ	:	Compact Data Acquisition
NI	:	National Instrument
MAX	:	Measurement & Automation Explorer
THD	:	Total Harmonic Distortion
RMS	:	Root Mean Square
SCRs	:	Silicon-Controlled-Rectifiers
IGBTs	:	Insulated-Gate-Bipolar-Transistors
c.pCO	:	Connected Programmable Controller
ExV	:	Electronic Expansion Valve
comp	:	Air Conditioning Compressor
CC	:	Compressor Contactor
FM	:	Air Conditioning Fan Motor

BM	:	Air Conditioning Blower Motor
BMC	:	Blower Motor Contactors
ECB	:	Electronic Control Board
BLDC	:	Brushless DC Compressor
CB	:	Circuit Breaker
pGD[1]	:	Programmable Graphic Displays
FBUS RTU	:	Frame Transport Bus for Remote Terminal Unit
IPM	:	Intelligent Power Modules
BMS	:	Building Management Systems
PID	:	Proportional, Integral and Derivative

LIST NOF NUMERICALS

$\dot{M}_{HVAC}$:   Mass supply air flow (kg/s)

M_{air} :   Air mass (kg)

C_p :   Air specific heat (J/kg.k)

R_{eq} :   Equivalent house thermal resistance ($R_{in}+R_{out}$).

Q_{int} :   The sum of convective internal load ($Q_{int} = Q_{Heat\ sources}$)

$T_{outdoor}$:   Out-room temperature (°C)

T_{room} :   In-room temperature. (°C)

T_{HVAC} :   Supply temperature (°C)

T_{House} :   The inside house temperature. (°C)

T_{mass} :   The inner mass temperature. (°C)

T_{out} :   The outside house temperature. (°C)

C_a :   The thermal mass of the air.

C_m :   The thermal mass of the building and furniture.

U_a :   The conductive of the building envelope ($U_a = 1/R_{out}$).

U_m :   The conductance between the inner air and inner solid mass ($U_m = 1/R_{in}$).

Q_a :   The heat flux consists of three gain factors (J/s)

Q_{in} :   Internal heat gain (J/s)

Q_{so} :   Solar heat gain (J/s)

Q_c :   Heating/Cooling gain (J/s)

Q_m :   Mass supply air flow rate (J/s)

A	:	Area (m^2)
H	:	Heat transfer coefficient
k	:	Thermal conductivity
h	:	Radiation coefficient
l	:	Thickness (m)
$T_{\_out}$	:	External house temperature (℃)
$T_{\_H}$	:	Internal house temperature (℃)
$T_{\_1}$	:	Internal roof temperature (℃)
$T_{\_2}$	:	Internal wall temperature (℃)
$T_{\_3}$	:	Internal windows temperature (℃)
$C_{\_Air}$	:	Specific heat of air (J/℃)
$M_{\_Air}$	:	Mass of air inside the house (kg)
$c_{\_Air}$	:	Heat capacity of air
$C_{\_Roof}$:	:	Specific heat of roof (J/℃)
$M_{\_Air}$	:	Mass of roof (kg)
$c_{\_Roof}$	:	Heat capacity of roof
$C_{\_Wall}$	:	Specific heat of wall (J/℃)
$M_{\_Wall}$	:	Mass of wall (kg)
$c_{\_wall}$	:	Heat capacity of wall
$C_{\_Wind}$	:	Specific heat of windows (J/℃)
$M_{\_Wind}$	:	Mass of windows (kg)
$c_{\_wind.}$	:	Heat capacity of windows
$Q_{\_Air}$	:	The energy stored in the space area of house. (J/s)

Q__Wall : The heat energy stored in the wall. (J/s)

Q__Roof : The heat energy stored in the roof. (J/s)

Q__Wind : The heat energy store in the windows. (J/s)

Q__(Heat house Sources): The heat energy supplied from activity human and furniture in the

space area of house. (J/s)

$\frac{dQ_{Cooler}(t)}{dt}$: The absorbed heat flow form air house by cooler.

K_0 : The effective cooler gain kg/K (default $K_0 = 1$ kg/K).

K_1 : The effective time cooler gain kg/s.K (default $K_1 = 1$ kg/s. K).

THESIS ABSTRACT

FULL NAME : [OMAR AHMED OMAR AL-TAMIMI]

THESIS TITLE : [MODELING OF A VARIABLE FREQUENCY DRIVE

CONTROLLER FOR RESIDENTIAL AIR CONDITIONING SYSTEM]

MAJOR FIELD : [ELECTRICAL ENGINEERING]

DATE OF DEGREE: [May,2017]

In recent years, research and development of energy saving for Heating, Ventilation, and Air Conditioning (HVAC) system has become a hot spot with the advance of science and technology. Achieving thermal comfort with minimum energy consumption is the main requirement in designing an air conditioning system. The Kingdom of Saudi Arabia (KSA) has a desert climate characterized by extreme heat during the day. Therefore, the air-conditioning systems become a necessity component in people's daily life. HVAC system is the chief contributor to energy consumption in a house which consumed about 60% of the energy used in the residential area in KSA. Developing a sophisticated and very precise thermal model for a house and air conditioning system is really needed to save the electric energy and to maintain the thermal comfort level. The aim of this work is to conduct an experimental and a simulation research for two different types of air conditioning systems installed in two identical houses located at KFUPM campus in Dhahran, Saudi Arabia. The thermal model for both houses has developed with two different types of air-conditioning systems, conventional HVAC system equipped with ON/OFF cycle and new technology HVAC system equipped with variable frequency drive (VFD) which has been modeled by three different control strategies (PID, PWM, and FLC). LabView platform is utilized for the experimental work to monitor the environment parameters and power consumption. Energy analysis shows that HVAC integral with PID, PWM and fuzzy logic controllers are better than ON/OFF HVAC control mechanism based on energy saving. Generally, with HVAC variable frequency drive fuzzy logic controller is better than PID and PWM controllers. The study shows that VFD-FLC is the most suitable control strategy, and the space temperature is able to be controlled with significant energy saving.

ملخص الرسالة

الاســــم الكامـــل : [عمر احمد عمر التميمي]

عنـوان الرسالـــــة : [نمذجة وحدة تحكم محرك التردد المتغير لنظام تكييف الهواء السكنية]

التخصـــــــــص : [الهندسة الكهربائية]

تاريخ الدرجة العلمية : [مايو- 2017]

في السنوات الأخيرة، أصبح البحث والتطوير لتوفير الطاقة للتدفئة والتهوية، وتكييف الهواء (HVAC) نظام بقعة ساخنة مع تقدم العلم والتكنولوجيا. تحقيق الراحة الحرارية مع الحد الأدنى من استهلاك الطاقة هو الشرط الرئيسي في تصميم نظام تكييف الهواء. المملكة العربية السعودية (KSA) لديها مناخ صحراوي يتميز بالحرارة الشديدة خلال النهار. ولذلك، فإن أنظمة تكييف الهواء تصبح عنصرا ضروريا في حياة الناس اليومية. نظام التكييف هو االمساهم الرئيسي في استهلاك الطاقة في المنازل ويستهلك حوالي 60٪ من الطاقة المستخدمة في المنطقة السكنية بالمملكة العربية السعودية. تطوير نموذج حراري متطور ودقيق جدا لمنزل ونظام تكييف الهواء هو في حاجة حقا للحفاظ على الطاقة الكهربائية والحفاظ على مستوى الراحة الحرارية. والهدف من هذا العمل هو إجراء بحوث تجريبية ومحاكاة لأنواع مختلفة من أنظمة تكييف الهواء المثبتة في منزلين متطابقين يقعان في حرم جامعة الملك فهد للبترول والمعادن في مدينة الظهران بالمملكة العربية السعودية. وقد تم تطوير النموذج الحراري لكلا النظامين مع نوعين مختلفين من أنظمة تكييف الهواء، ونظام HVAC التقليدي مجهزة دورة ON/OFF ونظام HVAC التكنولوجيا الجديدة مجهزة محرك التردد المتغير (VFD) الذي تم تصميمه من قبل ثلاث استراتيجيات التحكم المختلفة (PWM,PID وFLC). يتم استخدام منصة LabView للعمل التجريبي لمراقبة المعلمات البيئة واستهلاك الطاقة. ويظهر تحليل الطاقة أن التكامل HVAC مع PID، PWM و تحكم FLC أفضل ON/OFF آلية التحكم HVACعلى أساس توفير الطاقة. عموما، مع HVAC تردد متغير محرك تحكم FLC أفضل من PID و PWM تحكم. وتبين الدراسة أن FLC-VFD هو أنسب استراتيجية للتحكم، و قادرة على التحكم و السيطرة على مستوى درجة الحراره مع توفير كبير للطاقة

.

درجة الماجستير في العلوم

جامعة الملك فهد للبترول والمعادن

الظهران، المملكة العربية السعودية

CHAPTER 1

INTRODUCTION

1.1 Introduction

Heating, ventilation, and air conditioning (HVAC) is mainly made for maintaining thermal comfort in indoor environments, especially for hot and humid climate. Nowadays, air conditioning has become a necessity in residential area, commercial buildings and industrial processes, and it is considering one of the fastest growing energy consumers in Saudi Arabia. However, HVAC system is directly participating in increasing energy consumption. Therefore, making a sophisticated control system for indoor temperature is really needed at the current time to help saving the electric energy and maintaining the thermal comfort. This chapter is describing the background of this thesis, objectives and thesis structure.

1.2 Climate of Kingdom of Saudi Arabia (Dhahran City)

Saudi Arabia is characterized with high temperature, humidity, and dust storms. A temperature in Saudi Arabia follows the pattern of the desert climate, with the exception of the southwest. The average summer temperature is about 45° C, but readings of up to 54° C are not unusual. By the next years, climate change could make that extreme a typical hot summer day in the Arabian Gulf. And the worst heat could be in Dhahran, Saudi Arabia, according to a study published on October,26 2015 in Nature Climate Change [1]. Right now, typical summer days in the city crest

at 43°C and the humid air blowing off the coast of the Arabian Gulf can make daytime activities difficult without the aid of air conditioning. Figure 1.1 shows the outdoor temperature pattern as the highest recorded, daily mean and lowest recorded temperature in 2015. Dhahran city can be classified climatically as hot dry maritime subzone and it presents the Eastern Province weather. From Figure 1.1 the outdoor temperature pattern presents the hottest months in the year which Jun, July and August, they have very high temperature reach to 55 ˚C. The high outdoor temperature will increase demand for cooling over the years as well as the energy consumption.

Climate of Dhahran City (KFUPM Campus-2015)
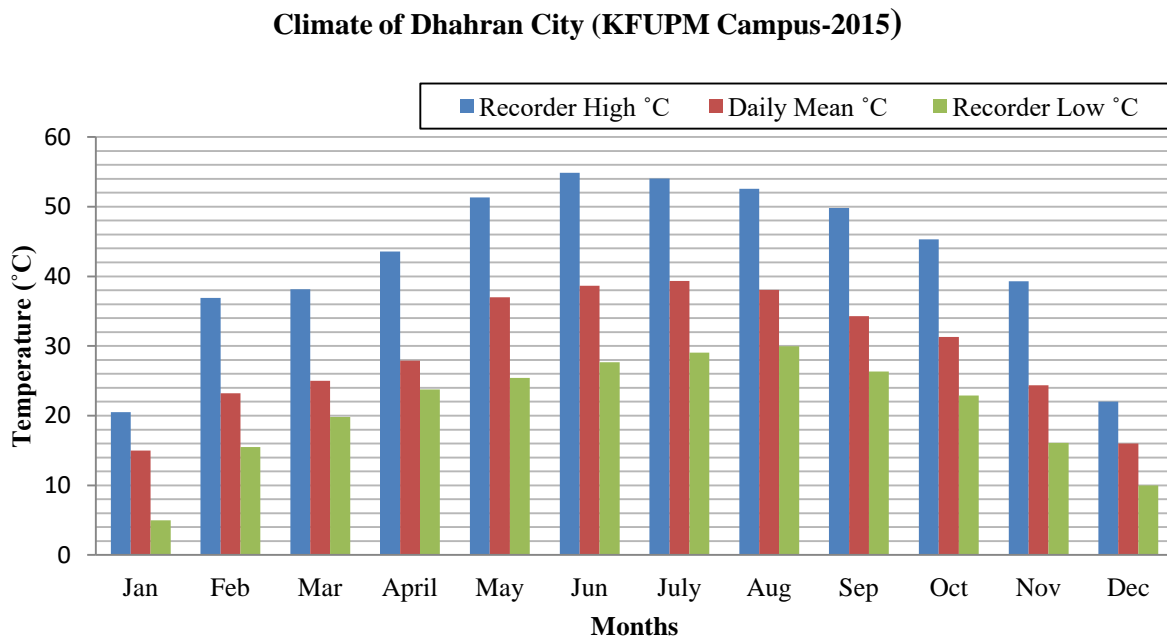
Figure 1.1 Temperature data for Dhahran city, Saudi Arabia, 2016

1.3   Energy Demand of HVAC System in KSA

The residential energy demands are the main source of substantial increase of the electricity consumption due to increase the use of air conditioning requirements. Energy consumption in the residential area is directly impact on with energy demands of HVAC systems. HVAC systems are the most energy end use in the residential and non-residential area. Some studies show that

air conditioning is responsible for 10% to around 60% of the total residential energy consumption, relying on the building type [2].

Energy consumptions in KSA have grown substantially over the previous years. Electricity consumption in KSA is considered one of the highest per capita consumption rates in the world around 8,161 kWh /capita which is approximately three times more than the world's average. The energy consumptions have witnessed a growth of around 5-8% annually. The peak load has been growing annually at a rate of 10.2 (2014-2015). Figure 1.2 presents the growth trend forecast peak load up to 2020 [3]. Due to the high cooling demand during the summer, when the temperature reaches beyond 45°C, energy consumption from the residential sector exceeds industrial and commercial sectors. The residential sector consumes about half of the electricity supply, closely followed by industrial, commercial/trade, and government facilities at 19%, 15%, and 13%, respectively [4]. Table 1.1 represents the comparison between 2013 and 2014 power consumption by residential sector [4].

Table 1.1 Comparative amount of power consumption for 2013-2014 by residential Sector

Consumption Category	2013	2014
Residential	48.96%	49.51%

Therefore, it can be inferred that residential consumption will drive the consumption of power in the country by 2016 and beyond. Residential segment has been driving the power demand in the Kingdom due to increased demand for cooling over the year. The Kingdom's electricity demand and consumption are unique in a way that it is the residential sector that drives the consumption

and not the industrial sector as is the case with the rest of the developed/developing countries globally.
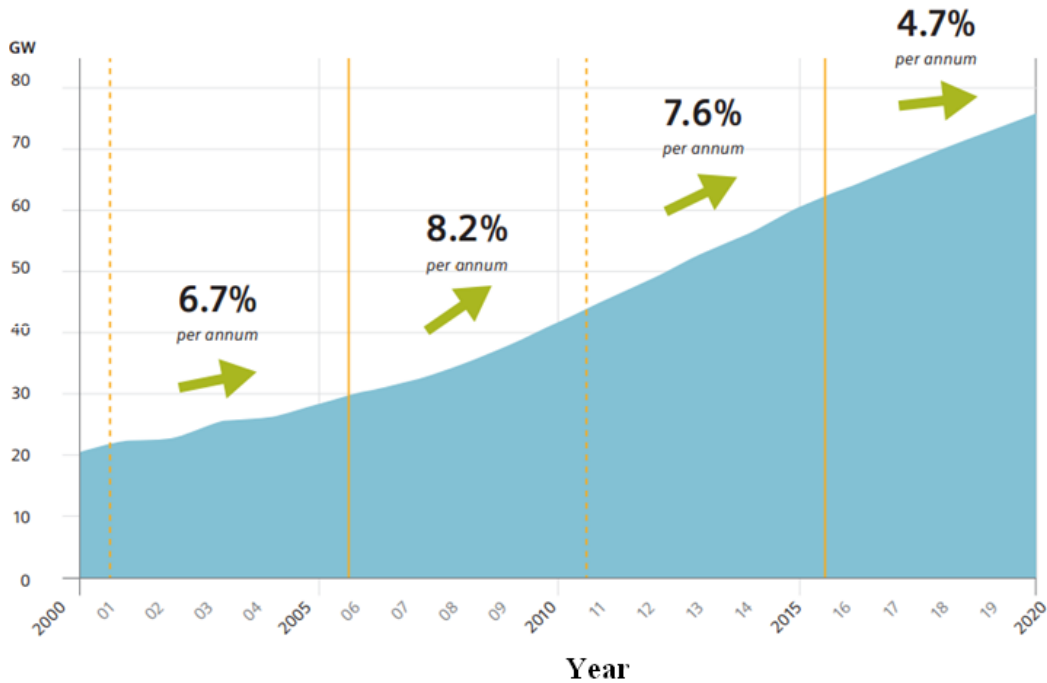
Figure 1.2 Growth trend and forecast peak loads to 2009

HVAC systems are considered the major energy consumptions in the residential area in KSA and it is accounted for approximately 60% of the energy utilized in the residential area. Air conditioning has been on the rise through the KSA because of the high humidity and hot temperature. To assess the energy consumption consumed by air conditioning, thermal modeling and simulation of the house have to be developed and two types of HVAC systems operation will be presented. One HVAC system operates ON/OFF cycle and the second HVAC system runs by using variable frequency driver (VFD). The major parameters of energy consumption in a house are graphically illustrated in Figure 1.3.
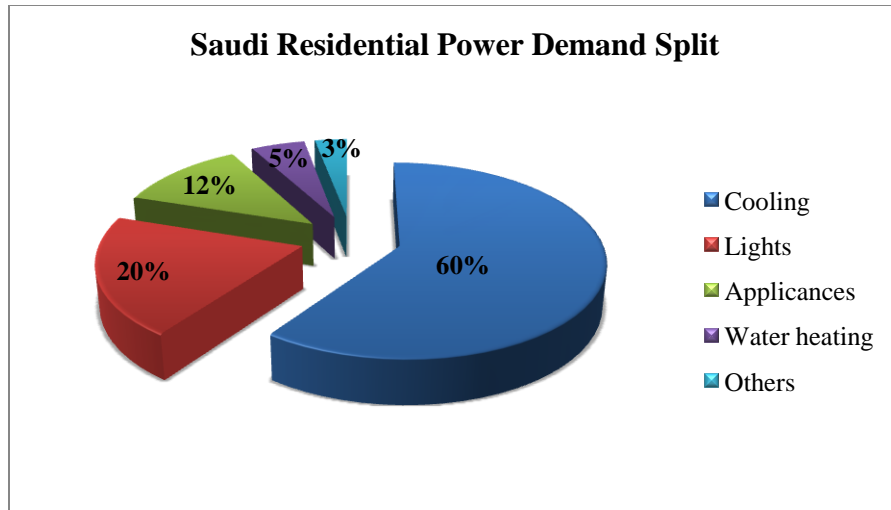
Figure 1.3 Saudi residential power demand split

1.4   Air Conditioning

Historically, air conditioning has implied cooling, otherwise, improving the indoor environment during the warm and hot months of the year. In modern times, the term has taken on a more literal meaning that can be applied to year-round environmental situations. That is, air conditioning refers to the control of temperature, moisture content, cleanliness, odor, and air circulation, as required by the occupants, a process, or product in the space [4]. This general definition has led to the alternative term 'environmental control'.

1.4.1 Conventional HVAC System (ON/OFF Cycle)

The air conditioner attains the desired temperature based on the temperature set point by its thermostat. When the compressor in the air conditioner is turned ON, it will remain ON until the room temperature decreases to desired temperature on the thermostat. Within the threshold the compressor will turn OFF until the room temperature increases again.

1.4.2 Variable Frequency Drive HVAC Systems

A Variable Frequency Drive is like the speed regulator on a car. It adjusts the speed of an HVAC fan and compressor motor based on demand, to save energy and to extend motor and mechanical components life. Without a VFD, HVAC fan or pump motor is either ON full load or OFF.

1.5 Problem Statement

KSA has high temperatures associated with humidity. Air conditioning system is considering the first contributor (60% to 65%) in energy consumption of every house in Saudi Arabia. The main reason of raising this amount of consumed energy because it is using the conventional HVAC system, which actually operating ON/OFF cycle. Each house has its desired set point of the temperature, when the indoor temperature less than the set point the HVAC system is OFF, then when the indoor temperature accessed the set point the HVAC system is ON. During the process of turning ON, the HVAC system needs a very high inrush current. This current leads to consume more power (huge energy consumption) for each cycle during the whole day. Moreover, the lifespan of the compressor is affected by the inrush current. At the same time the comfort level in indoor environment in the house is not achieved very well by using the conventional HVAC. To address the problem, alternative approach to reduce energy consumption is proposed in this study, which molding VFD HVAC unit by utilized three artificial intelligent control strategies, comparing them with the model of the conventional HVAC system, and evaluating the energy consumed by each model. Finally, the obtained simulation results will be validated with measurement results.

1.6   Research Aims and Objectives

The main objectives of the thesis are:

- To build a residential thermal model for two identical houses located at KFUPM campus using Matlab/Simulink software.

- To simulate the model of a house integrated with ON/OFF cycle air conditioning unit.

- To integrated the model of the house with three different models of VFD air conditioning (PID, FLC, and PI with PWM).

- To evaluate the amount of energy consumption of ON/OFF cycle unit, and VFD unit.

- To measure and analysis the amount of the energy consumption using LabView platform.

- Validate the amount of energy consumption obtained by simulation with the real measured energy consumption.

- To compare the energy savings from the simulation and the measured data and choose the suitable control strategy of VFD unit that provides more energy savings.

1.7   Scope of the Thesis

In this thesis, the scope of the experimental and the simulation work will be undertaken in the following development stages:

- Study of the air conditioning system based on three different control techniques of VFD.

- Matlab/Simulink simulation program is used to simulate house thermal model that integrated with ON/OFF cycle and VFD (PID, FLC, and PI with PWM) HVAC systems.

- LabView platform is used for instrument interfacing to measure the general forecast weather for the houses at KFUPM campus.

- Compare the energy savings of house thermal model with ON/OFF cycle and VFD HVAC system using (PID, FLC and PI with PWM).

1.8   Thesis Structure

The thesis is comprised of eight chapters. A brief summary of each chapter is described next.

Chapter 1 presents a background overview of basic idea of this work and states the statistical data for energy consumption of HVAC systems in residential area in KSA. Additionally, the basic objectives and the scope of the study have briefly discussed along with the thesis outline.

Chapter 2 gives the literature review from previous research studies about house thermal model and control techniques models of the HVAC system.

Chapter 3 provides the flowchart that shows the whole project process. It addresses the HVAC system configurations, defines the specification of the heat and cooling characteristics, discusses the load profile of the house and the general project data are also stated in this chapter.

Chapter 4 covers the mathematical thermal model development of a house and HVAC systems; and the ON/OFF HVAC simulation approach.

Chapter 5 gives a comprehensive explanation of VFD's operation. It will discuss VFD's model with HVAC system and how the energy can be saved by using variable frequency compressor for air conditioning systems.

Chapter 6 develops and investigates project monitoring & measurement system. However, the utilized sensors for the experimental work are presented as well.

Chapter 7 discusses and compares the results of the simulation and the experimental work. It will present the energy savings.

Chapter 8 illustrates the significant outcomes of this thesis and conclude it by offering several recommendations for further work.

CHAPTER 2

LITERATURE REVIEW

2.1   Introduction

The literature is rich with thermal house and air conditioning models. Nowadays, modelling and simulation are significant techniques for overcoming some design problems in several branches of engineering. Since this work is concerning about the modelling, design, and validation of the HVAC controllers, as well as developing the thermal house model. Chapter 2 gives a brief literature review of the published articles are stated below.

2.2   Thermal Model of Residential Sector

Models of thermal house properties, especially heat-cooling load of the house and its energy consumption as well as the global warming have been the main matter of several research papers he last twenty years. Those articles are considering a very useful to make this literature more valuable references.

A simple physical based model of thermal heating has been studied to assess the electric and heat energy consumption of residential HVAC system [5]. By using Matlab software researchers have implemented the model for several scenarios to present the impact of various technology

adoptions to be evaluated. Beside that they made a comparison and validation between their obtained results and the actual metered data of the residential load. Specific equipment and some regulation in developing energy and thermal performance of houses and HVAC system have achieved in [6]. They have built a mathematical model application for office buildings to test its toughness, also their obtained results have compared with changing of several locations.

By using Matlab/Simulink software, HVAC model of building has been proposed in [7] to predict the variation of the temperature inside the building and assume the amount of energy needed to achieve the comfort level. They used the building energy simulation test of (IEA) "International Energy Agency" to validate their model result. Also, the model they have developed was less computational and simpler. A highly aggregated accurate model and control of air conditioning loads for cooling demand has built based on a general second order equivalent thermal parameter [8]. They validated their model and the control strategy through realistic simulation utilizing GridLAB-D. The simulation results illustrate that the presented model can manage a very large number of space conditioning to give several damned response services.

An optimal control strategy for HVAC system in building energy management has been proposed to keep the building's indoor environment with high energy efficiency [9]. They used intelligent control strategy MOPSO "Multi-Objective Particle Swarm Optimizer" to calculate the energy dispatch for HVAC equipment. The result shows that using (MOPSO) optimizer for keeping the indoor comfort and energy saving is more effective. Also, they compared the simulation result with (CAV) (constant Air Volume) system and non-optimized (VAV) Variable Air Volume system. The proposed MOPSO has shown more capable of saving energy in building under the same environmental condition. The influence of the thermal insulation on the

thermal energy demand of a passive house in the Arabian Gulf area has been presented in [10]. They compared the yearly cooling demand from simplified (GSAS) "Global Sustainability Assessment System"; also they have found that the discrepancies in predicted yearly cooling demand between the simplified and detailed models did not exceed 15% for both static and dynamic operations of the passive house. A sensible heat transfer modeling for energy optimal control of a residential space conditioning system has been presented [11]. They made a comparison between the energy efficiency and thermal comfort under the different schemes. They found out that there is no big difference in energy consumption between the control schemes; therefore the proportional control is advantageous to the two position control for the thermal comfort.

Implementation and evaluation of physically based electrical load models for HVAC system has been conducted and tested in [12]. All these models were based on energy balances between the house constructive elements, the internal air, the conditioner appliances, and the external environment through discrete state-space equations. They have compared their data collected for one year in different locations and for different load performances with the simulated results.

The concept of using simulation as a tool for performance validation and energy analysis of HVAC systems has been presented in [13]. They described one way of making use of this new technology by applying simulations, configured to represent optimum operation; to monitor data. The idea is to use simulation predictions as performance targets with which to compare monitored system outputs for performance validation and energy analysis. They presented the

results from applying the concepts to a large dual-duct air-handling unit installed in an office building in San Francisco.

2.3   Electrical Model of HVAC System

Nowadays, the world demand for HVAC equipment is going up by 6.2% per year, reaching a total of $93.2 billion in 2014 [14]. Space-conditioning equipment will continue to overtake heating equipment globally with increasingly hot weather conditions. The increasing the demand for cooling equipment is leading to an increase demand of energy consumptions. Therefore, modeling of HVAC systems is gaining more interest for system performance assessment as well as energy saving. Modeling and simulation techniques for HVAC system design and analysis could be categorized with respect to the issues they are meant to deal with, such as desired comfort level and the amount of energy saving. This section reviews a brief survey of the electrical models, which are implemented by using several tools to run the HVAC systems.

Some of ASHRAE publications reference like the VFD's for residential system, presented different models of using variable frequency driver for HVAC system. Variable frequency operation of the compressor and blower in central space- conditioning system enables the system to match the compressor speed to match the cooling capacity of the cooling load of the residence. The airflow rate is proportional to the speed of the air blower. The airflow rate is varied in tandem with the capacity, maintaining dehumidification capacity and taking advantage of the speed cubed power law. The resultant of using variable frequency drives in the HVAC system is to increase the Seasonal Energy Efficiency Ratio (SEER) by 30%-40% compared to a conventional HVAC system with ON/OFF cycle capacity control, which reflect on electric energy saving [15].

VFD system can provide energy saving benefits, and it goes beyond energy saving, it enable to improve and enhance thermal comfort control and reduce the noise levels of the blower. Energy saving technologies for inverter HVAC system have been reviewed in [16]. They have presented the technology trends and the latest energy efficient technologies for compressor motor and power converters. Most applications of VFD systems involve variable torque loads such as fans and centrifugal pumps where the load power varies as the cube of the speed are discussed in [17]. Performance tests of VFD systems are planned to measure efficiency of the VFD units and the efficiency of the involved motor. On the other hand, the real benefit of VFD systems is the reduction of energy used to provide the quantity of end product (fluid or air) of the pump or fan. Therefore, many HVAC manufacturing companies have applied their motors to operate at 80% nameplate rating at rated speed. This means that the required hp per speed is now 80% of motor nameplate rating and the cubed curve effect. In fact, a 100 hp motor is operated at 80 hp for rated speed. Other operating plans will call for a new set of motor ratings for various speeds. Maximum savings of using VSD systems will occur where maximum times are spent operating at speeds that range below the 75% level for many hours per year. Most of the researcher's development branch of the industrial sectors focused on energy savings technology and promoted the development of high efficiency products.

One of the devices used in the VSD is brushless DC motor in compressor due to high efficiency through wide range of motor speed. The actual motor positions to commutate the motor current adequately. Depending on the inability of the hall position sensors to work well due to high temperature environment of refrigerants, sensor-less control patterns play an important part in the applications of inverter fed BLDC compressors [17]. They analyzed the sensor less circuits with many details to find the best design rules of the parameters for several compressor motors.

In addition, they limited the sensor less control circuits to improve a practical operation controller for BLDC compressors.

A dual mode control strategy for BLDC motor drivers with power factor correction (PFC) were proposed to use in high efficiency compressor applications in [18]. They developed modern control strategies "Pulse Amplitude Modulation" PAM mode and "Pulse Width Modulation" PWM mode with reduced switching frequency for efficiency optimization of the compressor motor drive to maintain a constant V/Hz ratio with specified current ripples. Based on their control system, innovative PWM control structures can be developed to improve the inverter efficiency and reduce the motor audio noise by controlling the PWM duties to achieve specified phase current profile. Modeling the induction motor with a variable frequency drive were presented in [19]. They simulated and analyzed the performance of the model using MATLAB/SIMULINK. The model achieved the control of the speed of the induction motor from zero to the nominal speed by varying the frequency of the applied ac voltage using pulse width modulation method.

2.4 Air Conditioning System Control

The early presented publications were dealt with HVAC system models. Controlling air conditioning can be achieved by utilizing a number of advanced control techniques such as proportional–integral–derivative controller (PID controller) and Fuzzy Logic Controller (FL controller). A brief overview about PID controller and FL controller, and review several published papers that have studied similar research methodologies for their HVAC system. The main components of the HVAC system are evaporator coil, blower fan, compressor and condensing coil. Figure 2.1 shows the schematic diagram of the HVAC system cycle.
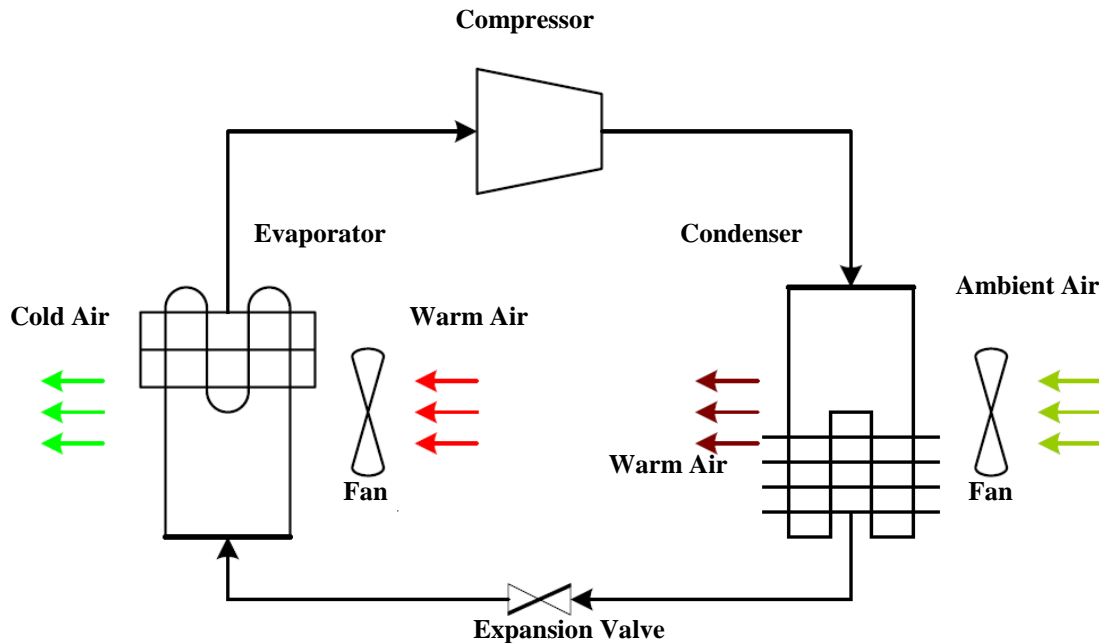
Figure 2.1 Schematic diagram of a typical air conditioner cycle

- **Evaporator** - Heat is absorbed to boil the liquid at a low temperature, and then a low pressure must be maintained in this section.

- **Compresso**r - The compressor works on the system to increase the pressure from the evaporator which draws in a low pressure, a low temperature, and a saturated vapour and to the condenser which delivers a high pressure and a high temperature vapour.

- **Condenser** - The high pressure, high temperature (superheated or saturated) vapour that enters the condenser has heat removed from it. Then the condenser is changing it back into a liquid phase.

- **Valve** - The high pressure liquid from the condenser is expanded through a valve, allowing its pressure to drop in the evaporator. The evaporator then again passes to the compressor in which its pressure is again increased and the whole cycle is repeated.

2.4.1 PID Controller

Most of the control systems over the entire world are operated by utilizing PID controller. Moreover, PID controller is used for a very wide range of issues such as motor drivers, automotive, instrumentation and process controlled. The PID algorithm is related the control signal supplied to the inverter to the error between the value of the set point temperature and the monitored temperature. PID is represented by the following equation [20-21].

$$u(t) = K_p e(t) + K_i \int_0^t e(t)dt + K_d \frac{de(t)}{dt} \tag{1.1}$$

The control variables are a sum of the following three terms: P-term is proportional to the error, the I-term is proportional to the integral to the error and the D-term is proportional to the derivative of the error. First, to use the proportional term only, one variable is needed which the proportional gain K_p for the control system meets the desired dynamic behaviour. Secondly, to use the proportional gain plus the integral gain (PI) controller, or proportional gain plus the derivative gain (PD) controller requires selecting two variables K_p and K_i or selecting K_p and K_d, to use (PID) controller all the three variables have to be chosen K_p, K_i and K_d. Figure 2.2 is illustrating process the PID controller.

Some of the recent published papers have proposed a PID, PI, and PD controllers to control their HVAC system. PI control implementation for building air conditioning system has proposed in [20]. They have used the PI controller to control the speed of the air conditioning compressor to match the cooling load inside the building as well as to have a higher energy efficiency with obtain the desired thermal comfort level. The experimental part has conducted and found that the

16

PI technique provides better temperature control with more energy efficiency compared to the conventional ON/OFF controller. Indoor temperature control and energy savings of a space-conditioning system utilizing PD controller is proposed in [21].The proposed ON/OFF controller and PD controller to monitor the energy consumption of a different controller is conducted. The emulation of the energy used shows that PD controller can provide higher energy efficiency compared to ON/OFF cycle. A study of potential electricity savings by using "Variable Speed Compressor" (VSC) for air- conditioning system is presented in [21].They used PID controller for air conditioning system. The simulation results shows that using PID controller with VSC gives the highest energy saving while having variable load condition, PD controller offers the best option.

One of the methods that has been suggested and investigated to maintain thermal comfort of an environment room and to reduce energy consumption from an air-conditioning unit is through the use of well-tuned controller for the air handling unit and variable speed compressor (VSC). This involves the development of various types of controller either for AHU or the compressor system. Among many control methods for HVAC application, the PID algorithm is very common. For example, the researchers reported the behaviour of the proportional and integral constants in combination to provide responsive, stable, and controlled in the HVAC system, [22-23]. Three-way bypass valve was used in this study and the results were validated for valve controller application. They developed and evaluated software package for self-tuning of three-term Direct Digital Control (DDC) using a searching technique for optimization. A simulation model for a practical air-handling system was studied the behaviour under a conventional system of PID controllers. A new controller based on system identification model was developed and

tested where input and actuating variables were incorporated into the system identification model . Their model could predict the new system status based on the past records and suggested the optimum control actions. Computer simulation had proved that such system identification based controller is superior to the conventional PID controller in at least three major aspects which adaptation to system change, response rate and energy conservation. The result of the study has not been tested for variable speed compressor and may be valid for only AHU controller mechanisms [24].
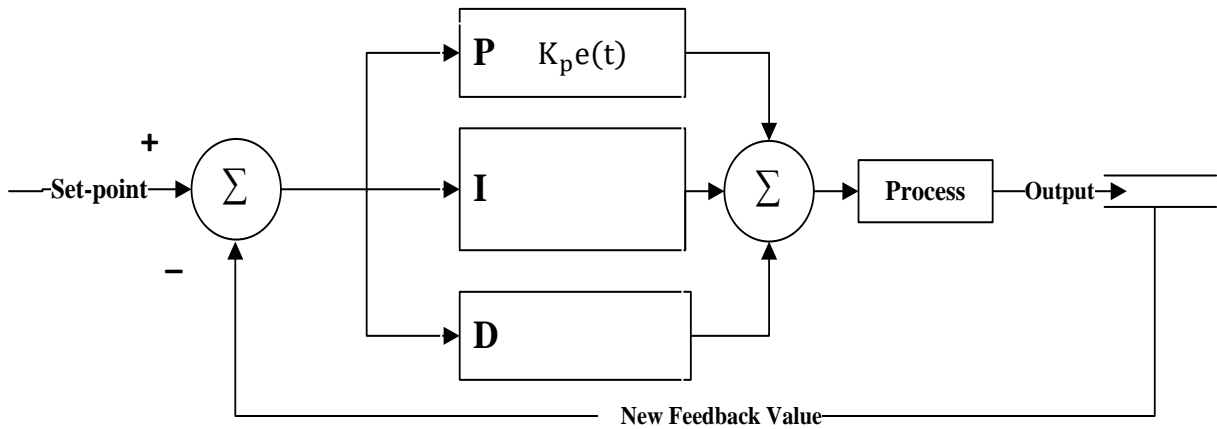
Figure 2.2 Block diagram of a PID controller

2.4.2 Fuzzy Logic Controller

Fuzzy Logic Control (FLC) originally is identified and set forth by Lotfi A. Zadeh in 1965. Fuzzy logic control is the one of the most powerful controller which can control non-linear system because of it non-linearity characteristic behavior. Fuzzy logic control is one of the intelligent control systems that are successful solution to many control problems. Figure 2.3 presets three basic processes of fuzzy logic controller [25].
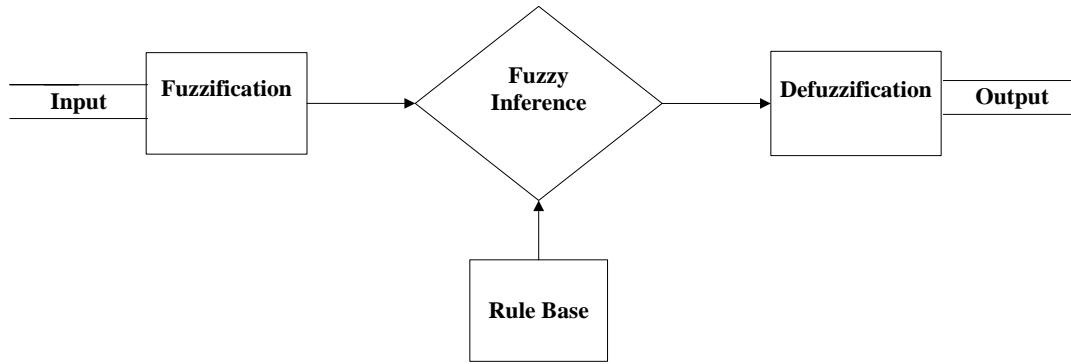
Figure 2.3 Main parts of fuzzy expert system

First process is fuzzification which defined as a process of mapping crisp numbers in the input data matrix to the fuzzy sets. Then there will be membership functions which play the major role during this process by mapping each input value to a degree of membership between 1 and 0, membership functions such as gaussian distribution, triangular, trapezoidal, sigmoidal functions and bell functions). Second process is fuzzy inference system which maps a fuzzy set into a several fuzzy set using logical operations and fuzzy rules. Furthermore, fuzzy rules are just like IF-THEN statements and they can be obtained by professionals or generated from the available numerical data using computing techniques (software) and evolutionary algorithms. Fuzzy inference systems have two principle types of Sugeno fuzzy inference and Mamdani fuzzy inference. Mamdani type is mostly accepted and more used while Sugeno type is especially used for dynamic non-linear systems.

Defuzzification process produced the aggregate linguistic which the output value can be derived from the former processes input of defuzzification. The main point is to have a single crisp value as the output that we are getting from the final process. In other words, fuzzy logic can demonstrate the thermal comfort linguistically and, moreover, can characterize the thermal comfort levels rather than temperature or humidity levels which result in improved thermal

comfort. There is different control methods obtained based on fuzzy logic control and they are briefly explained hereafter. First method is the fuzzy P controller which a technique used for fuzzy logic control that used in closed loop control. The inputs to the controller are derived from the process of measurements and the output of the fuzzy logic system is used to control the process. This process considered as a pure fuzzy logic system that indicated as fuzzy P controller [26]. Second method is the PID fuzzy controllers; they categorized it into two main types. The first type is fuzzy logic controller, which realized as a set of heuristic control rules. The second type is referred to PD or PI fuzzy controller, it comprises of a conventional PID controller in conjunction with a set of fuzzy reasoning mechanism and fuzzy rules to tune the PID gains online. Fuzzy logic control application to buildings is effective and suitable for non-linear system control [26]. If the fuzzy rules are designed to be more robust, fuzzy controllers can enhance the disturbance response by reducing undershoot and overshoot present in the controlling variable. On the other hand, in [27] the researchers utilized this technique to control discontinuously occupied buildings. Many other researchers have been working on the application of only fuzzy logic to control the thermal comfort of buildings [28]. They presented fuzzy logic based energy saving technique for a central air conditioning system. In [29] studied the development of a PID fuzzy controller for indoor temperature control consent to energy resources management in buildings. Moreover, the use of fuzzy PID, fuzzy PD and adaptive fuzzy PD for controlling thermal visual comfort and indoor air quality are presented in [29]. One of their main objectives was to reduce the energy consumption. Furthermore, fuzzy logic control of air-conditioning system in residential buildings or efficient energy operation and comfortable environment are investigated in [30]. The simulation has been done and fuzzy controller results are compared with conventional PID control. It was found that the proposed control strategy satisfies the load

and at the same time achieving the comfort zone, as defined by the ASHRAE code. It has been demonstrated that fuzzy logic controller makes the HVAC system more efficient and consumes less energy than the HVAC controller by PID control. The development of an algorithm for air condition control system based on fuzzy logic control to provide the conditions necessary for comfort living inside a building and reduces energy consumption has been discussed by [31]. They used MATLAB/Simulink to conduct the simulation of the controlling air conditioning system. Fuzzy logic control was developed to control the compressor motor speed and fan speed in order to maintain the room temperature at or close to the set-point temperature.

2.4.3 Summary

Variety of control methodologies employed in the control of building temperature and energy usage were reviewed in this chapter. At the beginning of this chapter different building control strategies and intelligent techniques were presented. Classical control methods are still the first choice in building control today, while advanced and intelligent methods are gaining more attention. The types of control systems and their advantages and limitations are listed and summarized in Table 2.1.

 In summary, the use of classical controllers is because of their low initial cost and simplicity of implementation. However, they admit high maintenance cost and higher energy consumption. Further, they cannot be used in MIMO systems efficiently. Advanced control methodologies could be an alternative approach in building control. These techniques require a good quality dynamic model of the building and they exhibit non-linear characteristics. HVAC systems are non-linear and time delayed processes, advanced control methods can handle them more smoothly than conventional methods. In intelligent control, no mathematical model is needed

and it is solely based on the human perception of the thermal comfort. Hence, it can provide improved thermal comfort to the occupants. Further, these controllers can be used to upgrade the existing traditional controllers [32].

Table 2.1 Advantages and limitations of building cooling control strategies

Control Strategy	Advantages	Limitations
On/Off Control	Low initial cost, simple structure, fast response, feedback type.	Accepts only binary inputs, often incapable of tracking the set-point accurately and hence could be inefficient, not versatile and effective in the long run.
PID control	Feedback types, derivative term, combat with sudden load changes in the system.	Little measurement and process noise can cause large variations in the output due to derivative term, energy inefficient, tuning is time consuming.
Fuzzy control	Non-linear control method and can be applied to HVAC systems effectively, high accuracy, rapid operation, increased energy savings, and cost effective.	Can use only a limited number of input variables, development of optimal number of fuzzy rules and determination of the membership function parameters are not straightforward.

2.5   Lab View Module

As the most popular workbench of virtual instrument, LabView has been widely used with graphical design and rich function. A monitor system of real-time data acquisition, processing, display, save is constructed based on LabView application. In this section, the literature survey

on the application and the fundamentals of data acquisition system for the thermal house and air condition system will be discussed.

Thermal model of building has a special importance for assessment and online evaluation since the air conditioning load is consistently varying, the efficient energy consumption became a priority. Monitoring and controlling process variables such as temperature, pressure, air flow and level control in HVAC system are built using LabView [32]. The corresponding values are measured and converted into digital signals using NI-DAQ and these are controlled in Lab View. A temperature measurement module using DS18B20 digital temperature sensor is developed to work as a standalone system [33]. The module is compared with other conventional temperature sensors used in space applications. A set of software by LabView language was compiled. The program is operated in a circular manner and automatically. Temperature measurement and control system for constant temperature reciprocator platelet preservation box is designed based on Fuzzy-PID control [36]. The humidity and temperature monitoring system in ammunition storehouse was very important to the quality of ammunition during storage time [37]. They improved the management efficiency of the storekeepers in storehouse, and by designing a monitoring system based on LabView. Developing a system to record and analyze parameters like wind speed, wind direction, pressure and temperature using LabView was reported [38]. Interfacing is done using data acquisition system. In addition, current and voltage from utility feeder were also monitored to measure power consumption and power factor. Based on the improved traditional steady-state method which combined with LabView virtual system in measuring of the thermal conductivity of poor conductor, the minutely monitoring of temperature on the two surfaces of a sample was realized in [39]. A multifunctional virtual

power quality monitoring system was designed and implemented in LabView environment [40]. The root

means square (RMS) value, the waveforms of three phase voltage and current, the harmonic components, the total harmonic distortion (THD) and S-transform analysis waveforms of the three-phase voltage and current signals can be calculated and displayed in the system. In this thesis, a performance monitoring and experimental test system for measuring metrological parameters and electrical parameters for HVAC system is proposed. Automatic data acquisition, DAQ, technology made by National Instrument (NI) is used as hardware for monitoring the HVAC system performance. The software of the data acquisition system based on LabView package is used to display, store, and process the collected data in the PC-hard disk

CHAPTER 3

METHODOLOGY

3.1   Introduction

In the modern era, HVAC system models require further enhancement to meet the new difficulties and obstacles that can improve the energy savings for the HVAC system in the residential area. In this thesis, a very comprehensive thermodynamic model for the house is presented with all the heating /cooling system characteristics and physical factors of the house taking to account the enhanced model and simulation capabilities.

This chapter provides the information of the research methodology to develop the thermal load heat model for the house. It includes stages such as flow of the process. Moreover, it describes the load profile of the house and the general project data input. Figure 3.1 illustrates the flowchart of the research development.

3.2   Flowchart of the Research Development
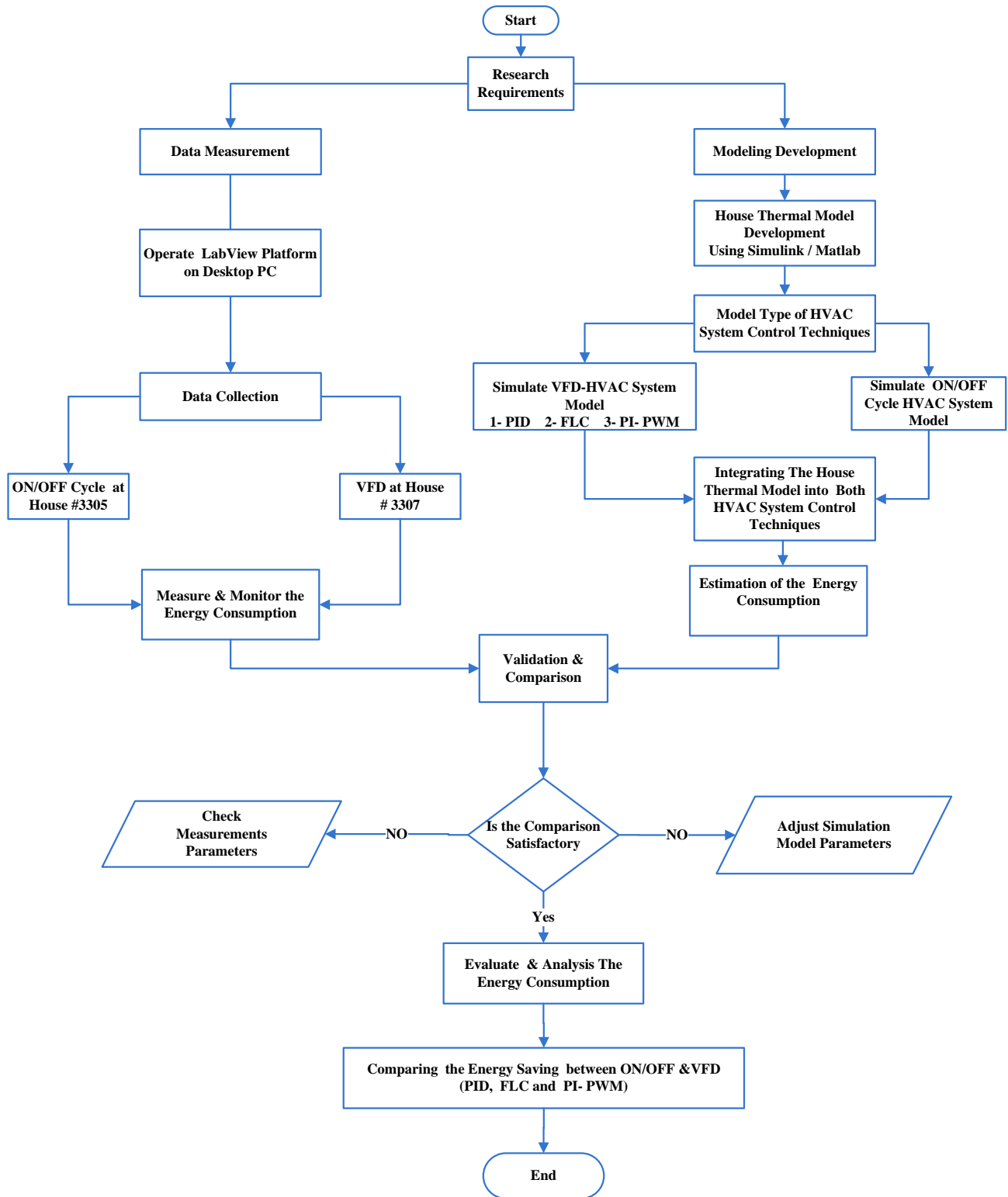
Figure 3.1 Flowchart of the research development

3.3   Development and Approach

In recent years, the need of thermal house models has increased in several fields of the energy saving studies. The major challenge of modeling the thermal properties of houses is the effect of climate on the indoor temperatures. For example, solar gain, wind, and outdoor environment temperatures have a greater impact on indoor environment temperatures than any other individual air vent register. Moreover, it is difficult to develop a model that totally captures the influence of climate on indoor temperatures due to outdoor climate conditions constantly change and rarely repeat. Therefore, the difficulty of attributing the influence on climate conditions on indoor environment temperature makes it hard to isolate the impact of the state of any particular air vent register on the indoor environment temperature. The aim of this work is to model and simulate two different heat load models (ON/OFF) cycle and variable frequency driver air conditioning systems with three different control techniques (PID, FLC, and PI-PWM) of a house located in Dhahran area at KFUPM campus and compare the thermal comfort and energy consumptions between these two models using Matlab/Simulink.

3.3.1 House Heat-Cooling Load Model

There are three categories to define thermal house load characteristics, space, room and zone. Group of rooms, or a partitioned room, or a site without partitioned, or a volume is called a space. Portioned space is mostly considered as a single load is called a room. Several rooms of unites of space having similar operating conditions is called a zone. A zone may be or may not be closed space, or it may comprise of many portioned rooms. The heat gain of conditioned space can be classified into three categories which are presented in the following section.

3.3.2 Definition of Heat

Transferred energy due to temperature variance is defined as heat. It simply passes energy from a warm object to a cold object. In addition, it is the flow of energy from a high temperature body to a lower temperature body. System international (SI) unit of the heat flow described as Watt, which is 1 J/s of flow. Measuring the capability of a material, or any thermal system, to pass heat energy to other thermal system is called temperature. Btu and Calorie are other definition heat energy where are amount of heat needs to raise 1 gram of water by 1°F, 1°C, or 1K respectively. Required the amount heat energy to increase the temperature is described by:

$$Q = c_p m \Delta T$$

(3.1)

The produced work can be expressed by

$$W = FL \qquad\qquad (3.2)$$

Or by $\qquad\qquad\qquad\qquad W = PAL \qquad\qquad (3.3)$

which are the mechanical work applied by pressure and volume respectively [41].

Where,

Q   Amount of heat   (kJ)

c_p Specific heat (kJ/kg.K)

m   Mass (kg)

ΔT Temperature difference between hot and cold side (K)

W Amount of mechanical work (Nm), (J), which 1 J = 1 Nm

F   Applied force (N)

L Length or distance moved (m)

P   Applied pressure (N/m2 (Pa))

A   Pressurized area (m2)

3.3.3 Types of Heat

- **Sensible Heat**: If heat is added or removed, it changes the temperature of the material.

- **Latent Heat**: if heat is added or removed, it does not change the state of the material.

- **Superheat**: once the liquid has change completely into vapor, adding more heat will increase the temperature.

- **Sub-cooling**: once the vapor has changed completely into a liquid, removing more heat will decrease the temperature.

- **Gas Laws**: if you compress a gas to reduce its volume, both the temperature and the pressure will increase, if you expand a gas to increase its volume, both the temperature and pressure will decrease.

3.3.4 Heat Transfer

Three different ways of heat transfer to manage transferring the heat through or between substances. Convection, conduction, and radiation are the heat transfer mechanisms. Figure 3.2 illustrates the basic heat transfer mechanisms.
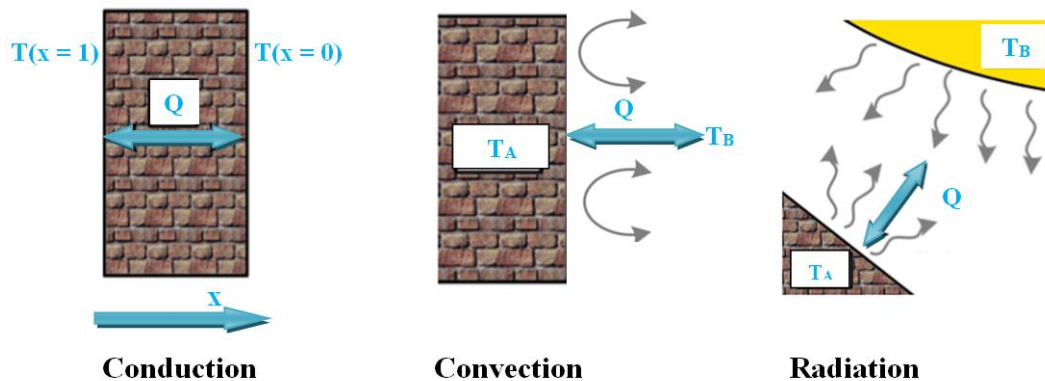
Figure 3.2 Heat Transfer Mechanisms

▪ Conduction

Conductivity of the thermal is defined as the heat energy flowing through a piece of material per second which is 1 meter in length, 1 m^2 in cross sectional area and has a temperature difference of 1°C between its each end.

$$Q_{cond} = k \times \frac{A}{D} \times (T_A - T_B) \tag{3.4}$$

Where,

Q_{cond} Heat energy flowing through the material (Conductive heat flow) (*Btu/hr*)

A   Area of the material through the heat flows (*m^2*)

D   Desistance between the layers or the length of the material through the heat flow (*m*)

T_A Temperature at face two, the higher temp (*°C*)

T_B Temperature at face one the lower temp (*°C*)

k   Material thermal conductivity (W*/m °C*)

Conductivity of the thermal of the substance (Silicon) S.I, units of k rearranging the equation making k the subject expressed as

$$k = \frac{QD}{A(\Delta(\Delta} \tag{3.5}$$

Unites are   (Joules meter) / (Secondsmeter^2 (Kelvin)) = (Joules) / (Seconds meters (Kelvin)) = Watts/ meter (Kelvin)

▪ Convection

Heat is Transferring between a solid surface and other movement substance (gas or liquid) is termed as convection heat where rating heat flow depends on moving temperature substance and on its flow rate.

$$Q_{conve} = k \times A \times (T_A - T_B) \tag{3.6}$$

Where,

Q_{conve} Convective heat flow (Btu/hr)

k   Convection heat transfer coefficient (W/m^2.K)

T_A, T_B Temperature of the bodies (^{o}C)

A   Surface area (m^2)

▪ Radiation

Heat transferring occurs when heat transferred in form of electromagnetic waves [42]. This energy originates from a hot object travels freely during absolutely transparent media. Depending on the surface and its temperature the amount of radiation energy directly effects. The heat transfer function is ruled by the Stefan-Boltzmann law and is defined by the following equation (3.7).

$$Q_{rad} = k \times A \times (T^4{}_A - T^4{}_B) \tag{3.7}$$

Where,

Q_{rad} Radioactive heat flow (W)

k   Radioactive heat transfer coefficient (W/m^2K^4)

A   Surface area (m^2)

T_A, T_B Temperature of the bodies (^{o}C)

All the three thermal mechanisms are considered simultaneously. First considering a wall located among a cold internal and a hot external. From the experience, the wall will be a little cool to the touch, so obtaining a thermal flow from the outer surface wall to the room through the convection and the radiation. The wall itself is conducting heat to the inside surface. Then radiation and convection carry heat away from there. The thermal energy is not being created or destroyed in the wall; the balance equation is presented as following:

$$P_{conv,in} + P_{rad,in} = P_{cond} = P_{conv,out} + P_{rad,out} \qquad (3.8)$$

The resistance values of conduction, convection, and radiation combine like resistors in a circuit, are shown for a conductive wall coupling to inside and outside through radiation and convection. Figure 3.3 shows the equivalent circuit of power heat flow.
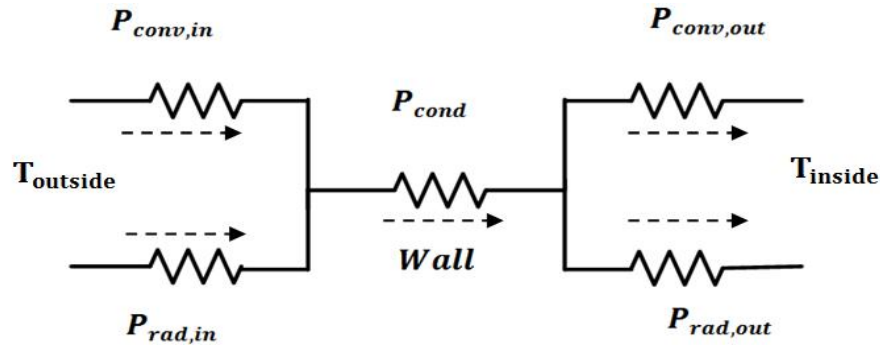
Figure 3.3 Equivalent circuit of power heat flow

3.3.5 Thermal Resistance Network

The principle of thermal resistance can be used to overcome the steady state heat transfer issues that involve series, parallel or combined series-parallel components. Thermal resistance is the resistance of a particular medium or system to flow the heat through its boundaries and depends upon geometry and thermal properties of the medium such as thermal conductivity. Thermal resistance networks are mostly employed in order to analyze steady state heat transfer. Thermal resistance networks have a similar functionality to electrical resistance networks utilized in electrical engineering and allow for easy calculation of the total thermal resistance in a system whether it is composed of resistances in series, parallel or both [43]. In industrial heat transfer issues thermal resistance is often in both series and parallel. For example the heat loss from the contents of an un-insulated tank will have the convective resistance of the tank contents followed by the conductive resistance of the tank walls in series followed by convective and radiative

resistance to the surround environment in parallel. This example is described by the thermal resistances network shown in the Figure 3.4.
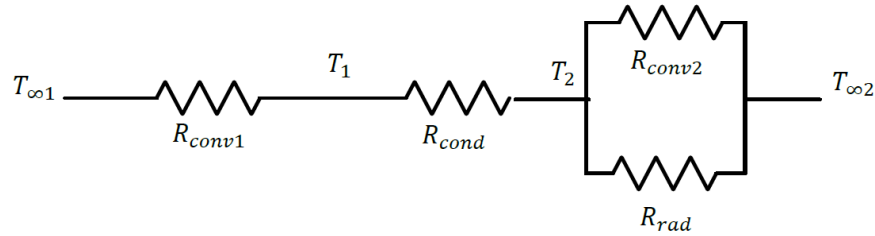
Figure 3.4 Thermal resistances network

Equation (3.9) shows the total resistance is calculated by adding the total resistance for the series segment and the total resistance of the parallel segment.

$$R_{total} = R_{conv1} + R_{wall} + \frac{R_{conv2} \times R_{rad}}{R_{conv2} + R_{rad}} \tag{3.9}$$

3.3.6 Calculation of Thermal Resistances

the design and optimization of industrial equipment are mostly required to determine a steady state temperature at some point along a thermal resistance network, for example, the temperature between a tank wall and the inside of its insulation [43]. Furthermore, to determine these temperatures one must first calculate the thermal resistances.

▪ **Conductive Resistance**

Table 3.1 Conductive resistance equations

Geometry	Resistance Equation	
Plane Wall	$R_{wall} = \dfrac{x}{kA}$	(3.10)
Cylinder Wall	$R_{Cyl} = \dfrac{\ln\left(\dfrac{r_2}{r_1}\right)}{2\pi L k}$	(3.11)
Spherical Wall	$R_{sph} = \dfrac{r_2 - r_1}{4\pi r_2 r_1 k}$	(3.12)

33

To calculate the conductive resistance of some common cases, equations in Table 3.1 will be used.

- ▪ **Convective Resistance**

The heat transfer of convection resistance is calculated by the following equation.

$$R_{conv} = \frac{1}{hA} \tag{3.13}$$

So to calculate the convective resistance the heat transfer coefficient (h) must be calculated first. Many correlations exist to calculate the heat transfer coefficient is depending on of the geometry of the system being considered.

- ▪ **Radiation Resistance**

The heat transfer of resistance radiation is calculated by the following equation (3.14)

$$R_{rad} = \frac{1}{h_{rad} A} \tag{3.14}$$

This allows radiative heat transfer to be easily grouped together with other heat transfer modes when considering total heat transfer for a given system; however the radiative heat transfer coefficient must first be determined.

Where,

R Thermal resistance (K/W)

R_{conv} Thermal resistance for convective heat transfer (K/W)

R_{rad} Thermal resistance for radiation heat transfer (K/W)

R_{cond} Thermal resistance for conductive heat transfer through a plane wall (K/W)

Q Heat flow (W)

T Temperature at a given point (K)

X Thickness of a plane wall (m)

A Heat transfer area (m^2)

K Average thermal conductivity (W/m.K)

r_1 Internal diameter (m)

r_2 External diameter (m)

L Length of a pipe (m)

h Heat transfer coefficient (W/m^2.K)

3.3.7 Combined Thermal Resistances Conduction, Convection, and Radiation

Now we can analyze the problems in which both conduction and convection occur, starting with a wall cooled by flowing air on each side [44]. A description of the convective heat transfer can be given explicitly as:

$$\frac{\dot{Q}}{A} = h_1(T_w - T_\infty) \tag{3.15}$$

This is representing a model of a plane wall with internal cooling. Figure 3.5 and equation (3.16) present the configuration of roof/wall/window section.
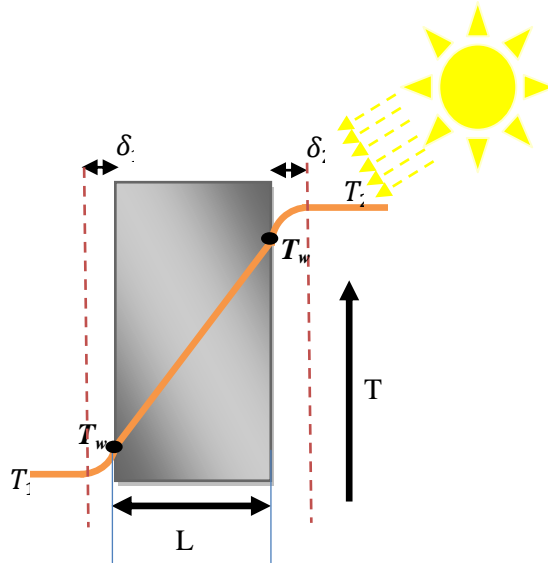
Figure 3.5 Conducting roof, wall and windows with convective-conductive heat transfer

$$\frac{\dot{Q}}{A} = h_1 (T_{w1} - T_1) \tag{3.17}$$

The heat transfer from outside air to wall/roof/windows is combined of convective and radiative resistances which are connected in parallel $R_{conv} // R_{rad}$ and it is given by (3.18) which is presented the heat flow:

$$\frac{\dot{Q}}{A} = (h_2 + h_{rad})(T_2 - T_{w2}) \tag{3.18}$$

Across the wall, we can get the heat transfer from outside wall to inside wall as a conductive heat by equation (3.19).

$$\frac{\dot{Q}}{A} = \frac{k}{L}(T_{w2} - T_{w1}) \tag{3.19}$$

The quantity $\frac{\dot{Q}}{A}$ is the same in all of these expressions. Putting them all together to write the

known overall temperature drop yields a relation between heat transfer and overall temperature

drop $(T_2 - T_1)$.

$$(T_2\text{-}T_1) = (T_2\text{-}T_{w2}) + (T_{w2}\text{-}T_{w1}) + (T_{w1}\text{-}T_1) = \frac{\dot{Q}}{A} = [\frac{1}{h_1} + \frac{L}{k} + \frac{1}{h_2 + h_{rad}}]$$ (3.20)

We can define a thermal resistance, R_{total} as before, such that

$$\dot{Q} = \frac{(T_2 - T_1)}{R_{total}}$$ (3.21)

$$R_{total} = [\frac{1}{Ah_1} + \frac{L}{Ak} + \frac{1}{A(h_2 + h_{rad})}]$$ (3.22)

Where, R is given by:

Equation (3.22) is reflected the thermal resistance for a solid wall with convection heat transfer on each side

For a plane wall in a house model, inside house temperature is a critical consideration. In terms of Figure 3.5, T_2 is the out-house temperature and T_1 is the in-house temperature. We wish to find T_{w2} because of the highest temperature to the outside surface house (walls, roof or windows) and the inside surface house temperature of T_{w1}. From equation (3.23), the outside surface temperature can be written as:

$$T_{w2} = T_2 - \frac{Q}{A(h_2 + h_{rad})} = T_2 - \frac{(T_2 - T_1)}{A(h_2 + h_{rad})}]$$ (3.23)

Using the expression for the thermal resistance, the wall temperatures can be expressed in terms of heat transfer coefficients and wall properties as

$$T_{w2} = T_2 + \frac{(T_2 - T_1)}{\dfrac{(h_2 + h_{rad})}{h_1} + \dfrac{(h_2 + h_{rad})}{k} + 1} \qquad (3.24)$$

Similarly, we can get T_{w1} by:

$$T_{w1} = T_1 + \frac{(T_2 - T_1)}{\dfrac{h_1}{h_2 + h_{rad}} + \dfrac{Lh_1}{k} + 1} \qquad (3.25)$$

Equation (3.24) provides some basic design guidelines. The goal is to have a value of T_{w1} close to desired temperature inside house. This means h_1 should be large, k should be small and L should be large (which mean using many layer for insulation). One way to achieve high insulation in buildings to utilize many layers shield with high h_1.

3.3.8 Thermal Model of the House Using Three Layers for Roof and Wall

In this study, a comprehensive heat model of the house is developed by using three layers for both roof and wall. Furthermore, in most climates, insulation is needed on all sides of a house: under the slab or lowest conditioned floor, at the basement walls, at the above-grade walls, and at the ceiling or roof. Because different insulation materials are good at doing different things, it makes sense to choose insulation based on the job it has to do. Heat flow is only part of the equation; moisture, air leakage, and drying potential are also important considerations to develop the thermal model for the residential house.

Figure 3.6 gives a very clear indication of how we can find the temperature at each desired point at surface or center of plaster, concrete, outside wall plaster or stucco. This will help us to calculate the suitable material with its thermal conductivity (k) and the appropriate thickness (L). The thermal model components for second order heat system are explained in details. The aim of

this section is improve the parameters such as type of building materials and thickness depending on the desired temperature in house. This means that at any instant the model able to represent the thermal aspects of a building in its present condition.
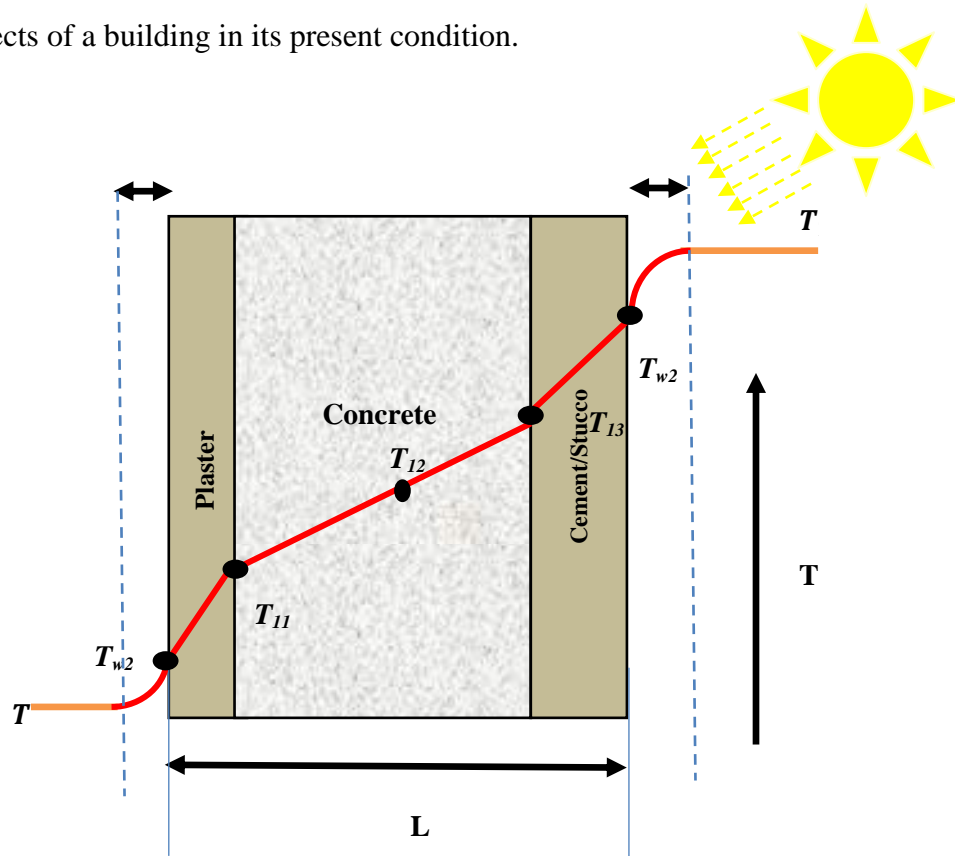
Figure 3.6 Conducting roof and wall with three layers and convective-conductive heat transfer

3.4   House Heating-Cooling Loads

3.4.1 Space Air and Equipment Loads

The cooling load (or heat gain) is the amount of heat energy to be removed from a house by the HVAC equipment to maintain the house at indoor temperature when worst case outdoor temperature is being experienced [45] . There are some classifications of the sensible and latent heat transfer among the space air and surroundings which listed as following:

- Space heat gain (Btu/h or W) gain either from an external sources or form internal source during a given time.

- Space cooling load (Btu/h or W) is the rate at which heat must be removed from the space to keep the comfort of the air temperature and relative humidity.

- The sensible cooling load is equal to the sum of the convictive heat transfer from the surface of the house envelope, furnishings, occupants, appliances, and equipments.

- Space heating load (Btu/h or W), which heat must be added to conditioned space to maintain the comfort level and relative humidity a constant.

- Space heating extraction rate (Btu/h or W) is the rate which heat is removed from the conditioned space by the air system.

- The heating coil (Btu/h or W) is the rate that is added to the conditioned air space from the hot water, steam or electric heating elements inside the coil.

- Refrigerating load (Btu/h or W) is the rate at which heat is absorbed by the refrigerant at the evaporator [45].

3.4.2 Components of Cooling Load

The cooling load can be categorized in two categories: internal and external. The schematic in Figure 3.7 shows the thermal system of the house with the most frequent objects of interest to develop the thermal system analysis for a house.

3.4.2.1 External Cooling Loads

These types of heat energy loads are formed from the heat gain in the conditioned space contributed from the external source such as houses envelope and partitioned walls. Outdoor loads are

- Heat gain from the exterior walls and roof.

- Solar heat gain transmitted through the windows.

- Speed of wind.

- Conductive heat gain.

- Heat gain from the partition walls and exterior doors.

- Infiltration of outdoor air into the conditioned space.

3.4.2.2   Internal Cooling Loads

There are several sources that contribute to internal cooling loads.

- Number of people living in a house

- Electric lights

- Equipment and appliances
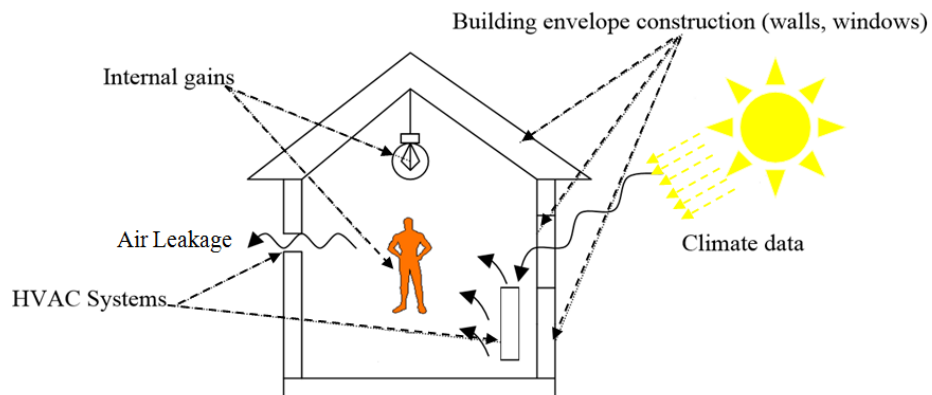
Figure 3.7 House as a thermal system

3.5   Cooling-Heating Equations

Latent , sensible cooling and heating equations are expressed in imperial units [46].

- **Sensible Heat**

The sensible heat in a heating or cooling process of air (heating or cooling capacity) can be expressed as:

$$h_s = 1.08 \, V \, dT \qquad\qquad (3.26)$$

Where

h_s Sensible heat (Btu/h)

V Air volume flow (cfm, cubic feet per minutes)

dT   Temperature different (°F)

- **Latent Heat**

The latent heat due to moisture in the air can be expressed as:

$$h_I = 0.68 \, V \, dw_{gr} \qquad\qquad (3.27)$$

Or
$$h_I = 4849 \, V \, dw_{lb} \qquad\qquad (3.28)$$

Where

h_s Latent heat (Btu/h)

V Air volume flow (cfm, cubic feet per minutes)

dw_{gr} Humidity ratio difference (grains water/lb dry air)

dw_{lb} Humidity ratio difference (lb water/lb dry air)

- **Total Heat - Latent and Sensible Heat**

Total heat due to both temperature and moisture can be expressed as:

$$h_t = 4.5 \, V \, dh \qquad\qquad (3.29)$$

Where

h_t Sensible heat (Btu/h)

V Air volume flow (cfm, cubic feet per minutes)

dh   Enthalpy difference (btu/lb dry air)

Total heat can also be expressed as:

$$\mathbf{h_t = h_s + h_1 = 1.08\,VdT + 0.68\,Vdw_{gr}} \tag{3.30}$$

3.6   Illustration - Heating Air

An air flow of one cfm is heated from 32 °F to 52 °F. Using equation (3.26) the sensible heat added to the air can be expressed as:

$$\mathbf{h_s = 1.08\,(1\,cfm)((52°F) - (32°F)) = 21(Btu/h)} \tag{3.31}$$

 Calculating indoor temperature and humidity loads as following.

Indoor climate is influenced by:

- Sensible and latent heat from people, lights, machines and electrical equipment and industrial processes.
- Pollution and gases from people, building materials, inventory and industrial processes.

The most important sources influencing the indoor climate may be summarized in [47].

1. sensible and latent heat from people
2. sensible heat from lights
3. sensible heat from electric equipment
4. miscellaneous loads

Each point will be described with a mathematical expression.

3.6.1 Sensible and Latent Heat from People

Sensible heat from people is transferred through conduction, convection and radiation also; latent heat from people is transferred through water vapor. The sensible heat can impact on the air temperature and latent heat can impact on the moisture content of air. The heat transferred from people depends on activity, clothing, air temperature and the number of people in the building.

3.6.2 Sensible Heat from Lights

Heat transferred to the room from the lights can be calculated as:

$$H_1 = P_{inst} \ K_1 \ K_2 \qquad\qquad (3.32)$$

Where:

H_l Heat transferred from the lights (W)

P_{inst} Installed effect (W)

K_1 Simultaneous coefficient

K_2 Correction coefficient if lights are ventilated. (1 for no ventilation= 0.3-0.6 if ventilated)

Table 3.2 used to estimate heat load from lights [47].

Table 3.2 The Estimate heat load from lights

Installed effect (W)	Illumination (lux)				
	200	400	600	800	1000
Incandescent lamp	38	75	110	145	180
Fluorescent tubes	15	25	36	48	60

The requirements for lighting levels in the rooms depend on the nature of the work in rooms itself. Table 3.3 shows the normal illumination of rooms.

Table 3.3 The Normal illumination of rooms

Room Activity	Illumination (lux)
Normal work	200
PC work	500
Archive	200
Drawing work, normal	500
Drawing work, detailed	1000

3.6.3 Sensible Heat from Electric Equipment

Heat transferred from electrical equipment can be calculated as:

$$H_{eq} = P_{eq} \ K_1 \ K_2 \tag{3.33}$$

Where

H_{eq} Heat transferred from electrical equipment (W)

P_{eq} Electrical power consumption (W)

K_1 Load coefficient

K_2 Running time coefficient

Carbon dioxide (CO_2) concentration in "clean" air is 575 mg/m^3. Huge concentrations can cause headaches and the concentration should be below 9000 mg/m^3. Carbon dioxide is produced by people during the combustion. The concentration of carbon dioxide in the air can be measured

and used as an indicator of air quality. The respiration and CO_2 generation per person at work conditions are explained in Table 3.4.

Table 3.4 The respiration and CO_2 generation per person

Activity	Respiration per person (m^3/h)	CO_2 generation per person (m^3/h)	Typical Heat Emission
Sleeping	0.3	0.013	80 W
Sitting, quietly	0.5	0.02	120W
Working, moderate	2 – 3	0.08 - 0.13	265W
Working, heavy	7 – 8	0.33 - 0.38	280W

3.7   Load Profile

The load profile is the variation of the space within a certain period, such as 24-hours operating cycle or an annual operating cycle. The load profile may be used to illustrate the load variation of air-conditioned space a room, a zone, a floor, a building or project. The profile's shape rely on the outside temperature, the latitude, and the orientation, structure of the building, the operating characteristics, and the variation of the load, Figure 3.8 shows the load profile of the typical floor.
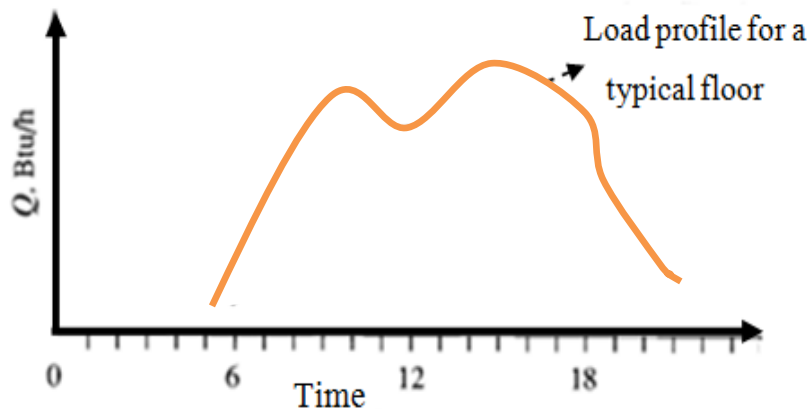
Figure 3.8 Load profile of a typical floor

46

3.7.1 Operation of Load Profile

Heating/Cooling loads are the measure of energy that need to be added or removed from a residence by the HVAC system to provide the desired level of comfort air within a house. The appropriate HVAC system begins with an accurate understanding of the heating/cooling loads on a house. The heating/cooling load calculation results will have a direct contact with the climate change, occupant behavior, and economic status of occupants, physical properties of building and characteristic of heating system.

Figure 3.9 shows the outdoor temperatures which are measured for 24 H's and we can observe the temperature is started around 30℃ and it goes up dramatically to 51℃ at midday, then it drops slowly and reach 35℃ at midnight. The daily house activity loads are displayed in Figure 3.12. It consists of one to three persons are living in the house, fluorescent 400 lux for light, kitchen tools (oven & fridge), computer, monitor, printer, and Wi Fi unit as presented in Table 3.6. Figure 3.10 and Figure 3.11 show the solar and mass heat gain of the house during hot day. The total house activities or the internal heat gain have been calculated based on Table 3.6. The typical house activity is presented in Figure 3.12 which will be used our simulation study [48].
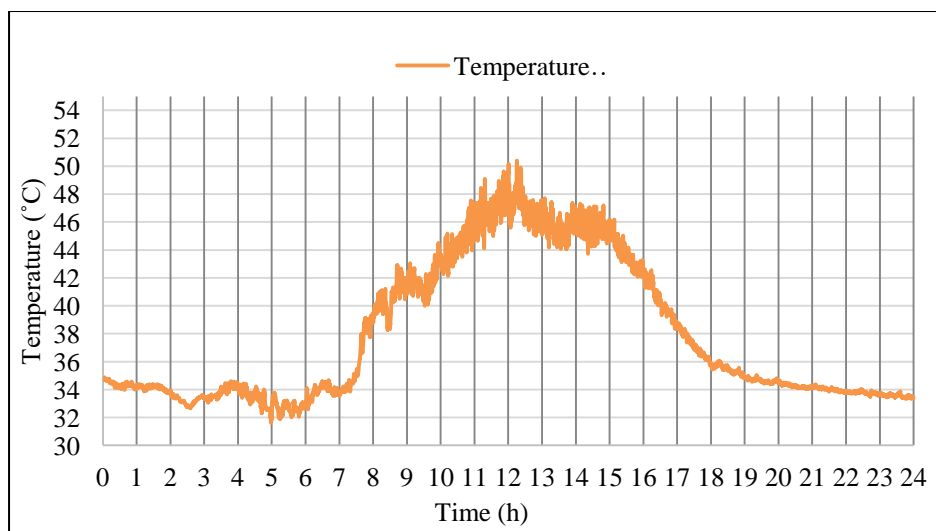
Figure 3.9 Outdoor temperature on 01.08.2016

Table 3.5 Solar heat gain and mass heat gain for warm and hot weather (Btu/h)

Time	Solar Heat Gain (Btu/h)	Mass Heat Gain (Btu/h)
12AM - 6AM	0	1000
6 AM - 12PM	2000	2500
12PM - 6PM	2000	3500
6 PM - 9PM	0	3500
9 PM - 12AM	0	1500
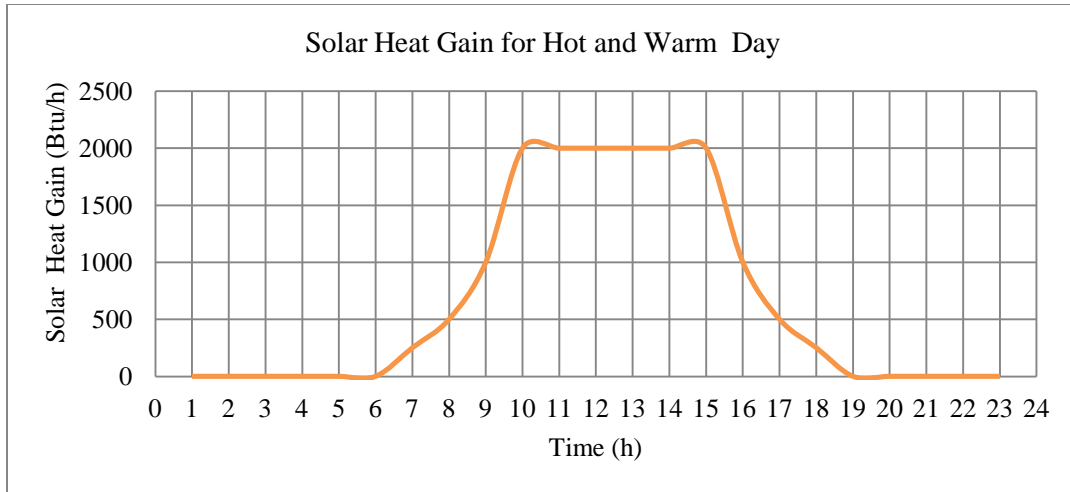
Figure 3.10 Solar heat gain
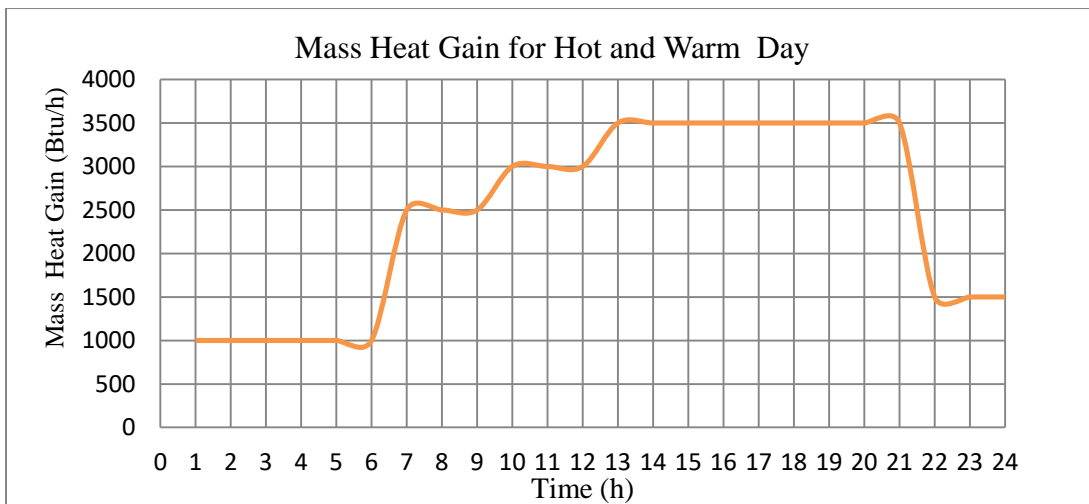
Figure 3.11 Mass heat gain

Table 3.6 Daily internal heat load (House Activities)

Internal Heat Gain									
Time (h) Full Day		**1-7**	**8**	**9-13**	**14**	**15-18**	**19**	**20**	**21-24**
Residents	**Male**	80	120	120	120	120	120	120	120-80
	Female	68	195.5	102	195.5	102	102	195.5	102.68
	Child	55	68	75	85	75	85	75	85
Fluorescent 400 lux 15-20 w/m2	**House area = 48.45 m^2**	0	0	0	0	0	658.71	658.71	658.71
	Kitchen Are=4.536 m^2	68.04	68.04	68.04	68.04	68.04	68.04	68.04	68.04
Computer (J/s)		150	150	150	150	150	150	150	150
Printer (J/s)		100	100	100	100	100	100	100	100
Monitor (J/s)		80	80	80	80	80	80	80	80
Wi-Fi Unit (J/s)		100	100	100	100	100	100	100	100
TV (J/s)		0	0	0	100	100	100	100	100
Oven (J/s)		0	1500	0	2500	0	0	2000	0
Fridge (J/s)		150	150	150	150	150	150	150	150
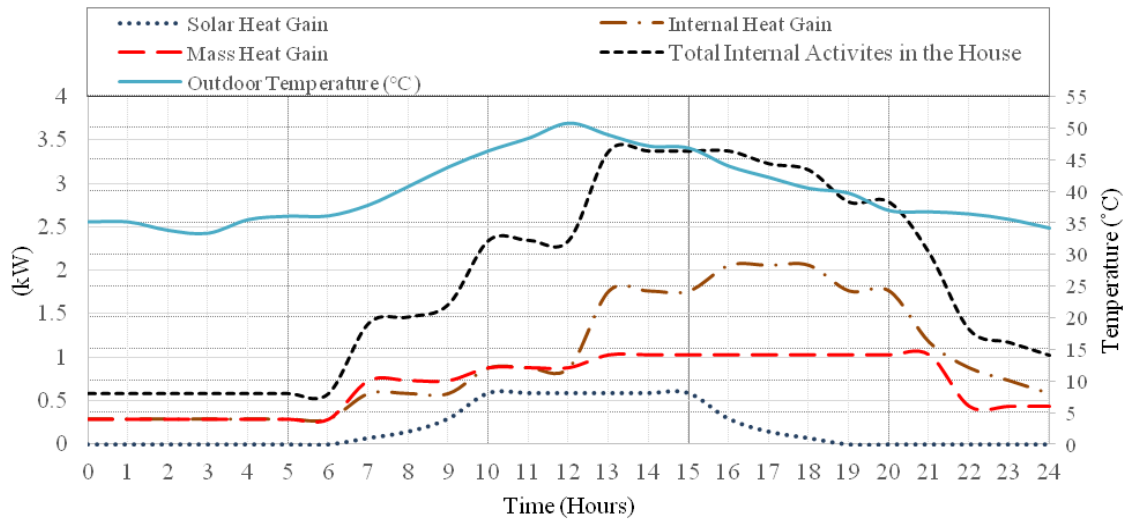
Figure 3.12 Internal heat load (House Activities)

CHAPTER 4

MODELING OF THERMAL HOUSE AND HVAC SYSTEMS

4.1   Introduction

When developing strategies to minimize energy consumption in buildings it is crucial to understand the dynamics of heat energy generation and losses. This chapter aims to investigate some of the contributions heat generation and losses studied through the development of several empirical models. The thermal model is derived to allow us building heat flows relations taking to account of the temperature variation. The developed models have adjustable parameters corresponding to different contributions of the heat budget by understanding the form of temperature variation. Therefore, the models aim to estimate the most important factors in the energy consumptions and productions within the building.

The objectives of the model to include the following:

1. To infer thermal properties of the buildings primarily achieved by modeling the process of heat loss within a building.

2. To infer heat production (i.e. to make a virtual energy meter) primarily achieved by looking at possible models of contributions to heat production.

To establish very precise thermal model researchers should think about the most obvious causes of heat generations and losses within a building. First, looking at cooling/heat losses, this is categorized into two forms, conduction and ventilation. Conductive heat losses can be thought in terms of heat flowing from a hot region to a cold region through windows and walls. Ventilation meanwhile represents the direct movement of hot air out of a building through cracks and gaps as well as through deliberate ventilation.

The standard method of modeling heat losses is making relation for both heat flows and the temperature difference between the two regions. In this investigation, the primary concerns with modeling losses that are the loss of conduction for a typical house in Saudi Arabia [49]. In addition, for heating/cooling losses, researchers need to consider how heating is generated in buildings to replenish the lost. Particular sources of interest included the buildings' heating system and the effect of sunlight as well as the effect of the buildings' occupants and many heat generating devices, which are common inside houses.

4.2   Second Order House Thermal Model

The thermal model of a house is illustrating in Figure 4.1. The model components for second order thermal system are addressed in the section. The aim of this section is to show the parameters extracted in real-time with a reasonable representation of the building. They could be used to control the cooling plant of a real building. This means at any instant the model would have to represent the thermal aspects of a building in its current condition, thus allowing predictions to be made. The thermal model is shown in Figure 4.2 by combining several resistances in series and parallel to achieve equivalent resistances $R_{11}, R_{12}, R_{21}, R_{22}, R_{31}$ and R_{32}.
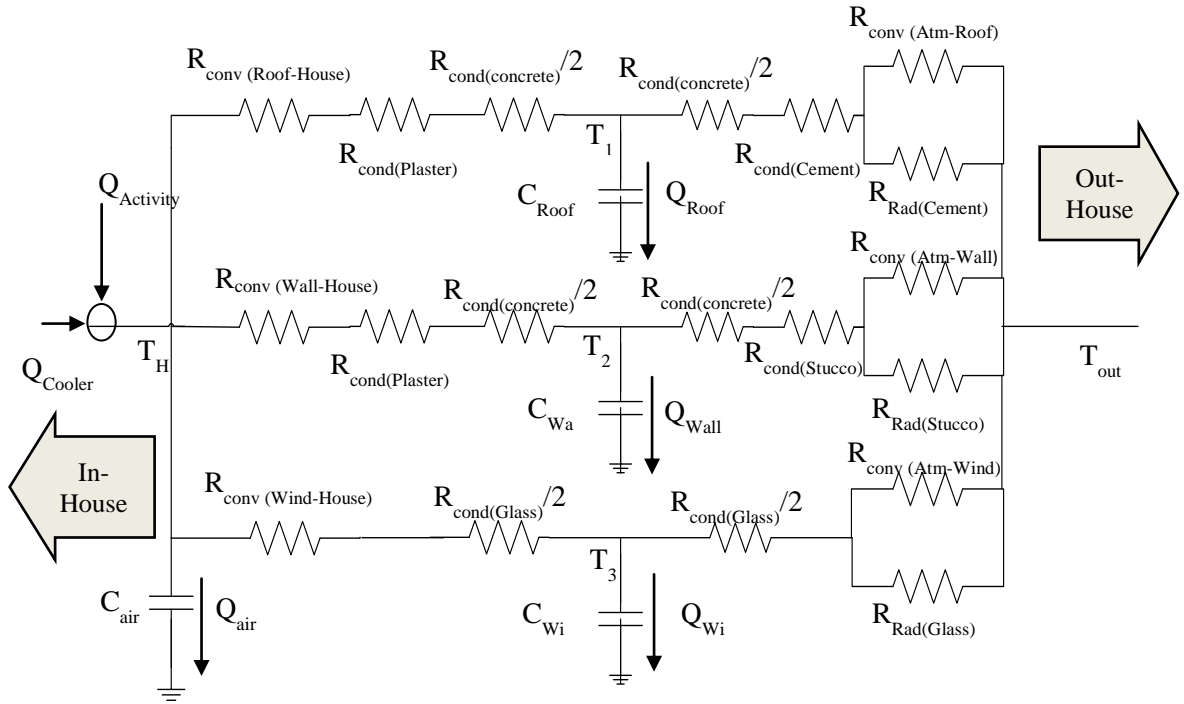
Figure 4.1 Thermal circuit model of the house thermal system
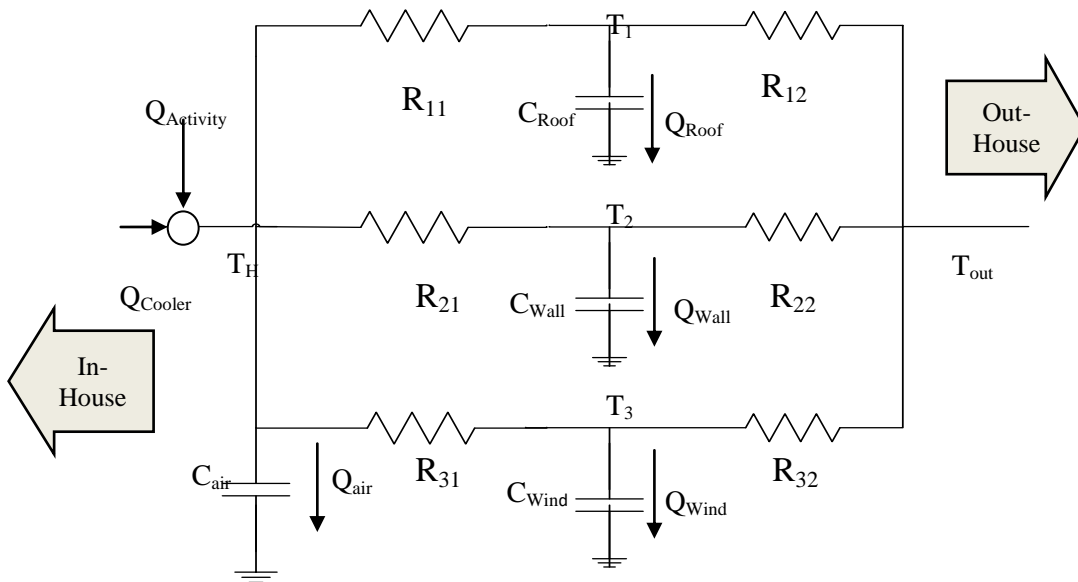
Figure 4.2 Reduced thermal circuit model of the house thermal system

The convective, conductive and radiative resistance values are offered by the following equations:

$$R_{\text{Convective}} = \frac{1}{H_{Conv} * A} \quad °C/W \tag{4.1}$$

$$R_{\text{Conductive}} = \frac{1}{k_{cond} * A} \quad °C/W \tag{4.2}$$

$$R_{\text{Radiative}} = \frac{1}{h_{rad} * A} \quad °C/W \tag{4.3}$$

The equivalent resistances for Figure 4.2 are presented by R_{11}, R_{12}, R_{21}, R_{22}, R_{31} and R_{32}

$$R_{11} = R_{conv(Roof+House)} + R_{cond(plaster)} + \frac{R_{cond(concrete)}}{2} \tag{4.4}$$

$$R_{12} = \frac{R_{cond(concrete)}}{2} + R_{cond(cement)} + R_{conv(Roof-Atm)} // R_{Rad(cement)} \tag{4.5}$$

$$R_{21} = R_{conv(wall-House)} + R_{cond(plaster)} + \frac{R_{cond(concerete)}}{2} \tag{4.6}$$

$$R_{22} = \frac{R_{cond(concrete)}}{2} + R_{cond(stucco)} + R_{conv(Atm-wall)} // R_{Rad(stucco)} \tag{4.7}$$

$$R_{31} = R_{conv(window-House)} + \frac{R_{cond(glass)}}{2} \tag{4.8}$$

$$R_{32} = \frac{R_{cond(glass)}}{2} + R_{conv(Atm-glass)} // R_{Rad(glass)} \tag{4.9}$$

Where, the conductance or U values equal to the inverse of equivalent resistances:

$$U_{11} = \frac{1}{R_{11}} \quad , \quad U_{12} = \frac{1}{R_{12}} \tag{4.10}$$

$$U_{21} = \frac{1}{R_{21}} \quad , \quad U_{22} = \frac{1}{R_{22}} \tag{4.11}$$

$$U_{31} = \frac{1}{R_{31}} \quad , \quad U_{32} = \frac{1}{R_{32}} \tag{4.12}$$

Based on the modified Figure 4.2, the absorbed heat in house air, floor, wall and windows are represented as thermal dynamic equations and we can rewrite these equations and represent them in following equations:

$$Q_{\text{Absorbed in the house Air}}(t) = \frac{dT_H}{dt} * C_{Air} \tag{4.13}$$

$$Q_{\text{Absorbed in the house Roof}}(t) = \frac{dT_1}{dt} * C_{Roof} \tag{4.14}$$

$$Q_{\text{Absorbed in the house wall}}(t) = \frac{dT_2}{dt} * C_{wall} \tag{4.15}$$

$$Q_{\text{Absorbed in the house window}}(t) = \frac{dT_3}{dt} * C_{window} \tag{4.16}$$

$$Q_{\substack{\text{Absorbed in} \\ \text{the house Air}}}(t) = Q_{\substack{\text{Heat passes} \\ \text{to house}}}(t) + Q_{\substack{\text{Heat} \\ \text{sources}}}(t) - Q_{cooler}$$
$$- \left(Q_{\substack{\text{Absorbed in} \\ \text{the house Roof}}}(t) + Q_{\substack{\text{Absorbed in} \\ \text{the house Walls}}}(t) + Q_{\substack{\text{Absorbed in} \\ \text{the house Windows}}}(t) \right) \tag{4.17}$$

The passing heat through roof, walls and windows and the absorbed heat in the roof, walls and windows are expressed in the following equations:

$$Q_{\substack{\text{Heat Passes} \\ \text{to the House}}}(t) = Q_{\substack{\text{Heat Passes} \\ \text{though Roof}}}(t) + Q_{\substack{\text{Heat Passes} \\ \text{through Walls}}}(t) + Q_{\substack{\text{Heat Passes} \\ \text{through Windows}}}(t)$$

$$\tag{4.18}$$

$$Q_{\substack{\text{Heat Passes} \\ \text{though Roof}}} = Q_{\text{Absorbed in the Roof}}(t) + U_{11}\big(T_1(t) - T_H(t)\big) \tag{4.19}$$

$$Q_{\substack{\text{Heat Passes} \\ \text{though Walls}}} = Q_{\text{Absorbed in the Walls}}(t) + U_{21}\big(T_2(t) - T_H(t)\big) \tag{4.20}$$

$$Q_{\substack{\text{Heat Passes} \\ \text{though Windows}}} = Q_{\text{Absorbed in the Windows}}(t) + U_{31}\big(T_3(t) - T_H(t)\big) \tag{4.21}$$

As result the following equations are presented the thermodynamic model for the house

parameters:

$$Q_{\substack{\text{Absorbed in} \\ \text{the House Air}}}(t) = U_{11}\big(T_1(t) - T_H(t)\big) + U_{21}\big(T_2(t) - T_H(t)\big) + U_{31}\big(T_3(t) - T_H(t)\big) +$$
$$Q_{\text{Heat Sources in the House}}(t) - Q_{\text{Cooler}} \tag{4.22}$$

$$\dot{T}_H(t) = \frac{1}{C_{Air}}\left(\begin{array}{l} \big(U_{11} \times T_1(t)\big) + \big(U_{21} \times T_2(t)\big) + \big(U_{31} \times T_3(t)\big) - T_H(t)\big(U_{11} + U_{21} + U_{31}\big) \\ + Q_{\text{Heat Sources in the House}}(t) - Q_{\text{Cooler}} \end{array}\right) \tag{4.23}$$

$$\dot{T}_1(t) = \frac{1}{C_{Roof}}\big(U_{12}\big(T_{out}(t) - T_1(t)\big) - U_{11}\big(T_1(t) - T_H(t)\big)\big) \tag{4.24}$$

$$\dot{T}_2(t) = \frac{1}{C_{Wall}}\big(U_{22}\big(T_{out}(t) - T_2(t)\big) - U_{11}\big(T_1(t) - T_H(t)\big)\big) \tag{4.25}$$

$$\dot{T}_3(t) = \frac{1}{C_{Window}}\big(U_{32}\big(T_{out}(t) - T_3(t)\big) - U_{31}\big(T_3(t) - T_H(t)\big)\big) \tag{4.26}$$

4.2.1 Heat Capacity of the House

There are four different parameters contributing to heat gain of a house. The heat gained by the house is mostly through the walls, windows, doors and roof. The following sections explained the heat capacity for second order thermal model. The residential house has bedroom, living room, kitchen and bathroom with four windows of glasses. We need to calculate the gain through each walls, roof, and windows. To determine the heat gained through roof, walls and windows we need to evaluate the thermal conductivity, convective and irradiative of the section of roof, walls and windows. The section of each roof, walls and windows are presented in Figure 4.3.

The thermal conductivity of any house structure type, U, can be found by calculating the thermal resistances for each section of the walls, roof and windows. The thermal conductivity (k) in (W/m.K), heat transfer coefficient (h) in (W/m^2.K) and radiation coefficient (h$_{rad}$) in (W/m^2.K^4) for material construction used in houses are shown in Table 4.1 [50].

<div align="center">(a)   (b)   (c)</div>
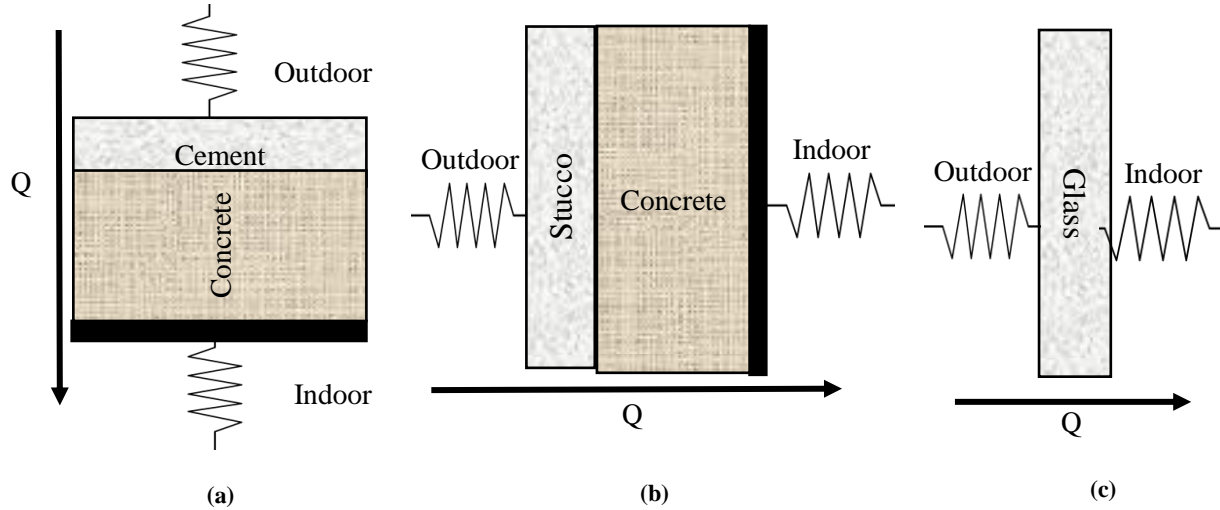
Figure 4.3 a. Roof section, b. Walls section, c. Windows section

Table 4.1 The Thermal conductivity, heat transfer and radiation coefficient

Type	Thermal conductivity (h_{cond}) W/m.K	Heat Transfer Coefficients (h_{conv}) W/m^2.K		Radiation Coefficients (h_{rad}) W/m^2.K
Low density Concrete	0.5	----------------------		----------------
High density Concrete	1.0	----------------------		--------------
Stucco	0.675	Atmosphere to Stucco 8.264		4.231*10^{-8}
Plaster	0.2	Plaster to in-house Air 16.95		-----------
Cement	0.71	Atmosphere to Cement 7.5		5.232*10^{-8}
Glass	0.78	Atmo. To Glass 32	glass to in-house Air 25	5.1773*10^{-8}

First, the wall resistance, which is depending on the wall consisting of stucco, concrete and plaster, then the roof also depends on the roof consisting of cement surfaces, concrete and plaster. The resistance values could be determined from the standard table of thermal properties of common building material, which is summarized in Table 4.2. The table shows the thermal resistances for walls, roof and windows in (K/W).

Table 4.2 The Roof, walls and windows thermal resistances [50]

Roof Thermal Resistances				
Type	Equation	Area (A) (m^2)	Thickness (x) (cm)	R (K/W)
Inside R	$R_{conv} = \dfrac{1}{h_{conv} * A}$	48.45	-------	$1.2177*10^{-3}$
Plaster	$R_{cond} = \dfrac{x}{h_{cond} * A}$	48.45	2	$1.2177*10^{-3}$
High density Concrete	$R_{cond} = \dfrac{x}{h_{cond} * A}$	48.45	30	$1.2177*10^{-3}$
Cement	$R_{cond} = \dfrac{x}{h_{cond} * A}$	48.45	2	$5.8140*10^{-4}$
Outside	$R_{conv} \parallel R_{Rad}$ $= \dfrac{1}{h_{conv}.A} \parallel \dfrac{1}{h_{rad}.A}$	48.45	----	$2.752*10^{-3}$
Walls Thermal Resistances				
Type	Equation	Area A (m^2)	Thickness x (cm)	R (K/W)
Inside R	$R_{conv} = \dfrac{1}{h_{conv} * A}$	90	-------	$6.55*10^{-3}$
Plaster	$R_{cond} = \dfrac{x}{h_{cond} * A}$	90	2	$1.1111*10^{-3}$

		Area A (m²)	Thickness x (cm)	R (K/W)
High density Concrete	$R_{cond} = \dfrac{x}{h_{cond} * A}$	90	30	$6.6667*10^{-3}$
Cement	$R_{cond} = \dfrac{x}{h_{cond} * A}$	90	2.5	$4.1111*10^{-4}$
Outside	$R_{conv} \ // \ R_{Rad}$ $= \dfrac{1}{h_{conv}.A} // \dfrac{1}{h_{rad}.A}$	90	----	$1.3445*10^{-3}$
Windows Thermal Resistances				
Type	Equation	Area A (m²)	Thickness x (cm)	R (K/W)
Inside R	$R_{conv} = \dfrac{1}{h_{conv} * A}$	12.1	-------	$3.3058*10^{-3}$
Glass	$R_{cond} = \dfrac{x}{h_{cond} * A}$	12.1	1	$1.0596*10^{-3}$
Outside $R_{conv(Atm-Glass)}$ $// \ R_{Rad(Glass)}$	$R_{conv} \ // \ R_{Rad}$ $= \dfrac{1}{h_{conv}.A} // \dfrac{1}{h_{rad}.A}$	12.1	----	$2.5826*10^{-3}$

Based on equations (4.4 - 4.9). The thermal resistances $R_{11}, R_{12}, R_{21}, R_{22}, \ R_{31}$ and R_{32} could be evaluated as following.

$$R_{11} = R_{conv(Roof-House)} + R_{cond(plaster)} + \frac{R_{cond(concrete)}}{2}$$

$$= \ 6.377655 \times 10^{-3} \ (K/W)$$

$$R_{12} = \frac{R_{cond(concrete)}}{2} + R_{cond(cement)} + R_{conv(Roof-Atm)} \ // \ R_{Rad(cement)}$$
$$= 6.43 \times 10^{-3} \ (K/W)$$

$$R_{21} = R_{conv(Wall-House)} + R_{cond(plaster)} + \frac{R_{cond(concrete)}}{2}$$
$$= 5.1 \times 10^{-3} \ (K/W)$$

$$R_{22} = \frac{R_{cond(concrete)}}{2} + R_{cond(stucco)} + R_{conv(Atm-Wall)} \ // \ R_{Rad(stucco)}$$
$$= 5.098 \times 10^{-3} \ (K/W)$$

$$R_{31} = R_{conv(Wind-House)} + \frac{R_{cond(Glass)}}{2}$$
$$= 3.84 \times 10^{-3} \text{ (K/W)}$$

$$R_{32} = \frac{R_{cond(Glass)}}{2} + R_{conv(Atom-Glass)} /\!/ R_{Rad(Glass)}$$
$$= 3.11 \times 10^{-3} \text{ (K/W)}$$

Where the U values or heat gains equal to the inverse of equivalent resistances is calculating by the equations (4.10) to (4.12). To calculate the heat gain for roof, walls and windows, assumed that the internal heat gain is due to the heat convection, Q_{int}. Table 4.3 shows required cooling load for each house, which consists of kitchen, bedroom, and living room [51].

Table 4.3 Required cooling load for houses

Outdoor-Conditions	48 ℃ Dry bulb temp./23.6 ℃ wet bulb temp
Indoor Conditions	24 ℃ / 50 % relative humidity
Lighting	15 W/m^2
Kitchen	1 persons, refrigerator, oven so internal heating dissipation is 1000 W.
Bedroom	2 persons, 1 laptop, so internal heat dissipation is 500 W.
Living/ Dining	2 persons, 1 Laptop, LCD, so the heat dissipation is 500 W.
Building Orientation	West and east big Windows

In building design, thermal mass is a property of the mass of a building that is the ability of a material to absorb and store heat energy. The thermal mass (J/K) is considered from the mass (Kg) of material and its specific heat (J/Kg.K). Table 4.4 presents the thermal mass for in- house air and building construction [52].

Table 4.4 Thermal mass for houses

Type	Mass (Kg)	Specific heat (J/Kg.K)	Thermal Mass(J/K)
Air	150.729	1005.4	$C_{Air} = 0.151543*10^6$
Roof	33430.5	835	$C_{Roof} = 27.914*10^6$
Walls	62100	835	$C_{Walls} = 51.8535*10^6$
Windows	412.5	840	$C_{Windows} = 0.3465*10^6$

Model data generated for the thermal house model and HVAC systems presented in Table 4.5.

Table 4.5 Model data generated for the thermal house model and HVAC systems

Item	Amount	Unit
Length of house	8.5	m
Width of house	5.7	m
Wall area	229.3	m^2
Roof area	48.45	m^2
Number of windows	4	-----------
Height of window 1	2.18	m
Width of window 1	2	m
Height of window 2	2.18	m
Width of window 2	2.52	m
Height of window 3	2.18	m
Width of window 3	1	m
Height of window 4	2.18	m
Width of window 4	1	m

Window area	14.2136			m^2
U_{11}	156.797			W/K
U_{12}	155.536			W/K
U_{21}	196.0784			W/K
U_{22}	196.502			W/K
U_{31}	260.718			W/K
U_{32}	312.298			W/K
C_{Air}	$0.101273*10^6$			J/K
C_{Roof}	$27.914*10^6$			J/K
C_{Walls}	$51.8535*10^6$			J/K
$C_{Windows}$	$0.3465*10^6$			J/K
T_{HVAC}	11			°C
M_{dot}	Air Speed two Outlet Ducks	4.19	2.24	(m/s)
	Tow Outlet Ducks Area	$0.4 \times 0.35 = 0.14$	$0.76 \times 0.14 = 0.1064$	(m^2)
	Volume Flow Rate	0.5866	0.23833	(m^3/s)
	Air Mass flow	$(0.5866+0.23833) \times 1.225 = 1.011$		(kg/s)
	ON/OFF Cycle	$\cong 3600$		kg/h
	VFD System	2200-3600		
Air Density	1.225			Kg/m^3

$T_{initial}$	24.5		°C
$T_{setting}$	24		°C
Power use	Compressor + Condenser	4.239	KW
	Blower Fan	0.82	

4.3   House Thermal Model Using Simscape Physical System

4.3.1 Simscape Physical System Modeling

With Simscape components, the thermal model of the house is built just as we would assemble a physical system. Simscape employs a physical network approach, also referred to as a causal modeling, to model building components corresponding to physical elements, such as pumps, motors, and op-amps, are joined by lines corresponding to the physical connections that transmit power. This approach allows us to describe the physical structure of a system rather than the underlying mathematics. The house model, which closely resembles a schematic, Simscape automatically, constructs the differential algebraic equations (DAEs) that characterize the system's behavior. These equations are integrated with the rest of the Simulink model, and the (DAEs) are solved directly. The variables for the components in the different physical domains are solved simultaneously, avoiding problems with algebraic loops.

Simscape allow us to create models of custom components by using the basic elements contained in its foundation libraries. Figure 4.4 shows the Simscape libraries of electrical, mechanical, hydraulic, and thermal building blocks for creating customized component models. Therefore, to build the house model different types of physical model components in needed. Modeling of electrical components and modeling of thermal effects are discussed as follows.

- **Modeling of Electrical Components:** Simscape toolbox provides electrical building blocks for representing electrical components and circuits. In addition to basic elements like resistors, capacitors, and inductors, more complex elements such as op-amps and transformers are also included. More elaborate electronic and electromechanical components are available in SimElectronics™.

- **Modeling of Thermal Effects:** Simscape provides thermal building blocks for modeling and simulating thermal effects for the house. Conductive, convective, and radiative heat transfer as well as the thermal mass of elements can be modeled. Using thermal source blocks, the temperature or heat transfer can be specified, using thermal sensor blocks, also the amount of heat transfer or temperature change can be measured.

4.4   House Thermal Model Development Using Simscape Physical

Building a simscape model required the following compomntes.

1. A model of the thermal mass,

2. A model of the convective, condictive and radative resistances,

3. A reference temperature,

4. A source temperature to specify intial temperatures $T_1, T_2 \& T_3$

5. A way to measure the house temperatures at the steady state T_{House} $T_1, T_2 \& T_3$. and

6. A way to measure the absorbed heat in air house and the house heat flow through roof, walls and windows.
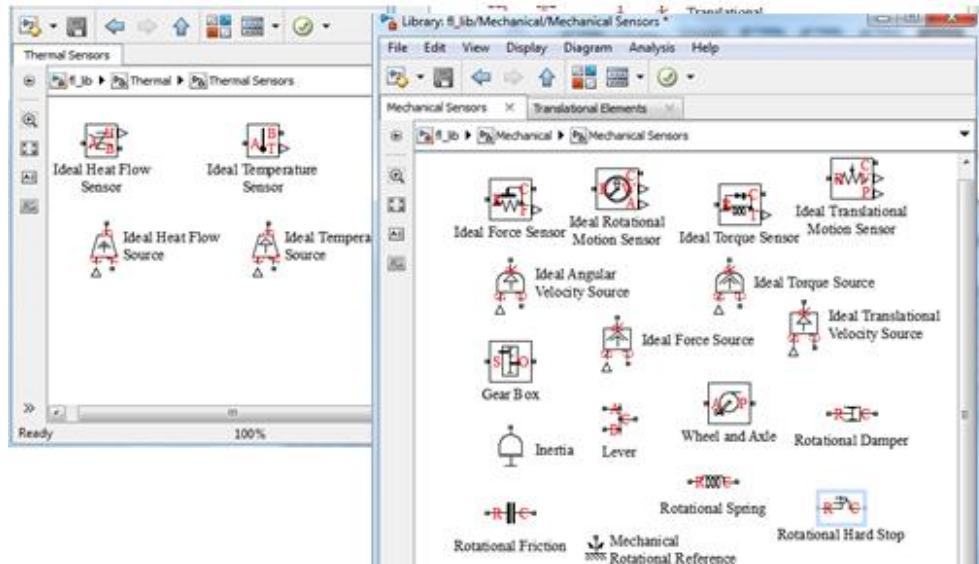
Figure 4.4 Simscape libraries of electrical, mechanical and thermal building blocks for creating customized component models.

A Thermal house model is displayed in Figure 4.5 that consists of a house structure with four thermally distinguishable parts: inside air, walls, windows, and roof. The house exchanges heat with the environment through its walls, windows, and roof. Each path is simulated as a combination of a thermal convection, thermal conduction, and the thermal mass. The physical roof model is presented in Figure 4.6. The roof consists of three layers plaster from inside, concrete and boxes of squares cement on outside roof. Therefore, plaster, concrete and squares cement layers have conductive thermal module. Plaster and cement layers have convective module. Out side cement layer also has radiative module. Thermal mass is added in the mid-thickness for roof weight which reflects the ability of a combination layers of roof materials to store internal energy.
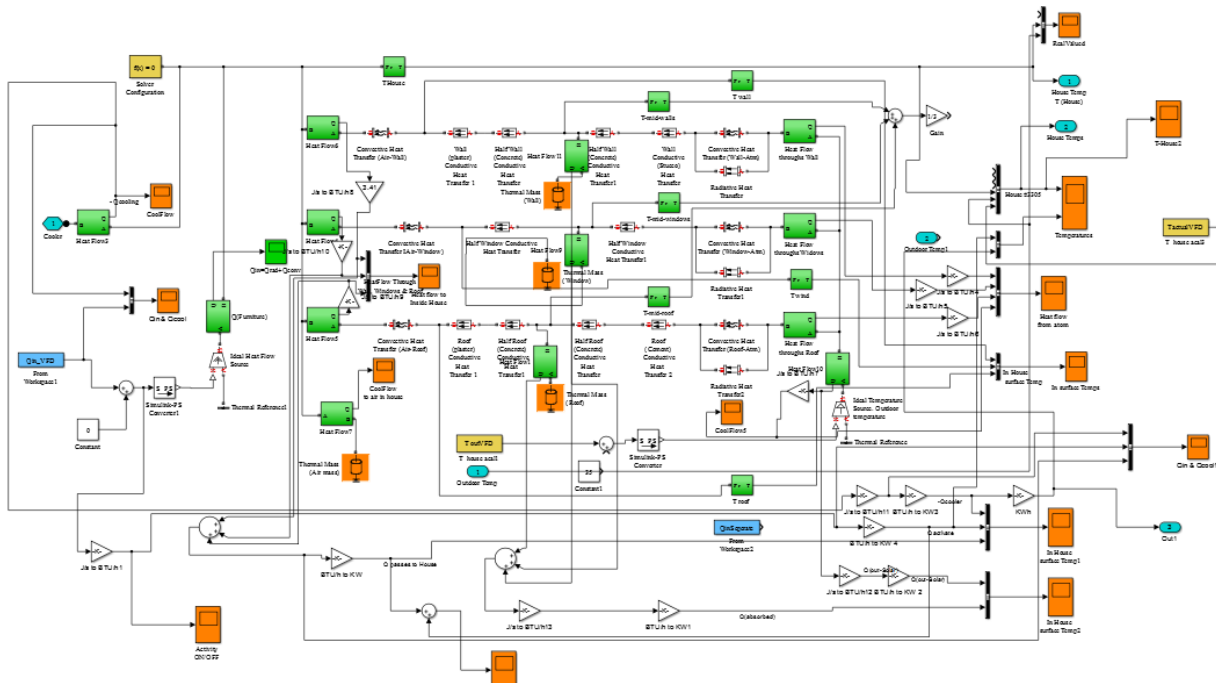
Figure 4.5 House thermal model using physical system
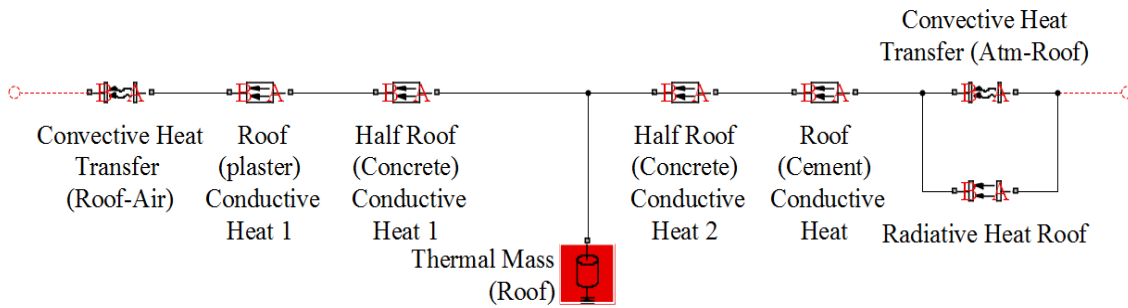
Figure 4.6 House roof thermal model using simscape physical systems

Similarly the physical walls model is presentd in Figure 4.7. The wall consists of three layers
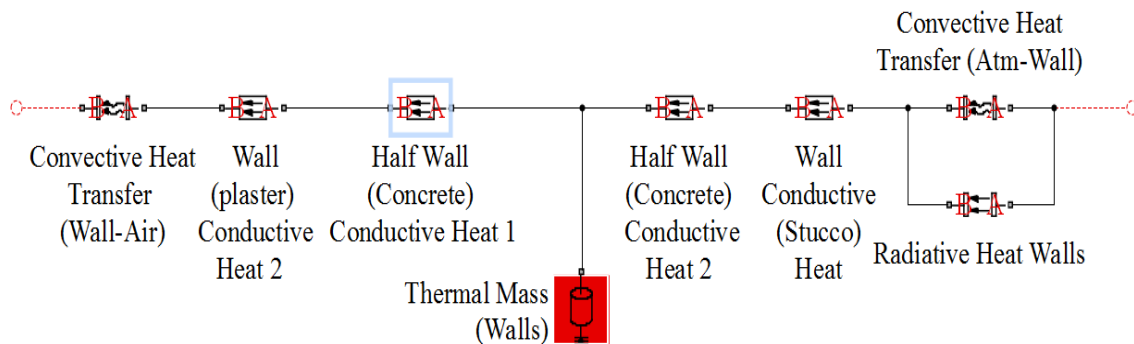
Figure 4.7 House walls thermal model using physical system

65

plaster from inside, concrete and stucco on outside. Therefore, plaster, concrete and stucco layers have conductive thermal module. Plaster and stucco layers have convective module. Out side stucco layer also has radiative module. Thermal mass is added in the mid-thickness for overall walls weight which reflects the ability of a combination layers of wall materials to store internal energy.
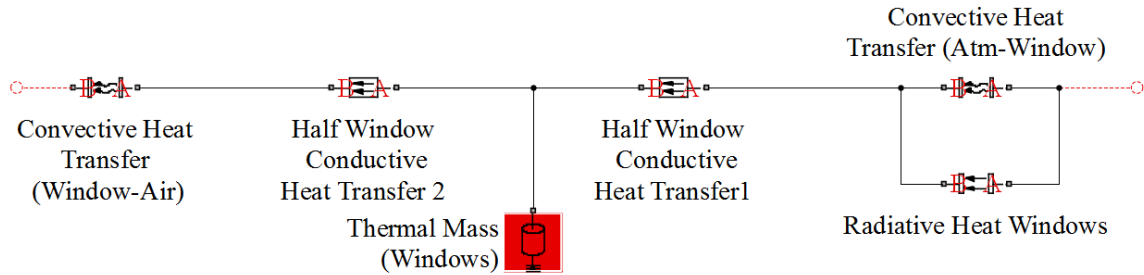
Figure 4.8 House Windows Thermal Model Using Physical System

The windows consist only of one glass layer which are explained in Figure 4.8. Therefore, they have conductive thermal model for glass thickness and convective model for inside house. They also have convective and radiative models for outside house. Thermal mass is added in the mid-thickness for overall windows weight which reflects the ability of a combination layers of windows materials to store internal energy.

(a): Q (cooler in house)

(c): Out house heat flow

(b): Q (activity in house
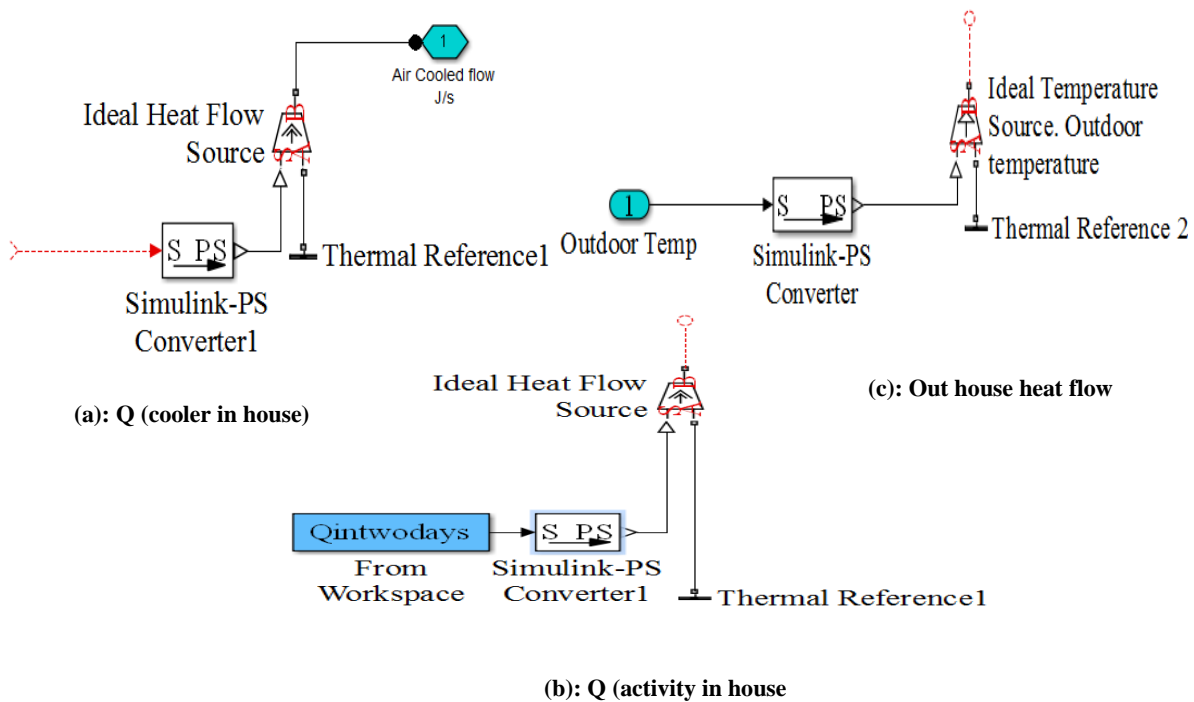
Figure 4.9 Block diagrams for convert untitled signal to simscape physical signal

The Simulink-PS (S-PS) converter blocks in Figure 4.9 are used to convert the input Simulink signal into a physical signal. We use these blocks to connect Simulink sources (heat flow or temperatures) to the inputs of a physical network diagram. The ideal heat flow source block in Figure 4.9 (a & b) represent an ideal source of thermal energy that is powerful enough to maintain specified heat flow at its outlet regardless of the temperature difference across the source.
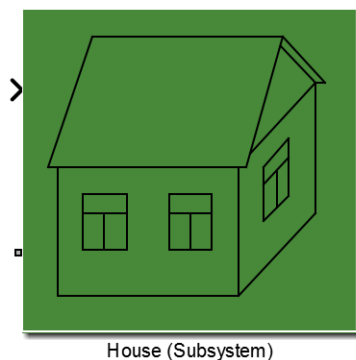
Figure 4.10 Thermal model of the house (Subsystem)

67

Figure 4.9(c) shows the ideal temperature source block, which represents an ideal source of thermal energy that is powerful enough to maintain specified temperature at its outlet regardless of the heat flow consumed by the system. Figure 4.10 represents the house as a subsystem in Matlab/Simlink.

4.5   HVAC system Model

The primary goal of controlling the building environment parameters is to maintain the thermal comfort of the occupants and to achieve good energy efficiency by using HVAC system. However, in most of the situations, achieving these goals may cause the other goal to be sacrificed to a certain extent. In building control, the common set-point for temperature inside a residential building is 24℃ with an operating band of +1℃ and – 1.5℃. Different strategies used for controlling the building thermal environment within the given ranges are roughly categorized into two classes in this thesis. They are: (i) conventional control technique (ii) intelligent and advance control methods.

The conventional air conditioning system usually employs an "ON/OFF" control. Since the speed of the compressor cannot be varied. It is either switched ON, working at full capacity or switch OFF by the thermostat. As shown in Figure 4.11 (a). The efficiency of this conventional technique is also low due to frequent starts and stops of the compressor as well as the operation of the compressor from a constant frequency source. The intelligent and advance control methods are used with variable speed driver for air conditioning which can deliver and enhance the performance over the conventional technique, while improving the overall energy efficiency as well as comfortability as shown in Figure 4.11 (b).

(a) Compressor speed for ON/OFF cycle & variable speed

(b) Indoor Air Temperature for ON/OFF Cycle &Variable Speed
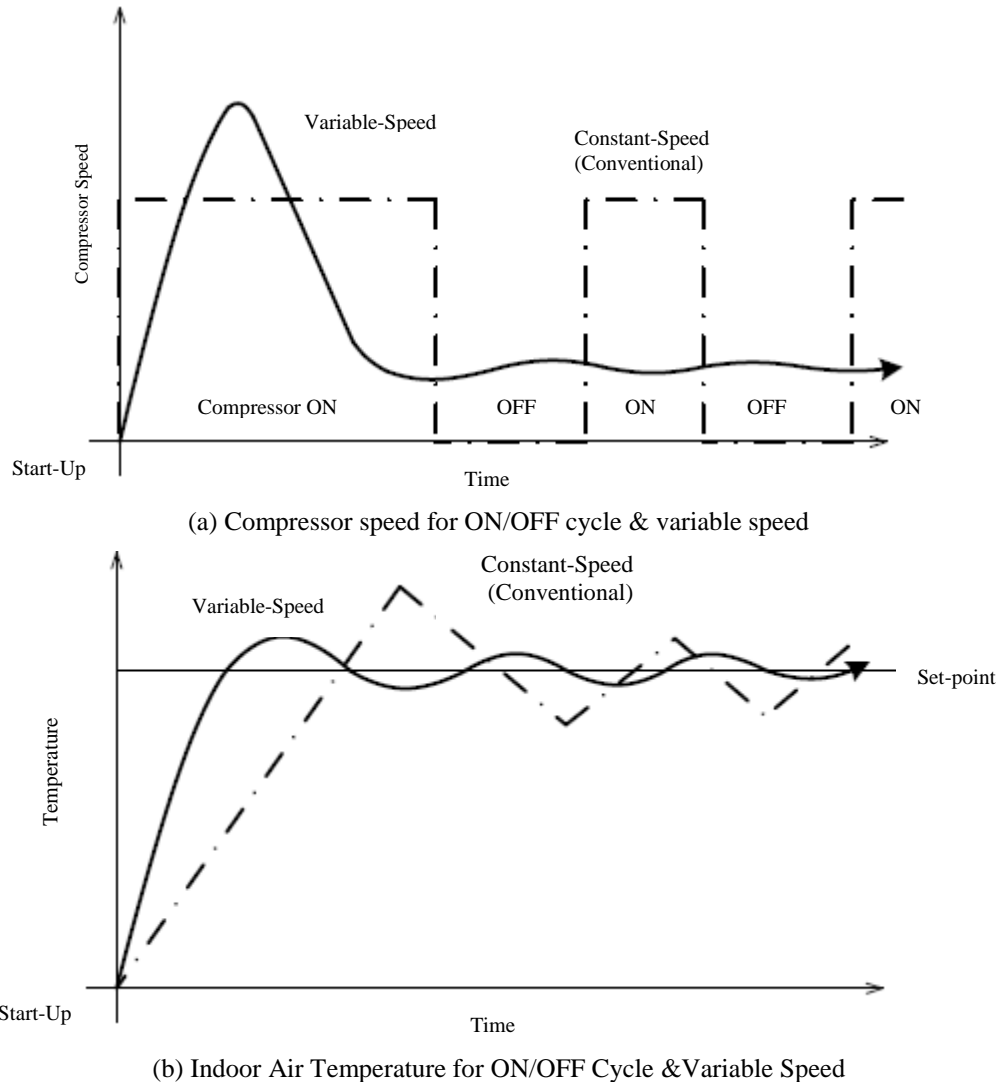
Figure 4.11 Compressor operations for constant and variable speed systems (a) compressor speed and (b) temperatures

4.5.1 Cooling Model of HVAC ON/OFF Cycle (Conventional Control)

The main classical controller used in building control is one-position control (ON/OFF) control. It has simple structure and low initial cost, which makes it the most used controller in HVAC systems in both commercial and residential buildings. ON/OFF control is one of the oldest techniques that is practiced in buildings for the purpose of energy saving and occupant thermal comfort. It is a simple, fast and inexpensive feedback controller that accepts only binary inputs

which is also known hysteresis control. The basic components of a thermostat are: (i) sensor to measure the temperature in the desired environment; (ii) switch/actuator to turn the heating or cooling equipment ON and OFF; (iii) feedback loop to find the offset and decide ON/OFF time; and (iv) user interface to display the current conditions.

Figure 4.12 displays the desired temperature (set point temperature) that is compared with the indoor house air temperature (T_{House}) and then it gives temperature error (T_{err}). The error is compared with the threshold value of thermostat relay. If T_{err} is above the threshold value, the relay is turned ON and if T_{err} is below the threshold value, the thermostat relay is turned OFF. The cooling air flow and outdoor temperature (T_{out}) is considered in the thermodynamic model for the house and T_{House}, mid parameter temperature such as roof, walls and windows are output.

Figure 4.12 also shows the block diagram of integrate ON/OFF cycle air conditioning system with thermal house model respectively based on the thermal dynamic equation
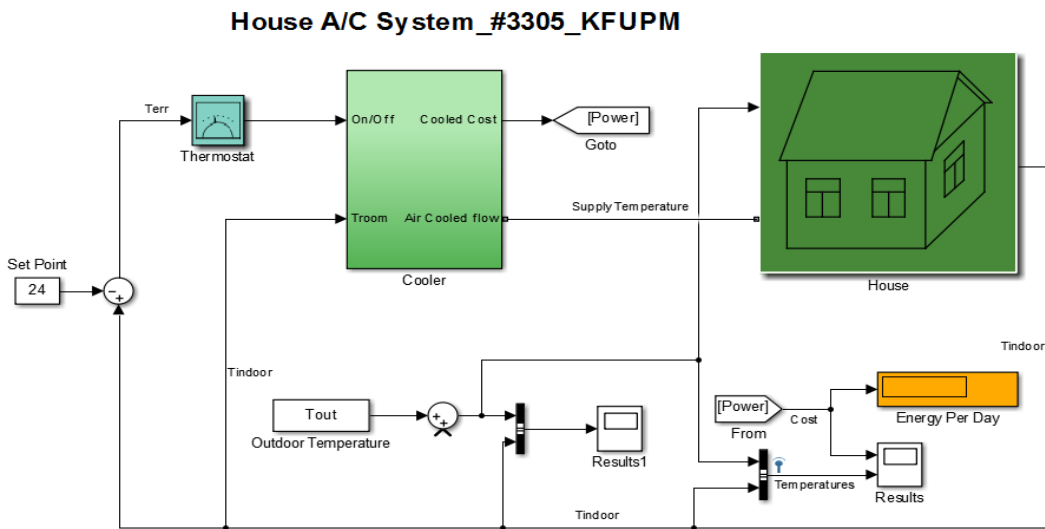
Figure 4.12 Integrate ON/OFF cycle HVAC unit with thermal house model

$$\frac{dQ_{Cooler}}{dt} = \left(\left(T_{HVAC} - T_{House} \right) \times \overset{\bullet}{M}_{HVAC} \times C_P \right) \tag{4.27}$$

The ON/OFF signal is coming from the thermostat relay. The cooling airflow (Q_c) into the house produced from the difference value between indoor temperature (T_{House}) and cooler air temperature ($T_{A/C}$) and then multiplied by cooling gain. Figure 4.13 presented the thermostat subsystem model.
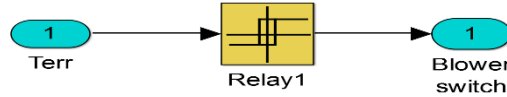
Figure 4.13 Thermostat subsystem model

The ON/OFF air conditioning will be ON or OFF depending on the set point and the outdoor temperature. Usually there is a dead-band of about +1°C to +1.5 °C to prevent ON/OFF cycling of compressor that will reduce its lifespan. In cooling mode, the compressor will turn ON when the outdoor temperature of the house is higher than the set point by 1°C, and it will only go OFF when the indoor temperature drops below -1.5°C (different manufacturer will have different value). Figure 4.14 is showing the measurement and simulation   operation range (+1°C to 1.5°C).
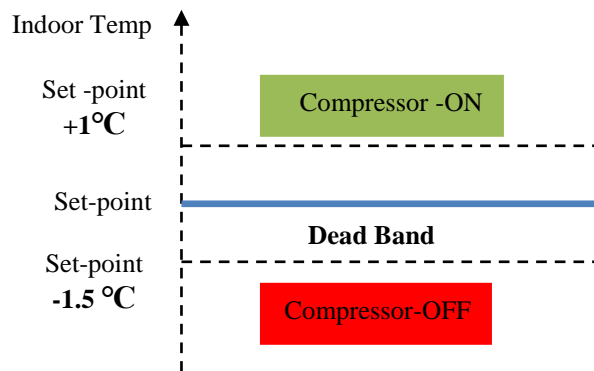
Figure 4.14 Thermostat operation range

The block diagram of the cooler subsystem is displayed in Figure 4.15 based on the following thermal dynamic equation
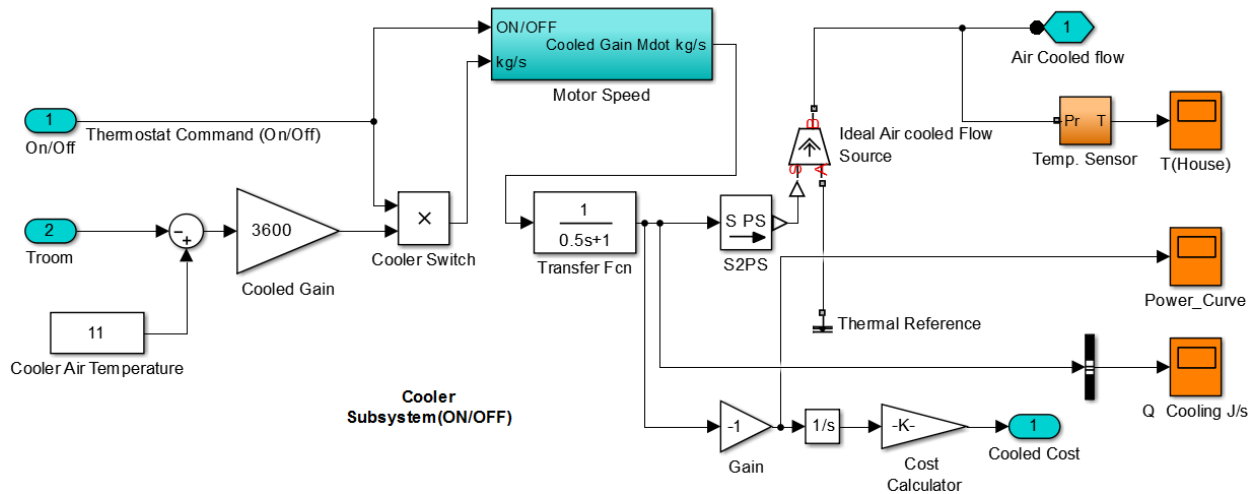
Figure 4.15 Cooler subsystem ON/OFF cycle system

Figure 5.16 shows the simulated indoor temperature and the actual outdoor door temperature for a hot and warm day. It can be noticeable that the indoor temperature varies between 23℃ to 25℃ which close to the set point temperature. The indoor temperature fluctuates in the operation's range for the whole day due to the HVAC system cycling ON/OFF. The conventional ON/OFF system is not provided the satisfaction of comfortable level inside the house. However, more energy is consumed by ON/OFF unit.
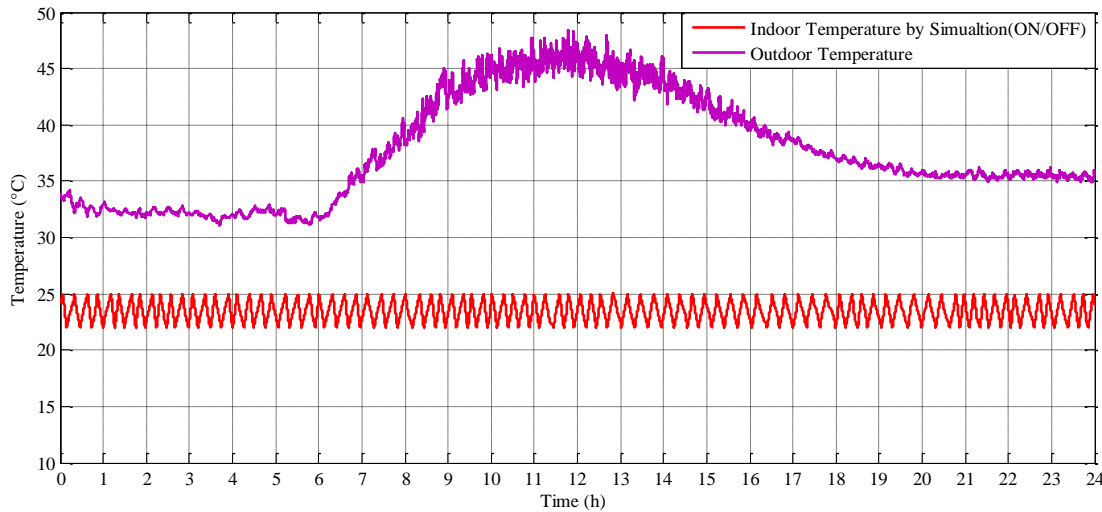
Figure 4.16 Simulated indoor temperature and the actual outdoor temperature for a hot day

4.6   Cooling Model of HVAC VFD System

Variable frequency driver has been employed for residential, industrial and commercial air conditioning applications and supposed to increase significantly in the next few years due to its energy savings capability and become a priority for consumers. Simulating the variable speed compressor by using intelligent and advance control methods can produce more energy savings. Intelligent control techniques can directly be used in HVAC control and they can also be employed to improve the existing traditional controllers, as well. These intelligent techniques are presented under three different methods (i) FLC (ii) PID and (iii) PI-PWM as it is presenting in Figure 4.17. By simulation in Matlab/Simulink , performance of each control method is going to be tested for a typical house in KSA. Modeling of VFD-HVAC will be presented in details with the three different controllers in the next chapter.
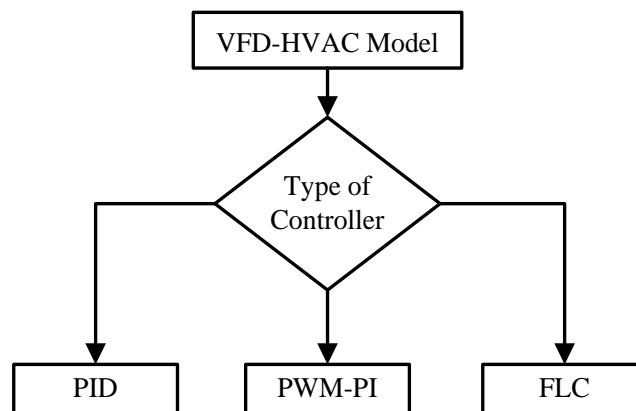
Figure 4.17 Intelligent and advance control methods of modeling VFD-HVAC

CHAPTER 5

MODEL OF HVAC VFD SYSTEM

5.1 Introduction

Variable frequency drive (VFD) has widely used in the HVAC application, including fans, pumps, compressors, etc. A better understanding of VFD will lead to improved application and selection of both equipment and HVAC systems. A variable frequency drive (VFD) is a type of adjustable speed drive used to control the speed of the compressor based on the system load requirements and operation schedule, resulting in a dramatic cut in energy consumption. VFD technology allows the air conditioner automatically vary its power output to specifically maintain room temperature at a desired or comfortable level. A non-inverter appliance maintains the temperature by repeatedly switching power ON and OFF, which consumes much more electrical energy upon starting. In the following sections, the operation principle of the variable frequency drive will present the benefit of VFD, and the model of the HVAC unit by using three different controllers will be provided with the integration of the thermal house model.

5.2 VFD Operation

A VFD is an electrical device used to control the rotation speed of an alternating current (AC) electric motor (compressor) by adjusting the frequency of the electrical power supplied to the motor. Figure 5.1, show VFD schematic diagram [53].
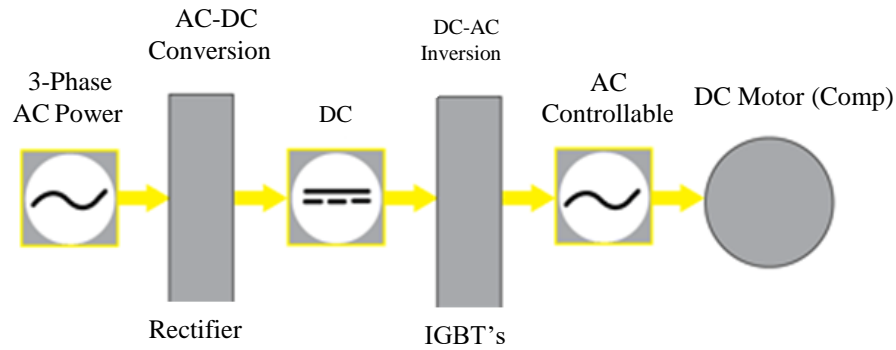
Figure 5.1 Schematic diagram of a variable frequency drive

The variable frequency drive consists of the rectifier unit, DC Bus, the inverter unit and controller circuit. For understanding the basic principle of VFD operation, a brief explanation of each component is presented as following. Figure 5.2, shows the VFD components.
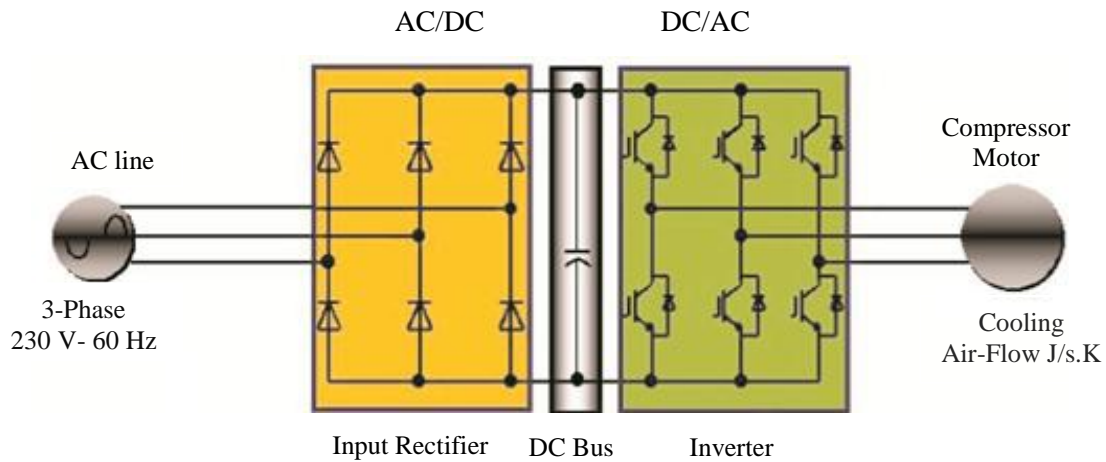
Figure 5.2 The VFD's components

- **Rectifier**

The rectifier in a VFD is used to convert three phase 60 Hz power from a standard 220V, 440V or higher utility supply to direct current (DC) power. Since most large power supplies are three phase, there will be a minimum of 6 rectifiers used in VFD. One rectifier is allowing the power to pass through only when the voltage is positive. A second rectifier is allowing the power to pass through only when the voltage is negative. Then there are two rectifiers which required for

each phase of power, conversion from AC to DC, and then back to AC, can cost as much 4-6% in energy losses for each conversion step.

- **DC Bus**

The DC bus comprises of capacitors to accept power from the rectifier, store it, and later deliver to keep the ripple to minimum that power through the inverter section.

- **Inverter**

The inverter contains six transistors that deliver power to the compressor motor. The "Insulated Gate Bipolar Transistor" (IGBT) is a common choice in modern VFD. The function of IGBT is to switch on and off several thousand times per second and precisely control the power delivered to the compressor motor. The IGBT uses a method called "Pulse Width Modulation" (PWM) to simulate a current sine wave at the desired frequency to the compressor motor.

- **Controller Circuit**

The controller is essential unit in the circuit and it's used to vary the output speed of the electric motor according to environment temperature degree, the compressor will be changed according to speed of motor. Controller circuit may incorporate many complex control units such as PID controller, sensors, PWM unit [53]. In the measurement part of this study PID controller use sample the current ambient air temperature and adjust the speed of compressor appropriately.

Most VFDs used in HVAC applications are inverters using sine coded PWM technology. The output voltage is adjusted by changing the width and number of the voltage pulse as shown in Figure 5.3, whereas the output frequency is varied by changing the length of the cycle [54].
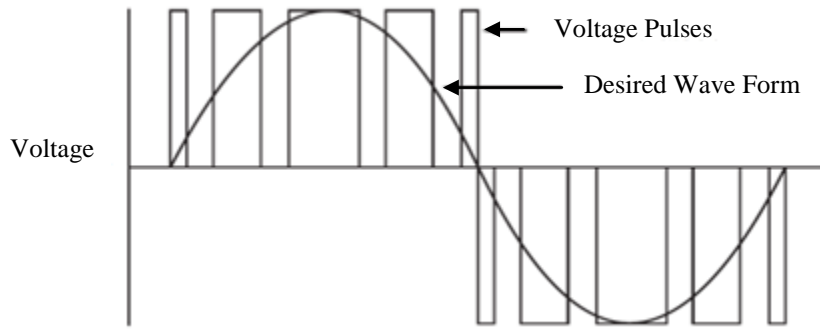
Figure 5.3 Sine coded PWM waveform

5.2.1 Variable Frequency /Speed fan

Variable speed fan is the fan equipped with VFD. Since its speed vary as the frequency of supply power changes, this fan is also called variable frequency fan. The operating characteristic of centrifugal fan makes it the excellent candidate for VFD applications. According to the fan and affinity laws, the fan power has a cubic relationship with the compressor motor speed. Therefore, significant power savings could be achieved by reducing the motor speeds with the proper controls. The variables related to the fan performance are rotation speed N, impeller diameter D, volume flow rate Q, gas/water density ρ, pressure P, power W, and mechanical efficiency η. In a typical application, the fan diameter is constant. The airflow, fan head, and power solely rely on the speed. These relations are given by the following equations [54].

$$\frac{Q_1}{Q_2} = \frac{N_1}{N_2} \tag{5.1}$$

$$\frac{P_1}{P_1} = \left(\frac{N_1}{N_2}\right)^2 \tag{5.2}$$

$$\frac{W_1}{W_2} = \left(\frac{N_1}{N_2}\right)^3 \tag{5.3}$$

77

Equation (5.3) is clearly indicating how the speed change affects the power change. The power demand of compressor motor varies with the cube of the speed of compressor motor. Power is proportional to $f(Speed)^3$ as shown in Figure 5,4. This means that a reduction of speed by 20% will result in reduction of power consumption by nearly a half, 50% saving. Since most HVAC equipment runs at full power, significant energy savings can be made with these variable speed drives
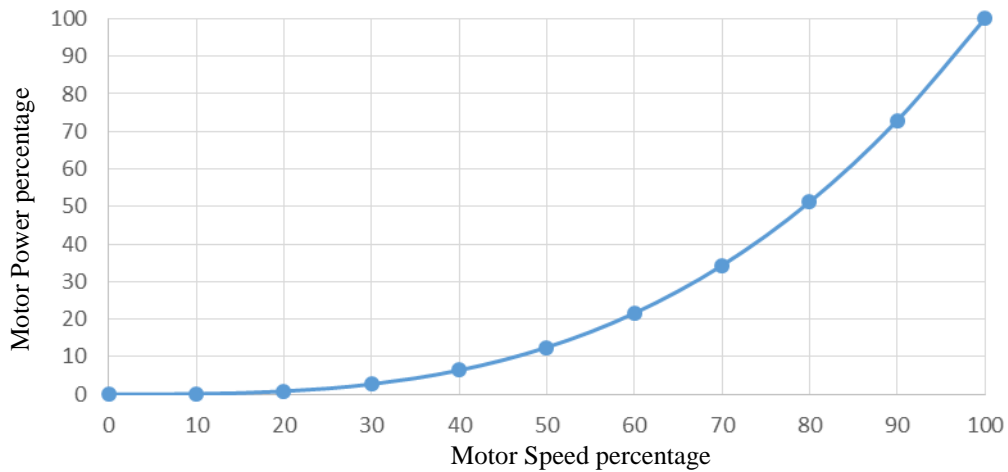
Figure 5.4 Relationship between power and speed

5.2.2 Variable Frequency/Speed Compressor

Variable frequency compressor or variable speed compressor is compressor equipped with VFD. In the HVAC industry, there are different types of compressors associated with the refrigeration systems such as, scroll, reciprocating, and centrifugal. All those types are applicable components for a VFD application. Refrigerant compressor is typically used in air conditioners, chillers or unitary air-handling units, in residential area and commercial buildings. In the experimental study of this research scroll compressor has integrated with brushless DC motor as it is especially suitable for a VFD due to its intrinsic structural design. Scroll compressor and reciprocating compressor are the most commonly used types on rooftop units (RTUs). The scroll

compressor seldom does not have a cubic relationship between power and frequency. Figure 5.5 shows linear relationship between power and frequency for a 5-ton RTU with a scroll compressor, based on the experimental study in [55]. This relationship clearly demonstrates how the compressor power changes with frequency.
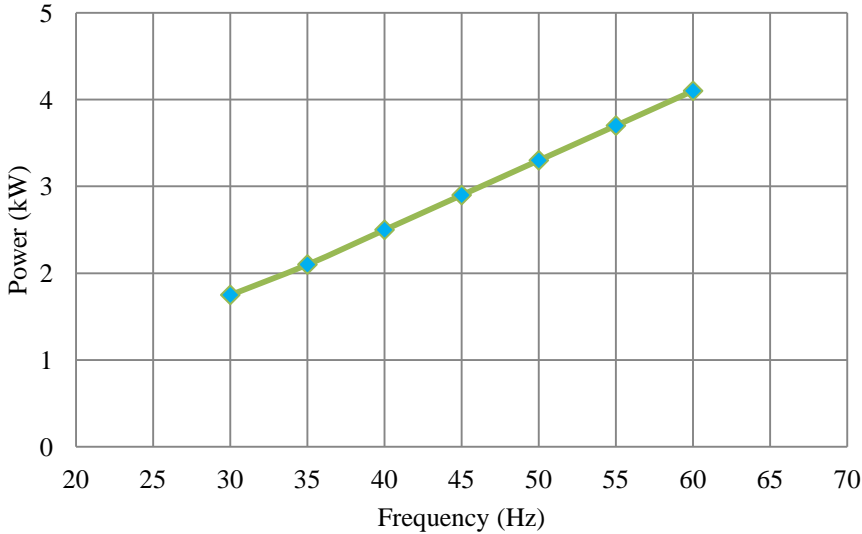
Figure 5.5 Relationship between compressor power and frequency for a 5-ton RTU

The electricity can be saved by using variable frequency compressor for air conditioning systems. Moreover, variable speed operation of the compressor and indoor air blower is one way to provide energy efficient capacity modulation. This is to take advantage of the speed cube power law. Compressors and blower are typically designed for worse case operating scenarios. Residential cooling loads vary greatly. Therefore, by operating systems at levels that vary below design maximum, significant energy and cost saving can be achieved [53].

5.3 Benefits of VFD

As VFD usage has increased dramatically in HVAC application, compressors, fans, pumps, air handlers, and chillers can benefit from speed control. Variable frequency drive can provide the follow benefits:

- Ideal soft start capability reduces the inrush current when motors start up, and thereby reduces thermal and mechanical stresses on the motor and improves the motor reliability.

- Reduces the motor power consumption significantly with proper controls (Energy savings).

- Improves the power factor of the entire drive system including VFD and motors (High power factor).

- Match the thermal comfort of the indoor temperature

- Reduce system maintenance and related costs.

These benefits boost the widespread utilization of VFD in the HVAC field. Moreover equipping a VFD in a new system or existing system increases the initial investment, the reduced VFD cost combined with the increased energy savings derived from a VFD result in short payback period.

5.4 Model of HVAC VFD System by PID

One of the methods that has been suggested and investigated to reduce the energy consumption from an air conditioning unit is through the use of well-tuned controller for the air handling unit (AHU) and variable speed compressor (VSC). Among many control methods for air conditioning, the proportional-integral-derivative (PID) algorithm is very common. In the unit that installed in the house #3307 the air temperature, the supply temperature and return temperature are controlled by using two types of PID controllers. The first PID is used to control on startup and the second PID is used to control during operation.

PID has the feedback control mechanism and the error which is the difference between measured process variable and the set point, and determines the control signal according to the error value. There are three separate techniques will be used in the PID control algorithm: (i) proportional term relates to the present offset, (ii) integral term depends on the accumulation of past errors, and (iii) derivative term predicts the future offset based on the current rate of change of the change. A control signal is delivered based on a weighted sum of these three actions. For modeling HVAC VFD two PID controllers will be used one will be used to control the cooling air conditioning and the second PID will be used to control the coil temperature of the system.

The complete block diagram for VFD air conditioning system with the thermal house model is displayed in Figure 5.6. If the indoor temperature T_{Indoor} varies nearby the desired temperature (Set Point), we immediately measure and calculate the desired speed depending on the setting and air house temperatures. The desired speed/frequency depends on measuring temperatures like supply air temperature, return air temperature, discharge and suction temperatures, discharge and suction pressure that are detected by "Connected Programmable Controller (C.PCO)". The desired value is calculated continuously using C.PCO through PID controller. The input of the VFD is desired speed/frequency (N/ F) that does as a controller to reduce or increase the speed of air conditioning compressor using IGBTs. Cooler gain of the air $\left(CoolerGain \dfrac{1}{s.K^{\circ}} \right)$ is the output of compressor that multiplied by the difference between T_{Indoor} and T_{Coil} to get appropriate cooling airflow J/s. T_{Coil} value depends on the electronic expansion valve (ExV) that is controlled using c.pCO through PID. The inputs into thermal house model are the outdoor house air temperature, and the smooth cooling airflow, and the output is T_{Indoor}.
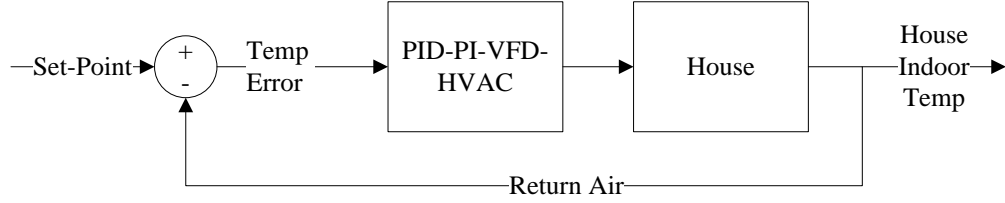
Figure 5.6 Integrate VFD-HVAC system with thermal house model

The Simulink in Figure 5.7 shows a house cooling system that consists of a cooler subsystem by using PID controller. Cooler has two options constant value and variable air flow rate, $\overset{\bullet}{M}_{HVAC}(t)$. Based on the equation 5.4, the variable airflow rate is delivered from cooler system using PI system. The air specific heat is multiplied with airflow rate to produce cooler gain by equation 5.5. The HVAC coil temperature T_{Coil} is a variable value that is controlled by PI system. Equation 5.6 is used to calculate the absorbed heat flow from air house. There is another optional to make the T_{Coil} a variable value between 11 $^{\circ}$C to 13 $^{\circ}$C but we find that it is not given accurate result, then we follow what have been used for the VFD HVAC unit which has to be variable during the operation of cooling.

$$\overset{\bullet}{M}_{HVAC} = K_0 \frac{d(T_{\text{setpoint}} - T_{Indoor}(t))}{dt} + K_1 T_{Indoor}(t) \tag{5.4}$$

$$\text{CoolerGain}(t) = \overset{\bullet}{M}_{HVAC}(t) \times C_P \tag{5.5}$$

$$T_{Coil} = K_2 \frac{d(T_{\text{setpoint}} - T_{Indoor}(t))}{dt} + K_3 T_{Indoor}(t) \tag{5.6}$$

$$\frac{dQ_{Cooler}}{dt} = (T_{Indoor} - T_{Coil}) \times \text{CoolerGain}(t) \tag{5.7}$$

Table 5.1 Values of PID variables

Term	K_0	K_1	K_2	K_3
Value	1	1	0.005	0.9
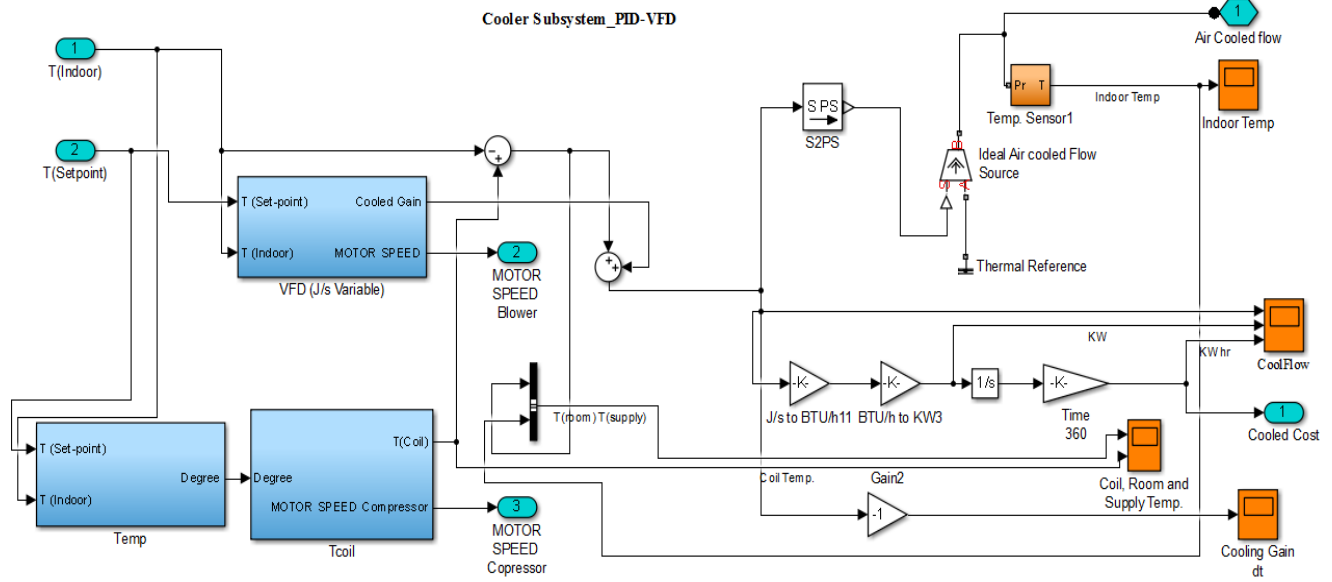
Figure 5.7 Cooler subsystem on VFD HVAC system

The block diagram of the cooler gain generator (J/s) sub-subsystem is presented in Figure 5.8 that contains of two block diagrams, one calculates the cooler gain and another one uses to calculate the desired speed/frequency that delivers to blower motor on VFD system.

Figure 5.8(a) displays the block diagram of the subsystem of cooler gain generate based on the thermal dynamic equation 5.4. The inputs of thermodynamic model of cooler are the T_{Indoor} internal temperature for house and $T_{setpoint}$ which is the desired temperature for house. The output of the model is the mass supply airflow $\dot{M}_{HVAC}(t)$ (kg/s) that multiplied by air specific heat C_P (J/kg.K^o) to produce the amount of absorbed heat flow from air house as in equation (5.5). Figure 5.8(b) shows the block diagram of the subsystem of desired speed generate based

on equations (5.1), (5.2) and (5.3). The input is the desired Q and the output is the RPM or desired speed/frequency (N or F) various time for the blower motor.
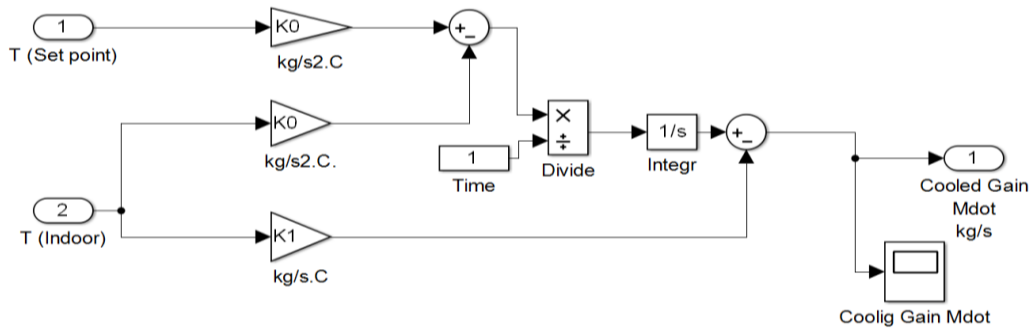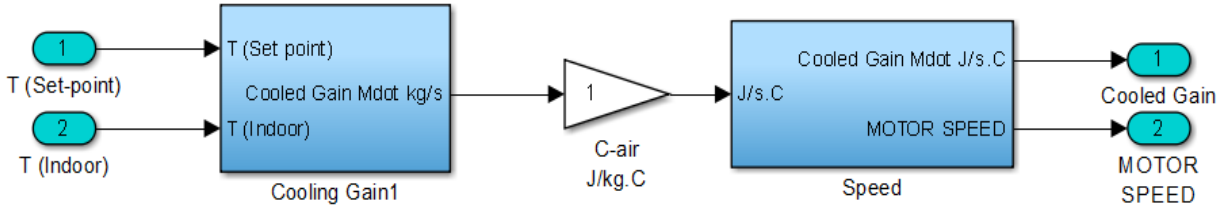
(a)
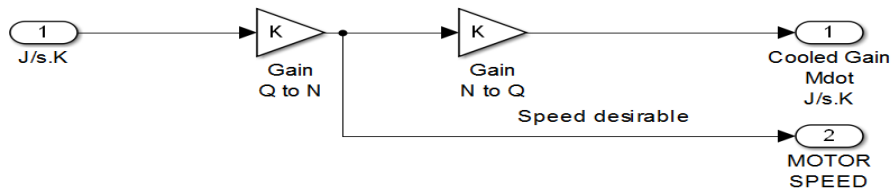
(b)

Figure 5.8 Cooler gain generator subsystem. (a): Cooler gain. (b): Desired blower speed

The block diagram of the HVAC coil temperature generator ($^{\circ}$C) sub-subsystem is presented in Figure 5.9 that also contains of two block diagrams, one calculates the HVAC coil temperature T_{Coil} and another one uses to calculate the desired speed/frequency that delivers to compressor motor on VFD system.

Figure 5.9 (a) shows the block diagram of the subsystem of HVAC coil temperature generate based on the thermal dynamic equation (5.5). The inputs of thermodynamic model of cooler are the T_{Indoor} internal temperature for house and $T_{setpoint}$.
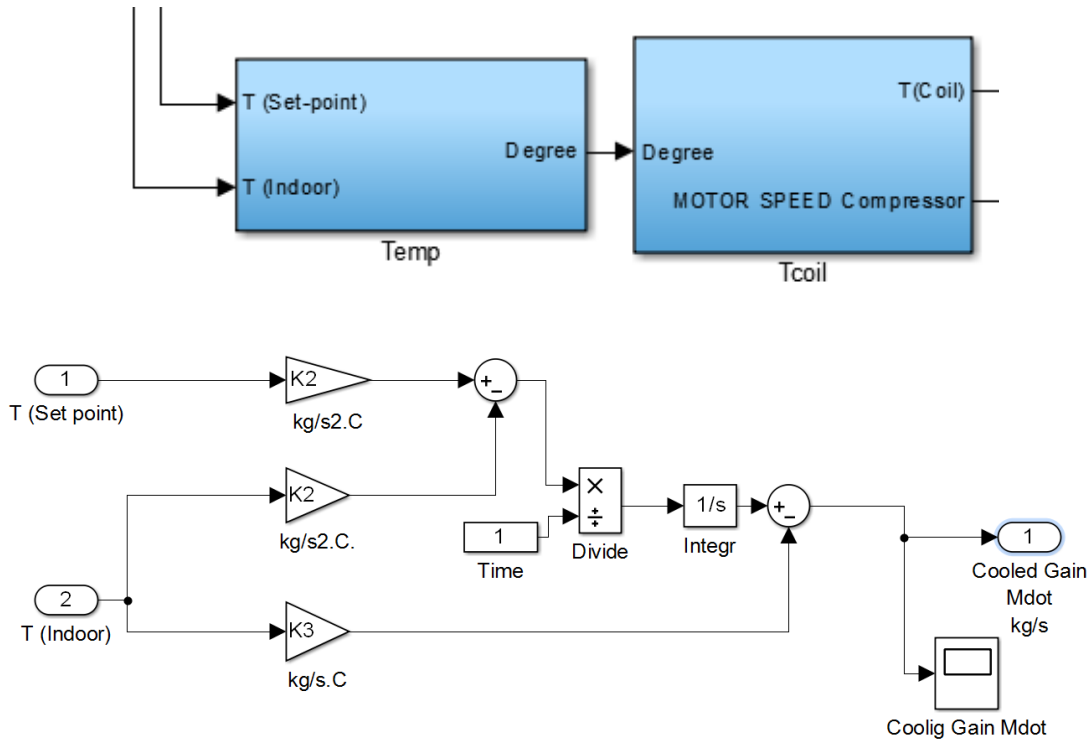
(a)
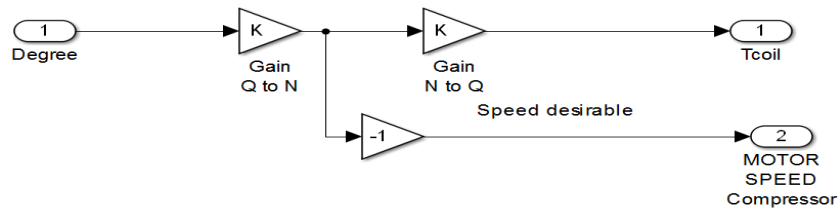
(b)

Figure 5.9 HVAC coil temperature subsystem. (a): HVAC coil temperature. (b): Desired compressor speed

The output of the model is HVAC coil temperature that adds to inside air house T_{Indoor} based on equation (5.7). Figure 5.9 (b) shows the block diagram of the subsystem of desired speed

generate based on equations (5.1), (5.2) and (5.3). The input is the desired T_{Coil} and the output is

the RPM or desired speed/frequency (N or F) with time for the compressor motor.

Figure 5.10 shows outdoor temperature and the simulated indoor temperature by using VFD-PID

controller for a hot and warm day. It can be noticeable that the indoor temperature varies at the

same level of the set point temperature, which makes the indoor environment more comfortable

for the occupants.
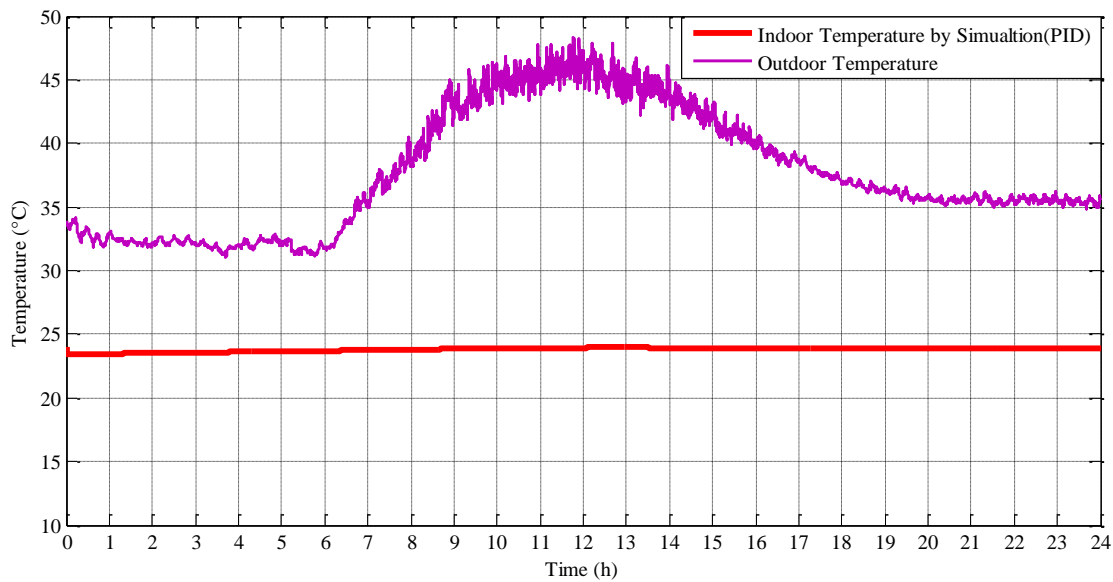
Figure 5.10 Simulated indoor temperature and actual outdoor temperature for hot and warm day

5.5 Model of HVAC VFD System by Fuzzy Logic Controller

The first model of the VFD controller has been developed for this thesis by using PID and here

in this section the second model of VFD controller has been done using fuzzy logic control.

Figure 5.7 shows the cooler subsystem of the PID replaced by FLC as it is the second proposed

method of modeling VFD-HVAC, then it will be integrated to the thermal model of the house.

Matlab/Simulink Fuzzy logic Toolbox will be used to develop and design fuzzy logic controller.

Basically, fuzzy logic controller comprised of four basic components: fuzzification, a knowledge

base, inference engine, and a defuzzification interface as shown in Figure 5.11. Each component affects the effectiveness of the fuzzy controller and the behavior of the controlled system. In the fuzzification interface, a measurement of inputs and a transformation, which converts input data into suitable linguistic variables, are performed which mimic human decision making. The results obtained by fuzzy logic depend on fuzzy inference rules and fuzzy implication operators. The knowledge base provides necessary information for linguistic control rules and the information for fuzzification and defuzzification. In the defuzzification interface, an actual control action is obtained from the results of fuzzy inference engine [56].
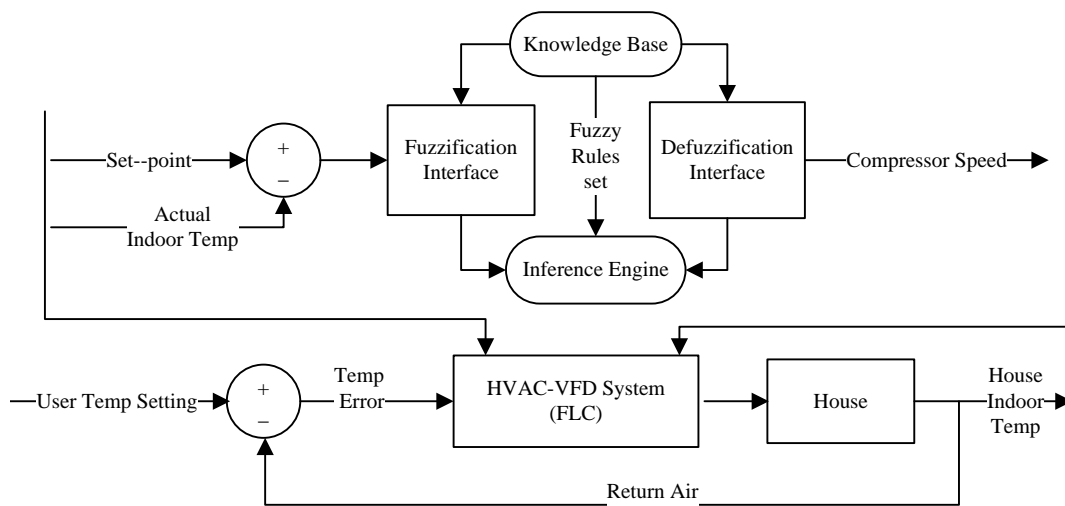
Figure 5.11 Simplified diagram for the proposed HVAC-VFD using FLC

5.5.1 Design of Fuzzy Logic Controller

The Mamdani techniques will be used in this system which consists of two control inputs and one control outputs as shown in Figure 5.12. The two inputs are the error (e) and the change rate of error (Δe). The output of the fuzzy control is variable speed compressor (Δz) and "centriod"

de-fuzzification method has chosen for controller design with the min and max inference method. The performance measurement is presented by the following equations.

$$e(t) = \text{Setpoint Temperature (t)} - \text{Actual Indoor Temperature(t)} \qquad (5.8)$$

$$e(t) = e(t) - e(t-1) \qquad (5.9)$$
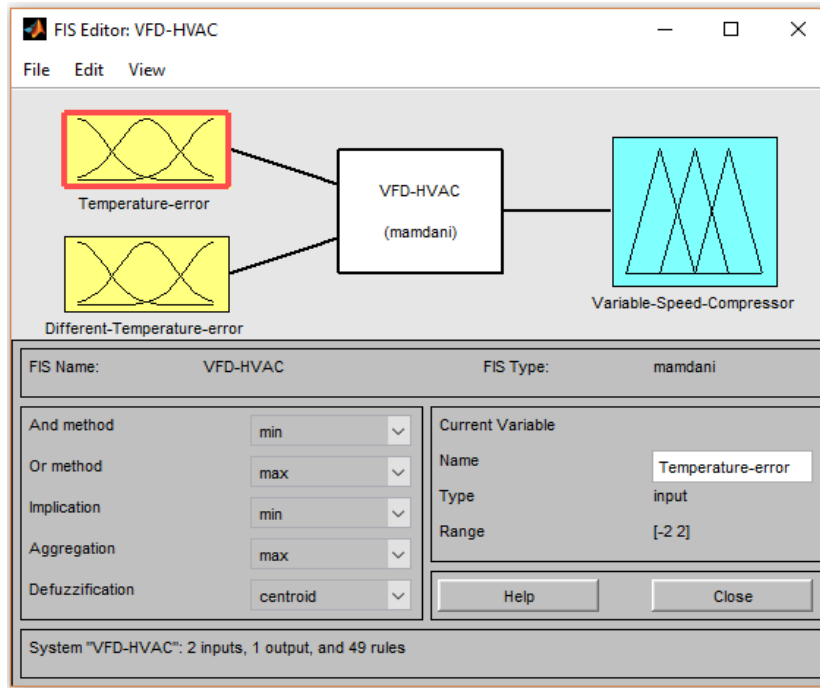
Figure 5.12 VFD-HVAC controller for the thermal model house

▪ **Input 1**

Fuzzification of temperature error (e), which is the set of the user decides temperature, as the most fluctuation bound of the temperature in the residential area is approximately $\pm 2^{o}$C. In this system (-2°C, +2°C) is the range of the temperature error. It is divided to seven memberships functions are used as zmf,smf and trigonometric membership function. Membership functions of the first input of the system are presented in Figure 5.13. In this system and the results simulation have to be validated with the measurement results, we decided to make the set point 24°C same as set-point of the house's unit (House #3307).
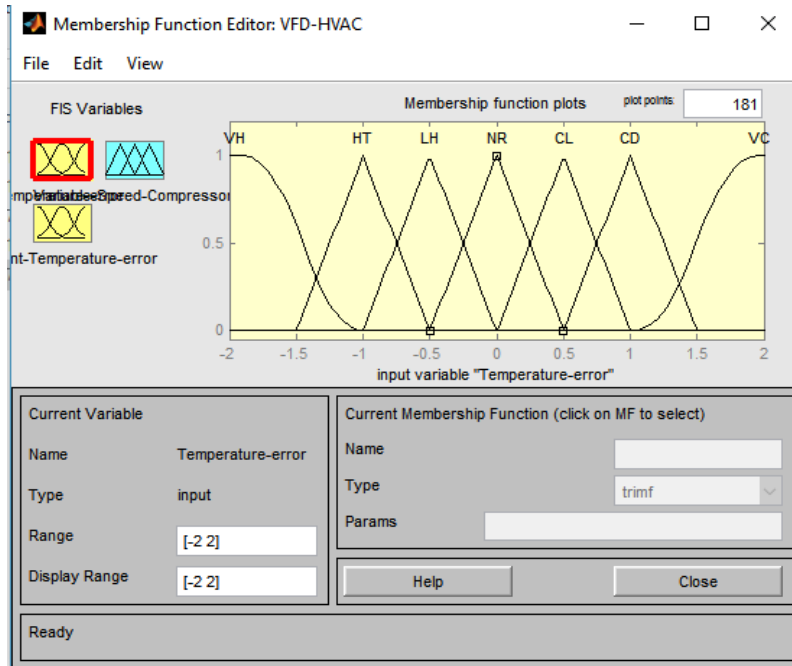
Figure 5.13 Membership function of the input 1 fuzzy variable (Temperature error)

Table 5.2 Membership function for the first input (Temperature error)

No of MF	MF (e)	Type of MF	Range (^{o}C)
MF1	Very Hot (VH)	zmf	[-2 -1]
MF2	Hot (HT)	trimf	[-1.5 -1 -0.5]
MF3	Less Hot (LH)	trimf	[-1 -0.5 0]
MF4	Normal (NR)	trimf	[-0.5 0 0.5]
MF5	Cool (CL)	trimf	[0 0.5 1]
MF6	Cold (CD)	trimf	[0.5 1 1.5]
MF7	Very Cold (VC)	smf	[1 2]

▪ **Input 2**

Fuzzification of the difference of the temperature error (Δe), the change rate of temperature error is the different sampling period. Temperature difference gives information on the difference between actual indoor temperature of the house and the set-point 24°C. The change rate of the temperature is range ±2°C. Temperature difference is divided into seven membership functions

are used as zmf, trapmf and trigonometric membership function. Membership functions of the second input of the system are presented in Figure 5.14.
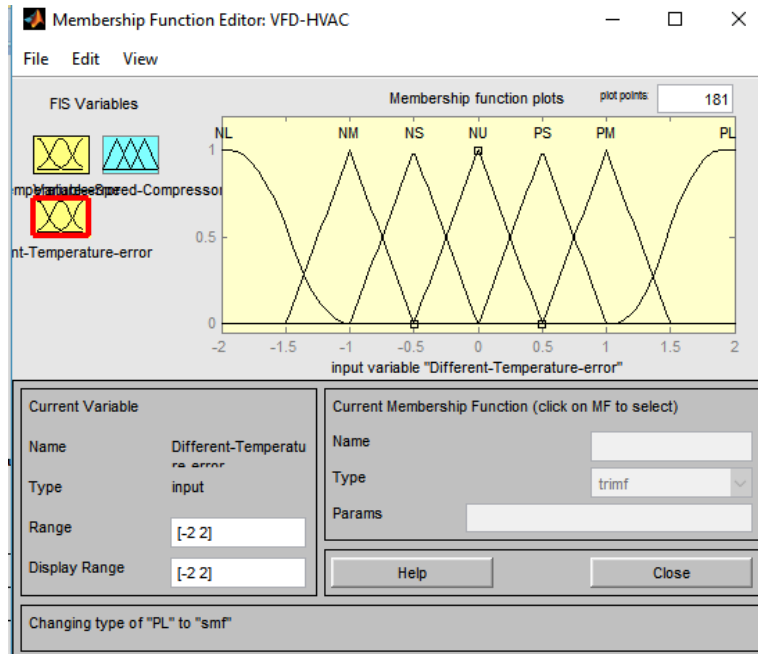
Figure 5.14 Membership function of the input 2 fuzzy variable (Different temperature error)

Table 5.3 Membership function for the second input (Different Temperature error)

No of MF	MF (Δe)	Type of MF	Range (°C)
MF1	Negative (NL)	zmf	[-2 -1]
MF2	Negative Medium (NM)	trimf	[-1.5 -1 0.5]
MF3	Negative Small (NS)	trimf	[-1 -0.5 0]
MF4	Neutral (NU)	trimf	[-0.5 0 0.5]
MF5	Positive Small (PS)	trimf	[0 0.5 1]
MF6	Positive Medium (PM)	trimf	[0.5 1 1.5]
MF7	Positive Large (PL)	smf	[1 2]

- **Output**

Fuzzification of the output is the variable speed compressor which is divided into seven membership functions and gives the required speed level of the variable speed compressor. The outlook for the system is presented in Figure 5.15. The range of this output is from 0 to 100 percentage of the speed of the compressor. In general, if the indoor temperature of the house is above the set-point then the compressor automatically gets on varies the speed according to the temperature difference.
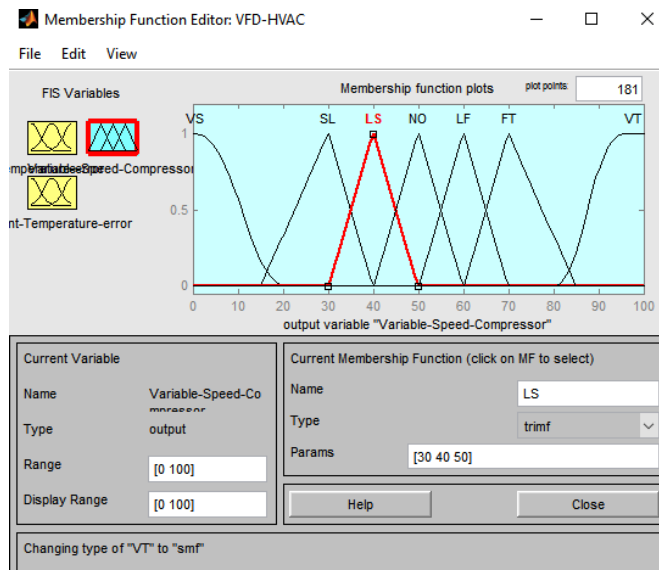
Figure 5.15 Membership function of the output fuzzy variable speed compressor

Table 5.4 Membership function for the output (variable speed compressor)

No of MF	MF(Δz)	Type of MF	Range (^oC)
MF1	Very Slow (VS)	zmf	[0 20]
MF2	Slow (SL)	trimf	[15 30 40]
MF3	Less Speed (LS)	trimf	[30 40 50]
MF4	Normal Speed (NO)	trimf	[40 50 60]
MF5	Less Fast (LF)	trimf	[50 60 70]
MF6	Fast (FT)	trimf	[60 70 85]
MF7	Very Fast (VF)	smf	[80 100]

91

- **Rules of the System**

This system contains 49 rules that cover the two inputs and one outputs membership function is presented in Figure 5.16 There is a combination of variable speed compressor in order to control the indoor temperature for the house. Three different rules as such example we are showing.

- 1. If (Temperature-error is VC) and (Different-Temperature-error is NL) then (Variable-Speed-Compressor is VS)

- 2. If (Temperature-error is VC) and (Different-Temperature-error is NM) then (Variable-Speed-Compressor is SL)

- 3. If (Temperature-error is VC) and (Different-Temperature-error is NS) then (Variable-Speed-Compressor is SL)
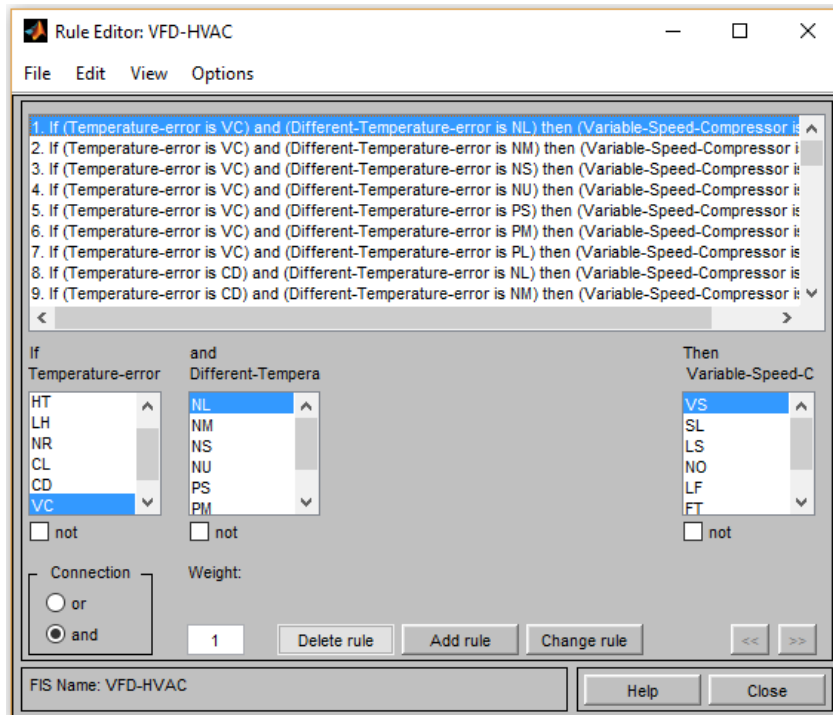
Figure 5.16 Rules editor in Simulink/Matlab

The rest of the rules are listed in Table 5.5.

Table 5.5 Rules of fuzzy control of VFD-HVAC

(Δz)		(e)						
		VC	CD	CL	NR	LH	HT	VH
(Δe)	NL	VS	VS	SL	LS	LS	NO	LF
	NM	SL	SL	LS	LS	NO	LF	LF
	NS	SL	LS	LS	NO	NO	LF	LF
	NU	LS	LS	NO	NO	LF	LF	FT
	PS	LS	NO	LF	LF	LF	FT	FT
	PM	NO	LF	LF	LF	LF	FT	VF
	PL	LF	LF	LF	LF	FT	VF	VF

The view features in the editor allow us to visualize the control space in three dimensions as shown in Figure 5.17.
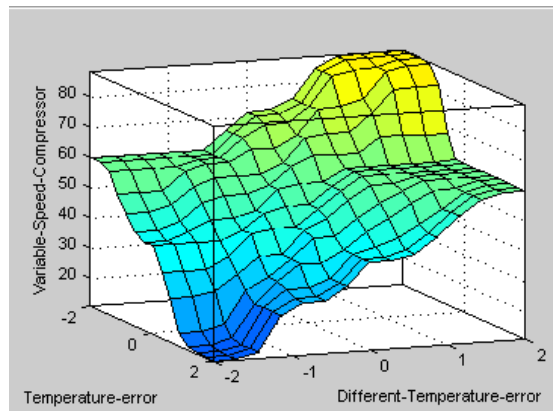
Figure 5.17 Variation of variable speed compressor

The Rule Viewer allows us to manually vary the inputs and observe the outputs result. As shown in Figure 5.17. FLC is implemented to control the compressor speed (air flow) according to the error between indoor temperature and the temperature set point. We have scaled and normalized the error as such (-2 to +2). Figure 5.18 shows the simulated indoor temperature and the actual outdoor door temperature for a hot and warm day. It can be noticeable that the indoor temperature varies at the same level of the set point temperature, which makes the indoor

environment more comfortable for the occupants. Comparing to the PID controller, FLC controller can achieve a typical indoor temperature with less energy consumption.
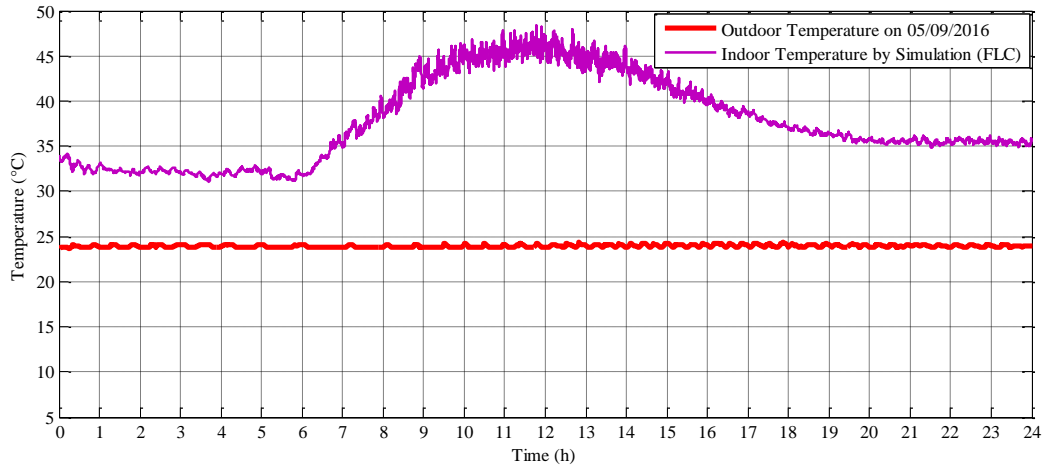
Figure 5.18 Simulated indoor and actual outdoor temperature for a hot and warm day

Figure 5.18 shows the indoor temperature distribution at temperature set point. The output signal of the error between set point temperature and indoor air temperature is generated to vary the speed of the compressor according to the error. The air flow speed is directly proportional to the frequency of the electricity provides to the motor. The controller minimizes the error between the set point temperature and indoor temperature. Beside that different set point temperature effect of the motor speed and room temperature in terms of taken to reach the required temperature. FLC will control the motor at the slow speeds to maintain the room temperature and its consequences use less energy.

5.6 Model of HVAC VFD System by PWM-PI

The block diagram of variable speed HVAC cooling air system is shown in Figure 5.20. It consists of two blocks, one block represents the PI controller and the second block represents the PWM to generate variable speed, which counts for flow rate of cooling air. The PWM block is already built in Simulink/Matlab and the main function of PWM in our simulation study is only

to integrate the signal coming from the PI and calculate the area under curve for evaluating the energy consumption.
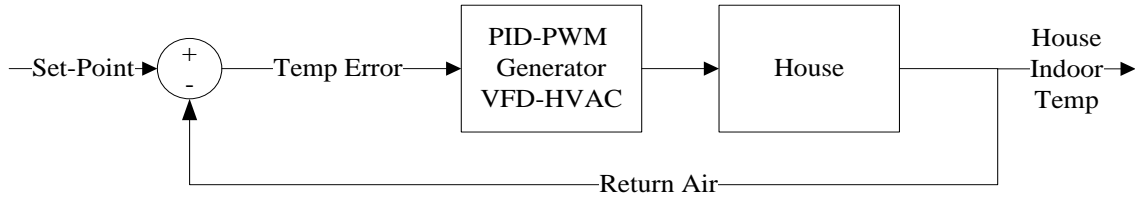
Figure 5.19 Simplified diagram for the proposed HVAC-VFD using PID-PWM
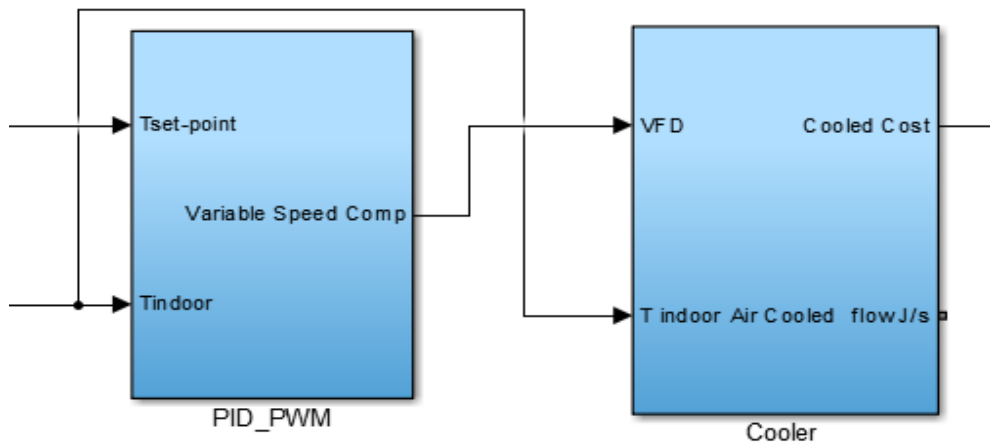
Figure 5.20 Cooler PID-PWM subsystems
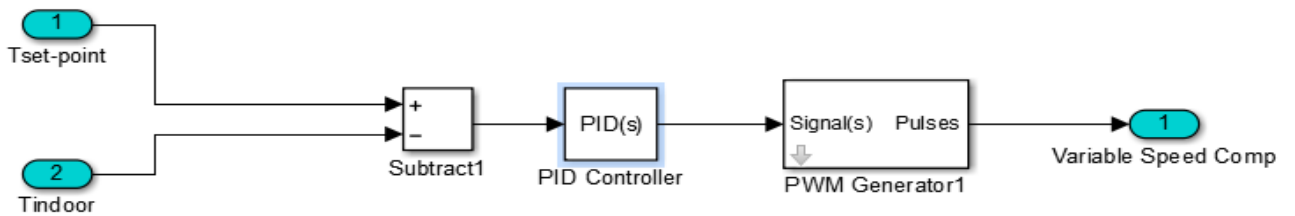
(a)
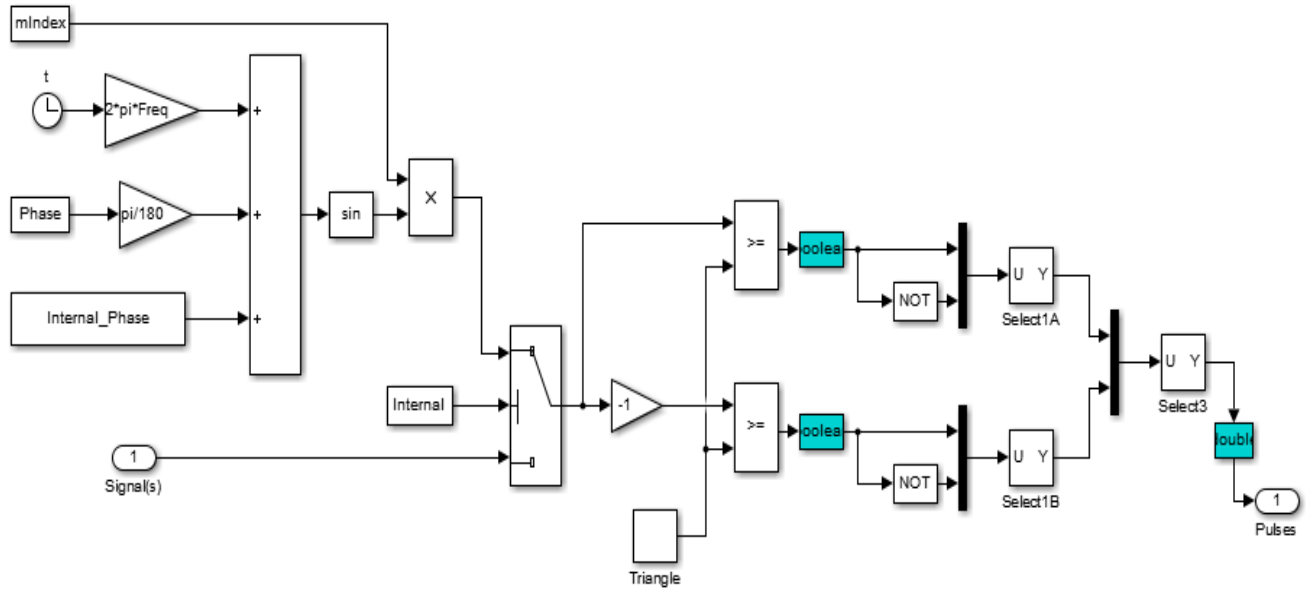
(b)
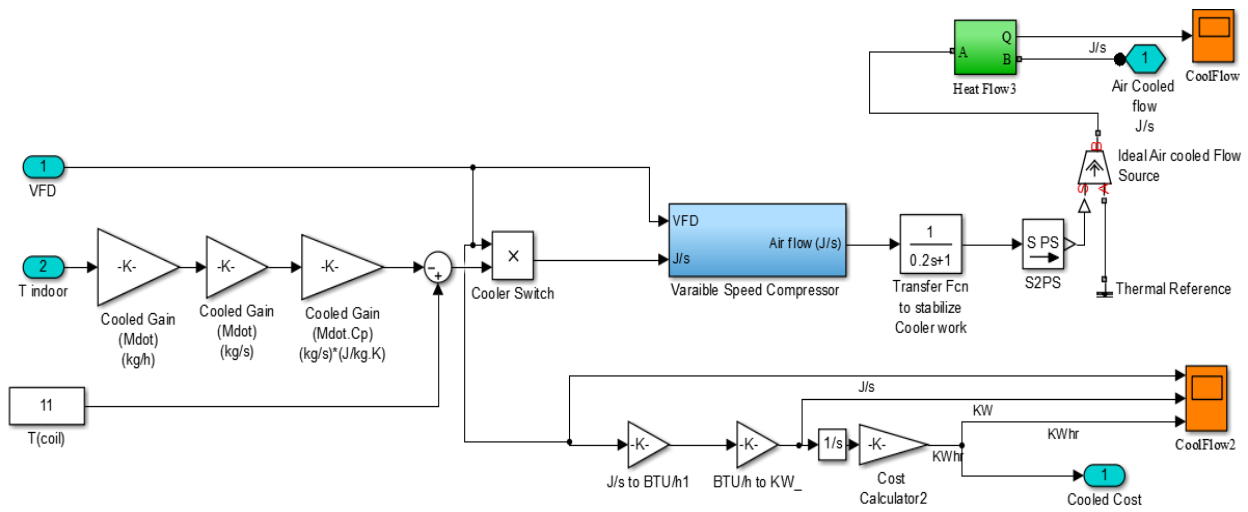
(c)

Figure 5.21 VFD-HVAC PID-PWM subsystems. (a): Desired compressor speed , (b): Cooler of HVAC ,(c): VFD-PI-PWM complete system

Figure 5.21 (a) shows the PI controller for the cooler system; it is used to controller the speed of the air flow which going to the thermal model of the house. Figure 5.21 (b) shows the pulse width modulation which has developed in Matlab/Simulink. The PWM block used to give

96

integrate the pulse that coming from the PI controller, as the error coming positive and negative, the modulation index is conducting the process of integration of the air flow.

Figure 5.21 (C) shows a complete design of the VFD-PWM-PI HVAC system which will be integrated to the thermal model of the house. Figure 5.22 shows the simulated indoor temperature and the actual outdoor door air temperature for a hot and warm day. It can be noticed that the indoor air temperature is almost constant, and it is in the same level of set point temperature throughout the day.
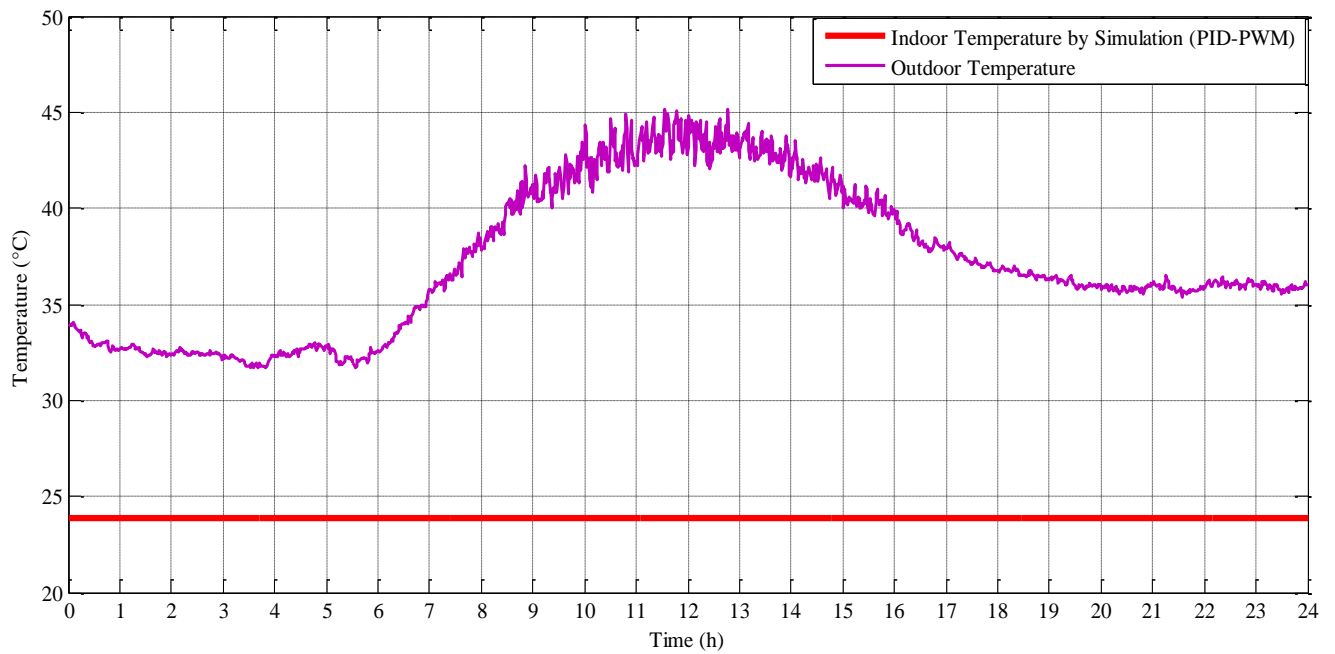
Figure 5.22: Simulated indoor and actual outdoor temperature for a hot and warm day

CHAPTER 6

EXPERIMENTAL SETUP OF HVAC SYSTEM

6.1 Introduction

This chapter will discuss the experimental HVAC systems setup for both houses in details. Monitoring and measurement system will be described, following by weather and environmental conditions. Figure 6.1 shows the schematic diagram of the experimental study.
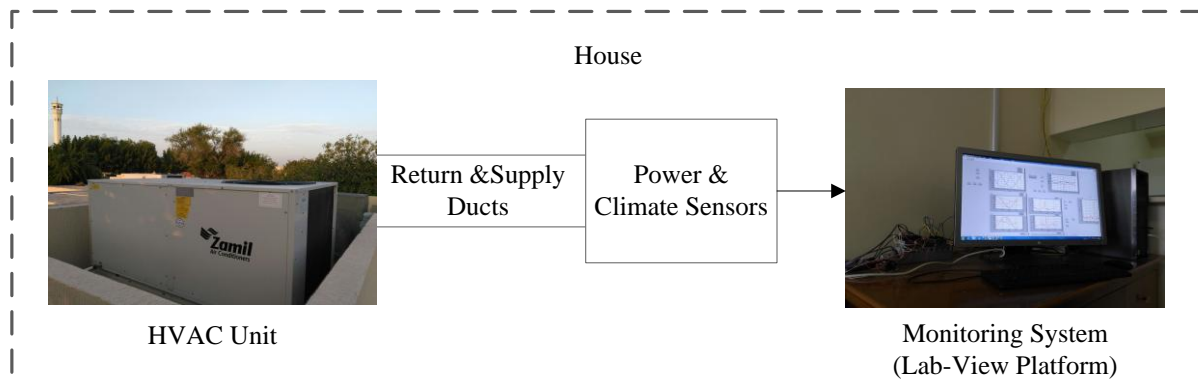
Figure 6.1 Schematic diagram of the experimental study

6.2 Experimental Analysis

The major role of the experimental work in this study is to confirm the validity of the simulation work and to evaluate the performance and energy consumption of the HVAC systems. The monitoring and measurement hardware systems comprise of four major blocks: two 5-ton Al-

Zamil air conditioning rooftop units, a data acquisition (DAQ) chassis with National Instrument modules (LabView), sensors, and a host computer. The National Instrument DAQ-chassis monitoring system has several modules such as voltage measurements, current measurements, and thermocouples. There are four thermocouple sensors (three sensors for indoor and one for outdoor temperature), two humidity sensors (indoor and outdoor), an irradiation sensor, barometric pressure sensor, three air flow sensors and two wind speed sensors. The host computer has the National Instrument (NI) software, which is the main communicator with DAQ-chassis. The host computer initiates the execution commands and stores the data in the hard drive and displays them on the monitor.

6.2.1 Experimental Set-up

The experiments were conducted in the Guest Houses at KFUPM campus, Dhahran, Saudi Arabia. The floor plan of both houses is shown in Figure 6.2. The 3D drawing of both houses is indicated in Figure 6.3(a), and the ducts plan is shown in Figure 6.3(b), each house consists of living room, bedroom, kitchen and bathroom. Moreover, all details of the houses which are integrated with ON/OFF and VFD HVAC systems are described in this section and followed by HVAC monitoring and measurement system.

6.2.1.1 Houses Details

General project information for houses #3305&#3307, location and environment parameters are presented in Table 6.1.

Table 6.1 The Environment parameters for project location

Weather reference city	Dhahran, Saudi Arabia
Project Location	KFUPM, Guest-Houses #3305&#3307

House #3305	ON/OFF HVAC unit
House #3307	VFD HVAC unit
Barometric pressure:	1007.652 mbar
Altitude	22.86 meters
Latitude and Longitude	26.288768 and 50.114103
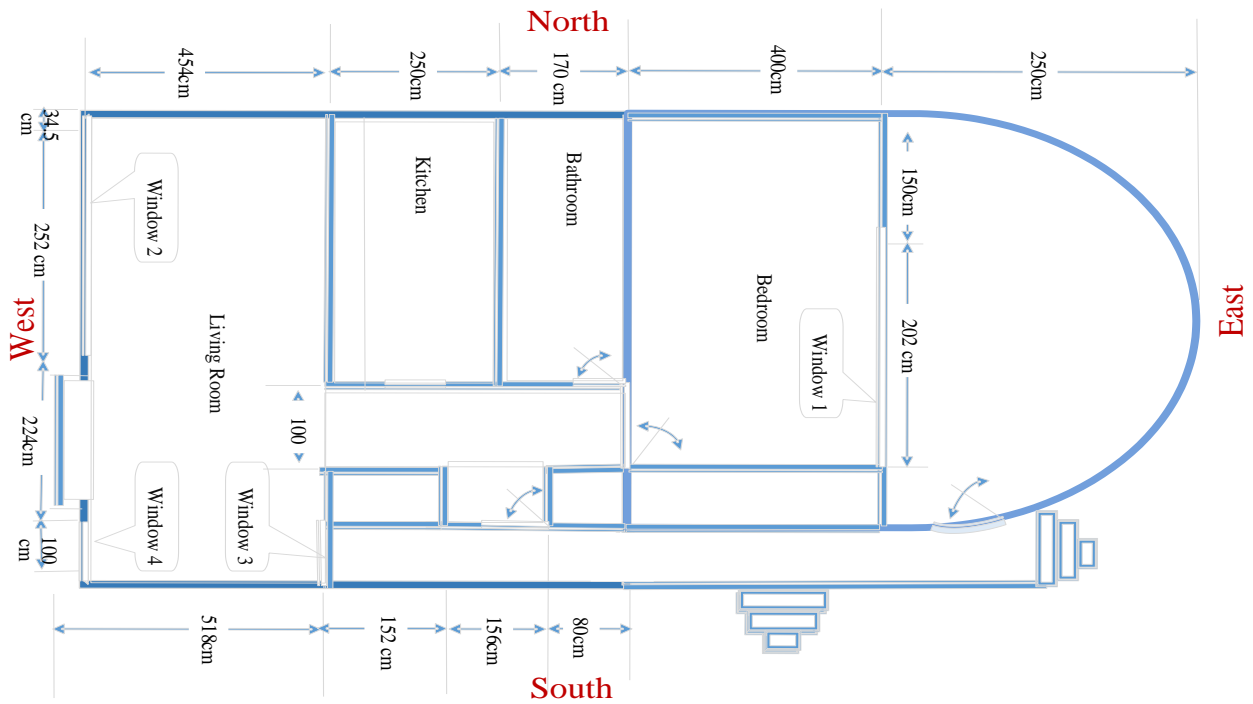
Figure 6.2 Floor plan for houses #3305& #3307
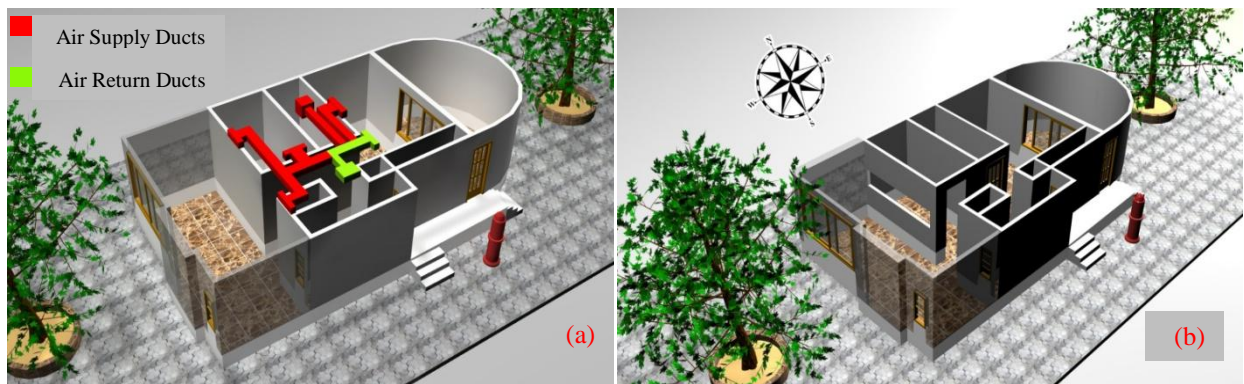
Figure 6.3 (a) 3D drawing for the houses (b): Ducts plan for #3305 and #3307 houses

6.2.2 Air Conditioning Units

In the tropical area and especially the summer time, high relative humidity, elevated air temperatures, and bright sunshine can sometimes combine to produce an uncomfortable indoor environment. An air-conditioning system can provide comfort for occupants by lowering the air temperature and the humidity level in the home. Two HVAC units are used in this study. Conventional ON/OFF cycle HVAC unit is installed in house #3305 and VFD HVAC unit is installed in house #3307. The two units have some common terms we will come across then comparing and determining the best choice for air conditioners:

1. The refrigerant is a substance that circulates through the air conditioner, alternately absorbing, transporting and releasing heat.

2. A coil is a system of tubing loops through which refrigerant flows and where heat transfer takes place. The tubing may have fins to increase the surface area available for heat exchange.

3. The evaporator is a coil that allows the refrigerant to absorb heat from its surroundings, causing the refrigerant to boil and become a low-temperature vapor.

4. The compressor squeezes the molecules of the refrigerant gas together, increasing the pressure and temperature of the refrigerant.

5. The condenser is a coil that allows the refrigerant gas to give off heat to its surroundings and become a liquid.

6. The expansion device releases the pressure created by the compressor. This causes the temperature to drop and the refrigerant to become a low-temperature vapor/liquid mixture.

7. The plenum is an air compartment that forms part of the system for distributing warmed or cooled air through the house. It is generally a large compartment immediately above the heat exchanger.

6.2.2.1   The ON/OFF Cycle HVAC System

The schematic diagram for conventional HVAC system is described in Figure 6.4. The compressor (CM) and the blower (BM) are fed in HVAC unit by three phase system with V_{LL}=230 V, connected to supply by compressor contactor (CC). The Fan motor (FM) is connected between two phases 230V and integrated with compressor motor. Electronic control board (ECB) is built for detecting and controlling the ON/OFF cycle unit. Thermostat device is connected to ECB to detect the setting and room temperatures. The CC and BMC is controlled by ECB continuously. Transformer 240V/12V is used to apply ECB and relays.

The unit was built and wired according to the Al-Zamil air conditioning standers and specifications. The main components of the ON/OFF unit, is the BLDC motor for the compressor, the ON/OFF frequency should be less than 250 cycles per day, which meant that the ON/OFF cycle shall not exceed on average of 10 times/hour. The set point of experimental study for the ON/OFF unit is fixed as 24 ^{o}C, and the condenser fan was set auto.

Table 6.2 Specifications of ON/OFF unit

Item	Description
ON/OFF	Run and stop operation.
Operation Mode	Switches between Cool /Auto/Fan/Heat.
Temperature Setting	The set point temperature for cooling in the following range: 15°C to 30°C.
Fan Speed Setting	Fixed high or low or it can be auto.
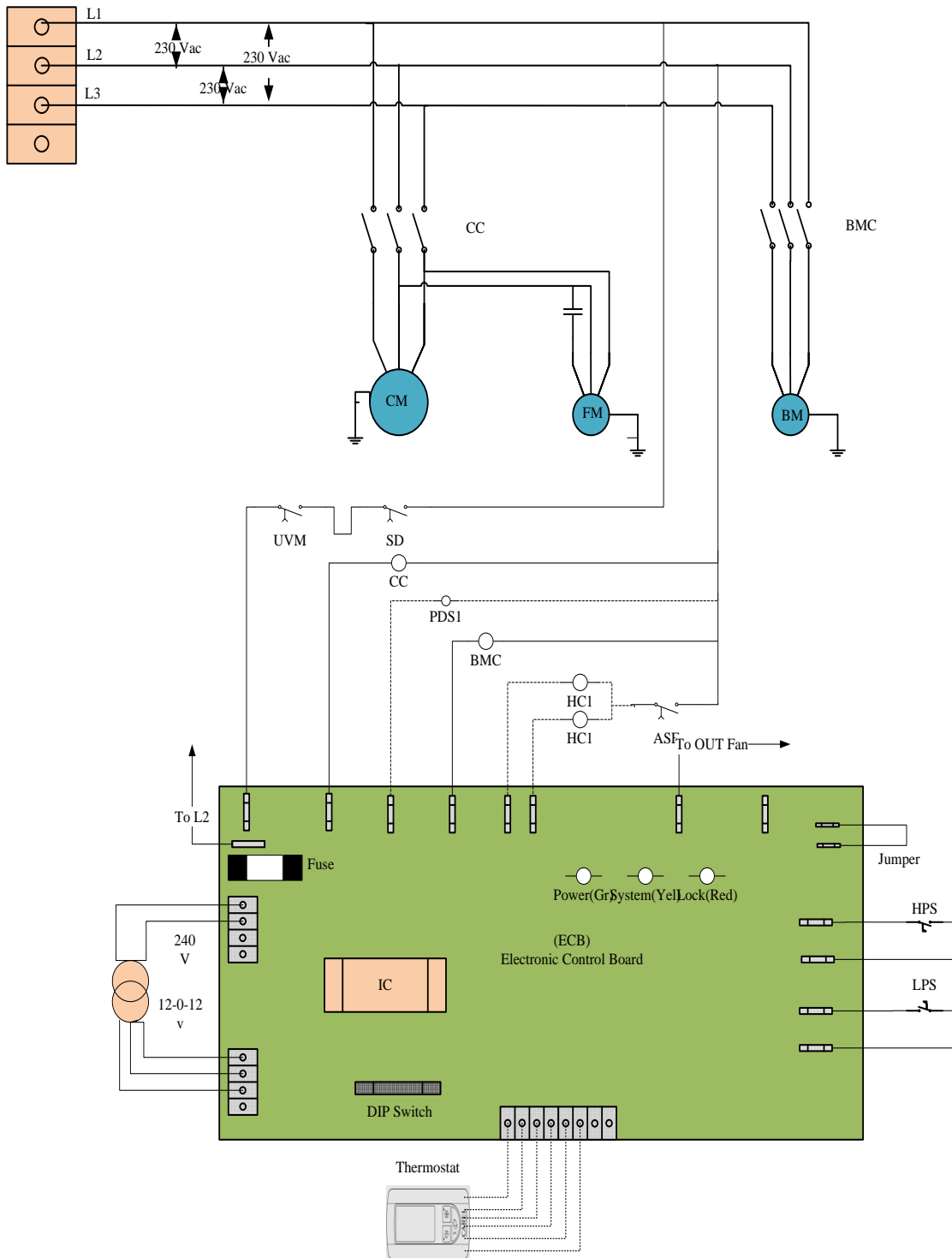
Figure 6.4 Schematic diagram for ON/OFF HVAC unit

L1
L2
L3

230 Vac
230 Vac
230 Vac

CC
BMC

CM
FM
BM

UVM
SD
CC
PDS1
BMC
HC1
HC1
ASF To OUT Fan

To L2
Fuse

240 V
12-0-12 v

IC

(ECB)
Electronic Control Board

Power(Gr) System(Yel) Lock(Red)

Jumper

HPS

LPS

DIP Switch

Thermostat

We are given some reported data for the motors and the compressor of the ON/OFF unit which have investigated experimentally in our study. Table 6.3 is presented the energy consumptions for different outdoor temperature with several heat capacities in the house. The power consumptions and the input current have also listed in the Table 6.3.

Table 6.3 Experimentally test data for the ON/OFF unit

Outdoor °C	Capacity Btu/hr	Unit Capacity kW	Power (W)	Input current (A)
24	76000	22.274	5282	15.55
29.4	72100	21.132	5796	16.17
35	66500	19.489	6415	18.3
37.8	62300	18.258	7100	20
46	57900	16.968	7842	21.8
51.5	52965	15.522	8657	23.86

- ## ON/OFF Unit Compressor Specifications

Table 6.4 shows the main specifications of the ON/OFF unit such as the unit model, voltage range and refrigerator type. Furthermore, the standard temperatures of the condenser, evaporator and return gas have also presented in the Table 6.4.

Table 6.4 Compressor data of ON/OFF unit

Compressor Information			
Compressor Model	ZP61KCE-TF5	Phase	3
Refrigerant	R-410A,Mid Pt	Frequency	60
Volts	200-230	Application	Air Conditioning
RLA(MCC/1.4) (Amp)	21.2	MCC (Amp)	29.7
RLA(MCC/1.56) (Amp)	19.0	LRA (Amp)	123.0
Inputs			
Condensing Temperature (°C)	54.4	Evaporator Superheat (°C)	-6.6
Evaporator Temperature (°C)	7.22	Compressor Superheat (°C)	-6.6
Return Gas Temperature (°C)	18.33	Total Sub-cooling (°C)	-9.44
Results			
Compressor Capacity (But/hr)	61,500	Refrigerant Flow Rate (lb/hr)	
Net Refrigeration Effect (But/hr)	61,500	Current (Amp)	16.8
Power (W)	5,700	Isentropic Efficiency (%)	72.0
Compressor EER (Btu/Wh)	10.79	Liquid Temp (°C)	46
Condenser Heat Rejected (Btu/hr)	80,954		

The Table 6.5 provides information for the compressor which it's varies as per condition of the

outdoor temperature change by step of 5.5°C from 24°C to 51.5°C.

Table 6.5 Compressor power varying per outdoor temperature

Outdoor °C	Power (W)	Current (A)
24	3960	12.7
29.4	4400	13.7
35	4900	14.9
37.8	5500	16.3
46	6100	17.8
51.5	6800	18.6

According to Al-Zamil air conditioning Company, Table 6.6 shows the data of blower motor for

ON/OFF unit.

Table 6.6 Blower motor data

Item	Unit	Stander	Unit motor Value
Break Down Torque	Nm	4.42	3.42
Locked Rotor Torque	Nm	1.16	0.82
Rated Torque (Full Load)	Nm	3.76	3.38
Rated Input Power (Full Load)	Watts	798	742
Rated Current (Full Load)	Amps	3.17	3.53
Locked Rotor Current	Amps	6.57	5.04

According to Al-Zamil air conditioning Company, Table 6.7 shows the data of condenser motor

for ON/OFF unit.

Table 6.7 Condenser motor data

Item	Unit	Stander
Break Down Torque	Oz.ft	50.75
Locked Rotor Torque	Oz.ft	20.7
Rated Torque (Full Load)	Oz.ft	50.4
Rated Input Power (Full Load)	Watts	749
Rated Current (Full Load)	Amps	3.59
Locked Rotor Current	Amps	7.9

7

6.2.3 The VFD HVAC System

Online block diagram for VFD HVAC system is described in Figure 6.5. The refrigerant cycle from compressor, condenser, expansion valve and evaporating is shown in Figure 6.5. Compressor driver "brushless DC compressor" is connected between controlling unit and BLDC compressor. Interface unit and thermostat device are joined to control the HVAC.
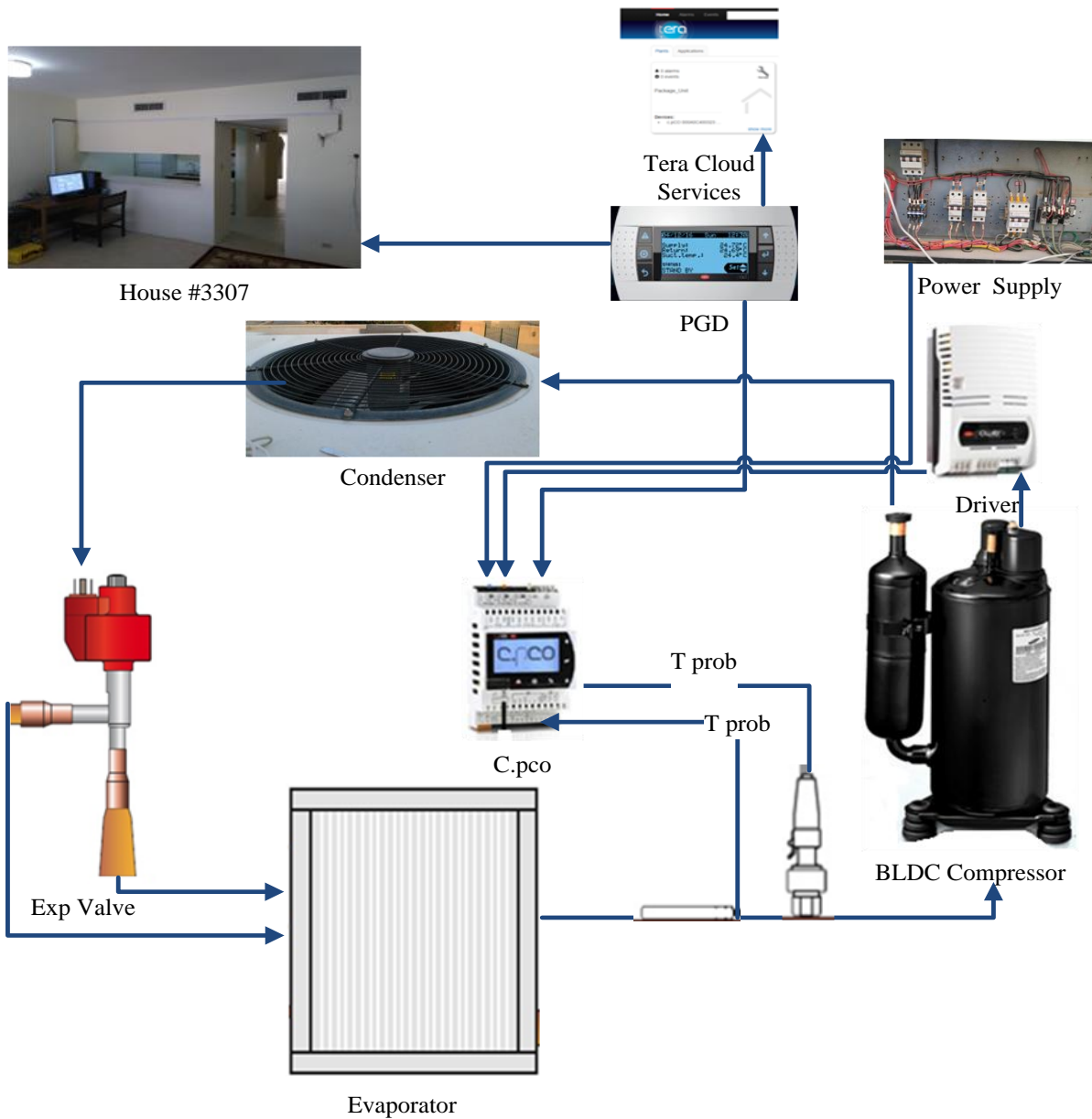
Figure 6.5 Online diagram of VDF air conditioning unit

The schematic diagram for VFD HVAC system is shown in Figure 6.6. One BLDC compressor (CM) is installed in HVAC unit through BLDC compressor driver. The driver is fed by three phase line 230 Voltage. Three phase circuit breaker (CB) is used to protect the compressor and driver. Fan motor (FM) and blower motor (BM) are connected to two phases 230 Voltage through two circuit breakers. The unit was built and wired according to the Al-Zamil air conditioning standard and specifications.
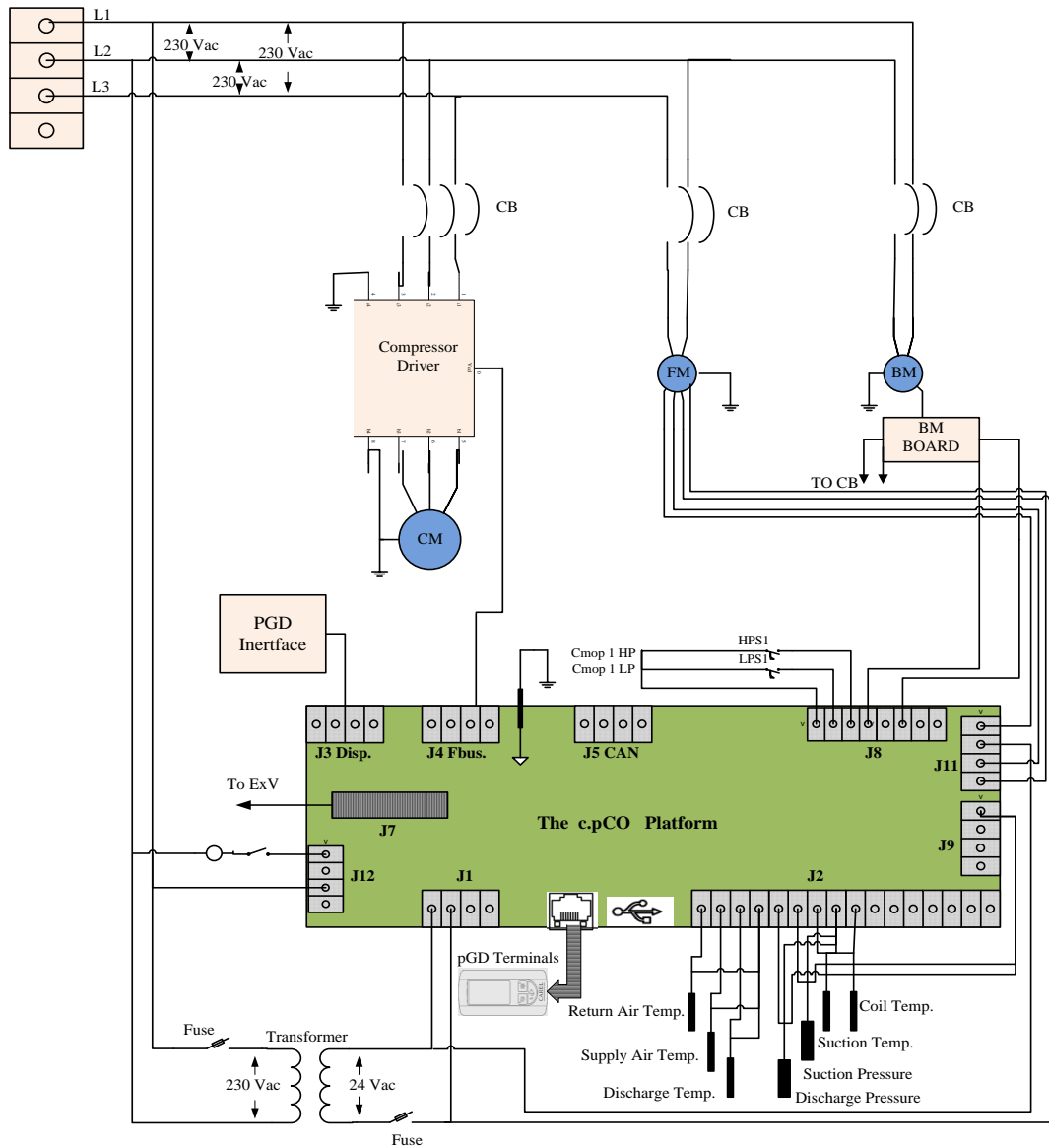
Figure 6.6 Schematic diagram for VFD- HVAC unit

6.2.3.1 Connected Programmable Controller (c.pCO)

The programmable controller (c.pCO) is built to control the compressor, fan motor, blower motor and electronic extension valve. The temperature and pressure sensors are fixed on the unit and they are connected to c.pCO. Supply air temperature, return air temperature, discharge and suction temperatures, discharge and suction pressure are detected by the controlled unit. The VFD HVAC system user interface is the Programmable Graphic Displays (PGD) terminal that is an electronic device allows graphic management using the icon-based display. The supply voltage to c.pCO unit is occurred using a step down transformer 230V/24V. The unit can be turned on and off from the user menu and the status can be displayed as shown in Figure 6.7, also the user can set the temperature set point from the same menu of PDG.
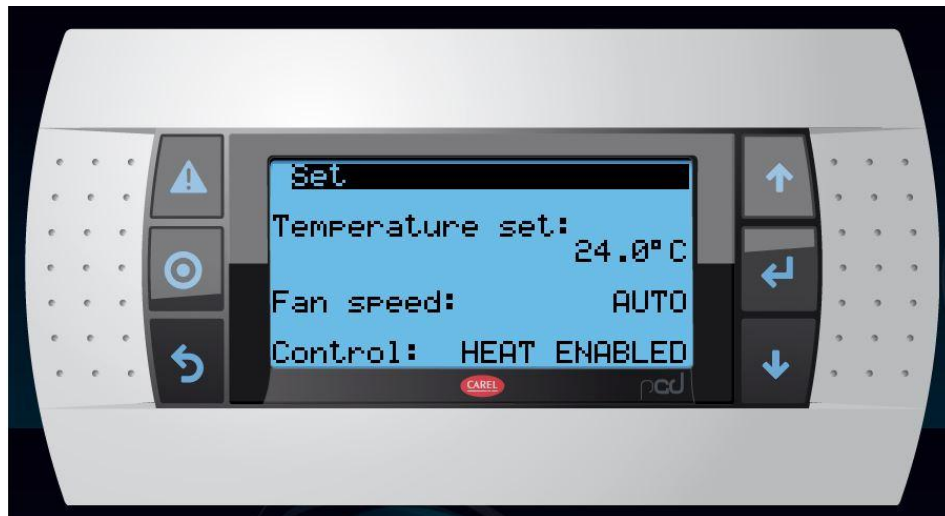
Figure 6.7 PDG screen for the user to set the set point and ON-OFF the unit

Microprocessor-based, programmable electronic controller (c.pCO) is featuring a multitasking operating system, compatible with the c.pCO. Sistema family of devices includes programmable controllers, user terminals, gateways, communication devices and remote management devices. These devices represent a powerful control system that can be easily interfaced with most

Building Management Systems (BMS) available on the market. The controller has been developed by manufacturers to provide solutions for several applications in air-conditioning, refrigeration and HVAC systems [43].

6.2.3.2   C.pCO Connection to cloud TERA

The c.pCO controller's family can establish a remote secure connection to the Carel cloud server platform called TERA. Every c.pCO with built-in Ethernet interface is natively integrated into TERA cloud platform and can access to linked services. Every c.pCO is uniquely identified by the Tera cloud using its MAC address. For this project we create a customized private portal according to our experiment specifications. TERA platform can provide us live reading for our system parameters we can set up from the office and monitor our system. Also we are able to create a report for different period of time for the HVAC unit. Figure 6.8 is presenting live different parameters such as supply and return temperature, frequency, discharge and suction temperature.
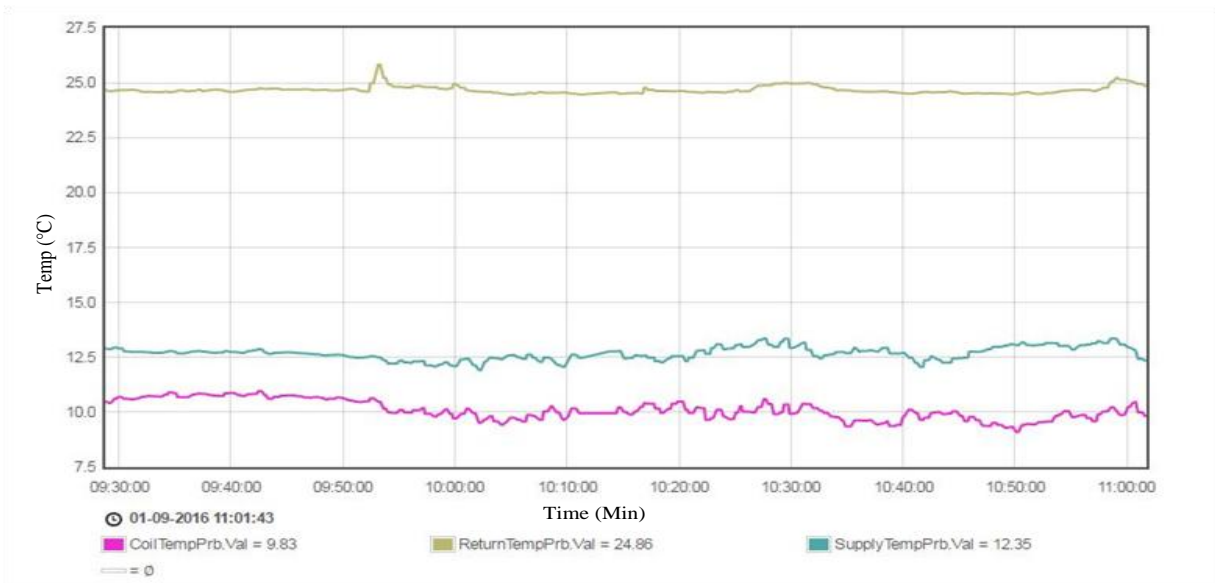
Figure 6.8 Live reading for HVAC unit's parameters

- **Temperature control**

The c.pCO unit allows the control of the supply and return temperatures for the unit.

PID Control: There are two types of Proportional, Integral and Derivative (PID) control.

- PID control on startup
- PID control during operation

The startup control must prevent an excess of requested power. Since at startup the status of the load is not known but only the temperature is, the power must be entered little by little, waiting for the reaction of the system. It can regulate on the value of the return temperature using a wide proportional band (2-3 times the nominal thermal gradient) and a large enough integral time that is greater than the system time constant.

The control during operation must be quick in order to follow any load variations and maintain the supply temperature as close to the set point value as possible. In this case, the time constant is given by the reaction of the compressor - evaporator system and is in the order of a few tens of seconds (slower with shell and tube evaporators, faster with plate evaporators). The PID controllers integrate the "anti-windup" function that limits the integral action when the request has reached the maximum and minimum limits.

- **Evaporator Fan**

A delay can be set between the fan startup and thermo-regulation enabling. A delay can also be set between the shutdown of the last compressor and fan shutdown.

- **Compressor Management**

Safety time control: The c.pCO ensures the compressor safety timings as:

- Minimum on time

- Minimum off time

- Minimum time for consecutive startups

These times are in the compressor menu and can be changed by accessing with service password.

- **BLDC Regulation**

The operating limits (hereafter defined as envelope) of the BLDC compressors are controlled. This control cannot be disabled in order to prevent the compressor from working outside of the safety limits dictated by the manufacturer. All the compressors are inserted thus contain the envelope data. Besides the operating limits specified by the manufacturer, there is the possibility of customizing the maximum condensation and minimum evaporation thresholds. These thresholds are considered only if they are more restrictive than the operating limits. The choice of a compressor with a type of gas is binding in the choosing the refrigerant type. The description of the work zones of a generic envelope are shown in Figure 6.9.
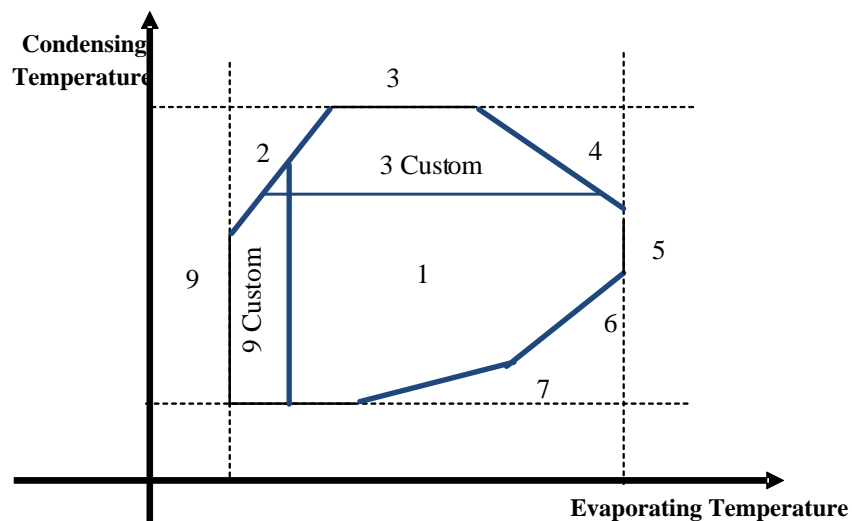
Figure 6.9 The operation limits for BLDC compressor motor

Table 6.8 shows the zone description for BLDC compressor motor, it describes the max and the min zone of each point of Figure 6.9.

Table 6.8 Zone description for BLDC compressor motor

Zone	Description
1	Zone inside the operating limits (the prevention is active to avoid going outside the limits)
2	Max compression ratio
3	Max condensation pressure
3 Custom	Max condensation pressure custom threshold
4	Max motor current
5	Max evaporation pressure
6	Min compression ratio
7	Min differential pressure
8	Min condensation pressure
9	Min evaporation pressure
9 Custom	Min evaporation pressure custom threshold

- **ExV device**

The EVD driver for the electronic expansion valve is a fundamental device/control in the c.pCO controller. It allows safe management of the compressor and circuit and reads all of the essential probes for regulating suction superheat, managing the work zone and the discharge temperature.

- **Pump-Down**

The purpose of the pump-down function is to reduce the quantity of refrigerant in the evaporator to limit the presence of liquid in suction during the compressor startup phase. Pump-down can be controlled by the electronic expansion valve (ExV). In general, the pump-down can be activated in two phases: at compressor start up or shut down. c.pCO manages the pump-down in both phases. In the compressor shutdown phase it stops when the evaporation pressure reaches the pump-down end set-point. In the compressor startup phase, the pump-down ends when the

pressure difference between discharge and suction reaches the nominal value if prevention is enabled or the minimum evaporation pressure threshold is reached.

- **Condenser Fans**

Control in chiller mode: Fan control can be modulating or ON/OFF and controls the saturated temperature value equivalent to the condensing pressure. The control diagram is displayed in Figure 6.10. From Figure 6.10 some offsets are given a numeric value that indicates that they cannot be changed from the display; they are fixed. The fan control set-point is related to the minimum condensation value of the envelope plus an offset.
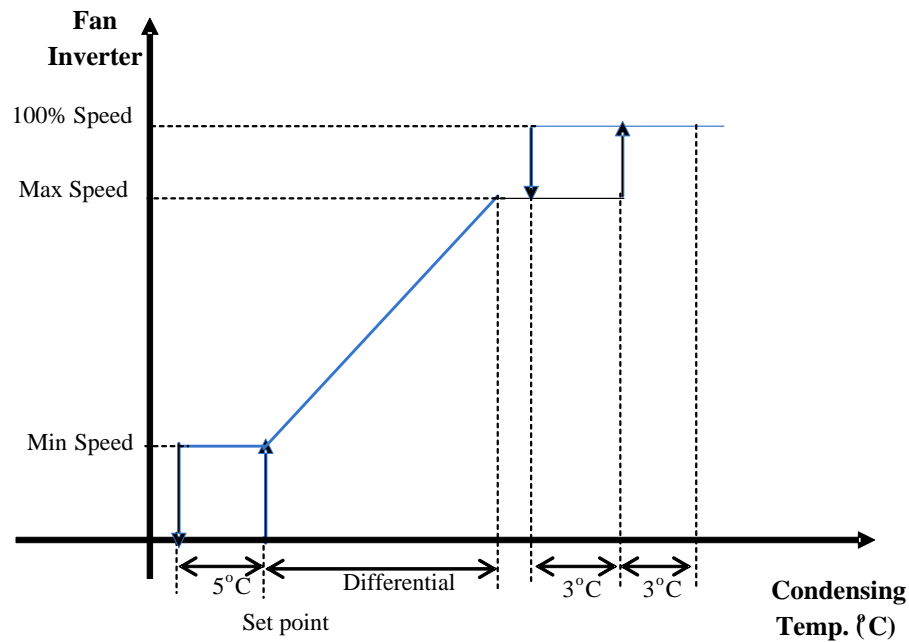
Figure 6.10 The control diagram of fan motor

6.2.3.3 BLDC Compressor Driver

BLDC compressor driver is a special inverter that can control compressor with permanent magnet brushless motors (BLDC/BLAC). The driver is integrated into c.pC. It brings significant energy savings by modulating compressor speed and consequently the cooling capacity of the

unit. Variations in load are managed precisely and with constant control of the compressor envelope. The standard specifications for BLDC compressor driver used in the VFD HVAC system are described in Table 6.9 [42].

Table 6.9 Standard specification for BLDC compressor driver

Inverter type	4THB F010i	
	Converter	3 Ø Diode Rectifier
Inverter Control method	Inverter	3 Ø IPM Inverter
	Method	Sensor-less Vector Control Method
	Voltage	3 Ø 200 - 240 V~
Power Supply	Frequency	50/60 Hz
	Tolerance Voltage	+10/-15% , Frequency ± 5%
	Operating Revolution	10 - 130 rps
PWM Control	Carrier Frequency	4 kHz
	Output Current	34 Arms
Ambient Temperature	-20°C to +70°C	
Relative Humidity	30 to 80 % (Don't condense, don't freeze)	
Vibration	Max. 5.9 m/s^2 (0.6g) 10 to 55Hz	

The function block diagram of BLDC compressor driver is shown in Figure 6.11. As we discussed in chapter 5, details of three main components of VFD were explained, a VFD's rectifier/converter accepts ac line voltage. Then its DC bus stores converted power on capacitor. Finally, the inverter creates desirable frequency/voltage sinusoidal output. Let us look at the driver circuit for the BLDC compressor that takes its supply from a three-phase power supply 230V- 60 Hz. There are two main sections of operation. The first section consists of a DC rectifier/converter. The DC converter converts the incoming power supply from 3-phase AC to DC using six diodes (Diode Module). DC reactor (Inductors) and capacitors are connected before the converter to reduce the electrical noise being introduced into the power supply due to the switching of the transistors. The second section is the inverter (Power Module) consisting of IGBT transistors. This section generates 3-phase voltage supply to the BLDC compressor motor.

The six discrete IGBT transistors are controlled by the c.pCO. The driver has ability to communicate with the Frame Transport Bus for Remote Terminal Unit (FBUS RTU) protocol via the RS485 communication link to c.pCO, which is one of the favorite industrial communications. In this mode, the driver receives frequency and control command from controller unit in order to drive the BLDC compressor.

The software is written in such a way that proper signals are being used to power ON or OFF each transistors at a correct timing depending on the feedback such as the position of the rotors in relation to the stator motor and the voltage levels detected. The BLDC motor of the compressor will receive close to a 3-phase sinusoidal voltage that turns the motor ON. The speed of the motor can be controlled from low to high by varying the frequency/Voltage (power supplied) to the motor through the switching of the transistors. In this way, capacity controlled HVAC can be achieved. When cooling or heating is needed immediately, the motor will turn at the highest speed. When the temperature of the room has stabilized, the motor will turn at a lower speed.

Intelligent Power Modules driving circuit (IPM), detection circuit, overload conditions and other parameters are built in an encapsulated casing. It looks like an integrated circuit except that it is very much bigger in size. The wiring diagram for online BLDC compressor driver is displayed in Figure 6.11. The following table is shown a test condition for the DC reactor 1mH, and load is 10kW. Table 6.11 shown the input and output data of the drive.

Table 6.10 Test condition

Item	Input of Driver	Output of driver	Unit
Voltage	206.58	191.31	V
Current	29.910	33.701	A
Frequency	49.96	50.00	Hz
Active Power	10.130	9.988	kW

Apparent Power	10.537	11.140	kVA
Power Factor	0.9612	0.8784	-

According to the recorded test the power loss is 342W and the efficiency = 96.62% and here the following table indicated the current drivers' harmonics. Table 6.11presnts the harmonic current of the driver's phase.

Table 6.11 Harmonic current of driver

Item	Value
THD_Phase R	29.6%
THD_Phase S	26.5%
THD_Phase T	27.1%
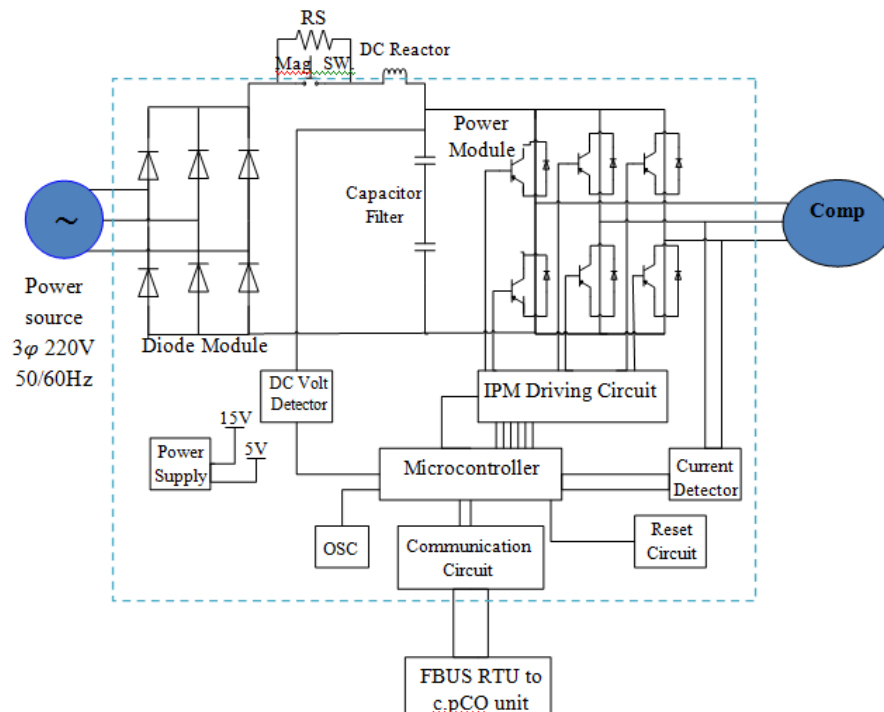
Figure 6.11 The Function block diagram of BLDC compressor driver

6.3   Monitoring and Measurement Systems

In this section of the thesis, a performance monitoring and experimental test system for measuring metrological parameters and electrical parameters for HVAC system are proposed. Automatic data acquisition, DAQ, technology made by National Instrument (NI) is used as hardware for monitoring the HVAC systems performance. The software of the data acquisition system based on LabVIEW package is used to display, store, and process the collected data in the PC-hard disk. The set up of the sensors, expermint tools, types of sensores and wires drawing of the system will be explained in detils.

6.3.1 Location of the Sensors in both Houses

Each HVAC unit is on the roof top of each house and linked by duct lines to indoor rooms. Figure 6.12 is presented the location of all the sensors for both houses. The duct air conditioners are designed to facilitate distribution cool air to the house. The short (light green) duct is used for the return air from the house to the unit, and the long or the bigger duct is used for the supply air from the unit to the house. Three thermocouple sensors are fixed on bedroom wall, corridor wall and living room wall, respectively. The yellow dots are indicating the three indoor thermocouple sensors (2, 4 and 5). The temperatures in Celsius degree are measured from three positions and then the average temperature is taken for the house. Airflow sensors are located near inlet air ducts to measure HVAC unit flow in kilogram per second. The green dots are indicating the airflow sensors (1, 3 and 6). Pressure sensor is also placed inside house to measure in house pressure. The dark blue dot (9) is indicating the barometric pressure sensor. Thermocouple sensor and irradiation sensors are placed outside of the house on roof top to measure the ambient temperature in degree and daily irradiation in watt per meter square. The two dark dots (7 and 8) are indication the irradiation and the outdoor thermocouple sensor. The wind speed and the

humidity have been measured for several days by using the Multi-Function Ventilation Meter VELOCICALC device.
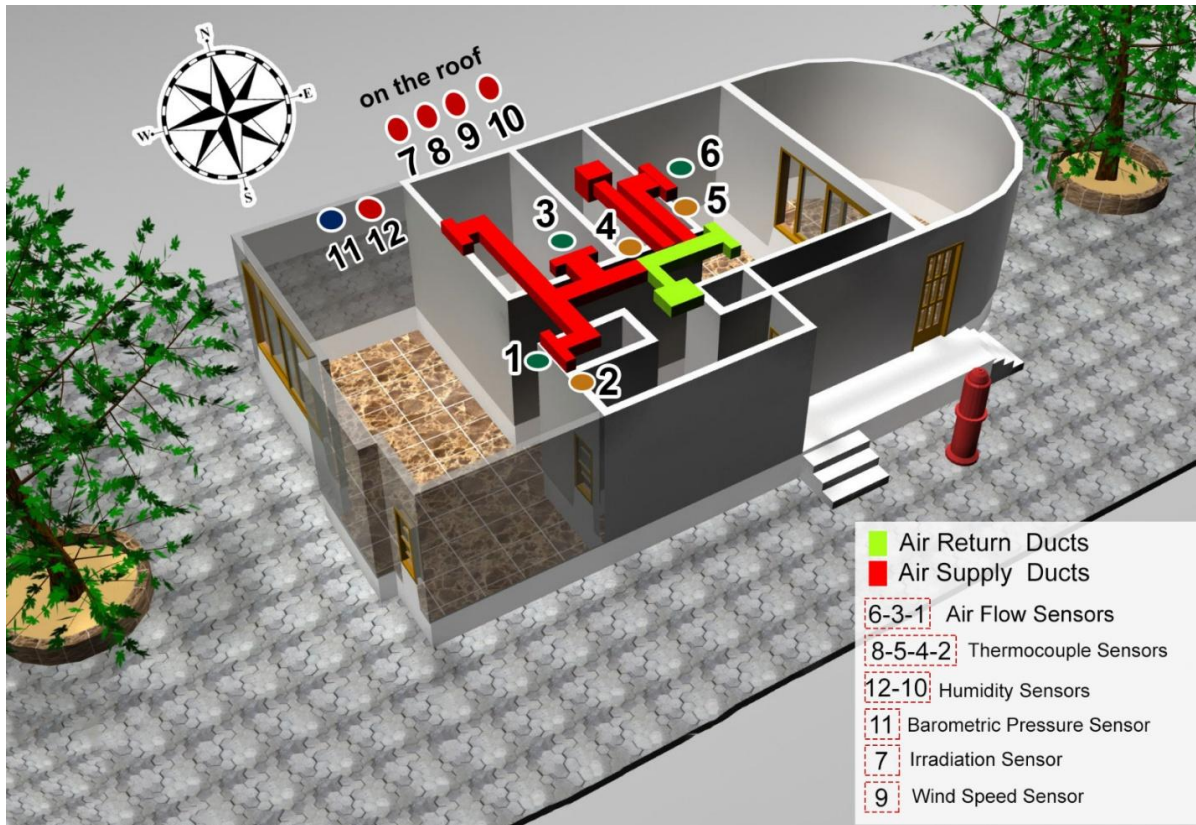
Figure 6.12 Ducts and sensors location for both houses

6.4 Experimental Setup Procedures

Monitoring and measurement devices hardware system are shown in Figure 6.13. The monitoring and measurement devices consist of four major blocks: an air conditioner, a DAQ-chassis with NI modules, sensors, and a host computer. The National Instrument DAQ-chassis monitoring system has several modules such as voltage measurements, current measurements, thermocouples, and universal module. There are two thermocouple sensors (indoor and outdoor temperatures), two humidity sensors (indoor and outdoor), an irradiation sensor, and air flow sensors. The host computer has the NI software, which is the main interface with DAQ-chassis.

The host computer will initiate the execution commands, store the data in the hard disk drive and display them on the monitor.
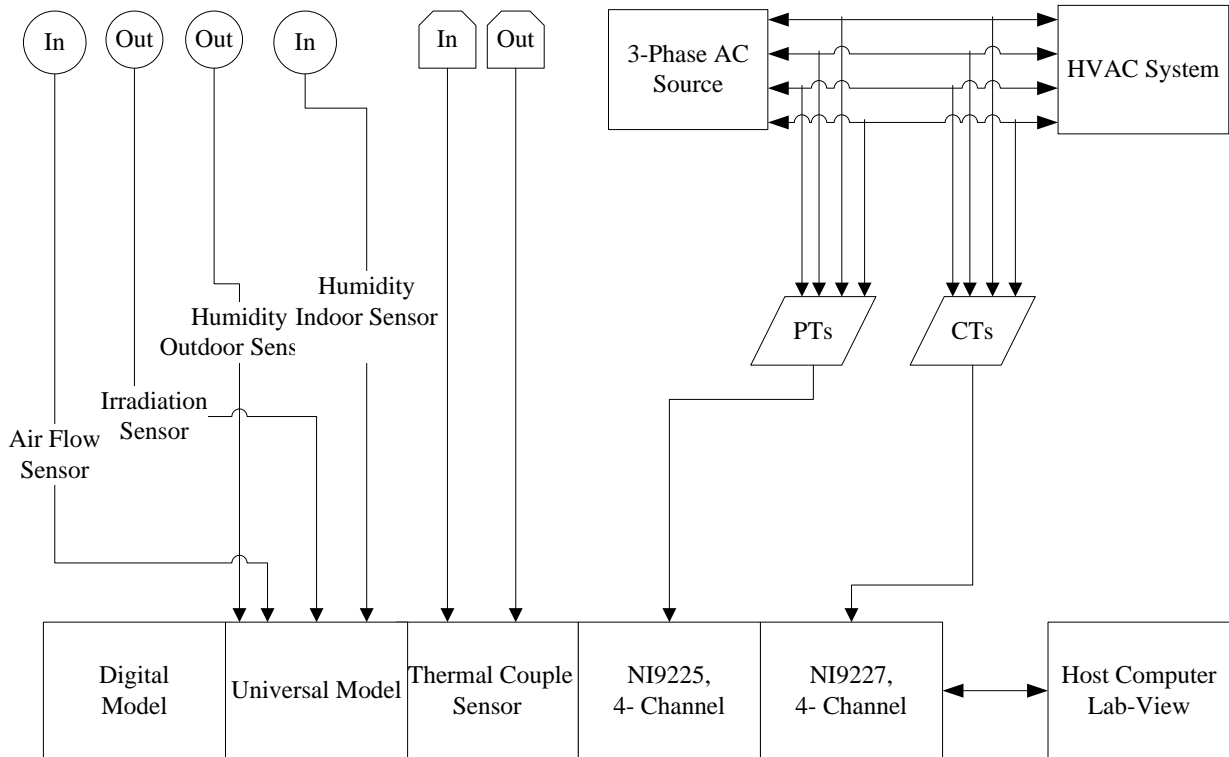
Figure 6.13 HVAC monitoring and measurement system

6.4.1 Experimental Tools

Several tools have been used to set-up the experimental work. This section provides the meaning of LabView and presents the instrument devices that have been used in the study for calibration, monitoring and measurement.

6.4.1.1   LabView

LabView is stand for Laboratory Virtual Instrument Engineering Workbench which a software program that normally taken as an instrument of virtual equipment and automation. It is used for system development to measure and analyze the data. In the LabView program setting, the graphic programming has replaced the traditional program writing style and can be derived easy

interface to use. Essentially our entire system involves the integration of sensor devices, personal computer (PC) and data acquisition (DAQ).

Next to the LabView platform, there are extra instrument devices have used during experimental work for calibration and validation. Table 6.12 is listed the extra devices.

Table 6.12 Listed the extra experimental tools for calibration

Instruments	Multi-Function Ventilation MeterVELOCICALC(9565)	Digital Handheld Multimeter (PeakTech-3315)	Power Quality Analysis (PQA-HIOKI 3197)
Measurements	Temperature, humidity, pressure, air velocity, and wind speed.	Current, frequency, and voltage, etc.)	Validate the measured power by Lab-View platform.
Accuracies	±3% of reading or ±0.015m/s ,(±0.28°C), ±3%RH	± (0.1% reading +0.2% range)	±0.3 % rdg . ±0.01% f.s within ±0.5°, ±3% at 40Hz to 5kHz
Appearances			

6.4.1.2   Sensors Specifications

Various sensors were utilized to measure and monitor the HVAC unit power and parameters as well as the weather conditions for indoor and outdoor environments. The specifications of all these sensors and LabView tools are represented in Table 6.13.

Table 6.13 Specification for the sensors, CT, PT and the data acquisition module

Components	Measurement	Specifications
Temperature Sensor	Measuring the indoor and the outdoor temperature	Type-K Thermocouple (Ni-Cr) , range -270 to +1372°C ,insulation range 73 to +482°C
Humidity Sensor VelociCalc-9565	Measuring outdoor Humidity	Multi-function ventilation meter, 0 to 5,000 ppm CO_2, 5 to 95% RH, (-10 to 60°C) Accuracy ±3% of reading or ±50 ppm, Resolution 1 ppm CO_2 0.1% RH 0.1°F (0.1°C)
Wind Speed (TV-110-L320)	Anemometer that measures the horizontal velocity of wind.	Operating Range is 0-100 mph. Less than1.1 mph (0.5 m/s) Distance Constant is Less than 16.5 ft (5.0 m)Accuracy +/- 1.0 mph (+/- 0.45 m/s). Temperature (-50 °C to +50 °C)
Air flow Sensors (AWM5104)	They measure flow as high as 20 standard liters per minute (SLPM)	Flow range 0-20 SLPM Performance characteristics at 10.0 ±0.01 VDC, 25°C
Barometric pressure (TB-2012M)	An active solid-state device to sense barometric pressure inside the house.	Supply Voltage is12 to 15 VDC, Accuracy is ±1.3Mb Operating Temperature Range is -40° to +50°C Output is 0-1 VDC
Irradiation (SP Lite2 Silicon Pyranometer)	A simple pyranometer for routine measurements of solar radiation	Spectral range (overall) 400 to 1100nm, Temperature range is -30 °C to +70 °C Expected output range (0 to 1500 W/m²)
Data acquisition module NI cDAQ-9188	Designed for remote or distributed sensor and electrical measurements. Measuring a broad range of analog and digital I/O signals and sensors.	An 8-slot NI Compact DAQ Gigabit ,measure up to 256 channels of sensor, analog I/O, and digital I/O signals
Power Supply (NI PS-15)	NI PS-15, 24 VDC power supplies for Compact DAQ	Full output power between -25 and +60 °C 115/230 V auto select input

NI 9205/9219/9225/ 9227 Module	Use with NI Compact DAQ and provides connections for 32 single-ended channels or 16 differential channels.	32-Channel , ±200 mV to ±10 V, Analog Input, 250 kS/s, 32 Ch Module
Current Transformer (CTs)METSECT 5CC010	Provide an isolated lower current in its secondary which is proportional to the current in the primary.	Secondary current 5 A [In] rated current 100 A. Current transformer Tropicalised DIN mount 100/5 for cables, rated insulation voltage 3 k, temperature range for operation -25 °C to 60. °C
Potential Transform (PTs) METSECT5CC0 10	Designed to present negligible load to the supply being measured and have an accurate voltage ratio and phase relationship to enable accurate secondary connected metering	Ration 240/6, temperature range for operation - 25. °C to 60. °C

6.5 Experimental Procedures

The data received from the cDAQ device needs to be processed for display and storage. A module is developed to display the entire data in an array and in a table for online continuous by and then saved in an excel file. On daily basis Variations data measurement the data is displayed as table's format for VFD unit as shown in Figure 6.14 (a) shows the date, time, four different temperatures, irradiation (W/m^2), pressure (Hg) and three air flow (kg/h). Figure 6.14 (b) shows RMS voltages (V), RMS currents (A), and power factor. The storage data for segregated and aggregate active and reactive power from cDAQ devices by LabView program are presented in Figure 6.14 (c). Figures 6.15 (a, b, c, d) shows the instantaneous values (peak to peak) line voltage and current with corresponding RMS values and total power consumption.

Array 0 | 31.8731 | 31.4331 | 31.3249 | 31.3253 | 0.70967

stop
STOP

date string: 4/25/2017
time string: ‫ص‬ 08:35

Temp1	Temp2	Temp3	Out Temp
31.873083	31.433117	31.324902	31.325329

Humidity In	Humidity Out
-0.000021	-0.000122

Irrad Amp	Irrad W/m2	Pressure V	Pressure Hg
0.007717	434.916768	30.258018	30.258

Air-flow 1 V	Air-flow 2 V	Air-flow 3 V
0.000163	-0.000165	0.000163

Air Flow1 SLPM	Air Flow2 SLPM	Air Flow3 SLPM
-4.99918	-5.00083	-4.99918

Table 2

Date	Time	T1	T2	T3	Tout	Irad (A)	Ima(W/m2)	Press (Hg)	Humidity In	Humidity out	Air Flow 1	Air Flow 2	Air Flow 3
4/20/2017	02:54	32.20038	31.58078	31.51954	31.43794	0.007989	466.672060	30.336767	-0.000064	-0.000029	0.000492	0.000163	0.000492
4/20/2017	02:54	32.08441	31.46423	31.40823	31.55662	0.007993	467.141044	30.337025	0.000036	-0.000029	1.306739	1.351725	1.280470
4/20/2017	02:55	32.06199	31.44622	31.34523	31.38111	0.007991	466.991806	30.336424	-0.000050	-0.000100	0.000492	0.000163	0.000163
4/20/2017	02:55	32.04071	31.44331	31.29580	31.18785	0.007988	466.549624	30.337583	-0.000114	0.000000	1.304112	1.344501	1.279813
4/20/2017	02:55	32.03012	31.44326	31.29203	31.20616	0.007981	465.791625	30.336639	0.000014	-0.000150	1.297873	1.352054	1.276201
4/20/2017	02:55	32.04862	31.45605	31.29200	30.96318	0.007990	466.793403	30.336167	-0.000072	-0.000086	0.000163	0.000163	0.000492
4/20/2017	02:55	32.03400	31.46496	31.30148	30.86912	0.008004	468.420726	30.336639	0.000014	-0.000107	1.325456	1.353696	1.281455
4/20/2017	02:55	32.00607	31.47374	31.31464	31.11017	0.008002	468.201750	30.336424	-0.000107	-0.000050	1.302799	1.353367	1.278409
4/20/2017	02:56	32.00620	31.49075	31.32668	31.32165	0.007994	467.251229	30.336553	-0.000007	0.000000	-0.000165	0.000163	0.000163
4/20/2017	02:56	31.99393	31.50609	31.33753	31.13320	0.007980	465.714565	30.336210	0.000007	0.000014	1.324799	1.381935	1.301485
4/20/2017	02:56	31.98682	31.50558	31.34210	31.18245	0.007973	464.840406	30.336038	-0.000007	-0.000093	0.000492	0.000163	0.000163

Table

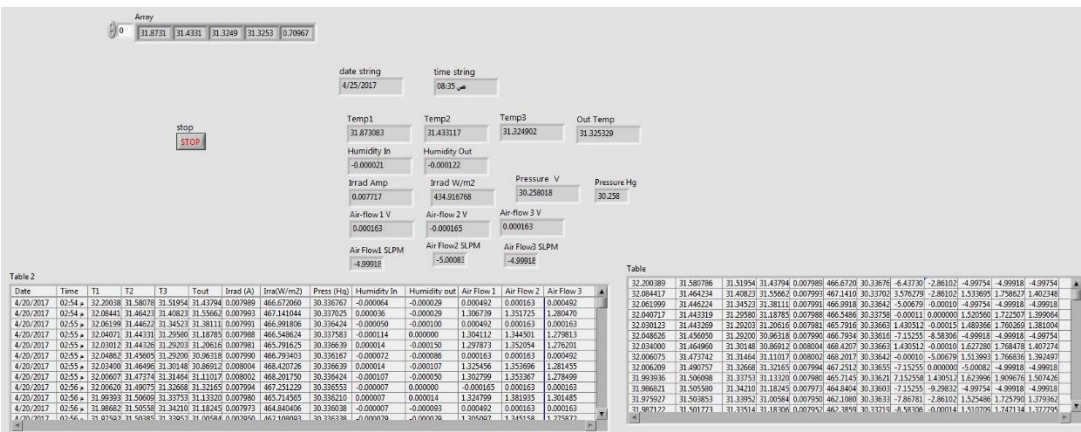|												
32.200389	31.580786	31.51954	31.43794	0.007989	466.6720	30.33676	-6.43730	-2.86102	-4.99754	-4.99918	-4.99754
32.084417	31.464234	31.40823	31.55662	0.007993	467.1410	30.33702	3.576279	-2.86102	1.533695	1.758627	1.402348
32.061999	31.446224	31.34523	31.38111	0.007991	466.9918	30.33842	-5.00679	-0.00010	-4.99754	-4.99918	-4.99918
32.040717	31.443319	31.29580	31.18785	0.007988	466.5486	30.33758	-0.00011	0.000000	1.520560	1.722507	1.399064
32.030123	31.443269	31.29203	31.20616	0.007981	465.7916	30.33663	1.430512	-0.00015	1.483366	1.760269	1.381004
32.048626	31.456050	31.29200	30.96318	0.007990	466.7934	30.33616	-7.15255	-8.58306	-4.99918	-4.99918	-4.99754
32.034000	31.464960	31.30148	30.86912	0.008004	468.4207	30.33663	1.430512	-0.00010	1.627280	1.768478	1.407274
32.006075	31.473742	31.31464	31.11017	0.008002	468.2017	30.33642	-0.00010	-5.00679	1.513993	1.766836	1.392497
32.006209	31.490757	31.32668	31.32165	0.007994	467.2512	30.33655	-7.15255	0.000000	-5.00082	-4.99918	-4.99918
31.993936	31.506098	31.33753	31.13320	0.007980	465.7145	30.33621	7.152558	1.430512	1.623996	1.909676	1.507426
31.986821	31.505580	31.34210	31.18245	0.007973	464.8404	30.33600	-7.15255	-9.29832	-4.99754	-4.99918	-4.99918
31.975927	31.503853	31.33952	31.00584	0.007950	462.1080	30.33633	-7.86781	-2.86102	1.525486	1.725790	1.379362
31.967122	31.501773	31.33514	31.18306	0.007952	462.3859	30.33719	-8.58306	-0.00014	1.510709	1.747134	1.377295

Figure 6.14(a) storage data from cDAQ devices by LabView program for VFD Unit, online data, time, four temperatures, solar irradiation, pressure and three air flow tables.

(Voltage & Current) RMS, PF and THD

Date	Time	V1 RMS (V)	V2 RMS (V)	V3 RMS (V)	I1 RMS (A)	I2 RMS (A)	I3 RMS (A)	PF1	PF2	PF3	THD V1 %	THD V2 %	THD V3 %	THD I1 %	THD I2 %	THD I3 %
12/7/2016	11:17:01	123.370321	125.147892	124.473963	0.589516	0.538463	0.343547	0.205623	0.309067	0.114329	2.079417	2.486260	1.771026	151.031781	198.278866	77.129055
12/7/2016	11:17:11	123.805041	124.908799	124.167764	0.600967	0.549836	0.343532	0.207696	0.307438	0.123423	2.051791	2.219067	1.691427	207.900293	219.825421	98.612793
12/7/2016	11:17:21	123.120885	125.069764	124.769472	0.586567	0.534020	0.341982	0.205518	0.314479	0.111465	1.976822	2.112654	2.012237	144.826706	192.912600	77.247562
12/7/2016	11:17:31	122.997179	124.612097	125.232403	0.591085	0.536946	0.340888	0.202304	0.316288	0.112719	1.992820	1.975081	2.196413	132.207034	193.785784	59.673551
12/7/2016	11:17:41	124.184822	124.305812	124.394352	0.597544	0.546705	0.343506	0.200861	0.303866	0.124588	2.310464	2.102407	1.675212	110.933072	95.181257	101.832192
12/7/2016	11:17:51	123.211365	125.119760	124.605516	0.592161	0.536699	0.342327	0.207937	0.309572	0.103472	1.989340	2.221429	1.896857	144.644635	188.261165	70.065319
12/7/2016	11:18:01	123.429169	124.151819	125.356265	0.600034	0.550326	0.341071	0.192247	0.308981	0.118795	2.157974	1.989122	2.145127	148.171857	85.659125	54.255953
12/7/2016	11:18:11	124.089220	124.365175	124.255194	0.594382	0.545437	0.344358	0.204950	0.309955	0.130478	2.255441	2.029743	1.684128	96.667723	98.748207	103.210106
12/7/2016	11:18:21	122.930617	124.679490	125.121131	0.589677	0.535970	0.339829	0.202176	0.315444	0.107484	1.963107	2.134701	2.269656	150.803638	207.268856	67.387316
12/7/2016	11:18:31	123.024607	124.364319	125.294077	0.588972	0.538111	0.340654	0.195599	0.314428	0.116069	2.000045	2.217099	2.511122	155.297612	223.047484	56.004419
12/7/2016	11:18:41	122.977139	124.922637	124.809822	0.598483	0.545245	0.341463	0.207099	0.314095	0.110073	2.075594	2.121786	1.952828	148.215762	198.768749	78.169463
12/7/2016	11:18:51	124.108983	124.064274	124.432215	0.586691	0.530380	0.341602	0.200746	0.295667	0.105838	2.606319	2.059028	1.755656	111.306947	84.759767	79.566165
12/7/2016	11:19:01	123.268078	124.114710	125.356488	0.567383	0.531331	0.341493	0.173120	0.293079	0.129464	2.199062	1.924947	2.250517	146.300488	85.129906	59.072699
12/7/2016	11:19:11	123.192278	124.269050	125.399702	0.560359	0.522167	0.341670	0.172115	0.294646	0.120495	2.084644	2.089480	2.629156	138.628877	211.785967	56.852341
12/7/2016	11:19:21	123.090860	125.050059	124.773315	0.601245	0.548313	0.342100	0.209163	0.315403	0.112532	1.951473	2.163296	2.036334	128.750972	182.332852	72.865830
12/7/2016	11:19:31	123.085689	124.346548	125.357539	0.596471	0.542947	0.340043	0.200045	0.315977	0.110900	2.052407	2.193657	2.657169	139.079464	204.615492	53.636729
12/7/2016	11:19:41	123.683030	125.051739	124.244507	0.586116	0.531370	0.342307	0.206540	0.300656	0.104811	2.065215	2.392942	1.734908	161.451881	203.956579	74.351492

Figure 6.14(b) Storage data from cDAQ devices by LabView program for VFD unit, online data RMS voltages, RMS currents, and phase angle

P (Watt), Q (VAR)

Date	Time	P1 (W)	P1 (W)	P1 (W)	P(Totral) (W)	Q1 (VAR)	Q1 (VAR)	Q1 (VAR)	Q (Total) (VAR)
12/7/2016	11:14:31	14.678045	20.859850	4.288975	39.826870	71.420225	63.369283	42.555988	177.345496
12/7/2016	11:14:41	14.758804	20.790708	4.159727	39.709239	72.051648	63.829367	42.524006	178.405021
12/7/2016	11:14:51	15.043698	21.470529	4.910519	41.424746	71.595496	64.289633	42.678124	178.563252
12/7/2016	11:15:01	11.568120	18.484458	5.050097	35.102674	67.828338	61.885499	42.637960	172.351798
12/7/2016	11:15:11	14.148727	20.786582	5.264926	40.200235	71.118996	62.945562	42.434234	176.498792
12/7/2016	11:15:21	14.640132	20.243453	5.208607	40.092192	71.510774	63.680788	42.556537	177.748099
12/7/2016	11:15:31	14.531094	20.573425	4.800467	39.904985	70.348528	63.235594	42.650105	176.234227
12/7/2016	11:15:41	14.918639	20.210259	4.993124	40.122022	72.215586	63.971761	42.572132	178.759480
12/7/2016	11:15:51	15.102541	20.837541	4.878913	40.818996	71.735277	64.427119	42.686811	178.849208
12/7/2016	11:16:01	14.773288	19.789402	4.185356	38.748046	71.256277	63.360818	42.546171	177.163267
12/7/2016	11:16:11	14.979545	20.466129	4.924468	40.370143	71.688858	64.304785	42.636241	178.629883
12/7/2016	11:16:21	14.852790	20.266710	4.414843	39.534343	71.582678	64.104514	42.570262	178.257454
12/7/2016	11:16:31	15.675831	21.210180	4.873134	41.759145	72.781491	64.950622	42.701428	180.433540
12/7/2016	11:16:41	11.322455	18.356540	5.178010	34.857005	67.328098	61.589315	42.668319	171.585732
12/7/2016	11:16:51	15.068508	20.503128	5.127734	40.699369	71.672811	64.231372	42.447375	178.351559
12/7/2016	11:17:01	14.954731	20.827286	4.888993	40.671010	71.174701	64.088241	42.482238	177.745180

Figure 6.14(c) Storage data from cDAQ devices by LabView program for VFD unit, online data the segregated and aggregate active and reactive power
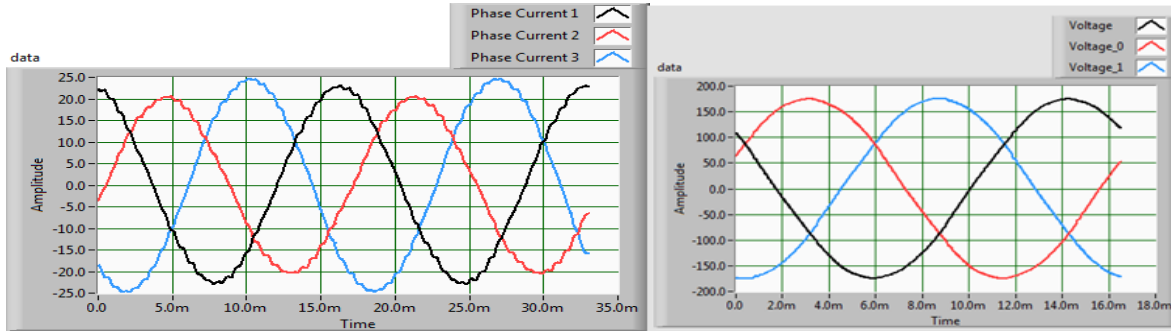
Figure 6.15 (a) Online peak to peak and RMS three phase currents and voltage for VFD unit
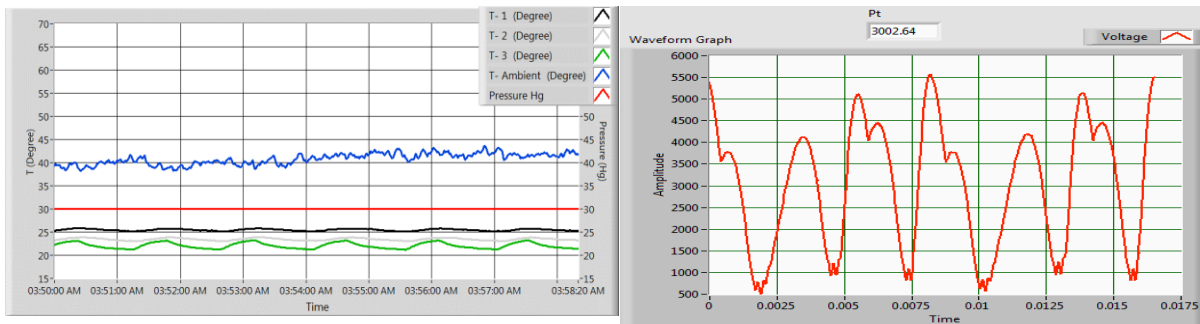
Figure 6.15 (b) Online Instantaneous values for four temperatures and pressure with time. Figure 6.15(c) online total power VFD unit

6.6 Climate Impact on HVAC

The Eastern Province is a vital region in Saudi Arabia because it's large land area, accounting for almost one third of the entire country. Dhahran represents the Eastern Province weather which is subject to hot-Dry Maritime subzone where the maximum temperature occasionally higher than other climate zones in KSA [44].

Buildings in a desert climate such as that of Saudi Arabia are subjected not only to high ambient air temperatures, but also to strong solar radiation throughout the day. This may draw the attention for designers and engineers to carefully consider the design of the various controllers of HVAC to minimize the energy consumption and provide an acceptable level of thermal comfort [45]. The excessive demand for air conditioning in the KSA is a direct result of the extreme

temperatures during summer, when the ambient temperature frequently reaches 46 $^{\circ}$C at night. About 65% of the electric energy generated in Saudi Arabia is used for operating buildings and 65% of this energy is consumed by air conditioning [46].

Climate conditions can impact the air conditioning operation, and according to M. B. Yurtseven et al. (2013) who has conducted an experimental study and compared the differences between the energy consumption of room type inverter and non-inverter air conditioners in the typical public office rooms, located in Istanbul Technical University (ITU). It is found that for the climates with varying temperature in a day, inverter technology yields high efficiency and is more favorable [47].

6.7   Climate and Environmental Measurement

The outdoor climate has a major impact on the energy use in a building. There are several factors related to the energy performance, including the outdoor temperature, the solar radiations, the long-wave radiations and the wind conditions. The indoor comfort is also affected by the outdoor humidity and the indoor surface temperatures. Figure 6.16 shows floor house plan with the direction of the sunshine in the morning. We can observe that the sunshine can directly affect the process of the cooling on the early morning as the sunshine is reflected directly to the window of the bedroom. Two big trees have grown one in the front of the house and the second tree is in the back yard of the house. These trees are help to reduce the effects of the outdoor temperature during the early morning and at the time of the sunset.
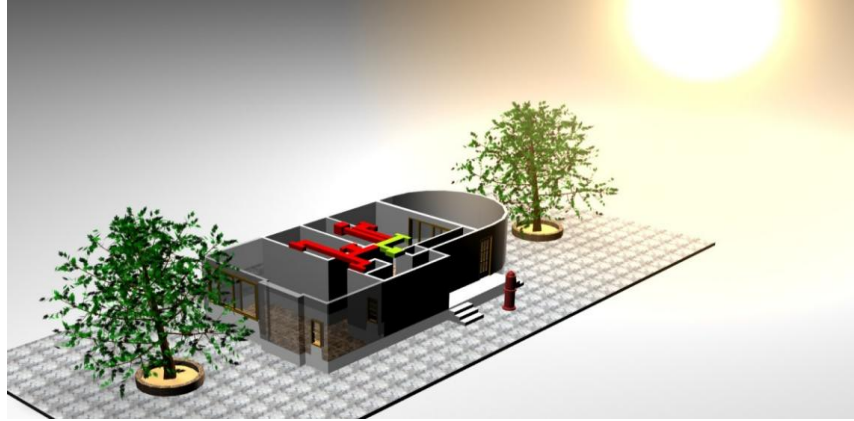
Figure 6.16 The direction and the Impact of the sunshine

6.7.1 Outdoor Temperature and Irradiations

All data for the outdoor temperature is taken directly from the LabView monitoring and measurement system. In Saudi Arabia, the irradiation may have a huge impact on the energy use of a building. All the following data have obtained from our monitoring and measurement system. Figure 6.17 shows the outdoor temperature for a warm day and the irradiation for the same day. We can notice the irradiation follows the pattern of the outdoor temperature during the day. There are some fluctuations on the irradiation pattern from 2:00PM to 3:00 PM; this is happened when the weather become cloudy during that time, or it might be form the tree moving due to the high wind speed, as the shadow of the tree is reflected on the irradiation sensor.
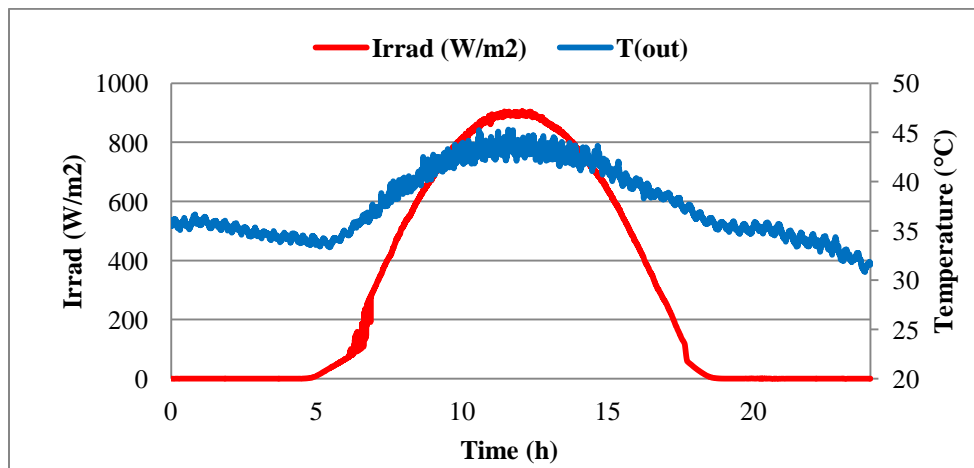
Figure 6.17 Outdoor Temperature and the irradiation for one day (3/10/2016) Dhahran, Saudi Arabia (2016)

6.7.2 Humidity and Wind Speed

Figure 6.18 shows the Outdoor humidity (%) and the wind speed (m/s) of Dhahran area. Relative humidity is changing from 45% to 8% through the day. It is high at the early morning's hours and it is drop to 8% at the midday and the getting increase to 30 at the midnight. It is clearly shown in the Figure 6.18 that wind speed fluctuates between 10 m/s - 45 m/s through the day. Both humidity and wind speed are considered as the external factors that can affect the cooling process.
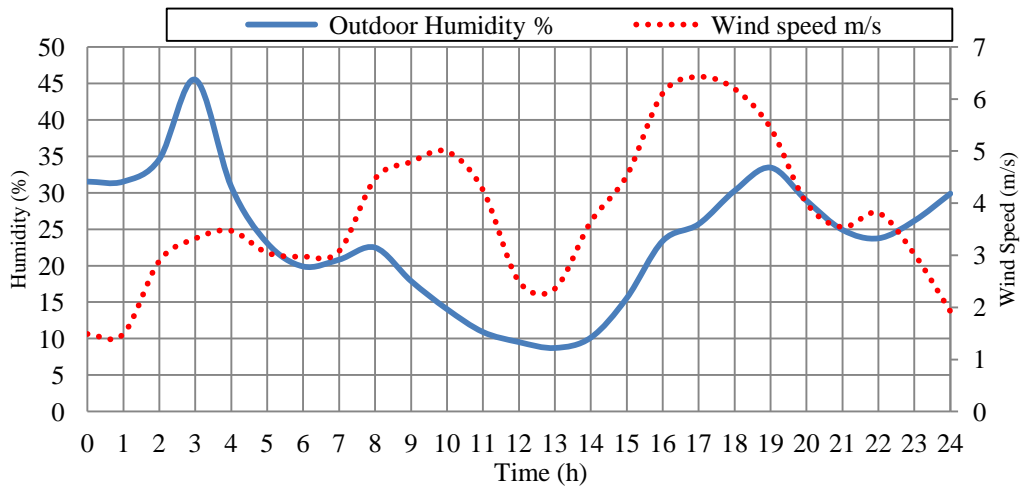
Figure 6.18 Humidity and wind speed data for one day (3/10/2016) Dhahran, Saudi Arabia (2016)

6.7.3 Indoor Climate for ON/OFF &VFD

The following figures are presenting the internal environmental parameters for both house #3305 and #3307. All data have obtained though our monitoring and measurement system. Figure 6.19 shows the outdoor temperature for house #3305 which equipped with ON/OFF unit. The indoor temperatures are presented from three different locations of the house. The average of the indoor temperature has taken of those three sensors. We can notice that the threshold of the indoor temperature is from 21 °C to 25 °C.
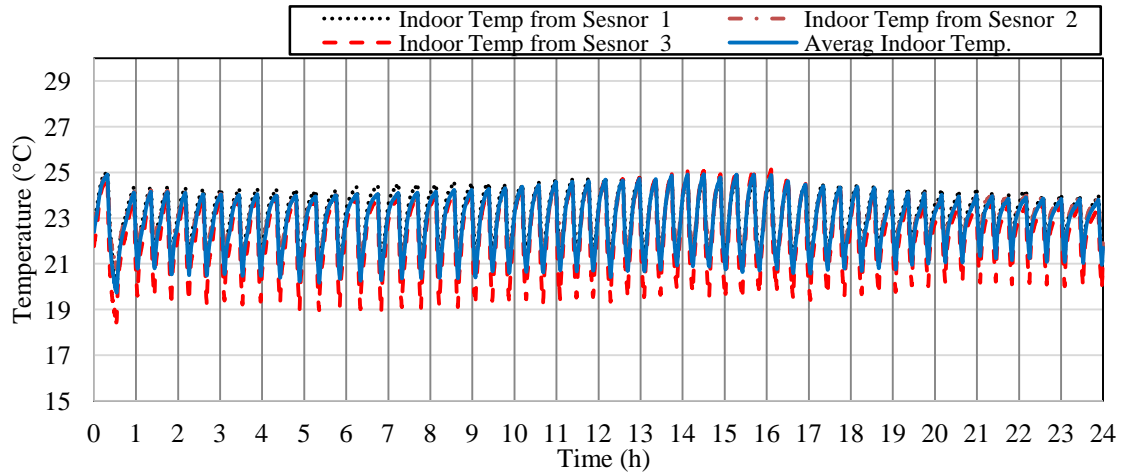
Figure 6.19 Indoor temperatures from three different places in the house #3305-ON/OFF unit. (3/10/2016)

Figure 6.20 shows the air supply temperature, the dew-point and the humidity. The air supply temperature is reached 13 °C during the midday as indoor temperature increased and more cold air is needed to reduce the indoor temperature to match the set point temperature. The dew-point temperature is following the pattern of the air supply temperature. Furthermore, indoor humidity of the house is fluctuating from 45% to 100% and it can be observed that 5:00 PM to 7:00 PM is varied from 40% to 80%. Figure 6.21 presents the barometric pressure of house #3305 and the air flow supplied into the house. The air flow pattern follows the ON/OFF cycle operation and as the blower fan is always ON during the day as it fixed at 70% of the speed.
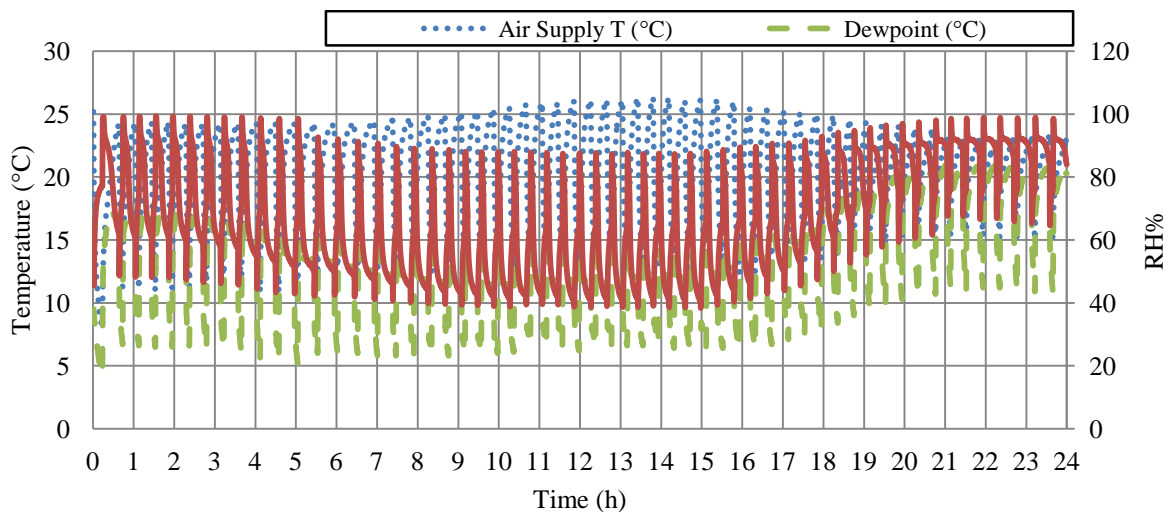
Figure 6.20 Air supply temperature, humidity and the dew point for house #3305-ON/OFF unit (3/10/2016)

128
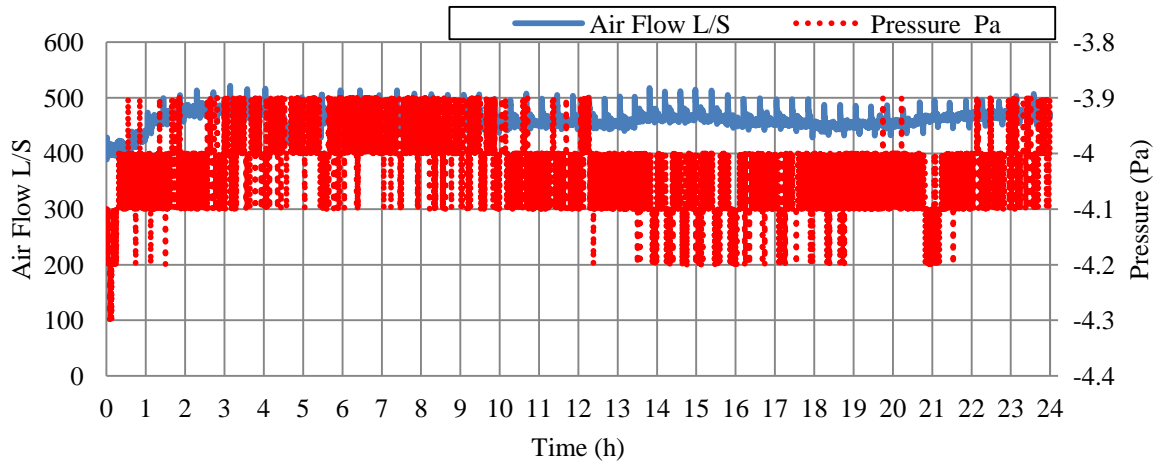
Figure 6.21 Air flow and pressure for house #3305-ON/OFF unit. (3/10/2016)

Figure 6.22 shows the air supply temperature and air return temperature for house #3307. It can be observed that the air return temperature pattern is almost the same as the set point temperature and it is only varied on the midday at 11:00 PM and it increased to 25 °C. The variation of the air supply temperature is varying from 14°C to around 24°C. At 11:00 AM. The air is supply temperature is 16 °C for almost one hour. Figure 6.23 presents the indoor temperatures from three different thermocouple sensors, and the average of the indoor temperature. It can be observed that the indoor temperature is varied from 22°C to 25°C. At the midday the indoor temperature is getting lower and reaches 22°C and that is a reflection of the high outdoor temperature at the midday time.
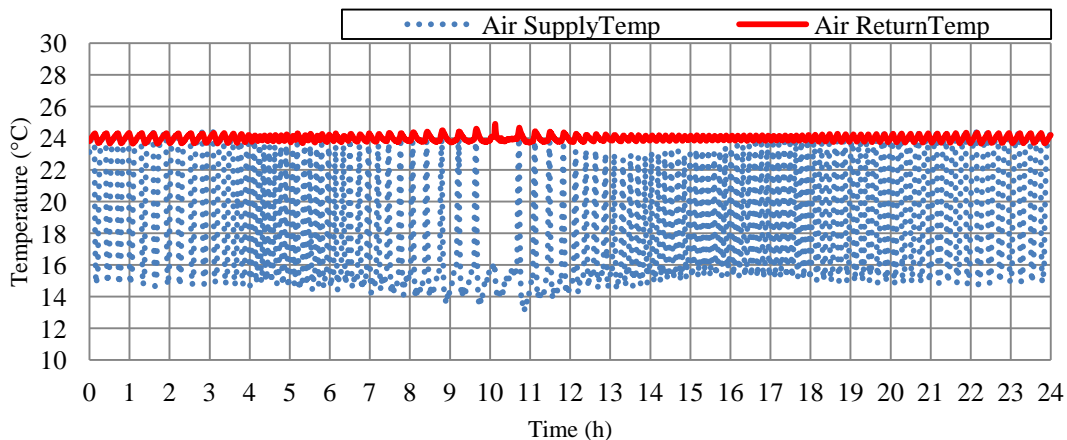
Figure 6.22 Air supply and air return temperature for house #3307-VFD unit. (3/10/2016)
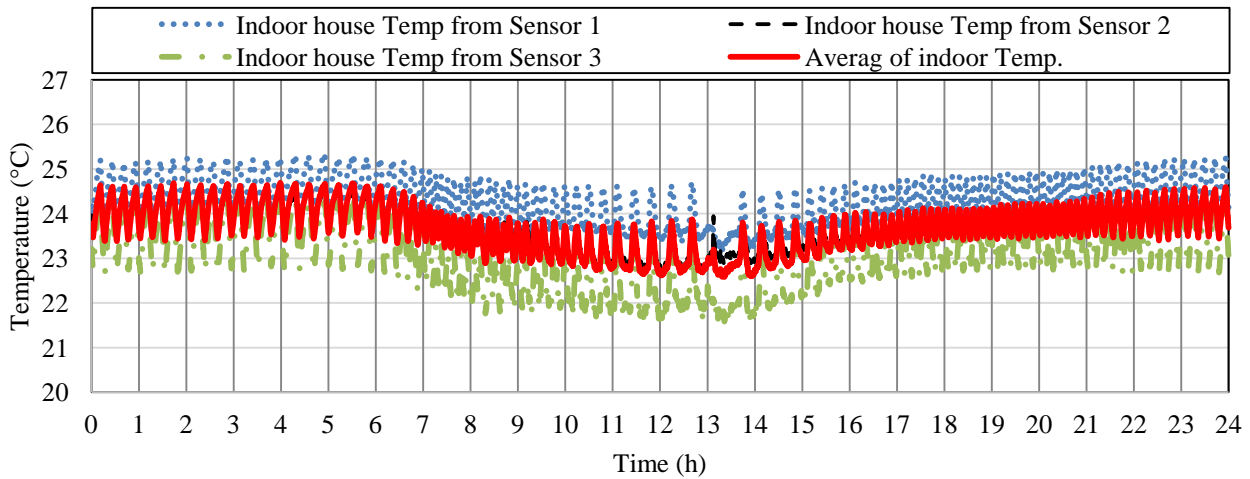
Figure 6.23 Indoor temperatures from three different places in the house #3307 VFD unit (3/10/2016)

Figure 6.24 shows the indoor humidity of house #3307, and the dew-points. The humidity varied from 50% to 80% from 8:00 AM to 12:00 PM, and then it is getting lower to less than 50% which is a reflection of the decreased indoor temperature in the midday. The dew-point curve follows the pattern of the indoor humidity.
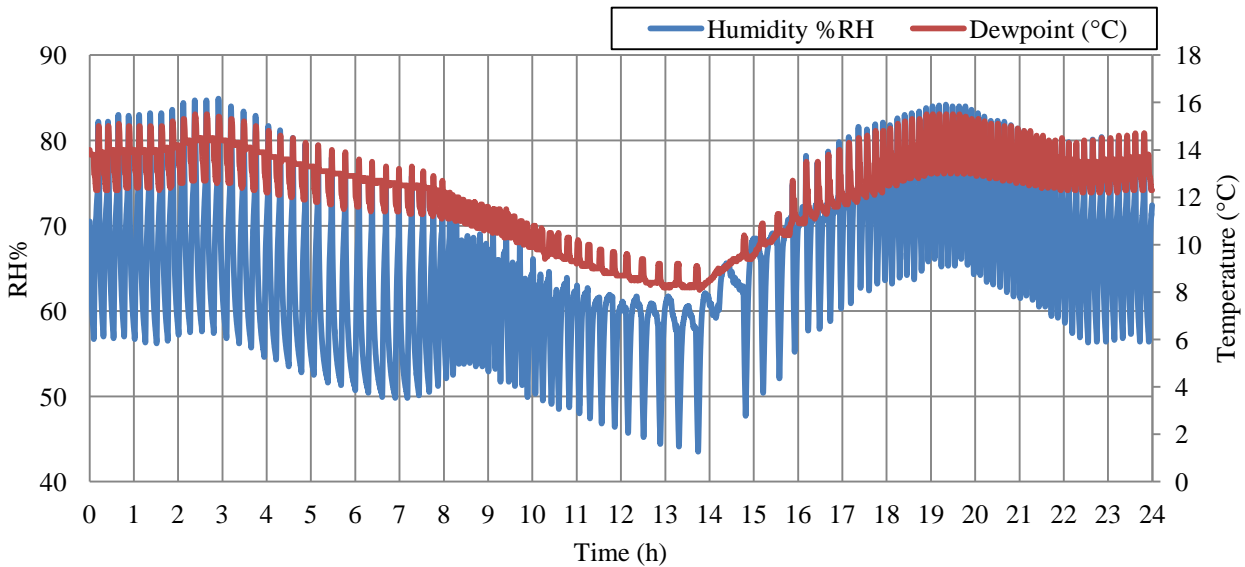
Figure 6.24 Humidity and the dew point for house #3307 VDF unit. (3/10/2016)

CHAPTER 7

RESULTS AND DISCUSSION

7.1 Introduction

This chapter presents the typical results from the implemented models of the thermal house and HVAC unites as well as the measurements results. The first section describes the temperature fluctuation that can be occurred in the thermal house parameters and the effect of the cooling process due to the occupant's activities and the weather environmental changes during the day. The second section presents the result for both HVAC systems and their power consumption. The final section will provide the validation of the simulation work with the experimental study.

7.2 Simulation ON/OFF Cycle HVAC System

Simulink/MATLAB thermal model of the house that has been developed in chapter 4 and used to simulate the functionality of both houses that integrated with of ON/OFF and VFD HVAC systems. The simulation results presented the indoor temperature, mid-wall temperature, mid-roof temperature, and mid-window temperature. Heat flow from atmosphere to indoor temperature through roof, walls and windows are also provided. Additional information is provides by the simulation such as HVAC operation time (ON time and OFF time), the length period length, and the duty cycle for ON/OFF system with the calculation of the consumed power (kW) by blower fan and compressor.

HVAC airflow rate used in this simulation is equivalent to a 5-tons air conditioner system. The outdoor temperature used in this simulation for hot and warm day (September 5, 2016) is taken in the Dhahran area. According to the monitoring and the measurement system, Table 7.1 gives the maximum, the minimum, the average of the outdoor temperature, average of outdoor humidity and wind speed as well as the average of indoor temperature for both houses #3305&#3307. The heights outdoor temperature reached in Dhahran area during the summer season of 2016 is 48.40 °C. However, the outdoor temperature varies between 31.03°C to 48.40°C is considered one of the highest temperature degrees in Dhahran area during the summer season, and the outdoor temperature varies between 48.40°C to 31.03°C. The set point for both houses is fixed as 24°C, and according to the experimental measurements the average of indoor temperature for ON/OFF house is a bit higher than the average of the indoor temperature of VFD house by approximately 1°C.
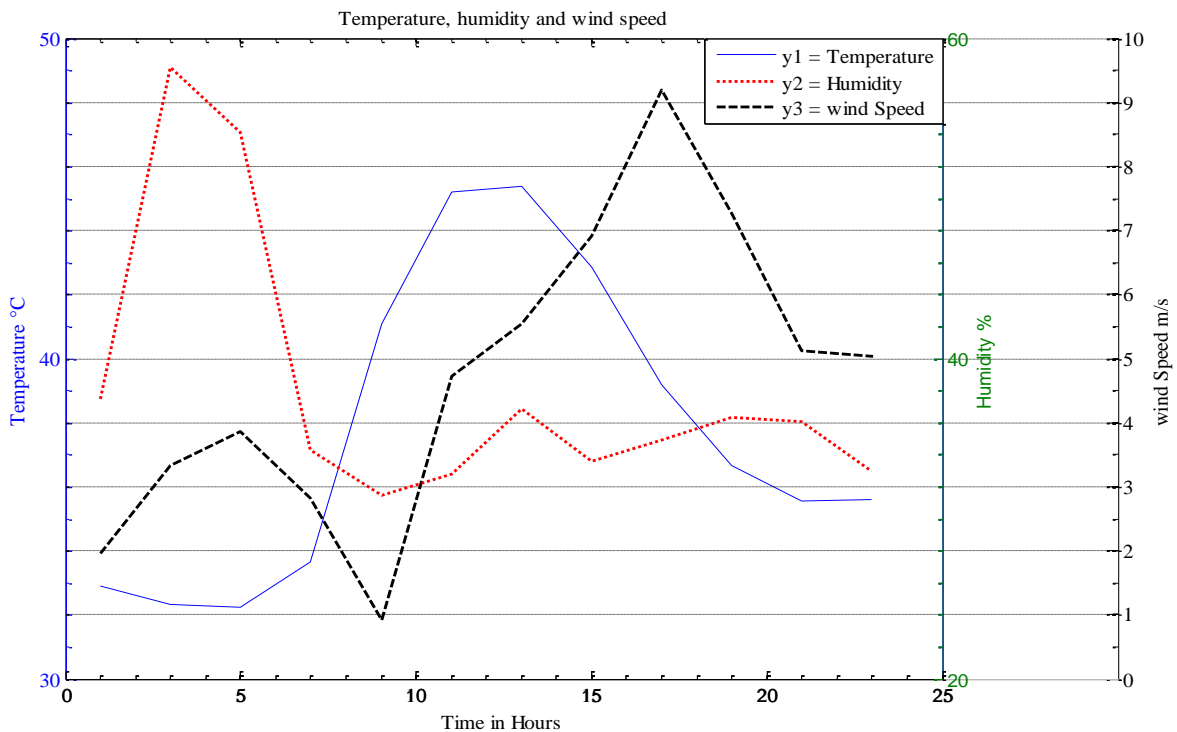
Figure 7.1 Average of outdoor temperature, outdoor humidity and wind speed on 5/09/2016

Table 7.1 Indoor and outdoor temperature for Dhahran area (KFUPM campus) on September 5, 2016

Temperature Data 5/09/2016	Max Outdoor Temp	Min Outdoor Temp	Average of Outdoor Temp	Average of Indoor Temp #3305-ON/OFF	Average of Indoor Temp #3307-VFD	Average of Outdoor Humidity (%)	Average of Wind Speed (m/s)
	48.40 °C	31.03°C	37.738 °C	24.28 °C	23.67 °C	38.36 %	4.48 m/s

Figure 7.1 illustrates the average of outdoor temperature, average of wind speed and the average of outdoor humidity of the Dhahran area on the 5th of September, 2016. The weather environmental parameters were obtained from the current study measurements and monitoring system. The outdoor temperature in this day reaches 48.48 °C at the midday and then it varies between 35°C to 40°C until the end of the day. The wind speed of the Dhahran area fluctuates between 1 m/s to 9 m/s though the day. However, the outdoor humidity is reaching 47% after the mid night until the 6:00AM. Then it fluctuates between 06:00 AM the 12:00 AM though the day.

Figure 7.2 shows the actual outdoor temperature, indoor temperature, mid house construction temperatures for walls, windows and roof. In this simulation, we used one of the hottest days in Dhahran, Saudi Arabia; the temperature is reached almost 48.40 °C on 5th of September 2016. The initial temperatures are used for the indoor temperature for the houses, mid-wall, mid-roof, and mid-windows are 24.5°C, 25°C, 25°C and 25 °C, respectively. From Figure 7.2, it can be observed that the mid-windows temperature is reached approximately 36.5°C and it is simply followed the pattern of the outdoor temperature for this day.
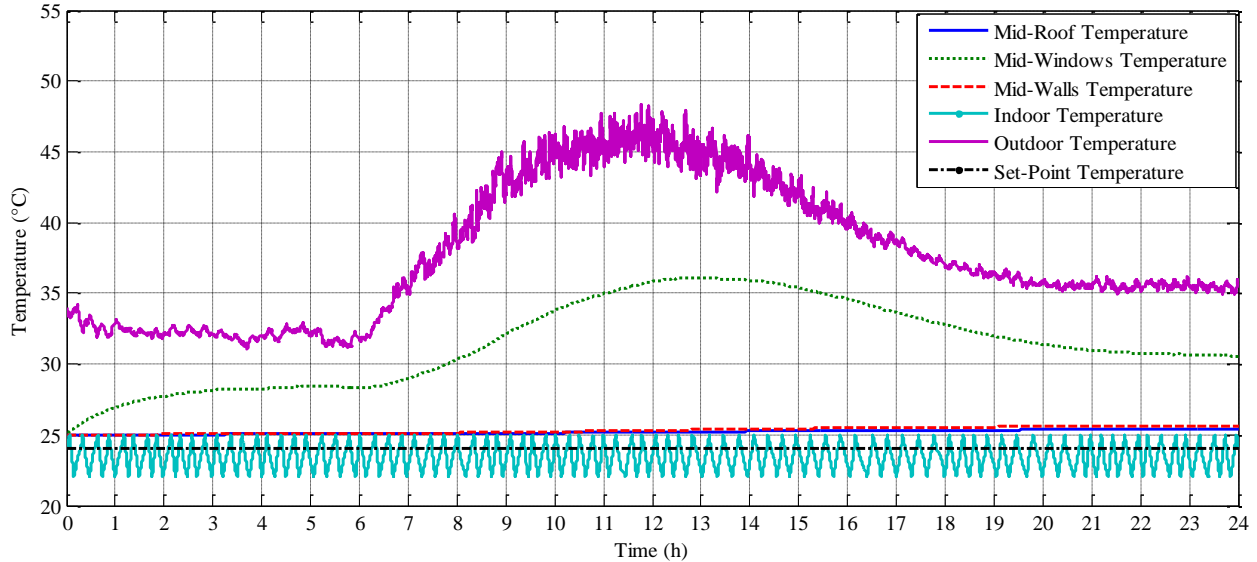
Figure 7.2 Outdoor temperature, indoor temperature, mid-wall temperature, mid-windows temperature, mid-roof temperature and set point temperature

Figure 7.3 represents the duty cycle in percentage, period or cycle length in minutes, and the air condition ON time in minutes. It is noticeable that the duty cycle of the air condition changing through the day and night with the association of the outdoor temperature. From midnight until 6 Am the duty cycle is more than 23% and the period length close to than 10 minutes, this is implying the air condition is turned on for less than 2-3 minutes and off for more than 8-9 minutes. At 6 Am, when the sunrise and household start their activities, the duty cycle starts rising up beyond 40 % and at the same time the HVAC on time reaches nearly 5 minutes per cycle. At midday, the HVAC on time goes up. From 12 PM to 6 PM, the outdoor temperature exceeds 48.5°C, and the duty cycles goes up almost 57 % and the period or cycle length reaches around 7 minutes, which means the HVAC is on for 5 minutes and off for 2 minutes. At 6 PM, the sunset and the outdoor temperature start declining. The duty cycles go down almost 40% with period or cycle length around 8-7 minutes until 9 PM. However, between 9 PM and midnight, the outdoor temperature continues in declining and the household activities are reduced close to bed time and the duty cycle goes to 26% with HVAC turning for short period of

time less than 3 minutes. The number of cycles is 91 per 24 h. The total time operation and the energy consumed for the HVAC system is presented in Table 7.2.
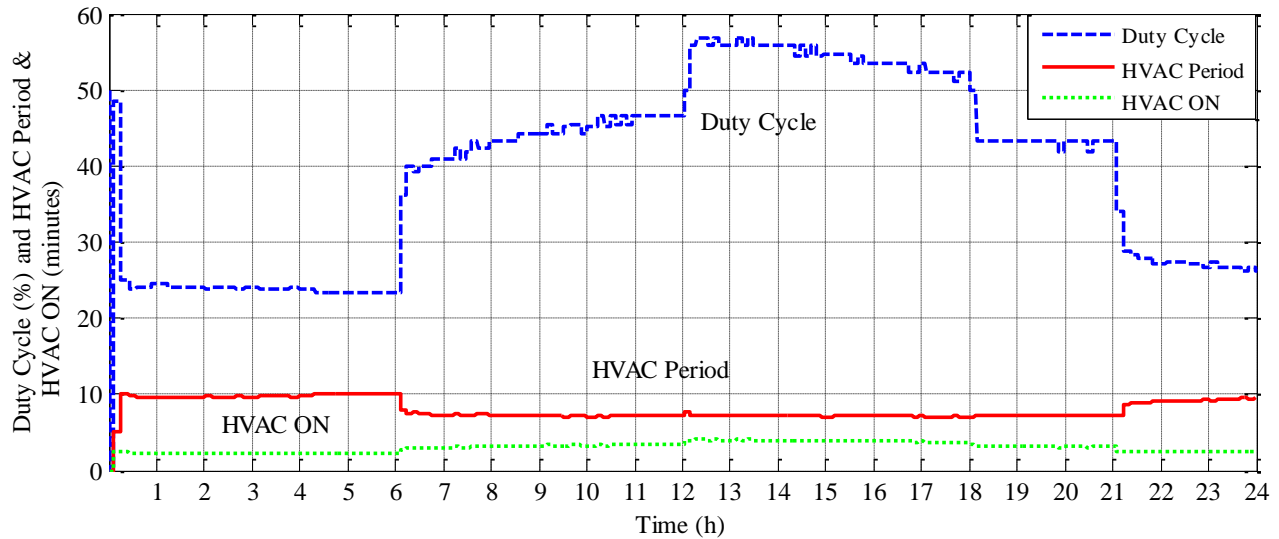
Figure 7.3 HVAC duty cycle, HVAC ON time and OFF time for one day

Table 7.2 HVAC On & Off time and energy used for 5th of September, 2016

Day	ON-Time	OFF-Time	Energy consumed by Compressor & Condenser	Energy consumed by Fan for ON Mode	Total Energy
05/09/2016	11.790 h	12.18 h	49.518 kWh	8.842 kWh	58.4098kWh

The internal wall, roof and windows surface temperatures for the house are presented in Figure 7.4. We show the surface temperatures of the house construction depend directly on the width. The windows have big area and smallest width so the inside surface windows effect by outdoor temperature and it reach at afternoon to 35 °C.
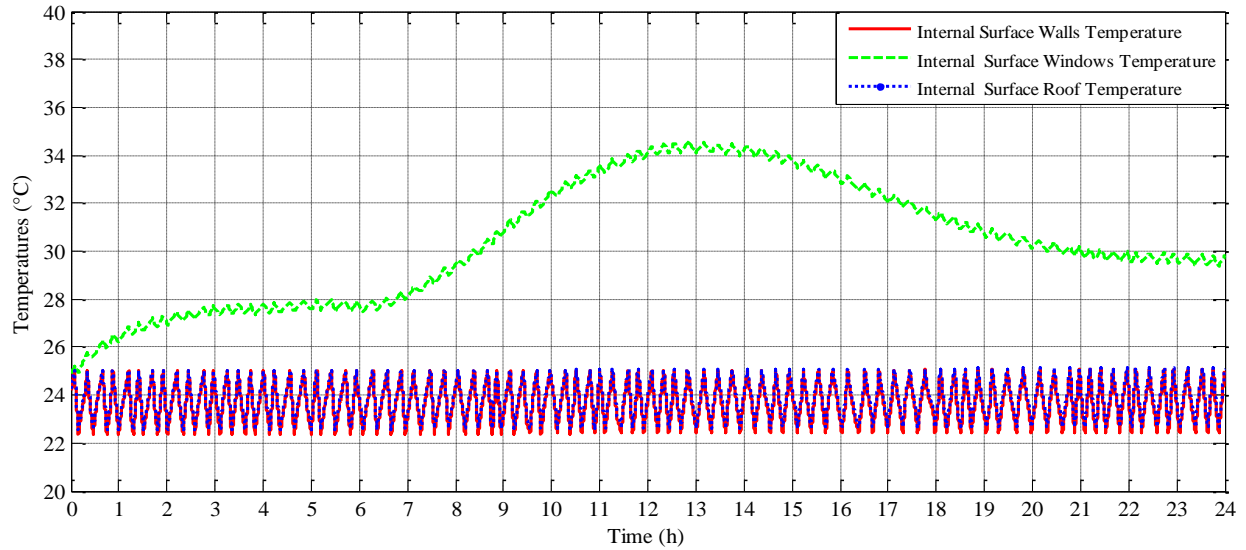
Figure 7.4 Internal wall, windows and roof surface temperatures

External heat flows from outside the house into the house through different ways. Figure 7.5 showed the heat flow to house through walls, windows and roof and it reached as maximum, (1.5 kW) heat in mid-day.
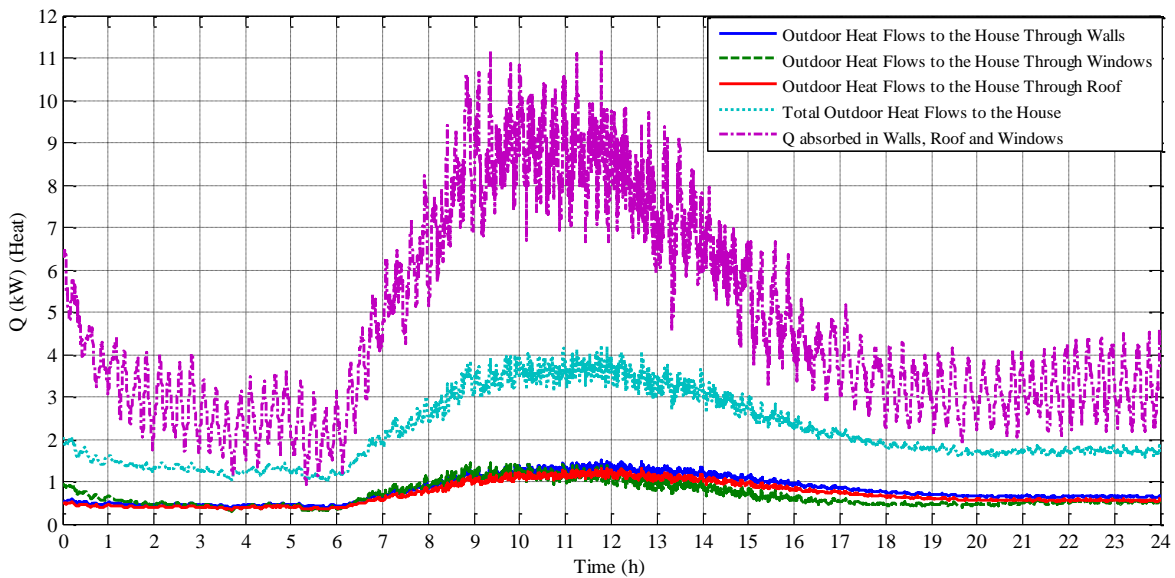
Figure 7.5 Total external heat flow and the stored heat in walls, windows and roof

Furthermore, the total absorbed heat in walls, roof and windows is reached between 10kW to 11kW in the afternoon, and the total outdoor heat flows to the house is reached around 4.12 kW at the mid-day.

The cooler flows in the house to recover the heat generated from the influence of the outdoor temperature for a typical day. Figure 7.6 presents the total power consumption of this day. The simulated energy consumption of the ON/OFF HVAC is 58.4 kWh. It can be observed that the rated power used is 4.95 kW. The system turned ON and OFF (cycling) for many time throughout the day. The number of cycling is 91 per 24 hour.
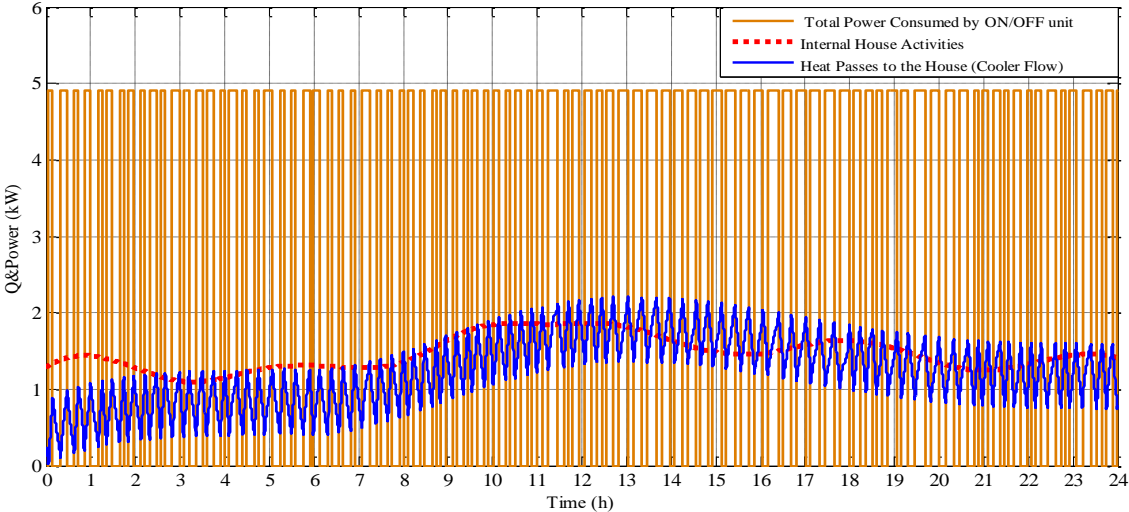
Figure 7.6 Power consumed by ON/OFF, internal house activity and heat flow passes to house (cooler flow)

Figure 7.7 show the accumulation of the total energy consumption by ON/OFF HVAC unit on Septmeber.5, 2016 by the average under the power area curve. The energy consumption is changing over time and the total energy is 58.40 kWh.
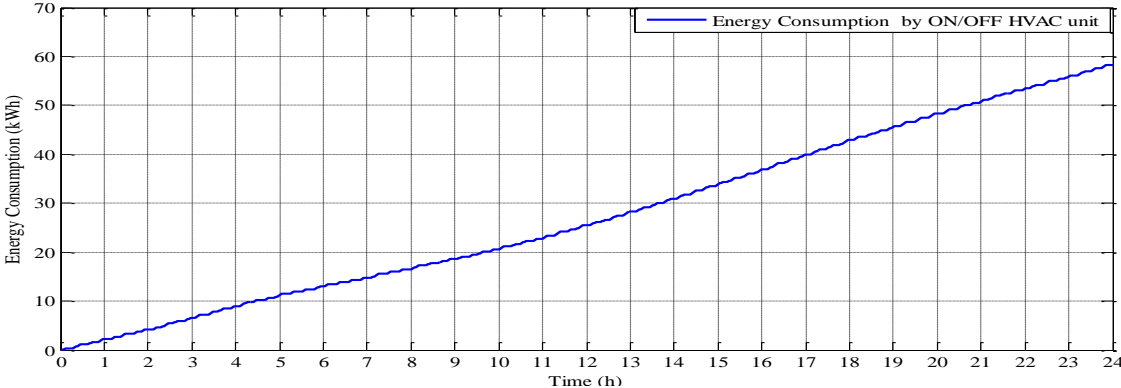
Figure 7.7 Total energy consumed by ON/OFF HVAC unit on 05/09/2016

137

7.3 Simulation of VFD HVAC System

In this section, different approaches of VFD HVAC simulation results are provided, starting by the simulation results of the thermal model of the house integrated with VFD-PID, VFD-PI-PWM and VFD-FLC air conditioning controllers. All results are presented with clear explanations and analysis.

Figure 7.8 shows the actual outdoor temperature, indoor temperature and mid house construction temperatures for walls, windows and roof. In the simulation, the outdoor temperature presents for one of the hottest and warm day (5th of September 2016) in Dhahran Saudi Arabia, as the outdoor temperature reaches almost 48.5 °C. In addition, the initial temperatures of house, mid-walls, mid-roof and mid-windows are 24.5 °C, 25 °C, 25 °C and 25 °C, respectively. HVAC cooling temperature and cooling gain and other parameters are explained in Chapter 4. Table 4.5. However, it is observed from Figure 7.8 that the indoor temperature very much follows the pattern of the set point temperature, which makes the thermal comfort level very comfortable for the occupants.
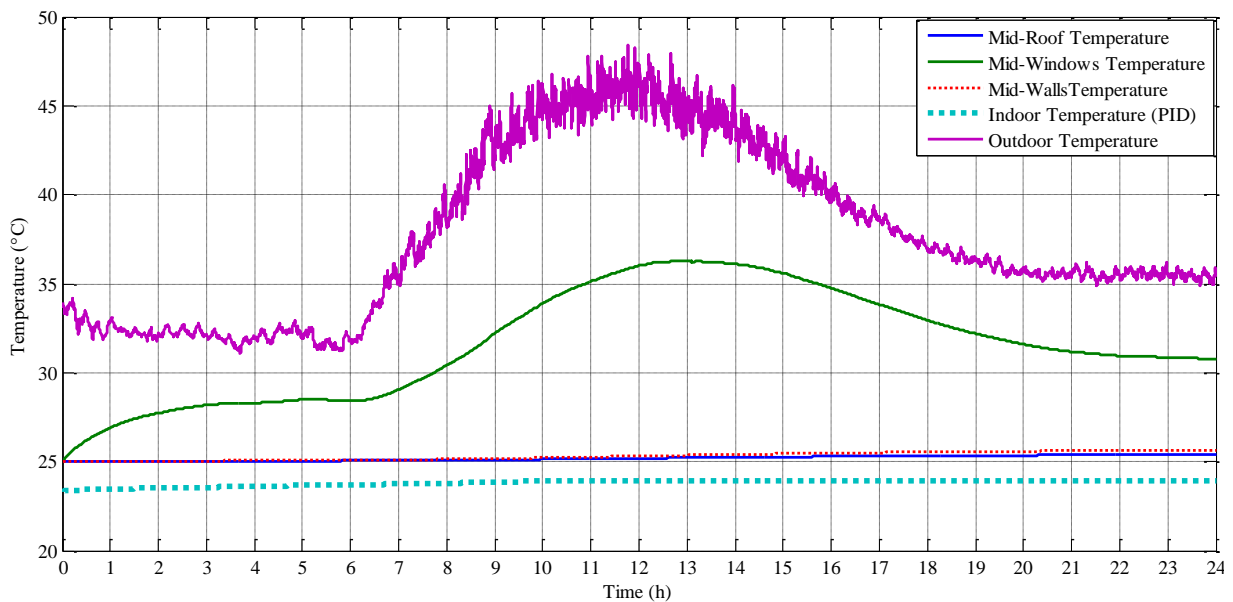
Figure 7.8 Outdoor temperature, indoor temperature, mid-wall temperature, mid-windows temperature, mid-roof temperature and set point temperature

138

The internal wall, roof and windows surface temperatures for the house are shown in Figure 7.9. The surface temperature of house construction depends directly on the depth and the insulation materials. The windows have big area and smallest width so the inside surface windows effected by outdoor temperature and it reaches by afternoon to 35 °C. It can be observed from Figure 7.9 that the internal walls and roof temperatures are almost similar as the set point temperature, due to the thickness of the walls and roof along the thermal insulation material which preventing the heat passes to the house.
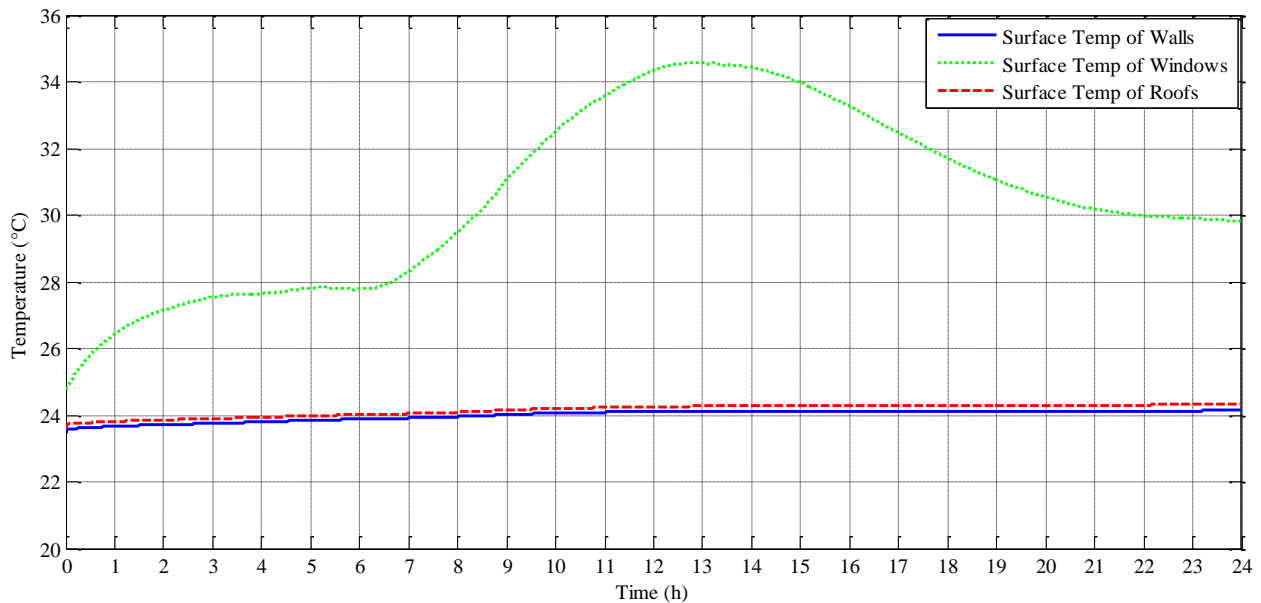
Figure 7.9 Walls surface, windows surface and roof surface temperatures

Figure 7.10 shows the house activities for VFD unit and the heat passes to the house. The same house activities pattern is used for simulating the three different techniques of VFD unit. It can be noticed that the heat penetration to the house follows the pattern of the outdoor. The increasing in the mid of the day due to the increase of the outdoor temperature, and then it decreases again to the normal level after the sunset. The amount of house activities and heat penetration to the house are converted from Btu/h to kW, (1 Btu/h = 0.00029307 kW).
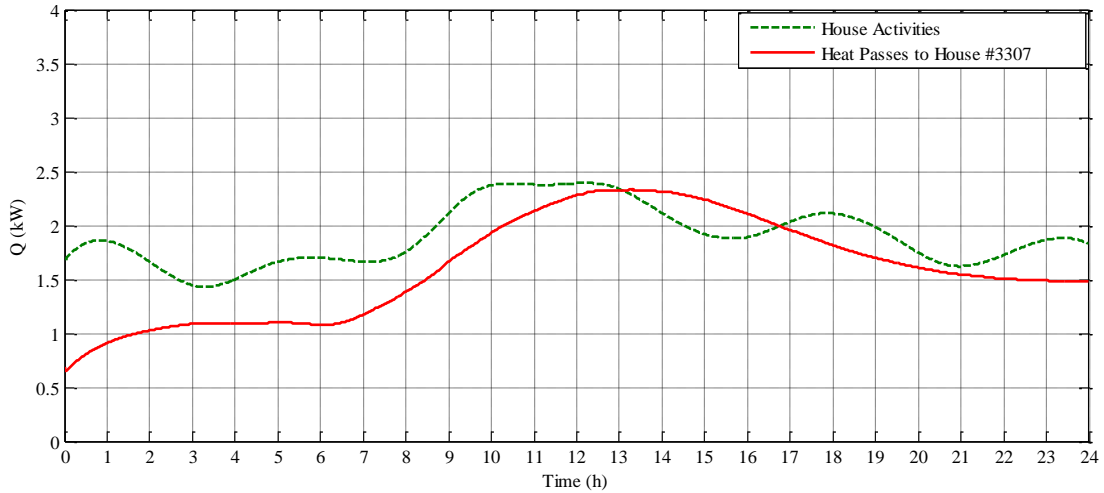
Figure 7.10 House activities for simulation VFD unit and the heat passes to the house

Figure 7.11 shows the simulated indoor temperature and the actual outdoor temperature. The indoor temperature has stimulated by using the VFD-PID HVAC system. It can be observed that the indoor temperature is varying in the same range of the set point temperature (24°C), however at the midday when the outdoor temperature increases and reaches around 48°C a small variation occurs on the indoor temperature and HVAC system performs well and makes a very satisfied conformable level in the indoor environment.
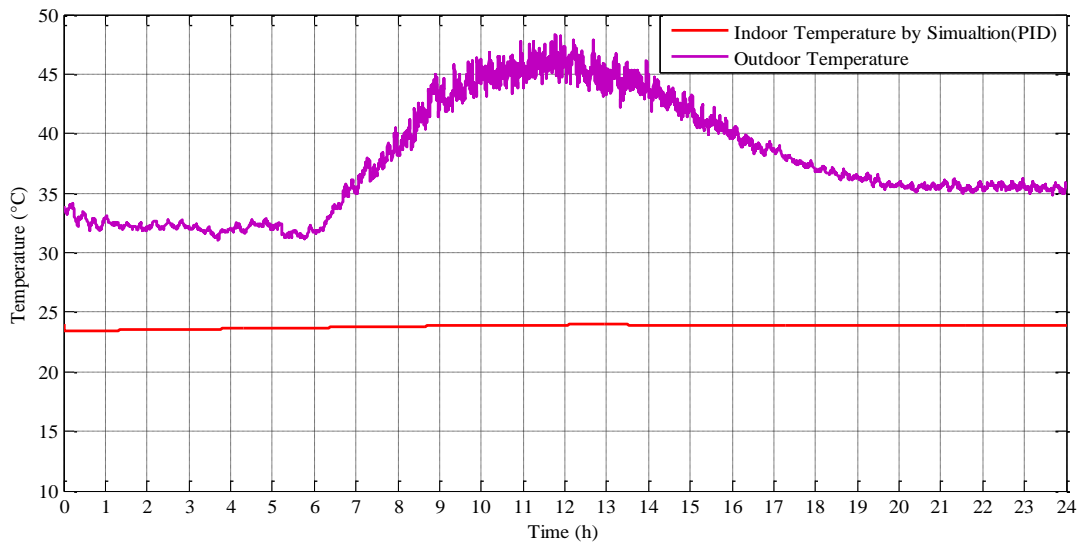
Figure 7.11 Simulated indoor temperature by using VFD-PID HVAC system and actual outdoor temperature
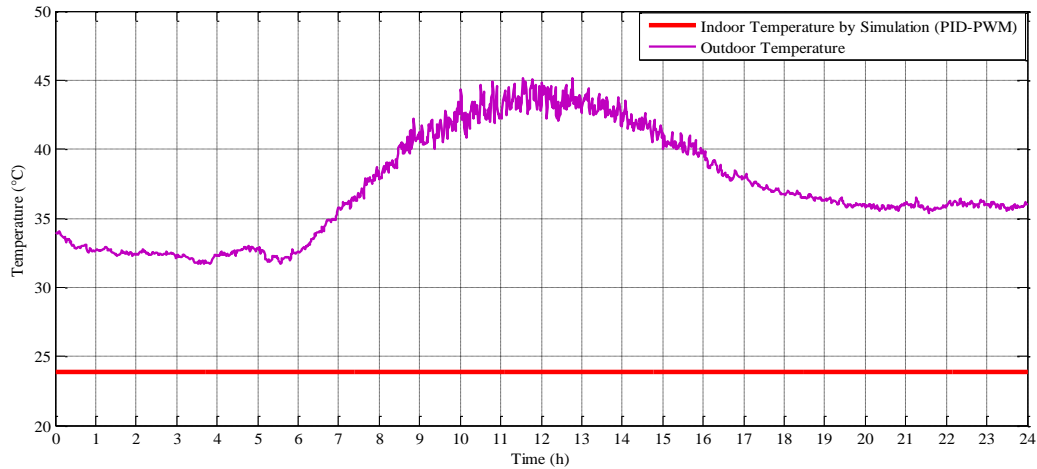
Figure 7.12 Simulated indoor temperature by using VFD-PI-PWM HVAC system and actual outdoor temperature

Figure 7.12 shows the simulated indoor temperature response using VFD-PI-PWM HVAC system and the actual outdoor temperature for hot day (05/09/2016). The result indicates that the indoor temperature is exactly following the set point temperature (24°C). In addition, keeping the indoor temperature at the same range of the set point temperature for the whole day is indicting that compressor motor performance with high capacity during the day to achieve a better indoor environment. This leads to consuming a great amount of energy consumption over the day. Moreover, it should be mentioned that should be at least a small fluctuation occurs in the indoor temperature throughout the door due to the internal house activities.
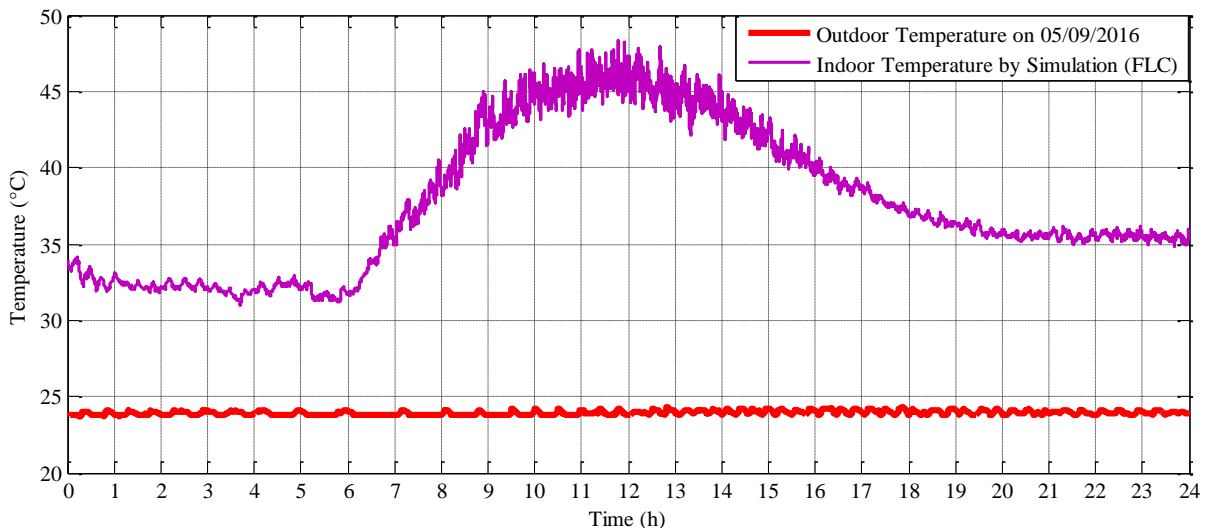
Figure 7.13 Simulated indoor temperature by using VFD-FLC HVAC system and actual outdoor temperature

141

Figure 7.13 shows the simulated indoor temperature response using VFD-FLC HVAC system, and the actual outdoor temperature for hot day (05/09/2016). There is a small variation occurs in the indoor temperature throughout the day. The indoor temperature varies around the desired temperature (24°C, ±0.5°C), due to the speed of the air flow changes based on the return temperature, which makes the compressor motor run at different speed to control the load capacity and to match the desired set point temperature. It is very reasonable and small variation happened in the indoor temperature during the operation of HVAC system though the day due to the internal changes in the house activities such as the cooking, door opening/closing, lights and TV. The simulation result obtained proved that the VFD-FLC varies the speed of air flow (compressor motor) and gives the occupants a very comfortable level of satisfaction compared to other VFD HVAC controllers.

7.4 Validation of Simulation Results with Measurement Data for One Day

7.4.1   Indoor Temperature Validation of ON/OFF Cycle HVAC System

In this section, comparison data measurement and simulation results for HVAC ON/OFF cycle. The simulated indoor air temperature will be validated with the actual measured indoor air temperature; also the simulated power consumption of ON/OFF unit will be validated with actual measured power consumption of the ON/OFF unit for the selected day (05/09/2016).

It should be mentioned that the internal house activities load has already calculated previously for one typical day and it has been used for this simulation. However, the same house activities load has been applied for all the simulation approaches in this study. In addition, the actual measured indoor air temperature is taken as an average of three thermocouple sensors located at three different places in the house #3305.
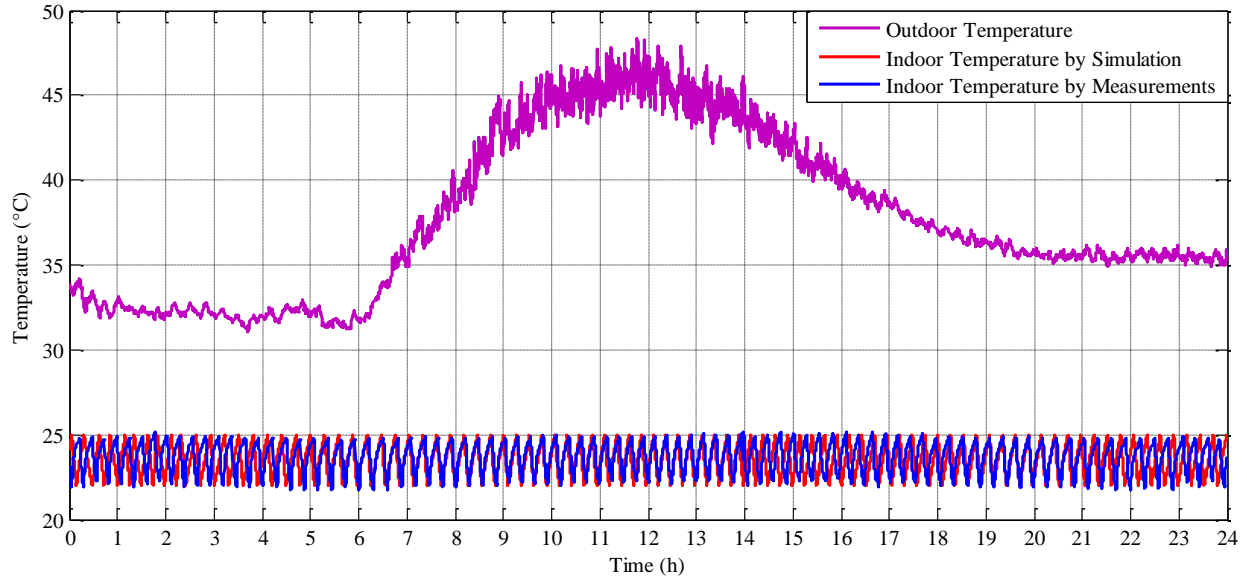
Figure 7.14 Validation of simulated and actual indoor temperature of ON/OFF HVAC system on 05th of Sept, 2016

Figure 7.14 shows the validation of the indoor air temperature on the 05th of September, 2016. The simulated indoor air temperature (Red Color) shifts in a narrow range of the actual measured air indoor temperature. It is clearly shown that the simulated indoor air temperature follows the pattern of the actual measured indoor air temperature throughout the day. The ON/OFF HVAC system turns on when the thermostat indicates that the indoor air temperature is greater than the set point temperature 24 ^{o}C, and then it turns off when the indoor air temperature is lower than the set point temperature. It is noticeable that the air conditioning system cycling during the day and both temperatures have identical cycle period without any extra variation. However, the operation time for simulation is (708 min = 11.8 hours and measurement is (710 min = 11.833 h). The outdoor air temperature has a great influence on the ON/OFF HVAC performance. It affects the number of ON pulses. The number of pulses is equal (91 per 24 h). Consequently, the simulation approach of ON/OFF HVAC study has achieved a typical result which identical with actual measured results.

143

7.4.2 Power Consumption Validation of ON/OFF Cycle HVAC System

ON/OFF control is one of the oldest techniques that is practiced in buildings for the purpose of energy saving and occupant thermal comfort level. The simulation and the measurement of the power consumption for the ON/OFF HVAC unit on the 05th of September, 2016 are presented in Figure 7.15.
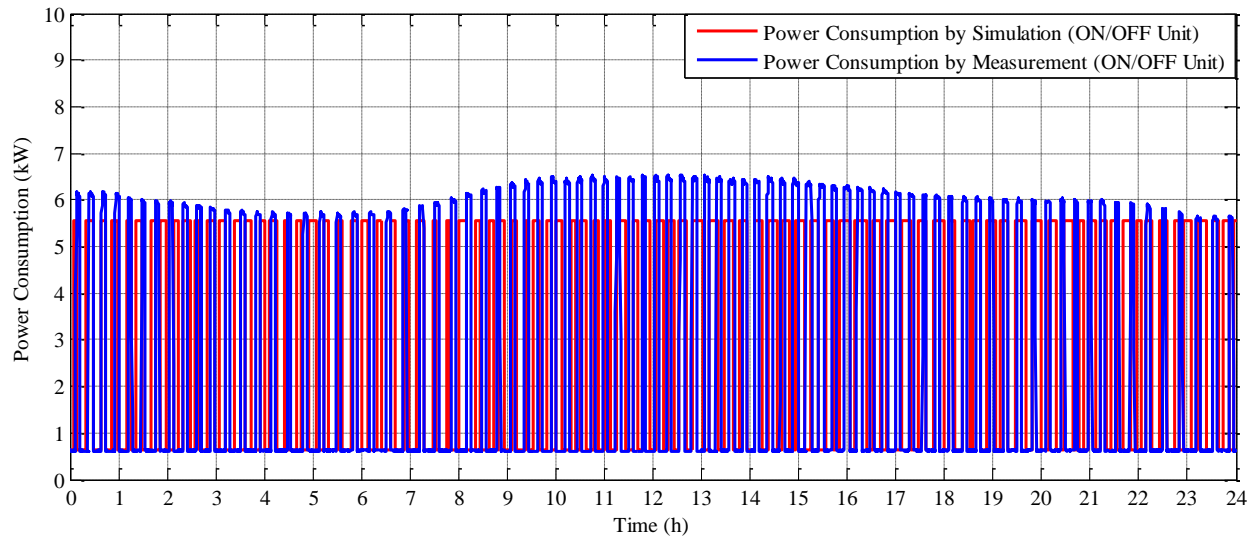
Figure 7.15Validation of simulated and measured power consumption of ON/OFF HVAC system on 05th of Sept

In central air conditioning unit, there are three motors are connected to the system, motor compressor, motor condenser, and motor blower. The motor compressor and motor condenser turn on and off together during the operation of HVAC system. The blower motor fan works continuously. In this study, it sets on the fixed mode. The performance of the ON/OFF system is running under one fixed compressor speed without any capacity control. In addition, the ON/OFF is using the full speed of the electric compressor that is equivalent to 5600 Watt.

It is clearly observed from Figure 7.15 under the ON/OFF HVAC system, the compressor motor speed fluctuates from equivalent 635 Watt to full speed and it cycles for several times as the blower motor is set on the fixed mode and it is working continuously during the whole day. The

simulated power consumption is similar to the measurement result (5.6 kW rated value), where the number of the ON/OFF HVAC system pulses are also equal 91 pulses. The total actual power consumption reached to 6.1kW as well as total simulated power consumption with slightly less than 6.1 kW. According to the experimental measurement data, it is found that the motor compressor and condenser motor consumed 39.6583kWh and blower fan motor consumed 19.9416 kWh. The total energy consumption by the simulation is 59.608 kWh and 58.4 kWh is the total energy consumption by measurement. The difference is 1.2 kWh, which is considered a very small difference in the energy consumption with the error percentage of 2.05%.

On the other hand, it is well established from experimental study in [8], that the compressor ON/OFF cycle causes significant amount of efficiency and capacity loss. In addition, it is experimentally found that efficiency loss of the system is 9% and the capacity loss is 11% due to compressor motor ON/OFF cycling. The frequent sharp pulse for compressor always generates noisiness and affects the lifetime of the motor seriously.

7.4.3 Indoor Temperature Validation of VFD-PID HVAC System

Figure 7.16 shows the validation of simulated and actual indoor air temperature of VFD-PID HVAC system on the 05th of Sept, 2016. It can be observed that the simulated indoor temperature has similar pattern of the actual indoor air temperature throughout the day. However, in the early morning until 5:00 AM, there is slightly variation happens on the actual indoor temperature above the simulated indoor air temperature. This is actually the impact of the outdoor air temperature as it fluctuates between 32 ^{o}C and 34 ^{o}C, and then it increases when the sunrises at 6:00AM. It rises continuously until it reaches 48 ^{o}C in midday. This action is having a great influence in the actual air indoor temperature which goes below the simulated temperature and reaches 23°C. The changes of the actual indoor air temperature continue at the same degree,

starting from 9:00AM until 4:00 PM as the outdoor air temperature fluctuates between 36 ^{o}C to 48 ^{o}C. However, increasing the demand of cooling air flow temperature, if rises the speed of the HVAC to supply cool air temperature. Consequently, the actual indoor temperature drops as the compressor run at the high speed to allow a faster heat recovery to the indoor environment until the set point temperature is upheld. In addition, the controller manipulates the motor speed so that indoor air temperature matches at the set point temperature from 5:00 PM until the end of the day. Finally, VFD-PID compressor could distribute conditioned air and matched the cooling capacity, which can control the indoor air temperature, furthermore, VFD-PID indoor temperature is having identical pattern as the indoor air temperature measurement data.

Figure 7.16 Validation of simulated and actual indoor temperature of VFD-PID HVAC system on 05th of Sept

7.4.4 Power Consumption Validation of VFD-PID HVAC System

Figure7.17 shows the validation of simulated and measured power consumption of VFD-PID HVAC system on the 05th of September, 2016. The simulated power consumption is appeared similar to the measured power consumption. It is clearly shown from Figure 7.17 a considerable amount of power consumptions vary between 1500 watts to 3000 watts. However, the amount of

power consumption increases and decreases smoothly depending on the internal house activities and the outdoor temperature.
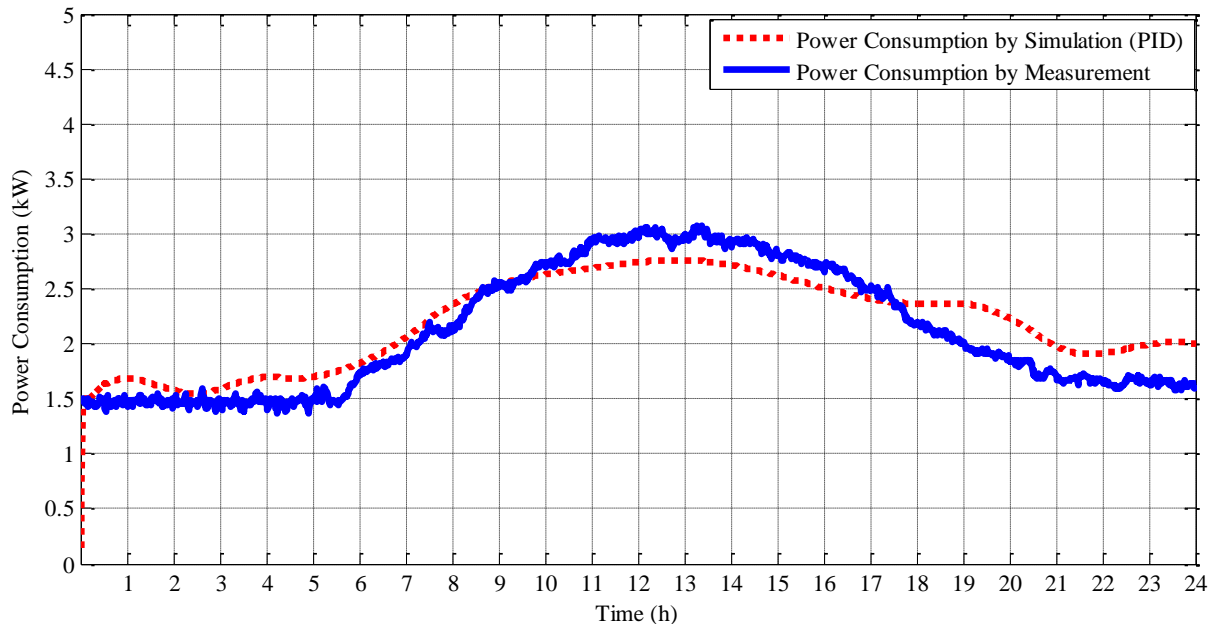
Figure 7.17 Validation of simulated and measured power consumption of VFD-PID HVAC system on 05th of Sept

It can be noticed that the power consumption flow is started to rise at 05:30 AM as the starting of the sunrise and the power consumption reaches maximum simulated power around 3 kW and 2.5 kW, from 11:00 to AM 14:00 PM due to the house activities, such as cooking breakfast/lunch, washing machine, open/close windows and door, ...etc.), and effect of outdoor air temperature. The power consumption decreases slowly till reach 2.5 kW at 17:00 and then it is dramatically deceases, due to drop in outdoor air temperature when the sunset and it continues to reach 1.6 kW throughout the remaining time of the day. On the other hand, the compressor capacity of the air conditioning system is matched the load by regulating the speed of the compressor motor. For example with low load, the compressor runs at low speed, and hence consumed less energy. However, there is slightly variation happens on the flow of the simulated power consumption as it is not exactly matching the measured power consumption. This is due the internal house

147

activities that occur by the occupants which leading to increasing the power consumptions. The energy consumption using VFD-PID HVAC approach is 46.67 kWh and the actual energy consumptions is 45.8418 kWh, there is a small difference between both energy consumptions (0.828 kWh), with the error percentage 1.77459 %.

7.4.5 Indoor Temperature Validation of VFD-PI-PWM HVAC System

Figure 7.18 shows the validation of simulated the VFD-PI-PWM HVAC system on the 05th of Sept, 2016. It can be observed that from the early morning of the day to 10:00 AM, the simulated indoor air temperature looks very similar to the actual indoor air temperature. The actual indoor air temperature seems to fluctuate in a narrow range between 23 ^{o}C to 23.5 ^{o}C from 10:30 AM until 03:00 PM, after that it matches the set point temperature till the end of the day. This action occurs due to the influence of internal house activities and the outdoor air temperature as it fluctuates between 35°C and 48 ^{o}C. However, increasing the demand of cooling air flow temperature in the midday gives raises the HVAC cool air temperature supply. Consequently, the actual indoor temperature drops as the compressor run at the higher speed. This action is taken to allow a faster heat recovery to the indoor environment until the indoor air temperature is upheld the set point. On the other hand, the simulated indoor air temperature fluctuates within ±0.5 around the set point temperature (24°C), which a very comfortable level of satisfaction. Consequently, VFD-PI-PWM controller manipulates the motor speed so that indoor air temperature matches the set point temperature throughout the day.
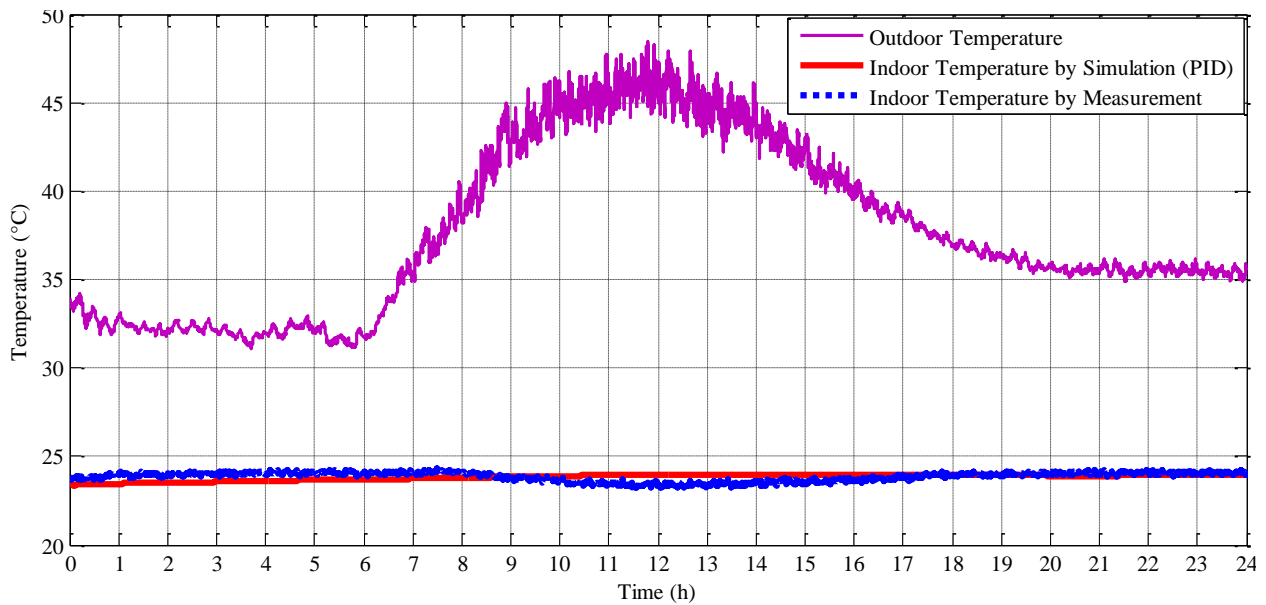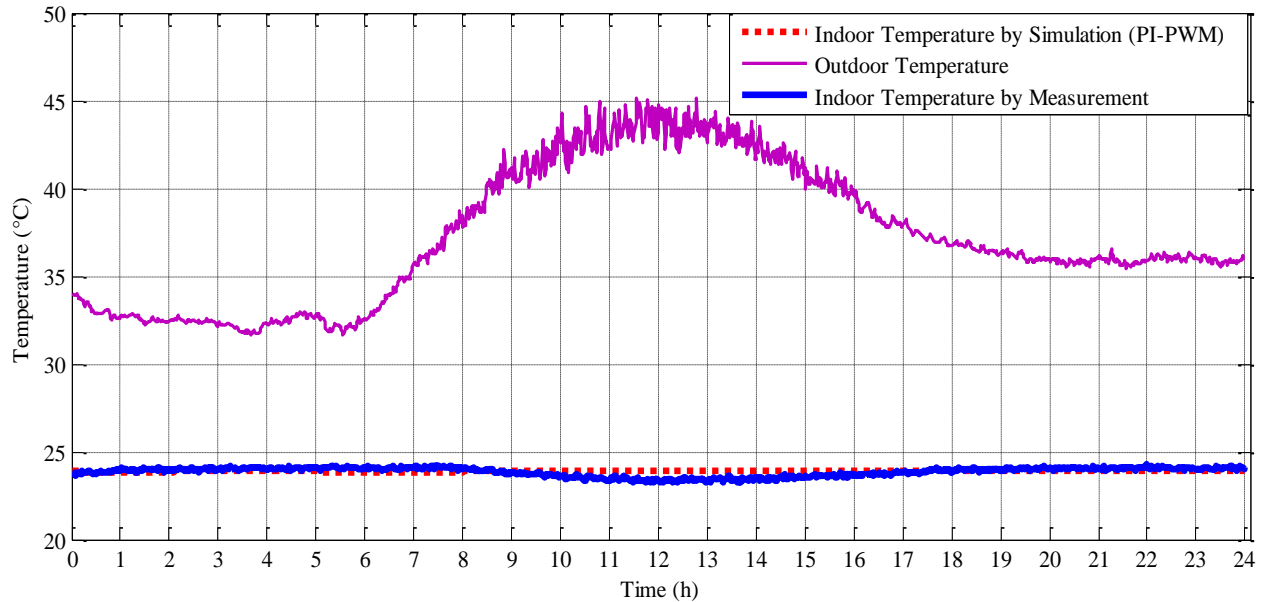
Figure 7.18 Validation of simulated and actual indoor temperature of VFD-PI-PWM HVAC system on 05th of Sept

7.4.6 Power Consumption Validation of VFD-PI-PWM HVAC System

Figure 7.19 shows the validation of simulated and measured power consumption of VFD-PI-PWM HVAC system on the 05th of Sept, 2016. The pattern of simulated power consumption result is appeared similar the measured power consumption. It is clearly shown from Figure 7.19 a considerable amount of power consumptions vary between 1500 watts to 3000 watts through the dat. However, the amount of power consumption increases and decreases smoothly depending on the internal house activities and the outdoor air temperature. On the other hand, the result indicates that the pattern of the simulated power consumption follows the same pattern of the measured power. It can be seen that at the beginning of the day the simulated power is slightly higher than the measured power as well as at the end of the day the power consumption becomes nearly constant (2.2 kW) or fluctuates in a narrow range around 2.2 kW. This actually is due to the internal actual heat gain. This phenomenon has a very significant effect on the PI-

149

PWM controller. However, it can be observed that at the midday the pattern of simulated power follows exactly the curve of the measured power.
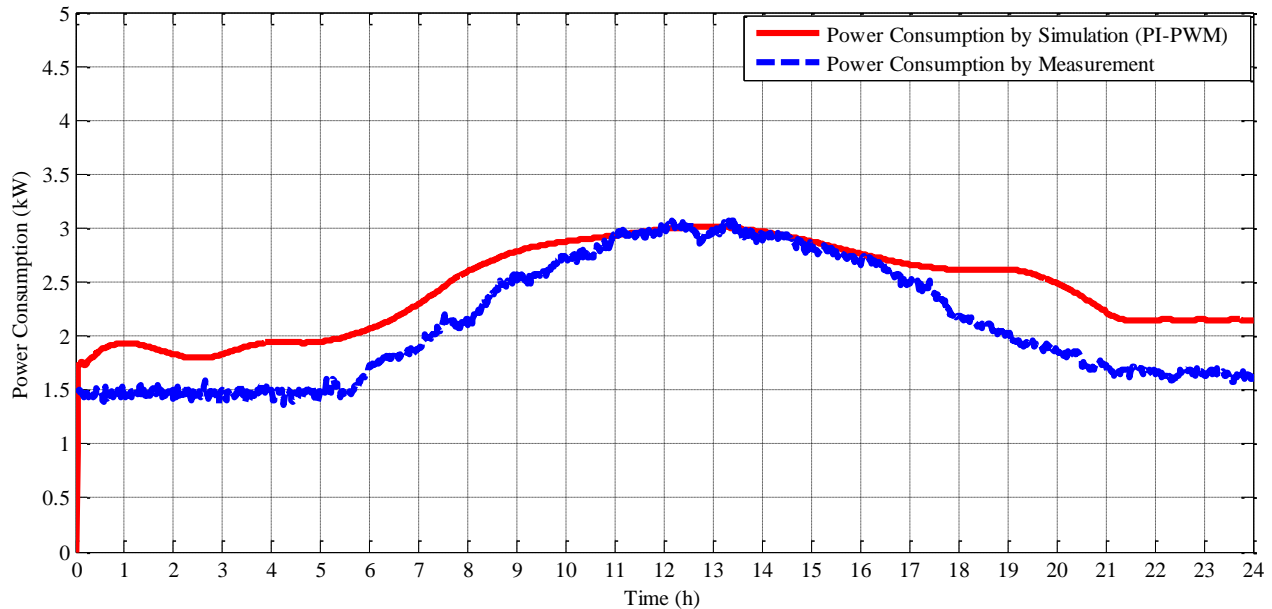
Figure 7.19 Validation of simulated and measured power consumption of VFD-PI-PWM HVAC system on 05th of Sept, 2016

The simulated energy consumption at this day is 48.98 kWh, and the energy consumption is 45.8418 kW. Moreover, the difference of the energy consumption between the simulated and actual measurements is 3.138 kWh in this particular day. The difference is a bit higher compared to the pervious approach; however, this should be still acceptable as the error is 6.4071%. As result, the VFD-PI-PWM shows that the simulation and the measurement values are both almost satisfactory.

7.4.7 Indoor Temperature Validation of VFD-FLC HVAC System

The simulation is conducted under the same conditions (outdoor air temperature & house activities) as those used for the VDF-PID and VFD-PI-PWM simulations. The simulated indoor temperature using VFD-FLC is compared with the measured data. Figure 7.20 shows the comparison of the simulated indoor air temperature with actual indoor air temperature of VFD-FLC HVAC system on the 05th of Sept, 2016. FLC provides the thermal comfort linguistically

and, therefore, can describe the thermal comfort levels rather than temperature or humidity levels which results in improving thermal comfort.
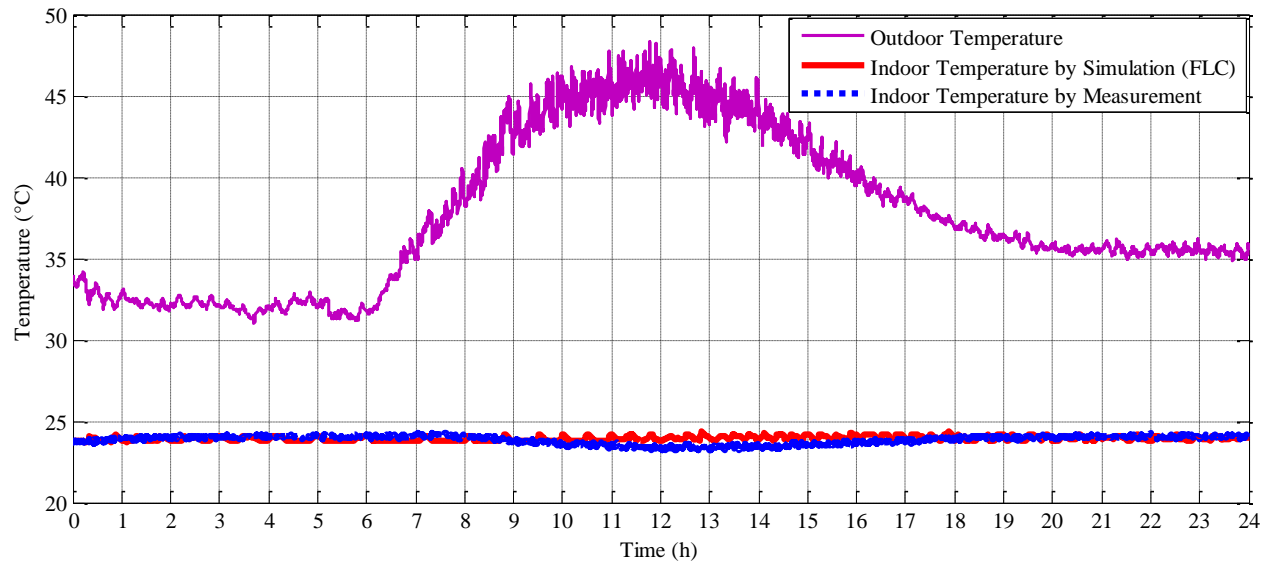
Figure 7.20 Validation of simulated and actual indoor temperature of VFD-FLC HVAC system on 05th of Sept

It is clearly shown that the response of the indoor air temperatures has similar patterns throughout the selected day, and it follows to the set point temperature. In addition, from 10:00 to 16:00, both simulated indoor air temperature and the actual indoor air temperature fluctuate in a narrow range between 23 $^\circ$C to 23.5 $^\circ$C before reaching it is steady state temperature 24 $^\circ$C. After the indoor air temperature is reached the compressor works at lower speed to maintain the indoor temperature. Furthermore, VFD-FLC HVAC system tracks the load by varying the operating conditions for better thermal comfort is achieved in the indoor environment. In cases where accurate control of temperature of an indoor environment is needed, there are some fluctuation occurs throughout the day which have achieved by the VFD-FLC HVAC approach. VFD-FLC HVAC system provides better thermal comfort for occupants compared to other approaches investigated.

7.4.8 Power Consumption Validation of VFD-FLC HVAC System

Figure 7.21 shows the validation of simulated and measured power consumption of VFD-FLC HVAC system on the 05th of Sept, 2016. The simulated power consumption is exactly similar to the measured power consumption. It is clearly presented in Figure 7.21 the amount of the power consumptions vary between 1500 watts to 3000 watts through the day for the compressor motor. The data could be observed by three distinct periods: 1:00 to 6:00, 6:00 to 19:00 and 19:00 to 12:00 for this particular day as shown in Figure 7.21. The first time period both power consumptions (simulated and measured) are varying in the level of the 1.5 kW and the trend lines fit to each other until matching the second period of time, when outdoor temperature air temperature begin to increase as the sun goes up and the occupants start their activities in the house. This is effected the performance of the HVAC system and the power consumptions dramatically increase until reach 3 kW in the midday.
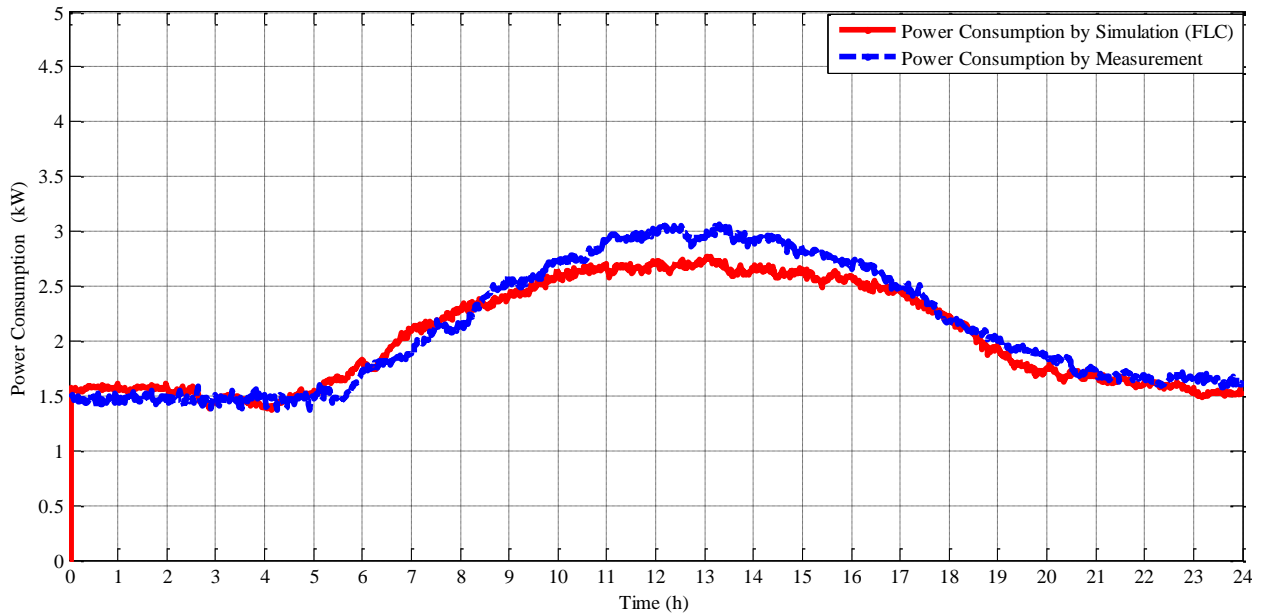
Figure 7.21 Validation of simulated and measured power consumption of VFD-FLC HVAC system on 05th of Sept

It is also noted that there is greater variation in the power at higher temperatures that occur in the afternoon hours than in the cooler morning hours. However, the power consumptions start decreases smoothly depending on the internal house activities and the outdoor air temperature until 19:00. Then the power consumptions follow each other in better fit until the end of the day compared to other controllers. Furthermore, the simulated trend line is slight below the measured power consumption pattern. This is due the accurate performance of the FLC controller, which can achieve the desired temperature set point with minimum power consumption. Regardless of slight variations, however, the power of the VFD-FLC HVAC system shows a strong relationship to outdoor air temperature. Moreover, Figure 7.20 reveals that the indoor air temperature dropped as the compressor ran at higher speed.

On the other hand, increasing the internal heat load (house activities) will cause the response of using the FLC controller is much faster than that controlled by PID and PI-PWM. VFD-FLC HVAC system gives the highest saving in comparison with other approaches studied. The energy consumption using VFD-FLC HVAC technique is 43.23 kWh and the actual energy consumptions is 45.8418 kWh. There is a small difference between both energy consumptions which is (2.6 kWh). However, the error is 6 %.

7.4.9 Daily Energy Consumption Analysis

Reducing energy consumption becomes one of the most important aspects in HVAC control system design because of the fact that 50% of the world energy is consumed by HVAC equipment in industrial and commercial buildings and residential area [2]. However, the power consumption is investigated experimentally and numerically. The total energy consumptions for both HVAC units are obtained for evaluate and analysis. Table 7.3 gives the total energy consumptions for both measurement and simulation. It provides a clear comparison for one

particular day measurement. The table shows that VFD-FLC HVAC unit consumed less energy compared to other VFD HVAC approaches and ON/OFF HVAC unit. The average of the VFD energy consumption done by VFD simulation strategies is 46.29 kWh.

Table 7.3 Energy consumptions for the different controllers studied for one day

Validation of Energy Consumptions of One Day (5th of September, 2016)					
Date	Energy Consumption by Measurement (VFD unit) per day	Energy Consumptions by Simulation (VFD unit) per day			Energy Consumption by Measurement per day	Energy Consumption by Simulation (ON/OFF unit) per day
	45.8418 kWh	VFD -PI-PWM HVAC unit	VFD–PID HVAC unit	VFD-FLC HVAC unit	59.6085 kWh	58.40 kWh
5/09/2016		48.98 kWh	46.67 kWh	43.23 kWh		

Based on the power consumptions data measurements for both units, it becomes an easy way to calculate and evaluate the energy consumption for compressor with condenser motor and the blower fan motor for selected day. Table 7.4 presents clearly the compressor energy consumption compressor and blower fan for both unites.

Table 7.4 Energy consumption by compressor and blower fan for both unites (Measurement data)

Energy used by Compressor and Blower Fan for One Day (5th of September, 2016)						
Day	Total Energy Consumed by ON/OFF Unit	Total Energy Consumed by ON/OFF (Comp & Fan Motor)		Total Energy Consumed by VFD Unit	Total Energy Consumed by VFD (Comp & Fan Motor)	
		Comp & Cond	Blower Fan		Comp & Cond	Blower Fan
5/09/2016	59.60 kWh	39.6583 kWh	19.94 kWh	45.841 kWh	24.124 kWh	21.717 kWh

7.4.10 Daily Energy Savings Analysis

The energy consumption is the power (P) multiplied with time operation (t) of the AC system. Whereas, the energy savings calculated and expressed in terms of percentage based on the difference between energy consumed by on/off control and energy consumed by the VFD control.

$$\text{Power} = \frac{\text{V} \times \text{I} \times \text{PF}}{1000}(\text{kW}) \tag{7.1}$$

Where is the current (Ampere), is V voltage (Volts), and PF is power factor.

$$\text{Energy} = \text{Power} \times \text{t}(\text{kWh}) \tag{7.2}$$

$$\text{Energy Saving} = \frac{(\text{ON/OFF HVAC Measured Energy Consumption}) - (\text{VFD HVAC Measured Energy Consumption})}{(\text{ON/OFF HVAC Measured Energy Consumption})} \times 100 \tag{7.3}$$

$$\text{Energy Saving} = \frac{(\text{ON/OFF HVAC Simulated Energy Consumption}) - (\text{VFD (PID-PI-PWM-FLC) HVAC Simulated Energy Consumption})}{(\text{ON/OFF HVAC Simulated Energy Consumption})} \times 100$$
$$\tag{7.4}$$

$$\text{Energy Saving} = \frac{(\text{ON/OFF HVAC Measured Energy Consumption}) - (\text{VFD (PID-PI-PWM-FLC) HVAC Simulated Energy Consumption})}{(\text{ON/OFF HVAC Measured Energy Consumption})} \times 100 \tag{7.5}$$

Equations (7.3), (7.4) and (7.5) are used to calculate the energy savings. Based on equations (7.3) and (7.4) the energy saving per day is shown in Table 7.5. However, the VFD-FLC provides the highest energy saving compared to other approaches for this day. The average of energy saving by VFD simulation strategies is 20.71%.

Table 7.5 Energy savings for the simulation approaches studied for one day.

Energy Savings of One Day (5th of September, 2016) by Simulation				
Date	Energy Saving by Simulation ON/OFF & VFD-PID HVAC unit	Energy Saving by Simulation ON/OFF & VFD-PI-PWM HVAC unit	Energy Saving by Simulation ON/OFF & VFD-FLC HVAC unit	Energy Saving by Measurements ON/OFF unit & VFD HVAC unit
5/09/2016	20.08%	16.13%	25.97%	23.09%

According to equation (7.5) the energy saving result from by the simulated VFD HVAC techniques compared to measured ON/OFF HVAC energy consumption is calculated. Table 7.6 provides the validation results of energy savings for the simulated VFD HVAC approaches with the measured ON/OFF unit. It is observed that the energy saving by VFD-PI-PWM HVAC and VFD-PID HVAC is lower than the energy saving by VFD- FLC HVAC. Moreover, the implemented simulation of VFD-FLC HVAC approach proved efficient in terms of model development energy consumption and most energy saving.

Table 7.6 Validation of energy savings for the VFD HVAC approaches with the ON/OFF unit.

Validation of Energy Savings of One Day (5th of September, 2016) by Simulation and Measurements			
Date	Energy Saving by Measurement & Simulation ON/OFF & VFD-PID HVAC unit	Energy Saving by Measurement & Simulation ON/OFF & VFD-PI-PWM HVAC unit	Energy Saving by Measurement & Simulation ON/OFF & VFD-FLC HVAC unit
5/09/2016	21.70%	17.82%	27.32%

After obtaining the energy consumption results, the error formula is used for determining the precision of the simulation approaches that have achieved in this study and compared them to the measured data. The formula is given by:

(7.6)

$$\text{Error \%} = \frac{\text{Expermintal Value - Simulation Value}}{\text{Simulation Value}} \times 100\%$$

Table 7.7 gives the error percentage for each approach; it can be noticeable that VFD-PID HVAC error percent is around -1.77%, which indicates that the simulation result is very close to the measurement value. VFD-FLC HVAC error percentage is +6.04%, which implies that the result of the VFD-FLC HVAC is lower than measurement data. Also the ON/OFF HVAC error percent is approximately 2 %.

156

Table 7.7 Error percentage of all the approaches

Variables	Experimental	Simulation	% Error
VFD-PID	45.8418	46.67	−1.77 %
VFD-IP-PWM	45.8418	48.98	−6.40 %
VFD-FLC	45.8418	43.23	+6.04 %

On the other hand, the error percent of VFD- HVAC is observed a bit high which about 6%, this indicates that the simulation value is less than the measurement value, which gives a clear indication that the VFD-FLC HVAC unit is the suitable control strategy.

It can be concluded that the use of a VFD to save energy in an air conditioning system is justified. Although different simulation approaches have been studied, and they had produced significant energy saving. However, VFD-FLC HVAC gives the most energy savings and performs better than the other control systems investigated. In addition, the use of a VFD unit will be economically justifiable and the result will be presented in end of this chapter.

Finally, the measurements results indicate than in VFD has the ability to maintain the indoor temperature close to the set point temperature without having to repeatedly turn the compressor on and off. But, it should be mentioned that when the HVAC inverter operates under one condition, in which if the load is less than minimum rated power, the operation of VFD shift to ON/OFF mode as can be seen some days. This action is only occurs in the experimental data.

7.4.11 Average Daily COP Variations

The coefficient of performance (COP) is commonly used to express the efficiency of an air-conditioning system. The main purpose of the HVAC system is to remove heat or to process load from the evaporator (Q_L). The energy required at the compressor (W_{com}) is to accomplish the refrigeration effect. Thus, the COP is expressed as:

$$COP = \frac{(h_1 - h_4)}{(h_2 - h_1)} = \frac{Q_L}{W_{com}} = \frac{\text{Internal Heat Gain (Energy Input) (kWh)}}{\text{Total Energy Consumption (kWh)}} \qquad (7.7)$$

Where, h_1 and h_2 (kJ/kg) are the enthalpy at the compressor inlet and the compressor outlet, respectively, h_4 (kJ/kg) is the enthalpy at the evaporator inlet, Q_L (kWh) is the refrigerating effect, and W_{com} (kWh) is the compression work.

The maximum theoretical COP for the air conditioning system is expressed by Carnot's theorem given by the following equation:

$$COP_{Maximum} = \frac{(T_C)}{(T_H - T_C)} \qquad (7.8)$$

Where T_C is the cold temperature and T_H is the hot temperature. The air conditioning system cools the house to 22.5 $^{\circ}$C for (ON/OFF) and 23 $^{\circ}$C for (VFD). The hottest outdoor temperature is 48.4 $^{\circ}$C, the theoretical maximum COP is:

$$COP_{Max(ON/OFF)} = \frac{(T_C)}{(T_H - T_C)} = 0.86 \qquad (7.9)$$

$$COP_{Max(VFD)} = \frac{(T_C)}{(T_H - T_C)} = 0.91 \qquad (7.10)$$

The total internal heat gain for the 5th of September, 2016 is calculated based on the solar heat gain, mass heat gain, and the internal house activities.

Total internal heat gain per day = 46.159 kWh (Heat Energy)

$$COP_{(ON/OFF)} = \frac{Q_L}{W_{com}} = \frac{46.159 kWh}{59.60 kWh} = 0.77 \qquad (7.11)$$

$$COP_{(VFD)} = \frac{Q_L}{W_{com}} = \frac{46.159 kWh}{45.84 kWh} = 1.006 \qquad (7.12)$$

The COP was calculated using equation (7.8). The results show that the average actual COP of 0.77 for ON/OFF unit and 1.006 for VFD unit. The value of the actual COP represents the motor

run at the maximum speed. It can observed that when the compressor energy consumption increases the COP decreases.

Table 7.8 gives a summary of the daily values of the Actual and Carnot coefficient of performance of both VFD HVAC and ON/OFF HVAC unites for 5th of September, 2016.

Table 7.8 Values of the Actual and Carnot COP for both unites on 5th of September, 2016

Temperature Set-point (24 °C)	Actual-COP		Carnot-COP	
	ON/OFF HVAC Unit	VFD HVAC Unit	ON/OFF HVAC Unit	VFD HVAC Unit
05/09/2016	0.774369427	1.006919449	0.86	0.91

7.5 Weather Environmental Analysis for (September, 2016)

In this section, monthly energy consumption profiles of the simulation and measurement data for both HVAC unites are presented and analyzed. However, to analyze the energy consumption accurately the climate data for this particular month, such as outdoor temperature, outdoor humidity, wind speed and radiation have to be obtained. Figure 7.22 presents daily average of outdoor humidity (%), daily average of the wind speed (m/s) and daily of irradiation (W/m^2).
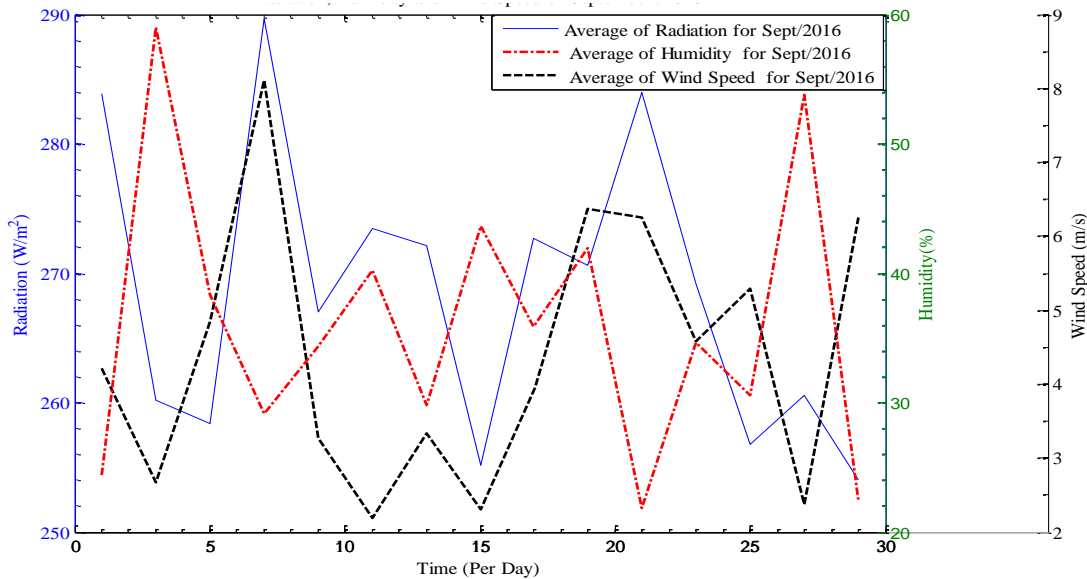
Figure 7.22 Daily average of the radiation, humidity, and wind speed of September, 2016

It can be observed from Figure 7.22 that the outdoor humidity varies between 22% - 60% during

the month of September, 2016. Moreover, the humidity seems a bit high in the early days of the

month and reaches around 60%, and then it continues its variation between 35% and 45% until

the end of the month. It is noticed that the wind speed fluctuates between 2.2 m/s to 8 m/s

throughout the month. Furthermore, the level of the radiation fluctuates between 250 W/m^2 to

290 W/m^2 through this particular month. However, all these changes occur in the weather is

definitely having a strong effect on the energy consumption of the HVAC unites.
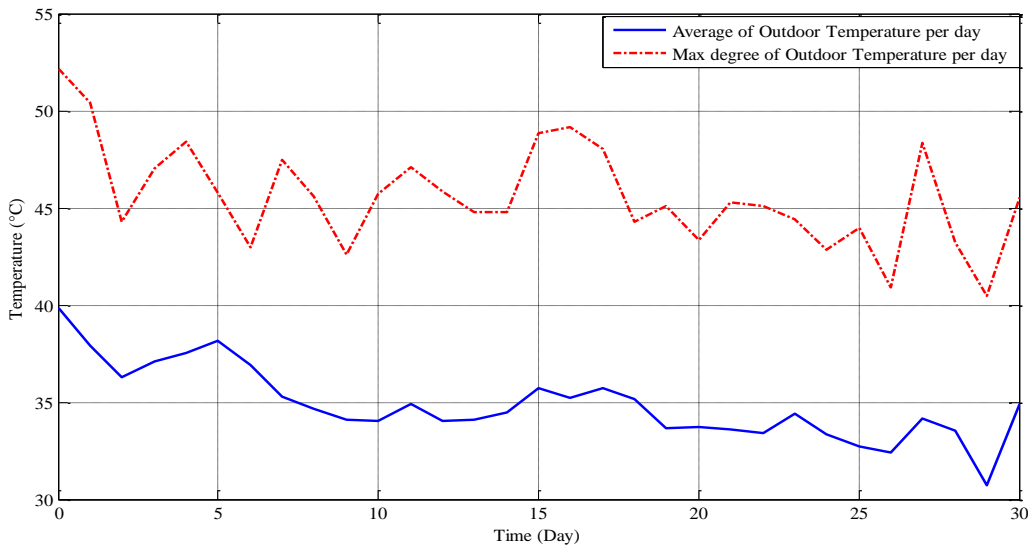
Figure 7.23 Daily average of outdoor temperature with the maximum degree in each day of September, 2016

Figure 7.23 shows the daily average of the outdoor temperature and maximum degree of outdoor

temperature for each day of September, 2016. According to the approaches that have been

investigated previously in this study, the outdoor temperature has a significant influence on the

performance of the HVAC system. However, when the outdoor temperature increases the energy

consumption increases. The average outdoor temperature is varies between 33°C to 40 ^{o}C

through the month and the maximum degree of the outdoor temperature fluctuates between 41°C

to 52.5^{o}C.

7.5.1 Energy Consumption by ON/OFF HVAC unit for (September, 2016)

The simulation study for ON/OFF HVAC unit has been conducted for each day separately and by using the same simulation's conditions that previously mentioned. Figure 7.24 presents the validation of the simulation results of the energy consumption compared with the measured energy consumption by ON/OFF HVAC unit for September, 2016. It is observed that the simulated energy consumption pattern follows the same trend line of the measured energy consumption. The high energy consumptions are registered in the first four days of September reading, as it is high than 70 kWh per day. Then it drops dramatically till 13th of September, as it goes up to 60 kWh. After that, it continues decreasing till the end of the September. Moreover, it is clearly seen from the figure that the difference of the energy consumption between the first five days and the last days of the month is a great different; this is due to the outdoor temperature and outdoor humidity influences. Consequently, the consumption of HVAC energy correlates to the outdoor temperature.
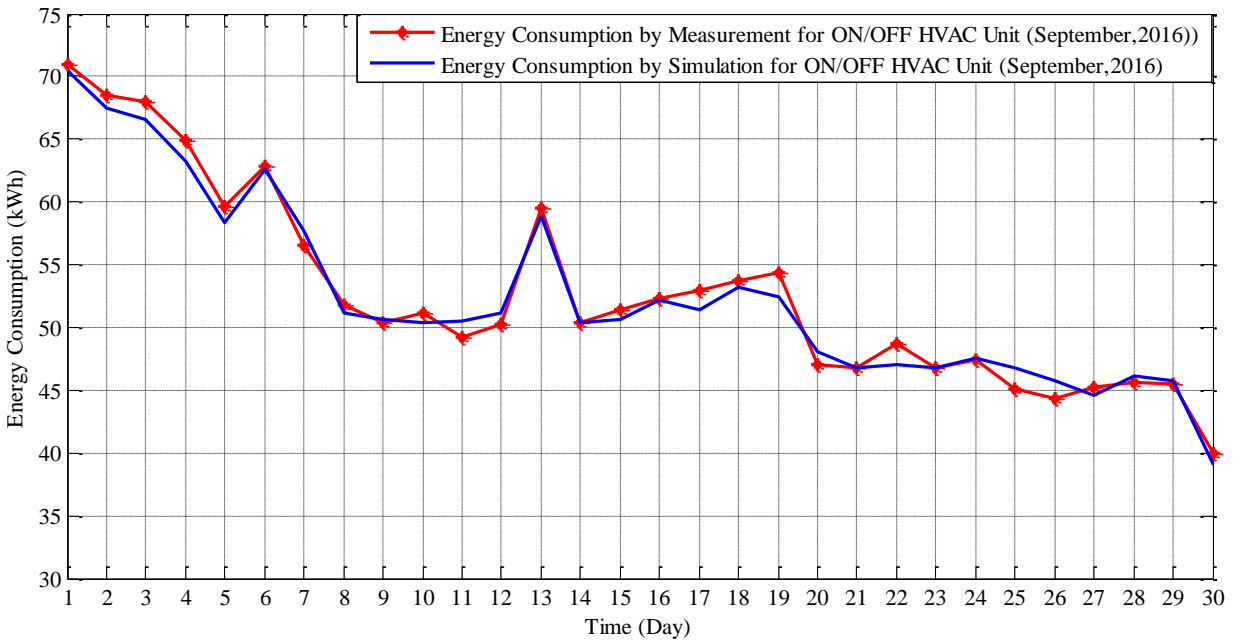
Figure 7.24 Comparison of the simulated and the measured energy consumptions of ON/OFF unit in September, 2016

Monthly average energy consumption for ON/OFF HVAC system profile by both simulation and measurement is 53.02 kWh and 53.57 kWh, respectively. The monthly total energy consumption of the ON/OFF HVAC by simulation and measurement is 1590.62 KWh 1598.21KWh, respectively. The error percentage is 0.48%.

7.5.2 Energy Consumption by VFD HVAC unit for (September, 2016)

Figure 7.25 displays the simulation of the energy consumptions of the VFD HVAC compared with the measured energy consumption. It can be notice that the simulation results follow the pattern of the measurement results. However, VFD-FLC HVAC unit is slightly lower the measured energy consumption curve and the rest of the VFD's approaches are at or upper the measured energy consumption curve. Consequently, VFD-FLC HVAC system offers lower energy consumption as compared to other investigated VFD HVAC controllers. It should be mentioned that VFD-PID energy consumption pattern is the closest to the actual measured energy, this is due to the use of the PID controller in the actual unit. VDF-FLC HVAC can be implemented to enhance the operation of HVAC system to consume less energy.
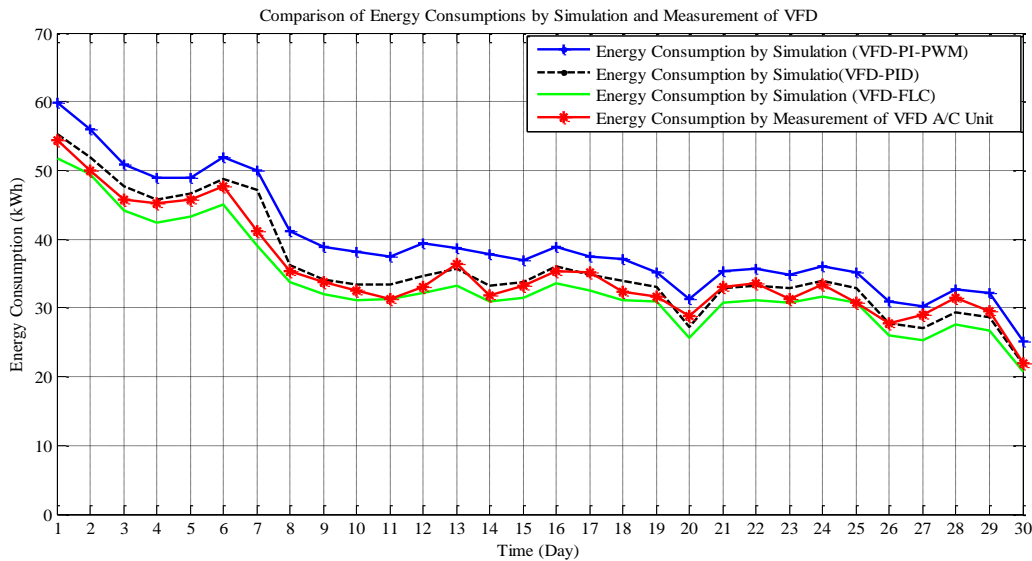
Figure 7.25 Comparison of a daily simulated energy consumption by VFD HVAC approaches with measured energy VFD HVAC unit for September, 2016

The total and operational measured energy consumptions are calculated for the month of September by multiplying the power consumption of the motors and the actual operating hours. Figure 7.26 shows the energy consumptions demand and energy saving for VFD HVAC in comparison with ON/OFF HVAC unit. The results indicate that energy consumption for VFD unit is lower than ON/OFF HVAC unit. As the performance of the ON/OFF system is running under one fixed compressor speed without any capacity control, and VFD HVAC unit has the ability to vary its speed, which controls the load capacity and as the compressor reduces its speed, a significant reduction in power consumption is achieved.
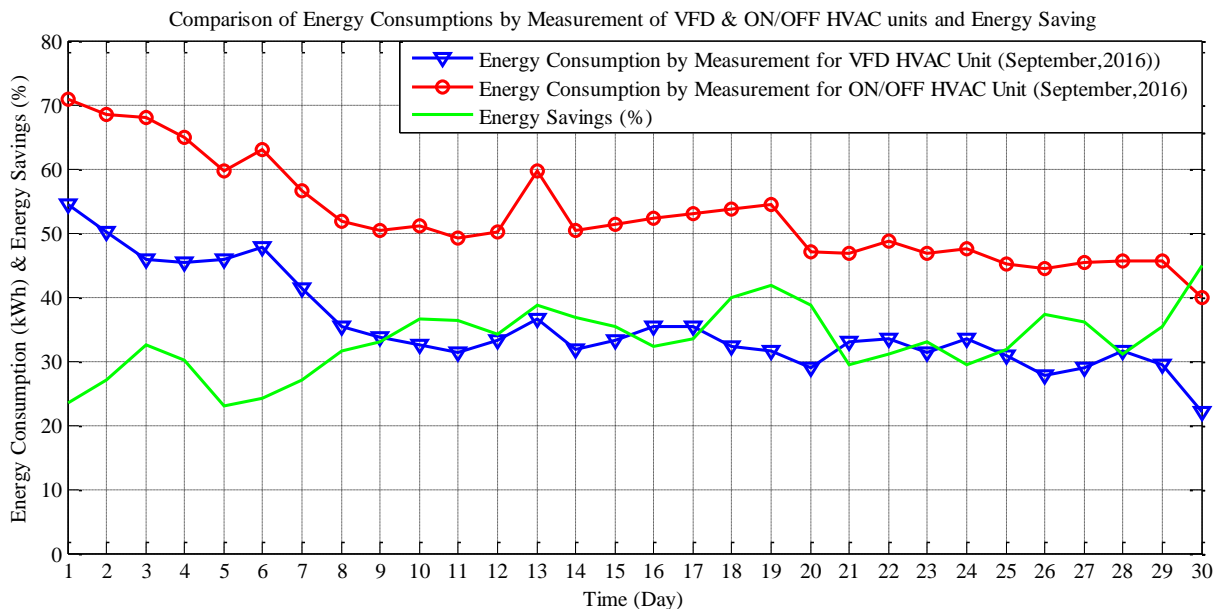
Figure 7.26 Comparison of daily measured energy consumptions for ON/OFF and VFD HVAC and energy saving for September, 2016.

On the other hand, it is clearly shown that HVAC unites energy demand is affected by outdoor temperature and outdoor humidity that have a direct influence on energy consumption. It can be claimed that the fluctuation that occurs in the demand of the energy consumptions is also due to the internal house activities, which have a great impact on the performance of the HVAC operation as well as the energy consumption. In addition, the results indicate that there is slightly

increasing in the energy consumption on 13th of September, 2016 by ON/OFF HVAC unit comparing to the previous and following day for the same unit. This is due to the increase in the internal load gain that occurs in the house, which reflects to increasing the energy consumption. However, the total energy consumption by measurements test in September by both VFD HVAC and ON/OFF HVAC is 1963.037 kWh and 1598.21kWh ,respectively. The average of the measured energy consumption in September by both VFD HVAC and ON/OFF HVAC is 35.43 kWh and 53.57 kWh, respectively.

7.5.3 Energy Savings for (September, 2016)

Figure 7.27, presents considerable amount of savings of energy occur by the VFD HVAC compared to ON/OFF HVAC unit throughout the month of September for the measurements test. The highest amount of energy saving occurs on the last day of September , reaches which 44.94%, this is due to the lower energy consumed by the VFD HVAC compared to the ON/OFF HVAC energy consumed, as the weather was become cooler at the end of the September. However, the average of energy saving for September, 2016 is 33.86% which considered a great amount of saving.
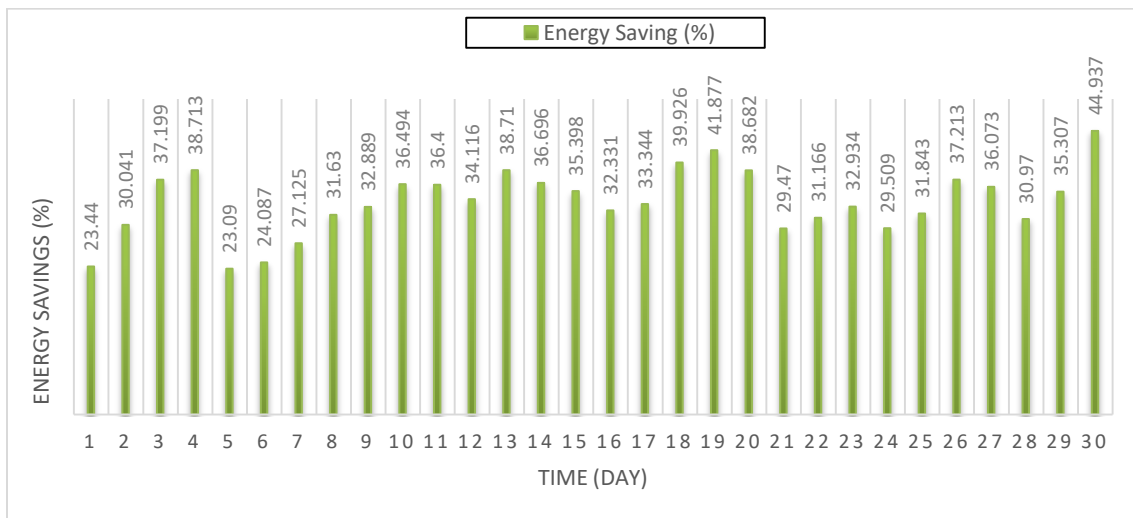
Figure 7.27 Energy savings of the VFD HVAC compared to the ON/OFF HVAC unit, (measurement)

Table 7.9 provides the validation results of energy savings for the simulated VFD HVAC approaches with the measured ON/OFF unit. It is observed that the energy saving by VFD-PI-PWM and VFD-PID is lower than the energy saving by VFD-FLC HVAC. Moreover, the implemented simulation of VFD-FLC HVAC approach proved efficient in terms of model development energy consumption and most energy saving.

Table 7.9 Energy savings for the simulation approaches studied for September, 2016

Energy Savings of September, 2016 by Simulation				
Date	Average of Energy Saving by Simulation ON/OFF & VFD-PID HVAC unit	Average of Energy Saving by Simulation ON/OFF & VFD-PI-PWM HVAC unit	Average of Energy Saving by Simulation ON/OFF & VFD-FLC HVAC unit	Average of Energy Saving by Measurements ON/OFF unit & VFD HVAC unit
5/09/2016	31.90 %	25.59 %	36.73 %	33.86%

It is clearly shown in Figure 7.28 that VFD-FLC HVAC provides the highest energy saving comparing to other controller techniques in September, 2016. However, the average of energy saving by VFD simulation strategies is 31.41.71%.

Figure 7.28 Validation of energy savings of the VFD approaches compared to the ON/OFF unit, (simulation)

Figure 7.29, presents energy savings comparison between the simulated VFD HVAC approaches with the measured ON/OFF HVAC unit. It is observed that the energy saving by VFD-PI-PWM HVAC and VFD-PI HVAC is lower than the energy saving by VFD-FLC HVAC. Moreover, the implemented simulation of VFD-FLC HVAC approach proved e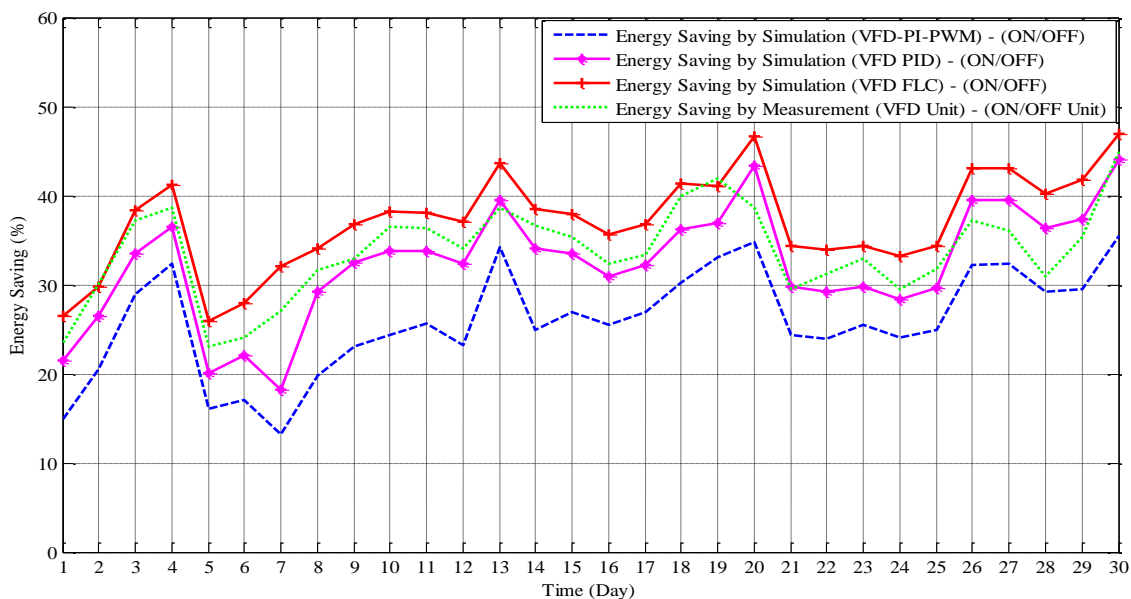fficient in terms of model development, energy consumption and most energy saving. Table 7.10 provides the validation results of energy savings for the simulated VFD HVAC approaches with the measured ON/OFF HVAC unit.
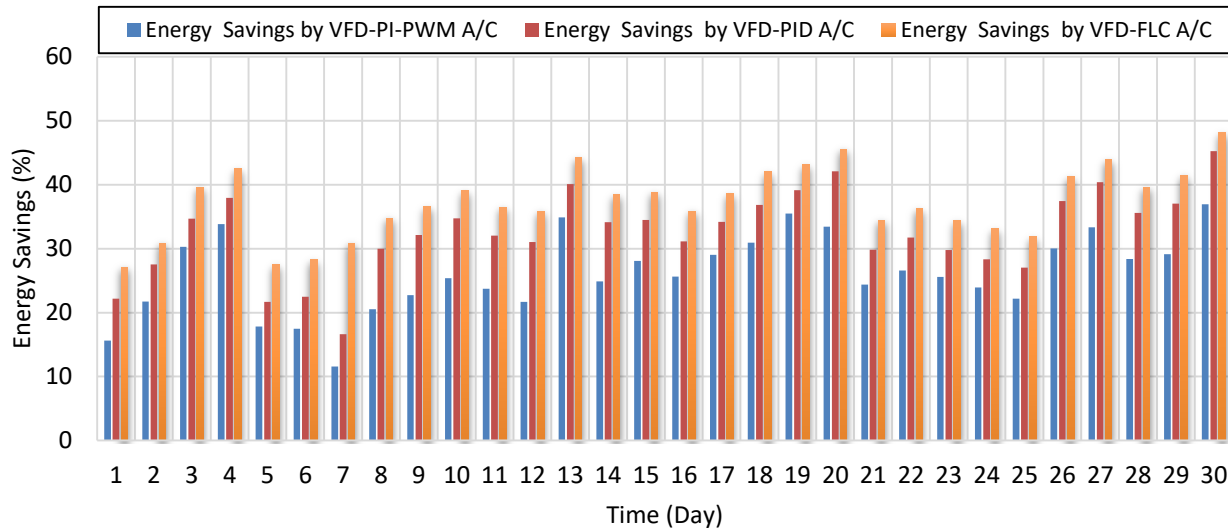
Figure 7.29 Comparison of the VFD HVAC simulation approaches with the measured ON/OFF HVAC energy savings

Table 7.10 Validation of energy savings of September, 2016 by simulation and measurements.

Validation of Energy Savings of September, 2016 by Simulation and Measurements			
Date	Energy Saving by Measurement & Simulation ON/OFF & VFD-PID HVAC unit	Energy Saving by Measurement & Simulation ON/OFF & VFD-PI-PWM HVAC unit	Energy Saving by Measurement & Simulation ON/OFF & VFD-FLC HVAC unit
5/09/2016	32.58 %	26.17 %	37.33 %

It can be concluded that the use of a VFD to save energy in an air conditioning system is justified for one complete month with several data comparison. Although different simulation approaches have been studied, and they had produced significant energy saving.

7.5.4 Average Monthly COP Variations

Based on equations (7.7) and (7.8), the measured energy consumptions and the internal heat gain (September, 2016), the monthly average actual coefficient of the performance, COP variation is calculated. The daily average of internal heat gain for the month of September in both houses = 42.922 kWh (heat). The daily average of the measured energy used for the month of September by the ON/OFF HVAC unit = 53.57 kWh, and the daily average of the measured energy used for the month of September by the VFD HVAC unit = 35.34 kWh.

$$\text{COP}_{(\text{ON/OFF})} = \frac{Q_L}{W_{com}} = \frac{42.922\,\text{kWh}}{53.57\,\text{kWh}} = 0.8 \qquad (7.13)$$

$$\text{COP}_{(\text{VFD})} = \frac{Q_L}{W_{com}} = \frac{42.922\,\text{kWh}}{35.34\,\text{kWh}} = 1.2 \qquad (7.14)$$
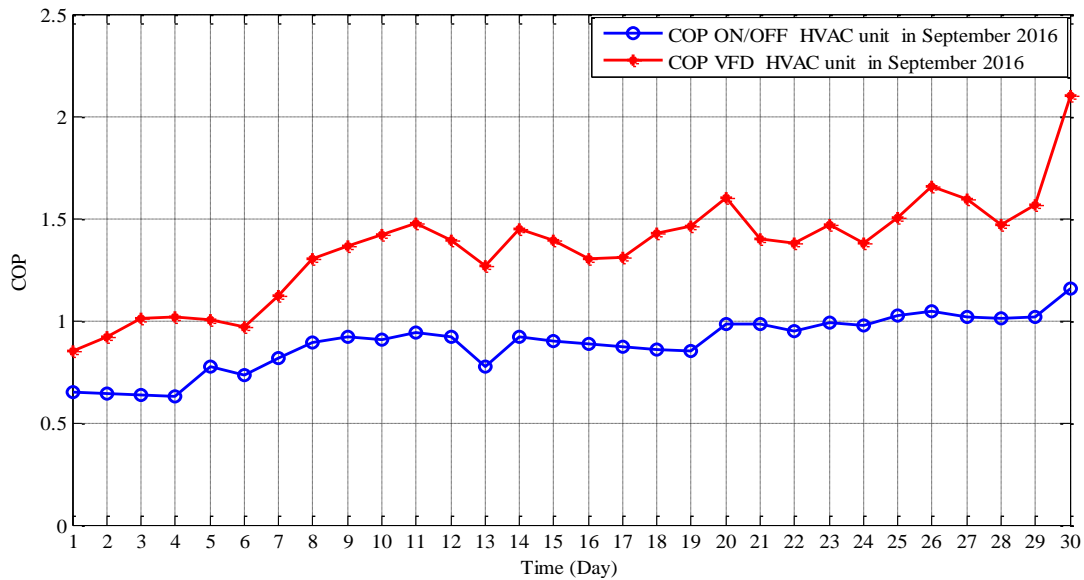
Figure 7.30 Comparison of the VFD HVAC COP and ON/OFF HVAC COP for September, 2016.

Based on equations (7.13) and (7.14), the average COP of the ON/OFF HVAC unit and VFD unit is 0.8 and 1.2, respectively. The results indicate that the COP of ON/OFF unit is less than the COP of the VFD, due to the increasing of energy consumption by ON/OFF unit. On the other hand, Figure 7.30 shows a comparison of daily actual COP of both HVAC unites. Consequently,

it can be claimed that the energy consumption can be reduced by improving the performance of the compressor or the coefficient of performance, which relies on the speed of the compressor motor. COP values will be larger at the lower compressor speed which results in low energy consumption. However, increases in compressor speed results increase in energy consumption with low COP. With VFD technology, compressor speed can be varied by changing the frequency, voltage and current of the compressor motor, leads to minimum energy consumption and then larger COP.

7.6 Annual Weather Environmental Analysis

Figure 7.31 presents the maximum outdoor temperature, the average outdoor temperature and the minimum outdoor temperature for the year of 2016. It can be observed that June, July, August, and September of 2016 are the hottest months of the year as the maximum outdoor reaches approximately 55°C and the minimum outdoor temperature reaches 36°C. Increasing the outdoor temperature will lead to increase the demand of the cooling systems over the year, which means that more energy is required.
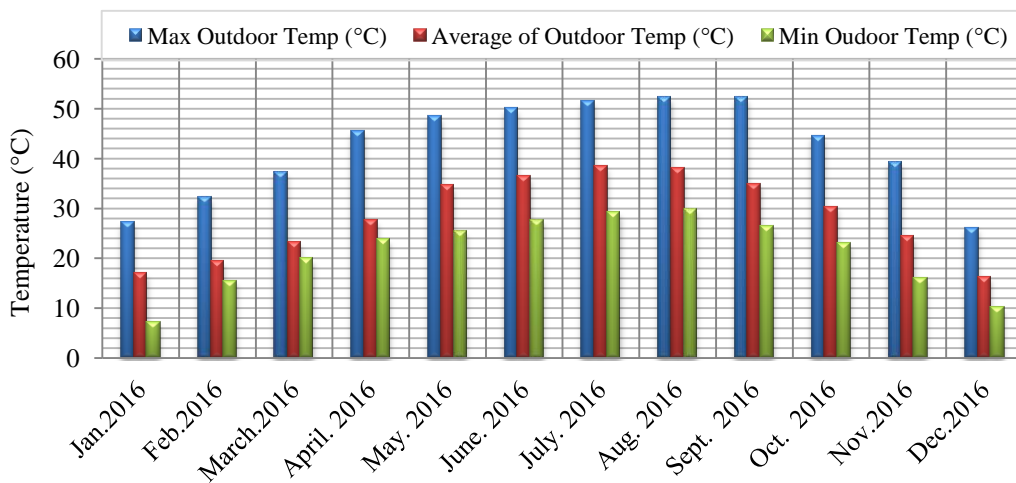
Figure 7.31 Temperature data for KFUPM campus at Dhahran, Saudi Arabia (2016)

The data collected based on average hourly of outdoor humidity. Figure 7.32 shows the relatively humidity variation during the year, 2016. The humidity fluctuates between 5%-90% throughout the year. It can be observed that the humidity is low during two months of the year, April and May compared to other months of the year. The outdoor humidity can affect the performance of the HVAC operation. Also, with such an extreme weather conditions in the Saudi Arabia, comfortable lifestyle has become the first priority, thereby pushing up the cooling demand.
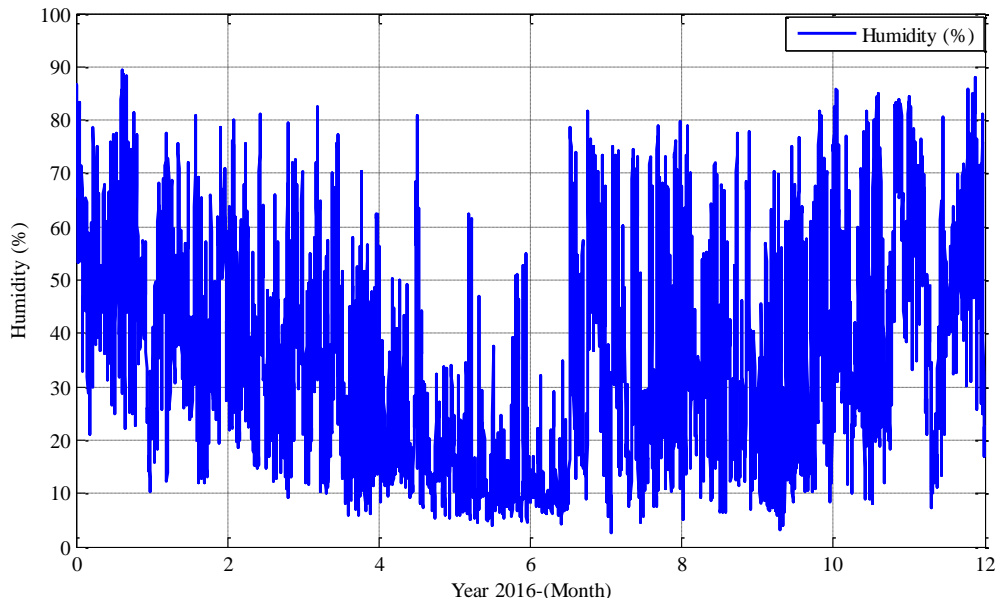
Figure 7.32 Hourly average of humidity of Dhahran area, 2016.

7.6.1 Annual Energy Consumption by Measurement

The most important finding of the monitoring and measurement system in this study is that HVAC systems account for a large part of energy consumption within the residential sector. With such an extreme weather conditions in the Saudi Arabia, comfortable lifestyle has become the first priority, thereby pushing up the demand of the energy consumption over the year. However, reducing the energy demand of the residential sector directly leads to a reduction in HVAC energy demand. A monthly energy consumption profile was measured for the both VFD HVAC and ON/OFF HVAC systems for the year, 2016.

169

7.6.2 Annual Energy Consumption by Measurement for ON/OFF & VFD

Figure 7.33 shows total of monthly energy consumption by both ON/OFF HVAC unit and VFD HVAC unit for year, 2016 by measurement. It can be observed from the figure that the highest energy demand occurs in summer season due to the warm, hot, and humid weather. In correspondence to the highest cooling demand, monthly energy consumptions during the summer months could be up to 2200kWh for ON/OFF HVAC unit and 1650 kWh for VFD HVAC unit, while the monthly total energy consumption in the winter months is less than 500kWh.
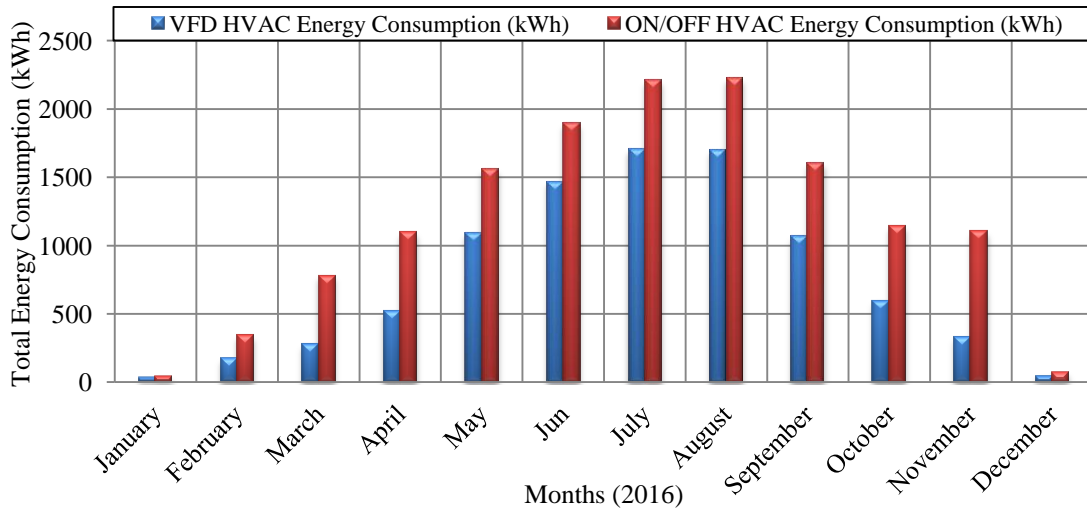
Figure 7.33 Annual energy consumptions by ON/OFF HVAC and VFD HVAC units, 2016.

However, the highest months used energy in the summer is Jun, July and August, 2016, as they used 1469.238 kWh, 1705.818 kWh, and 1696.081kWh,repesctilvly, for VFD HVAC unit, and 1894.732kWh , 2211.168 kWh ,and 2225.915 kWh, respectively, by ON/OFF HVAC unit. The total annual energy consumptions used by both ON/OFF HVAC and VFD HVAC unit is 14073.69 kWh and 9006.146 kWh, respectively. And the monthly average for both units is 1172.8 kWh and 750.51kWh, respectively.

On the other hand, based on the measurement data of energy consumptions by both HVAC units, Figure 7.34 shows the monthly average of year, 2016, for ON/OFF HVAC unit, and VFD HVAC

unit, and the monthly average of the outdoor temperature for Dhahran area. This graph is created

to link the relationship of the outdoor temperature with the energy demand. It can observe that

the patterns of the average energy consumptions of both HVAC units are similarly follow the

pattern of the outdoor temperature over the year. As would be expected when the average

outdoor temperatures drop significantly lower, the average monthly of energy consumptions

drops as well, especially during the summer period and we can say that "Air conditioning

drivers' seasonal change in electricity consumption".
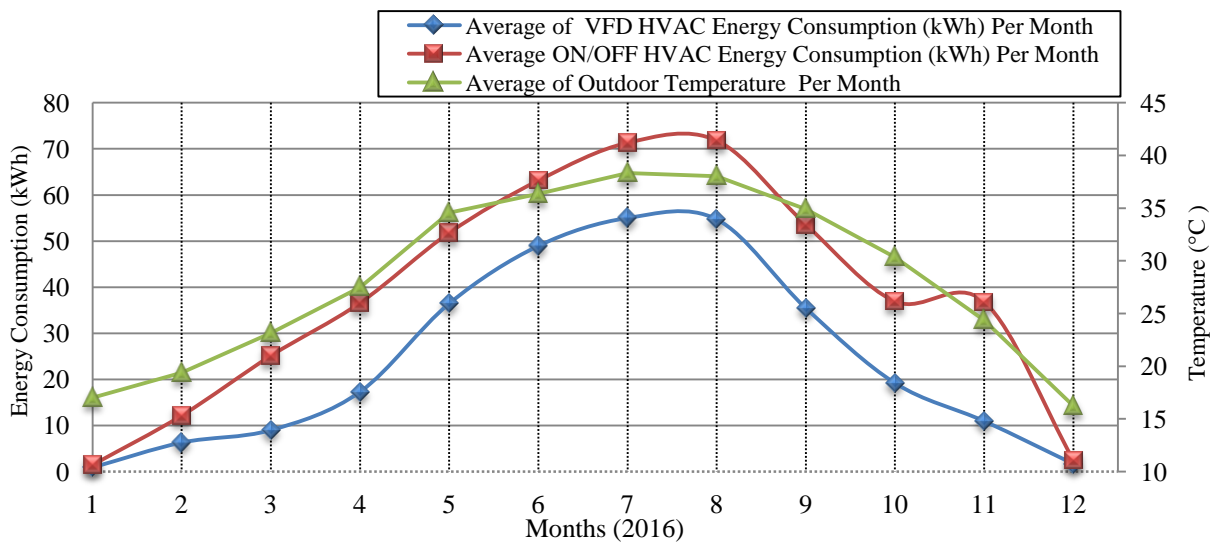
Figure 7.34 Monthly measured average energy consumptions by ON/OFF and VFD HVAC units, 2016.

The highest recorded average outdoor temperature is 37.29 ℃ on August and on January the

lowest average outdoor temperature is 16.31 ℃, however, the average monthly energy

consumptions in summer months is approximately 74 kWh for ON/OFF HVAC and 57 kWh for

VFD HVAC unit. Moreover, due to the high cooling demand during the summer, when the

temperature reaches beyond 45°, energy consumption from the residential sector exceeds

industrial and commercial segments. Consequently, comparing the behavior of the power

demand with the temperature curve shows a clear and strong correlation between them. Finally,

"the Kingdom's electricity demand and consumption are unique in a way that it is the residential

sector that drives the consumption and not the industrial sector as is the case with the rest of the developed/developing countries globally" [57].

7.6.3 Annual Energy Consumption by Simulation for ON/OFF & VFD

Dhahran city in Saudi Arabia has 9 months of warm, hot, and humid weather and four mild and cold. Based on the climate data obtained from our experimental study. We have selected the warm and hot months to be simulated to calculate and assess the energy consumption by each month. Figure 7.35 shows the simulated energy consumptions by both VFD HVAC and ON/OFF HVAC unites for the nine months of warm and hot weather in the year, 2016, starting from March to November, 2016.

For every simulation in each HVAC units, the total energy consumptions are calculated through an integrator of the blower (Air flow) over the whole simulation period. However, for VFD HVAC unit, the FLC VFD HVAC system has been used to simulate the energy consumptions of VFD unit for all these months. It is clearly shown in the Figure 3.35 that the VFD HVAC consumed less energy comparing to the ON/OFF HVAC unit. However, in the month of May, Jun, July, August and September which are warm and the hottest months among the nine months, the energy columns of ON/OFF HVAC seems nearly close to each other, as well as for VFD HVAC unit simulated energy consumptions. Comparing those five months to the other rest simulated months, there is a great difference between ON/OFF HVAC unit and VFD-FLC HVAC unit energy consumption.
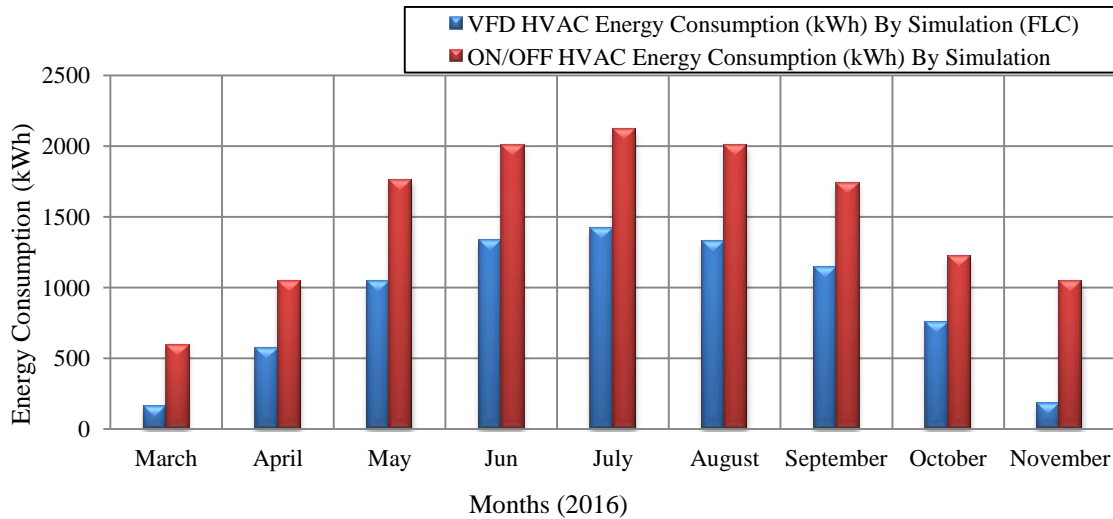
Figure 7.35 Monthly simulated energy consumptions by ON/OFF HVAC and VFD- FLC HVAC units, 2016

As can be concluded at the end of this section, energy consumptions for the nine months of year 2016 have been simulated for both HVAC units. The total of nine months energy consumptions used by both ON/OFF HVAC and VFD HVAC unit is 13529.002 kWh and 7925.485 kWh, respectively. And the monthly average for both units is 1503.224 kWh and 880.609 kWh, respectively. Finally, the validations of the simulated energy consumptions with measured energy over the year, 2016 is shown in the next figure.

The validation of simulated with measured monthly electricity energy consumption of the VFD HVAC unit and the ON/OFF HVAC unit for nine months is shown in Figure 7.36. For the simulation part, the models predicted total monthly energy consumption; however, the monthly energy consumption was compared with the actual consumption from utility electricity energy. Though an 8.6% deviation existed between predicted and actual consumption of the VFD HVAC unit, it can be observed that the predicated and the actual consumption followed the same trend for the ON/OFF HVAC unit. Since the deviation between actual and predicted value exceeded 0.3%, an adjustment procedure was adopted to adjust the model predictions to acceptable

deviation. The adjustment procedure would ensure suitability of the model for evaluating thermal and energy performance when evaluating different energy conservation measures. In addition, the error percentages of the energy validations have been calculated based on the total energy consumptions by simulation and measurement of both HVAC units, and according to equation (7.6) the results shown above in percentage. As described previously, the observed HVAC unites energy profiles by measurement and simulation show a high correlation of HVAC demand to outdoor temperature. Now this is proven by using the simulation data.
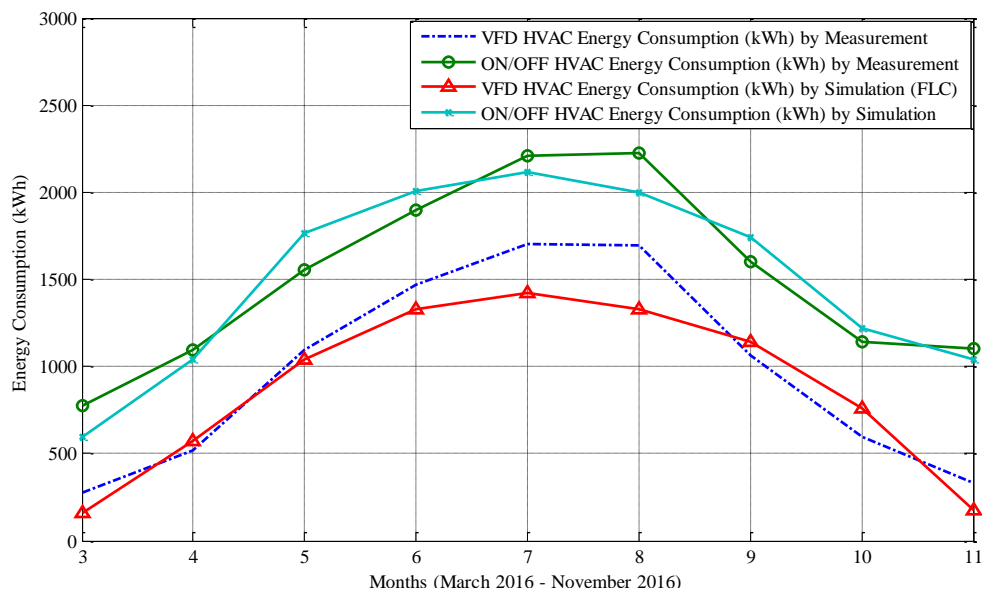
Figure 7.36 Validation monthly simulated and measured energy consumptions by ON/OFF and VFD-FLC HVAC units, 2016

It is noticeable that significant amount of energy consumption is used to operate the HVAC units throughout the year, and this main reason behind this kind of energy waste is the design of an HVAC systems especially ON/OFF HVAC unit, should be fundamentally based on thermal comfort need of the human body, but as the current trend on design seems to oversize the system to compensate for faster cooling time during the peak temperature, which leads to consume more energy over the year.

7.6.4 Monthly Energy Saving

Based on equation (7.3), which has mentioned in the previous section, the monthly energy saving of each month of year, 2016 has calculated. Figure 7.37, presents annual considerable amount of savings of energy occur by VFD HVAC compared to ON/OFF HVAC unit throughout the year for the measurements test. The results indicate, the higher the energy consumption the smaller is the energy saving. The highest amount of energy saving is on November which is 70%, due to the lower energy consumed by VFD HVAC compared to ON/OFF HVAC energy consumed as the weather was become cold. However, the average of energy saving for March, 2016 is reaching 65%, which considered a great amount of saving. In addition, the energy savings of other months fluctuate between 22% - 50%.
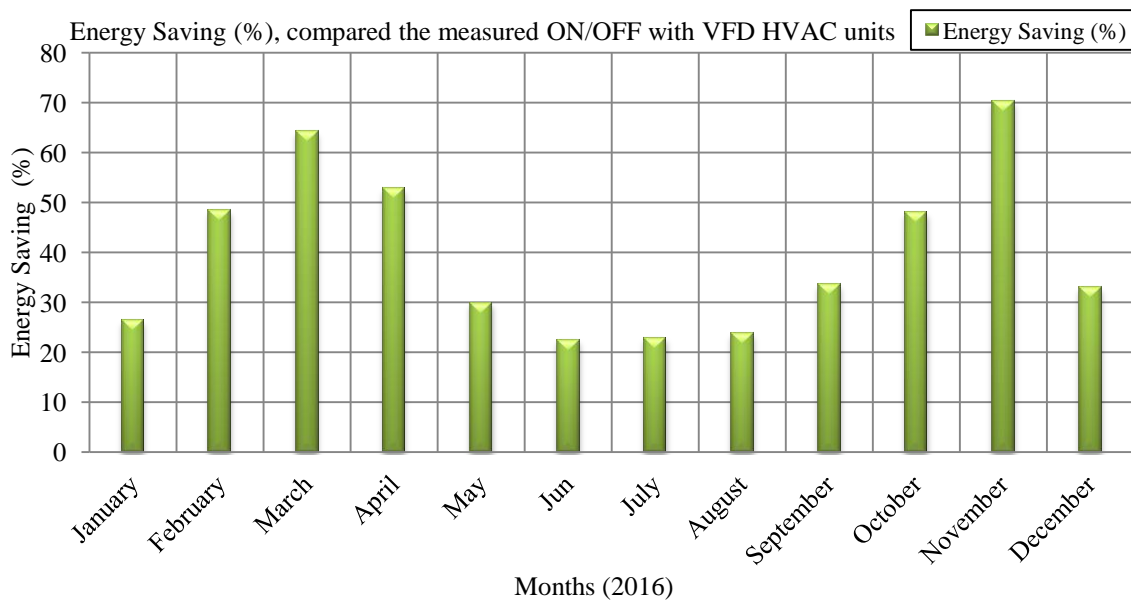
Figure 7.37 Energy savings of energy measurement data of the VFD HVAC with the ON/OFF HVAC unit.

According to equation (7.4), the energy savings by the simulated VFD HVAC techniques energy consumptions with simulated ON/OFF HVAC energy consumption is calculated. Figure 7.38 shows the energy savings of the simulated VFD-FLC HVAC system with the measured ON/OFF

HVAC unit. It is observed that the energy savings looks similar to the energy savings of the measured data.

Energy Saving (%), compared the simulated ON/OFF with VFD HVAC units
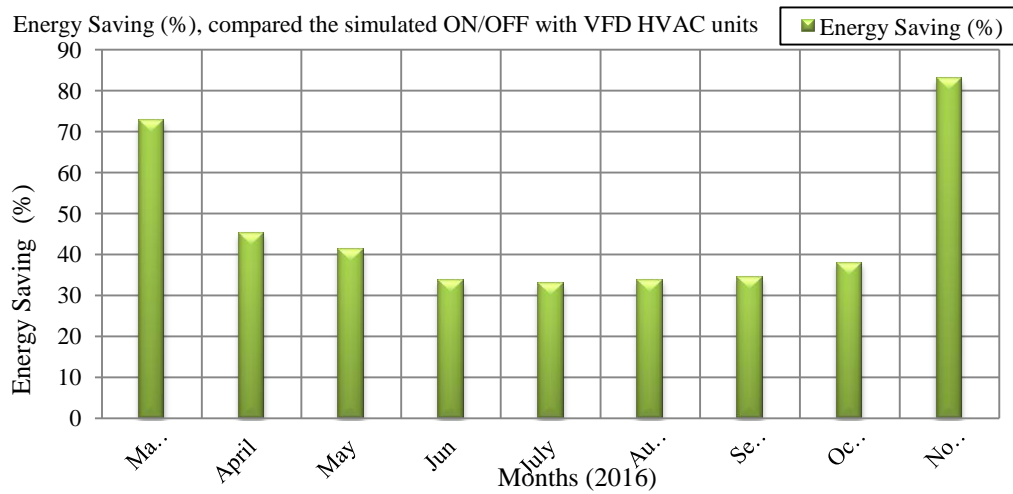
Figure 7.38 Energy savings of energy simulation data of the VFD HVAC with the ON/OFF HVAC unit.

Figure 7.39 shows monthly energy savings of the year, 2016, and based on the measurements data. The result indicates average energy saving ratios achieved, however, the higher the energy consumption the smaller is the energy saving. However, it can be observed that the energy savings fluctuates between 25% -70% throughout the year.
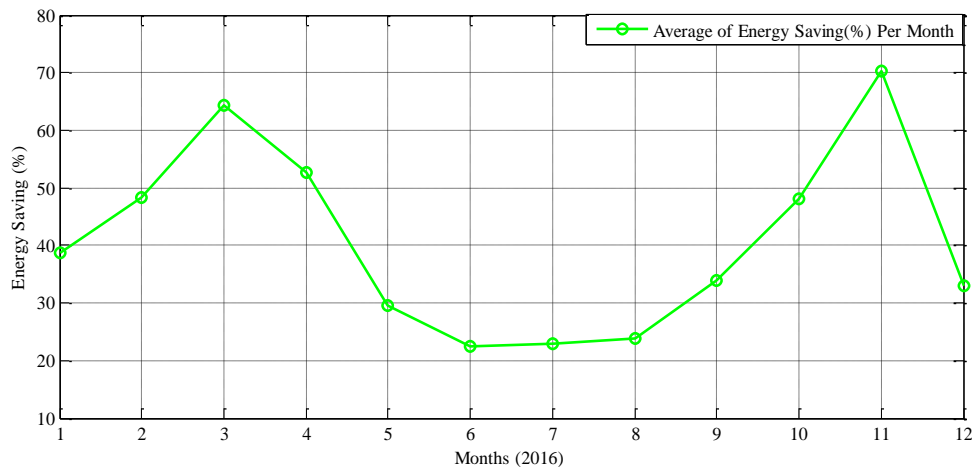
Figure 7.39 Average of energy savings of energy consumption data of the VFD HVAC with the ON/OFF HVAC unit of year, 2016.

176
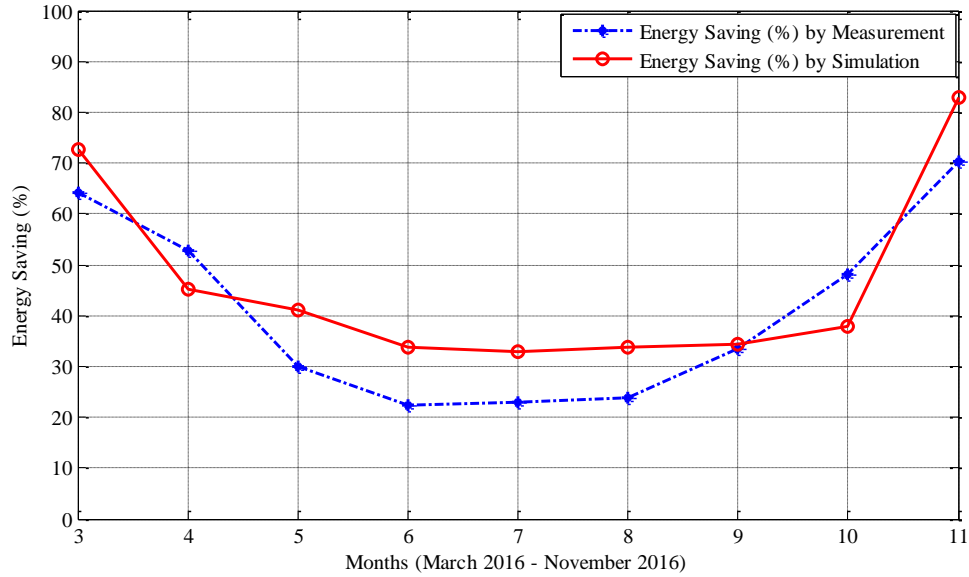
Figure 7.40 Energy savings of energy consumption data of the VFD HVAC with the ON/OFF HVAC unit of year, 2016.

According to equation (7.5), the energy saving by the simulation energy consumptions with measurement energy consumption is calculated. Figure 7.40, presents energy savings comparison between the simulated with the measured data. It is observed that the energy saving by measurement is slightly lower than the energy saving by simulation. Moreover, the implemented simulation of VFD-FLC HVAC approach proved efficient in terms of model development, energy consumption and most energy saving over the year, 2016. Finally, it is clearly shown from figure that huge amount of energy can be saved by using the simulation approach, and this is due to the lower energy consumption.

7.7 Cost Analysis of both the ON/OFF and the VFD HVAC System

The payback period is calculated by counting the number of years it will take to recover the cash invested in installing the VFD HVAC unit instead of the conventional ON/OF HVAC unit. The payback period for setting the temperature to 24 ^{o}C can be calculated by the following formula.

$$\text{Payback Period} = \frac{\text{Additional Cost}}{\text{Annual Saving}} \qquad (7.15)$$

The prices of both HVAC are given in table 7.9, the prices are provided by AL-Zamil Air Conditioning Company, Saudi Arabia.

Table 7.9 Prices of HVAC units

HVAC Unit	ON/OFF	VFD
Price	12750 SR	21500 SR

The cost difference between the ON/OFF unit and the VFD unit is about 40% (8750SR) in which the VFD unit is higher cost than the conventional ON/OFF unit. As previously mentioned, the experimental part of this study the annual energy consumed by both units is measured for each day for the whole year, as well as the energy saving.

Electricity prices in the Kingdom of Saudi Arabia are among the lowest in the world, Figure 7.41 shows global electricity price comparison with the Saudi Arabia in year, 2014 (US Cents/kWh). The residential tariff of the electricity is illustrates in table 7.10.
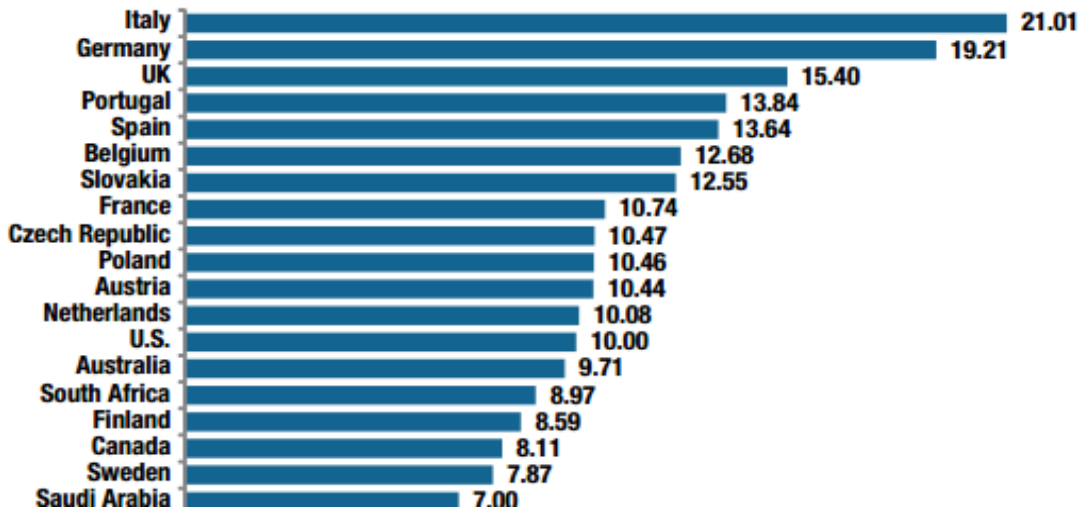
Figure 7.41 Global electricity price comparison with the Saudi Arabia in year, 2014 [57].

Table 7.11 Payback Period for a Residential HVAC

Electrical Energy Cost [58]		Annual Consumption		Annual Energy Savings	Annual Cost Saving	Payback Years
Residential Sector		ON/OFF	VFD			
kWh	Halalah					
1- 2000	5					
2001- 4000	10	13216.402 kWh	8734.918 kWh	34% 4481.484 kWh	4481.484 kWh* 0.3 Hala=1325.54SR	6 years & 6 months
4001- 6000	20					
6001- 8000	30					
8000 <	30					

Based on the calculation performed in Table 7.11, the payback period is six years and 6 months, so if the user installs a VFD HVAC system, he can recover the extra paid money within 6 years and 6 months. During the time after the payback period, the user will start to get the benefit of having the VFD HVAC in the house as the energy consumption is going to be less than that of having an ON/OFF unit.

Table 7.12 gives the time period of the life span of the both unites. The VFD installation is not economical in any county; there may be individual fields with large elevation changes where it is possible to attain the payback period less than 15 years. VFDs can be more beneficial in the cases where two or more fields of lower hydraulic demands are nearby and are irrigated from a single well and the cost of the VFD can be distributed over more acreage [59].

The life cycle of HVAC equipment in commercial buildings is typically 15 to 20 years, so a one- or two-year payback period can generate a substantial savings over time. Converting to a VFD system helps save money, increase the comfort of the building occupants   and reduce equipment maintenance costs and downtime. The system contributes to the house's overall comfort level by optimizing and regulating air flow and temperature into the house's occupant space. These

benefits extend beyond occupant comfort levels and encompass other house spaces that may need regulated temperature control, such as warehouse storage area.

Table 7.12 life Span of HVAC units

No Maintenance (0 Items)	Little Maintenance (2 Items)	Some Maintenance (2-3 Items)	High Maintenance (4 Items)
15-18 years	18-20 years	20-25 years	20-25 years

In addition, the analysis pertinent to the assessment of energy consumptions, energy savings, and the cost of the payback period have been evaluated. In general, the variable frequency drive controller provides higher efficiency and low cost of HVAC system. The cost analysis and the payback period have been calculated. It is found that the user needs only 6 years and a half to recover the additional cost. In the near future, if there is any further drop in the price of the VFD unit, it will become a catalyst in the promotion of energy conversion through the use of a VFD unit. Overall, it was found that the cost of the VFD was not extremely high to be paid back within the VFD's economic life.

CHAPTER 8

CONCLUSIONS AND FUTURE RECOMMENDATION

Chapter eight presents the conclusion to the research undertaken and attempts to draw recommendations from the results obtained in the simulation and the experimentations study.

8.1   Conclusions

The HVAC systems incorporating with the ON/OFF controller and the three control strategies of VFD are considered to determine the compressor power consumptions. Thermal analysis is carried out in line with the experimental conditions to assess the energy consumption of the HVAC systems. The experimental set-up is developed incorporating the LabView based data acquisition monitoring and measurement system. The thermal model considers different types of HVAC system controller (ON/OFF, VFD-PID, VFD-PI-PWM and VFD-FLC) units. The predictions of the power consumptions of the HVAC system have been compared with those of the measured data. The developed mathematical thermal house model is integrated with the cooling source model of an ON/OFF cycle and VFD air conditioning systems. The developed thermal models are simulated by using Simscape physical components in Matlab/Simulink environment. In addition, the analysis pertinent to the assessment of daily, monthly and annually energy consumptions, energy savings, and the cost of the payback period have been evaluated. In general, the variable frequency drive controllers provide higher efficiency and low cost of

HVAC system. In addition, the specific conclusions and focuses derived from the present study are listed as follows:

- The indoor temperature, energy consumptions and energy savings have been investigated for one day (5th of September, 2016). However, the performance of ON/OFF HVAC unit and VFD with the three control strategies are simulated and compared with measurements. It is found that all VFD control strategies HVAC units consumed less energy than the ON/OFF HVAC unit. It is found that VFD-FLC is suitable controller which consumed less energy than VFD-PID and VFD-PI-PWM. However, VFD-FLC gave the occupants a very satisfaction level of thermal comfort and the time response is faster to cool down the indoor air temperature.

- The energy consumptions and energy savings have been examined for one warm month of the year (September, 2016). The energy consumptions of both HVAC units have investigated by simulation and measurement. It is found that using VFD-FLC gives the most energy savings and performs better than the other investigated control systems.

- The energy consumptions have been examined for several months and it is demonstrated that the energy savings reach between 22% - 49% during the period from March 2016 to November 2016. It has been noticed that the performance the HVAC system simulation is affected by the outdoor temperature and the indoor activities during the day. Energy savings with VFD is reached 40% where the outdoor temperature around 30ºC. The simulation results matched significantly with the data measurement with an average error of approximately 3.07%.

- The daily and monthly average COP variations of actual and ideal systems are calculated and the finding revealed that VFD unit has higher COP than the ON/OFF cycle.

- The cost analysis and the payback period have been calculated. It is found that the user needs only 6 years and a half to recover the additional cost based on AL-Zamil Air Conditioning Company. In the near future, if there is any further drop in the price of the VFD unit, it will become a catalyst in the promotion of energy conversion through the use of a VFD unit.

- The utilization of VFD is economically justified and the result has shown that installing a VFD for a residential HVAC system gives considerable energy savings over the ON/OFF cycle.

8.2   Future Recommendation

Due to the wide scope of the present work from application point of view, the following recommendations are suggested for further study.

Saudi Arabia is facing a sharp rise in the demand for power consumption, due to the higher cooling demand during the summer. However, the calculated payback period seems to be low enough to encourage people to use VFD for their air conditioning, to achieve better thermal comfort level with minimum energy consumption.

- The design of HVAC system should be fundamentally based on thermal comfort need of the human body, but the current trend on design seems to oversize the system to compensate for faster cooling time during the higher temperature. Optimum resizing for the HVAC to reduce energy consumption.

- Implementing the VFD Fuzzy Logic Controller for the experimental study of VFD HVAC unit.

References

[1] Pal, J. S., & Eltahir, E. A. (2016). Future temperature in southwest Asia projected to exceed a threshold for human adaptability. *Nature Climate Change*, *6*(2), 197-200.

[2] Al-Shaalan, A., Ahmed, W., & Alohaly, A. (2014). Design guidelines for buildings in Saudi Arabia considering energy conservation requirements. In *Applied Mechanics and Materials* (Vol. 548, pp. 1601-1606). Trans Tech Publications.

[3] Alawaji, S. H. (2012). Saudi Arabia: a Proactive Approach to Energy. *Living Energy (7)*, 76-81.

[4] Liu, D., & Garimella, S. V. (2005). Analysis and optimization of the thermal performance of microchannel heat sinks. *International Journal of Numerical Methods for Heat & Fluid Flow*, *15*(1), 7-26.

[5] Matar, W., Murphy, F., Pierru, A., & Rioux, B. (2015). Lowering Saudi Arabia's fuel consumption and energy system costs without increasing end consumer prices. *Energy Economics*, *49*, 558-569.

[6] Bertagnolio, S., & Lebrun, J. (2008, September). Simulation of a building and its HVAC system with an equation solver: application to benchmarking. In *Building Simulation* (Vol. 1, No. 3, pp. 234-250). Tsinghua University Press, co-published with Springer-Verlag GmbH.

[7] Riangvilaikul, B., & Kumar, S. (2010). An experimental study of a novel dew point evaporative cooling system. *Energy and Buildings*, *42*(5), 637-644.

[8] Yu, C. H. P. (2001). *A study of energy use for ventilation and air-conditioning systems in Hong Kong*.

[9] Nasution, H. (2006). Energy analysis of an air conditioning system using PID and fuzzy logic controller. *Universiti Teknologi Malaysia: PhD Thesis*.

[10] Bruno, F. (2011). On-site experimental testing of a novel dew point evaporative cooler. *Energy and Buildings*, *43*(12), 3475-3483.

[11] Muratori, M., Marano, V., Sioshansi, R., & Rizzoni, G. (2012, July). Energy consumption of residential HVAC systems: A simple physically-based model. In *Power and Energy Society General Meeting, 2012 IEEE* (pp. 1-8). IEEE.

[12] Nasution, H. (2006). Energy analysis of an air conditioning system using PID and fuzzy logic controller. *Universiti Teknologi Malaysia: PhD Thesis*.

[13]   Teodosiu, C., Lungu, C., Colda, I., & Damian, A. (2006, July). Simulation of HVAC systems energy consumption. In *Environment Identities and Mediterranean Area, 2006. ISEIMA'06. First international Symposium on* (pp. 139-143). IEEE.

[14]   Salsbury, T., & Diamond, R. (2000). Performance validation and energy analysis of HVAC systems using simulation. *Energy and buildings*, *32*(1), 5-17.

[15]   Kulkarni, M. R., & Hong, F. (2004). Energy optimal control of a residential space-conditioning system based on sensible heat transfer modeling. *Building and Environment*, *39*(1), 31-38.

[16]   Zhang, W., Lian, J., Chang, C. Y., & Kalsi, K. (2013). Aggregated modeling and control of air conditioning loads for demand response. *IEEE transactions on power systems*, *28*(4), 4655-4664.

[17]   Elsarrag, E., & Alhorr, Y. (2012). Modelling the thermal energy demand of a Passive-House in the Gulf Region: The impact of thermal insulation. *International Journal of Sustainable Built Environment*, *1*(1), 1-15.

[18]   Wen, Y., & Burke, W. (2013, April). Real-Time Dynamic House Thermal Model Identification for Predicting HVAC Energy Consumption. In *Green Technologies Conference, 2013 IEEE* (pp. 367-372). IEEE.

[19]   Molina, A., Gabaldon, A., Fuentes, J. A., & Alvarez, C. (2003). Implementation and assessment of physically based electrical load models: application to direct load control residential programmes. *IEE Proceedings-Generation, Transmission and Distribution*, *150*(1), 61-66.

[20]   Nasution, H., Jamaluddin, H., & Syeriff, J. M. (2011). Energy analysis for air conditioning system using fuzzy logic controller. *TELKOMNIKA (Telecommunication Computing Electronics and Control)*, *9*(1), 139-150.

[21]   Khayyam, H., Kouzani, A. Z., Hu, E. J., & Nahavandi, S. (2011). Coordinated energy management of vehicle air conditioning system. *Applied thermal engineering*, *31*(5), 750-764.

[22]   Judkoff, R., & Neymark, J. (1995). *International Energy Agency building energy simulation test (BESTEST) and diagnostic method* (No. NREL/TP--472-6231). National Renewable Energy Lab., Golden, CO (US).

[23]   Penman, J. M. (1990). Second order system identification in the thermal response of a working school. *Building and Environment*, *25*(2), 105-110.

[24]   Nesler, C. G., & Stoecker, W. F. (1984). Selecting the proportional and integral constants in the direct digital control of discharge air temperature. *ASHRAE transactions*, *90*(2), 834-845.

[25]   Nesler, C. G. (1986). Automated controller tuning for HVAC applications. *ASHRAE Trans.;(United States)*, *92*(CONF-8606125-).

[26]   Ho, W. F. (1993). Development and evaluation of a software package for self-tuning of three-term DDC controllers. *ASHRAE, ATLANTA, GA(USA).*, (29-534).

[27]   Tamura, G. T. (1983). International Energy Agency: Energy Conservation in Buildings and Community Systems Programme: Annex IX: Minimum Ventilation Rates: Literature Review to Special Research Fields and Proposal of R & D Projects: Final Report.

[28]   Nasution, H., Jamaluddin, H., & Syeriff, J. M. (2011). Energy analysis for air conditioning system using fuzzy logic controller. *TELKOMNIKA (Telecommunication Computing Electronics and Control)*, *9*(1), 139-150.

[29]   Khayyam, H., Kouzani, A. Z., Hu, E. J., & Nahavandi, S. (2011). Coordinated energy management of vehicle air conditioning system. *Applied thermal engineering*, *31*(5), 750.

[30]   Judkoff, R., & Neymark, J. (1995). *International Energy Agency building energy simulation test (BESTEST) and diagnostic method* (No. NREL/TP--472-6231). National Renewable Energy Lab., Golden, CO (US).

[31]   Attia, A. H., Rezeka, S. F., & Saleh, A. M. (2015). Fuzzy logic control of air-conditioning system in residential buildings. *Alexandria Engineering Journal*, *54*(3), 395.

[32]   Ali, I. M. (2012). Developing of a fuzzy logic controller for air conditioning system. *AJES*, *5*, 180-187.

[33]   Penman, J. M. (1990). Second order system identification in the thermal response of a working school. *Building and Environment*, *25*(2), 105-110.

[34]   Stefanovic, M., Cvijetkovic, V., Matijevic, M., & Simic, V. (2011). A LabVIEW-based remote laboratory experiments for control engineering education. *Computer Applications in Engineering Education*, *19*(3), 538-549.

[35]   Valentini, L., Armentano, I., Kenny, J. M., Cantalini, C., Lozzi, L., & Santucci, S. (2003). Sensors for sub-ppm NO 2 gas detection based on carbon nanotube thin films. *Applied Physics Letters*, *82*(6), 961-963.

[36]   Monostori, L. (2014). Cyber-physical production systems: Roots, expectations and R&D challenges. *Procedia CIRP*, *17*, 9-13.

[37] Jiang, X., Zhang, L., & Xue, H. (2008, October). Designing a temperature measurement and control system for constant temperature reciprocator platelet preservation box based on LabVIEW. In *Natural Computation, 2008. ICNC'08. Fourth International Conference on* (Vol. 5, pp. 48-51). IEEE.

[38] Xiang, H., Wang, K., & Li, Z. (2011, October). Monitored Control System of Temperature/humidity for Ammunition Storehouse Based on LabVIEW. In *Instrumentation, Measurement, Computer, Communication and Control, 2011 First International Conference on* (pp. 172-175). IEEE.

[39] Aiswarya, V., & Prakash, N. K. (2013, August). Wind turbine instrumentation system using LabVIEW. In *Global Humanitarian Technology Conference: South Asia Satellite (GHTC-SAS), 2013 IEEE* (pp. 218-222). IEEE.

[40] Li, J., Xu, L., & Li, H. (2011, July). The application of automatic controlling and measuring system based on LabVIEW in thermal conductivity of poor conductor experiment. In *Multimedia Technology (ICMT), 2011 International Conference on* (pp. 6082-6084). IEEE.

[41] Tang, Q., Teng, Z., Guo, S., & Wang, Y. (2009, April). Design of power quality monitoring system based on labview. In *Measuring Technology and Mechatronics Automation, 2009. ICMTMA'09. International Conference on* (Vol. 1, pp. 292-295). IEEE.

[42] Široký, J., Oldewurtel, F., Cigler, J., & Prívara, S. (2011). Experimental analysis of model predictive control for an energy efficient building heating system. *Applied Energy*, *88*(9), 3079-3087.

[43] "Heat, Work and Energy." [Online]. Available: http://www.engineeringtoolbox.com/heat-work-energy-d_292.html. [Accessed on 9th of April,2016]

[44] Q. Mechanics, "Types Of Heat Transfer," *Energy*, 1979. [Online]. Available: http://physics.bu.edu/~duffy/py105/Heattransfer.html, [Accessed on 9th of April,2016]

[45] O. F. Metallic, "Thermal resistance," 1964. [Online]. Available: https://neutrium.net/tag/thermal-resistance, [Accessed on 9th of April,2016]

[46] T. Notes, "Combined Conduction and," *Notes*. [Online]. Available: http://web.mit.edu/16.unified/www/FALL/thermodynamics/notes/node123.html, [Accessed on 11th of April,2016]

[47] Cooling Loads - Latent and Sensible Heat." [Online]. Available: http://www.engineeringtoolbox.com/latent-sensible-cooling-load-d_245.html[Accessed on 16th of April,2016]

[48]   "Cooling   Loads   -   Latent   and   Sensible   Heat."   [Online].Available:
        http://www.engineeringtoolbox.com/latent-sensible-cooling-load-d_245.html.

[49]   "Cooling   and   Heating   Equations."   [Online].
        Available:http://www.engineeringtoolbox.com/cooling-heating-equations-d_747.html.
        [Accessed on 10th of April,2016].

[50]   "Calculating Indoor Temperature and Humidity Loads." [Online]. Available:
        http://www.engineeringtoolbox.com/indoor-temperature-humidity-d_114.html.   [Accessed
        on 10th of April,2016]

[51]   T. Al-Shemmeri, "Building's Heat Gains," 2011. [Online]. Available:
        http://www.wiley.com/legacy/wileychi/al_shemmeri/supp/powerpoints/chapter_5.pdf.
        [Accessed on 10th of April,2016].

[52]   Ryder-Cook, D. (2009). Thermal modeling of buildings. *Cavendish Laboratory,
        Department of Physics, University of Cambridge, Tech. Rep*.

[53]   Crawley, D. B., Hand, J. W., Kummert, M., & Griffith, B. T. (2008). Contrasting the
        capabilities of building energy performance simulation programs. *Building and
        environment*, *43*(4), 661-673.

[54]   Bidwell, C. C. (1940). Thermal conductivity of metals. *Physical Review*, *58*(6), 56 Grant,
        E, & Halstead, B. J. (1998). Dielectric parameters relevant to microwave dielectric
        heating. *Chemical society reviews*, *27*(3), 213-224.

[55]   Li, Y. (2015). Variable Frequency Drive Applications in HVAC Systems. In *New
        Applications of Electric Drives*. InTech.

[56]   Handbook, A. S. H. R. A. E. (1996). HVAC systems and equipment. *American Society of
        Heating, Refrigerating, and Air Conditioning Engineers, Atlanta, GA*.

[57]   Chamber, J. Sectorial report on Saudi Arabia-electricity. www.jeg.org.sa. 2016 [accessed 10.12.2016].

[58]   Saudi   Electricity   Company.   https://www.se.com.sa/en-
        us/customers/Pages/TariffRates.aspx.Consumption Tariff. 2016 [20.12.2016].

[59]   Li, Y., Liu, M., Lau, J., & Zhang, B. (2014). Experimental study on electrical signatures
        of common faults for packaged DX rooftop units. *Energy and Buildings*, *77*, 401-415.

VITAE

Name: Omar Ahmed Omar Al-Tamimi

Email: omer2333@hotmail.com

Address: Damoon- Tarim- Hadramout – Yemen

Qualification: **MS (Electrical Engineering)**

King Fahd University of Petroleum & Minerals

Dhahran, Saudi Arabia

BE (Telecommunication Engineering)

APU University

Kuala Lumpur, Malaysia

Publications

Status: **S**=Submitted   **UP**= Under Preparation

No	Publication Type	Paper Title	Status
1	Journal	Innovative Design of a HVAC System for Energy Savings and Economic Analysis.	S
2	Journal	Local Thermal Disturbance on Energy Content of HVAC Systems.	S
3	Conference	Indoor Temperature Control and Energy Saving of Air Conditioning System Using FLC.	UP